



UNIVERSITÀ DEGLI STUDI DI CATANIA

DIPARTIMENTO DI FISICA E ASTRONOMIA

CORSO DI DOTTORATO IN FISICA

FILIPPO CONTINO

IMPACT OF NEW PHYSICS BEYOND THE STANDARD MODEL ON
THE STABILITY OF THE ELECTROWEAK VACUUM

TESI DI DOTTORATO

RELATORE:

CHIAR.MO PROF. VINCENZO BRANCHINA

XXXIII CICLO

*Ai miei genitori Sarino e Giuseppina,
per avermi accompagnato e sostenuto in questo cammino
con affetto*

Cronache di un dottorato

*"In realtà non ce ne sono,
ma se proprio dobbiamo trovare un difetto,
direi il fatto che lui sia instancabile..."*

"il che implica che devo essere instancabile pure io..."
- quando mi chiedono quali sono i difetti di lavorare con Branchina

"Chi è, la zita?" - gli amici quando Branchina
mi telefona per la quarta volta in un giorno

"Dov'è il nostro amico sperimentale?" - Branchina ad ogni studente
di fisica sperimentale che si iscrive ai suoi corsi di QFT

"Ma io mi sono iscritto a teorica per fare i conti con carta e penna!"
- Filippo Contino alle prese con un codice Wolfram

*"Siamo quattro teorici che cercano di aggiustare una porta...
in un corridoio pieno di sperimentali...
togliamoci di qua prima di diventare una nuova barzelletta"*
- scherzi a parte, alla fine non riuscimmo a riparare la porta

*"Guarda, se tu vuoi andare, vai tranquillo...
io torno in albergo..."*

- Branchina sornione, quando ci fermano
a Varsavia invitandoci a uno strip club.

Abstract

Our current knowledge of particle physics, in particular after the discovery of the Higgs boson, tells us that our Universe is not sitting in its most stable state, which is its ground state. Since everything in Nature tends to reach such a state, the Universe will decay towards it, with inevitable consequences on its very existence. The results we obtain from the Standard Model tell us that this decay will take place after a time that is enormously greater than the current age of the Universe. However we also expect that there is still unknown New Physics that completes our knowledge on the interactions between fundamental particles, and such physics can have an impact on the stability of the electroweak vacuum. In particular, several works published in the last decade have shown that, in a flat spacetime background, this New Physics could trigger a more rapid decay towards the ground state. In this Ph.D. thesis, the problem of the stability of the Universe was therefore studied in a more complete context, i.e. considering also the presence of gravity. Using general models of New Physics, it has therefore been shown that gravity tends to have a stabilizing effect on the decay of the electroweak vacuum. Nonetheless, gravity fails to wash out the effects of the New Physics, so in some situations it would imply a very near decay or even a decay that should have already occurred. In the latter case, the corresponding New Physics model must obviously be discarded, as it cannot describe the Universe we observe. However, it has also been shown that the introduction of a direct coupling between the Higgs boson and gravity can provide a stabilizing mechanism that saves the Universe from this decay, as it generates a washing out of the New Physics effects. Finally, we went on to investigate the problem of the stability of the electroweak vacuum in two specific New Physics models. First of all, theories of minimal embeddings of the Standard Model in Supergravity framework have been studied, showing that in these contexts it is possible to introduce further stabilization mechanisms through the use of appropriate discrete symmetries. Secondly, this problem has been studied in the Two Higgs Doublet Model, which is a model that presents a rich proliferation of vacuum states and particles, and the calculation of the decay time has been used as an additional discriminant to reduce the space of the parameters of the theory. However, in the latter case, the study of the stability of the electroweak vacuum was limited only to the case of flat spacetime, leaving the inclusion of gravity for future studies.

Contents

1 Electroweak theory	9
1.1 Gauge principle and Yang-Mills theory	10
1.2 Introduction to electroweak theory	10
1.3 The Higgs mechanism	18
1.3.1 Spontaneous breaking of the symmetry and Goldstone theorem	18
1.3.2 Higgs mechanism. Spontaneous symmetry breaking of symmetry in the electroweak theory	20
2 Quantum correction to the Higgs potential	27
2.1 Effective potential in scalar theories	27
2.1.1 Computation of the effective action	32
2.1.2 Effective action for Linear Sigma Model	35
2.2 Standard Model one-loop effective potential	39
2.2.1 Scalar contribution	40
2.2.2 Gauge contribution	40
2.2.3 Fermionic contribution	43
2.3 Renormalization group improved effective Higgs potential	45
3 Instanton physics and vacuum decay	49
3.1 Tunneling in quantum mechanics	49
3.2 Tunneling with functional formalism	53
3.2.1 Application to the double well potential and instantons	57
3.2.2 Application to the decay of a metastable state and bounce solutions	64
3.3 Quantum tunnelling in systems with N degrees of freedom	69
3.4 Quantum tunneling in QFT	71
3.4.1 Bounce in QFT: vacuum decay	72
3.4.2 Bounce in QFT: inclusion of gravity	76
4 New solutions in the presence of New Physics beyond the Standard Model	79
4.1 Stability problem of the electroweak vacuum in Standard Model . . .	79

4.2	New physics: Higher order operators	86
4.3	New physics: large mass particles	90
5	Direct Higgs-gravity interaction and stability of our Universe	95
5.1	Non-minimal coupling of Higgs field to gravity	95
5.2	Effect of Planck scale New Physics	98
6	Stability of the EW Vacuum in SUGRA frameworks	105
6.1	Theoretical background	105
6.2	Planckian New Physics Effects	106
6.2.1	Planck-Scale Scenarios with $M = M_P$	107
6.2.2	Planck-Scale Scenarios with $M = M_P/10$	109
6.3	Protective Mechanisms in SUGRA	113
6.4	EW Vacuum Stability in SUGRA Models	118
6.4.1	SUGRA Scenarios with $M_S = 10^9$ TeV	118
6.4.2	SUGRA Scenarios with $M_S = 10$ TeV	121
7	Electroweak vacuum lifetime in two Higgs doublet models	123
7.1	The Two-Higgs Doublet Model potential	124
7.1.1	Theoretical constraints on quartic couplings	126
7.1.2	The electroweak-breaking minimum	127
7.1.3	Experimental constraints on the 2HDM	129
7.2	Coexisting minima in the 2HDM	130
7.3	Tunneling and bounces	133
7.4	Tunneling to degenerate vacua	138
7.5	2HDM Numerical Scans	141
7.5.1	General scans for type I and II models	142
7.5.2	First benchmark scenarios: safe regions	144
7.5.3	Second benchmark scenario: considerable exclusion	147
8	Conclusions and outlook	149
A	Standard Model β and γ functions	155
B	Potential with a single minimum: computation of the functional determinant	157
C	Mathematical appendix to the instanton computation	161
D	Numerical computation of the bounce solution	169

Chapter 1

Electroweak theory

The Standard Model is a *gauge theory* [1–5] based on the symmetry group $SU(2)_L \otimes U(1)_Y \otimes SU(3)_C$ that describes three of the fundamental interactions (the electromagnetic, weak and strong ones) between the elementary constituents of the matter (quark and leptons) in terms of the exchange of spin-1 particles that employ the role of mediators of these interactions. In particular, the *electroweak theory*, developed in the 60’s by Weinberg, Salam e Glashow, for the first time provided a unified description of the electromagnetic and weak interactions [6–12]. Successively in the 70’s the *quantum chromodynamics* was developed to describe the strong interactions.

However, for symmetry reasons, the theory imposes that all the particles have to be massless, contrary to what we see from phenomenological evidences. Then we have to consider a mechanism to give mass to the particles, i.e. the *Higgs mechanism*, obtaining the modern formulation of the Standard Model. According to the Higgs mechanism, additionally to the fields giving rise to particles and interactions, in the Universe there is a further scalar field to which corresponds the Higgs boson, and via this field we have a potential that generates a set of infinite minima for the ground state of the Universe. As we shall see, choosing one of the possible minima, the symmetry mentioned above is spontaneously broken and the particles acquire mass. This minimum is called *electroweak vacuum*.

However, the Standard Model provides also the possibility of a metastable scenario: in fact, considering the quantum corrections due to the interaction of the Higgs boson with the other particles, the Higgs potential presents a second minimum, whose relative height respect to the electroweak vacuum depends mostly from the mass of the Higgs boson m_H and from the mass of the top quark m_t . Considering the precise measurement of these masses, we can see that this minimum is lower than the electroweak minimum, so that it would decay in the stable minimum of *true vacuum* through tunneling effect, while the minimum of *false vacuum* in which our Universe currently sits is a metastable minimum. Before delving into the theory of stability of the electroweak vacuum, we provide a description of the electroweak sector of the Standard Model.

1.1 Gauge principle and Yang-Mills theory

In the search of a theory that is able to describe the fundamental interactions, the *symmetries* characterizing the physical systems play an extremely important role: for instance, the Lorentz invariance (more in general the invariance under Poincaré transformations) dictated by the principles of Special Relativity [13–15], permits to reduce the spectrum of possible interactions between quarks and leptons. The symmetry principle that allows to determine the correct form of the interaction between elementary particles is the *gauge principle* [8, 9, 13, 16]. According to this principle, given a physical system described by a lagrangian having a *global internal symmetry* (associated with a given symmetry group), the correct expression of the interaction is the one obtained imposing that the internal symmetry characterizing the lagrangian is also a *local symmetry*.

This can be implemented introducing a number of *gauge fields* commensurate to the number of generators of the symmetry group of the lagrangian, and then properly modifying the derivatives of the fields in such a way that they transform as the fields themselves. Thus we obtain in the lagrangian an additive term that describes correctly the *minimal interaction between the fields of matter* and that is written as the product of the introduced gauge fields and the Noether current associated to the global internal symmetry of the starting lagrangian.

In 1954 Yang and Mills propose a generalization of the gauge principle, until then used to obtain QED that is a gauge theory based on the group symmetry $U(1)$, characteristic of the electromagnetic interaction, in such a way to apply it to non-abelian gauge theories. The *Yang-Mills theory* [7, 8, 10, 11, 13] was then used in the 60’s to formulate the electroweak theory and afterwards, around 1974, for the development of the field theory of strong interactions.

1.2 Introduction to electroweak theory

The fermions of the Standard Model, i.e. quarks and leptons [17–21], can be organized into three families

$$\begin{array}{lll} \begin{pmatrix} \nu_e \\ e \end{pmatrix} & \begin{pmatrix} \nu_\mu \\ \mu \end{pmatrix} & \begin{pmatrix} \nu_\tau \\ \tau \end{pmatrix} \\ \begin{pmatrix} u \\ d \end{pmatrix} & \begin{pmatrix} c \\ s \end{pmatrix} & \begin{pmatrix} t \\ b \end{pmatrix} \end{array} \quad \begin{array}{l} \text{Leptons} \\ \text{Quark} \end{array} \quad (1.1)$$

In particular, the phenomenology allows us to assert that the leptonic doublets belonging to the different families are identical from the point of view of the interaction and they differ only for the masses. The same discussion is valid for the quarks doublets. For instance, the muon μ and the tauon τ are exact copies of the electron

e from the point of view of quantum numbers, but respect to the latter they have much more larger masses.

The *charged leptons* and the *quarks* are massive particles of 1/2-spin, and then can be described via Dirac fields [13]. We know that a generic Dirac field $\psi(x)$ can be written, using chirality projection operators, as a sum of Dirac fields purely left-handed and right-handed:

$$\psi(x) = \frac{\mathbb{1} - \gamma_5}{2}\psi(x) + \frac{\mathbb{1} + \gamma_5}{2}\psi(x) = \psi_L(x) + \psi_R(x). \quad (1.2)$$

In the case of *neutral leptons* we can not use the same representation because (despite of the fact the last experiments on the neutrinos oscillations have shown that these particles have a mass [22]) the neutrinos and the antineutrinos are described in the Standard Model as massless fermions, and then have to be described by left-handed and right-handed Weyl spinors respectively. Thus in the case of the neutrino we can do the identification

$$\psi_\nu(x) \equiv \psi_\nu^L(x) = \frac{\mathbb{1} - \gamma_5}{2}\psi_\nu(x). \quad (1.3)$$

The electroweak theory is a gauge theory based on the symmetry group $SU(2)_L \otimes U(1)_Y$, that is the group associated to the internal symmetries of *weak isospin* and of *weak hypercharge*. To understand the way in which this theory is constructed we have to introduce some phenomenological observations that allow to determine the properties and the symmetries characterizing the weak and electromagnetic interactions [23–25], and that allow to build the modern *unified field theory of the electroweak interactions*:

- The W^+ , W^- and Z^0 bosons are massive particles of 1-spin;
- The interactions between quarks and leptons that take place through the exchange of the W^\pm bosons, that are the *weak interactions with charged currents*, show the following properties:
 - only the left-handed fermions and the right-handed antifermions couple to the vector bosons W^+ and W^- , i.e. the weak interaction does not preserve parity;
 - the W^\pm bosons couples only to left-handed (right-handed) fermions (antifermions) belonging to the same doublet;
 - the partners of quark up, charm and top in the weak isospin doublets are linear combinations of quark down, strange and bottom;
 - all the fermionic doublets couple to the W^\pm bosons with the same coupling constant.
- The interactions between quarks and leptons that take place through the exchange of the Z^0 boson or through the exchange of a photon, i.e. the *weak interactions with neutral current*, present the following characteristics:

- all the interaction vertices preserve the flavour;
- the electromagnetic interactions depend by the electric charge that defines in a unique way the coupling, so that the neutral leptons, i.e. the neutrinos, can interact only through weak interactions;
- the electromagnetic interaction preserves parity, so that the photons couple to left-handed fermions and to the corresponding right-handed antifermions in the same way;
- the Z^0 boson couples to fermions in different way depending on the chirality.

Starting from these observations, since the fields that describe the interacting particles constitute, from the point of view of group theory [13], the base for a representation of the symmetry group characterizing the electroweak interactions, is possible to determine the symmetry group itself. In *quantum electrodynamics* the electromagnetic interaction between quarks and leptons [16] is described by the interaction lagrangian

$$\mathcal{L}_{QED}^{int} = q \bar{\psi}(x) \gamma^\mu \psi(x) A_\mu(x), \quad (1.4)$$

i.e. as said above, the interaction is described in terms of a gauge field $A_\mu(x)$ and the Noether current $J_\mu(x)$ associated to the global internal symmetry $U(1)$ of the Dirac lagrangian that describes free quarks and leptons. The density lagrangian that describes the weak interaction between leptons can be built similarly, considering that the possible *leptonic charged current* have to be consistent with the phenomenological properties: then we deduce that the form of these current is of the kind

$$J_\mu(x) = \sum_f \bar{\psi}_f^L(x) \gamma_\mu \psi_{\nu_f}^L(x) = \sum_f \bar{\psi}_f(x) \gamma_\mu \left(\frac{\mathbb{1} - \gamma_5}{2} \right) \psi_{\nu_f}(x) \quad (1.5)$$

$$J_\mu^\dagger(x) = \sum_f \bar{\psi}_{\nu_f}^L(x) \gamma_\mu \psi_f^L(x) = \sum_f \bar{\psi}_{\nu_f}(x) \gamma_\mu \left(\frac{\mathbb{1} - \gamma_5}{2} \right) \psi_f(x) \quad (1.6)$$

where Eqs. (1.5) and (1.6) are written, for simplicity, only for the leptons and the sum over f denotes a sum over the flavours. It is worth to note that the charged currents are written in terms of the difference of a vectorial current and an assial one (pseudovectorial) and this defines the so called *V-A structure of the weak interactions*. As said, since the W^\pm boson couples to left-handed fermions belonging to the same doublets, it is useful to define relatively to a given flavour family the Dirac field doublet:

$$\Psi_f^L(x) = \begin{pmatrix} \psi_{\nu_f}(x) \\ \psi_f(x) \end{pmatrix}_L. \quad (1.7)$$

Then the charged currents introduced in the Eqs. (1.5) and (1.6) can be written as

$$J_\mu(x) = \sum_f \bar{\Psi}_f^L(x) \gamma_\mu \sigma^+ \Psi_f^L(x), \quad (1.8)$$

$$J_\mu^\dagger(x) = \sum_f \bar{\Psi}_f^L(x) \gamma_\mu \sigma^- \Psi_f^L(x), \quad (1.9)$$

where we have introduced the matrices $\sigma^\pm = \frac{1}{2}(\sigma_1 \pm i\sigma_2)$ built with the Pauli matrices σ_1 e σ_2 . Having carried out these considerations, the currents $J_\mu(x)$ e $J_\mu^\dagger(x)$ can be interpreted as the Noether currents associated to a symmetry of the lagrangian: since they are written in terms of Dirac field doublets and of combinations of the Pauli matrices, that are the generators of the group $SU(2)$ in its fundamental representation, we can hypothesize that the symmetry group that characterizes the electroweak interactions is precisely the group $SU(2)_L$, where the index L refers to the fact that the weak interaction does not distinguish the particles constituting the left-handed doublets, and then the symmetry is referred to the invariance under rotations in the internal space of the left-handed doublets. Thus we suppose that the introduced doublets constitute the basic fields for the fundamental representation of $SU(2)_L$.

It is worth to note that the conserved Noether current associated to the third generator of $SU(2)$, i.e. the Pauli matrix σ_3 , is given by

$$J_\mu^3(x) = \sum_f \bar{\Psi}_f^L(x) \gamma_\mu \sigma_3 \Psi_f^L(x). \quad (1.10)$$

However, the current given by Eq. (1.10) does not coincide with the electromagnetic current introduced in Eq. (1.4), and thus the corresponding gauge field to which it would be coupled can not be interpreted as the photon field. The most simple way to introduce the electromagnetic field in the theory is to generalize the symmetry group through an abelian symmetry group

$$SU(2)_L \rightarrow SU(2)_L \otimes U(1)_Y.$$

At this point, we can proceed with the actual construction of the electroweak theory: for simplicity of notation, we suppose to have only a lepton family and that these are massless. The generalization to the case of more families and the inclusion of the quarks families is trivial, while to consider the fermion masses we have to introduce the Higgs mechanism. Denoting

$$\Psi_1(x) \equiv \begin{pmatrix} \psi_{\nu_l}(x) \\ \psi_l(x) \end{pmatrix}_L \quad \Psi_2(x) \equiv \psi_{\nu_l}^R(x) \quad \Psi_3(x) \equiv \psi_l^R(x), \quad (1.11)$$

the lagrangian describing the free leptons is a Dirac lagrangian that, in terms of the fields in Eq. (1.11), is written as

$$\begin{aligned} \mathcal{L}_0 &= \sum_{j=1}^3 i\bar{\Psi}_j(x) \gamma^\mu \partial_\mu \Psi_j(x) \\ &= i\bar{\psi}_{\nu_l}^L(x) \gamma^\mu \partial_\mu \psi_{\nu_l}^L(x) + i\bar{\psi}_l^L(x) \gamma^\mu \partial_\mu \psi_l^L(x) \\ &\quad + i\bar{\psi}_{\nu_l}^R(x) \gamma^\mu \partial_\mu \psi_{\nu_l}^R(x) + i\bar{\psi}_l^R(x) \gamma^\mu \partial_\mu \psi_l^R(x) \\ &= i\bar{\psi}_{\nu_l}(x) \gamma^\mu \partial_\mu \psi_{\nu_l}(x) + i\bar{\psi}_l(x) \gamma^\mu \partial_\mu \psi_l(x). \end{aligned} \quad (1.12)$$

The free lagrangian of Eq. (1.12) has a global internal symmetry associated with the transformations of the group $\mathcal{G} \equiv SU(2)_L \otimes U(1)_Y$, that is the set of simultaneous global transformations of the spinors:

$$\Psi_1(x) \xrightarrow{\mathcal{G}} \Psi'_1(x) = \exp(iY_1\beta) \exp\left(i\frac{\sigma_i}{2}\alpha^i\right) \Psi_1(x) \quad (1.13)$$

$$\Psi_2(x) \xrightarrow{\mathcal{G}} \Psi'_2(x) = \exp(iY_2\beta) \Psi_2(x) \quad (1.14)$$

$$\Psi_3(x) \xrightarrow{\mathcal{G}} \Psi'_3(x) = \exp(iY_3\beta) \Psi_3(x) \quad (1.15)$$

where the parameters $\alpha \equiv (\alpha_1, \alpha_2, \alpha_3)$ and β are the variables that define the particular transformation of the group \mathcal{G} . The generic phase transformation

$$U_L = \exp\left(i\frac{\sigma_i}{2}\alpha^i\right) \quad U_L \in SU(2)_L \quad (1.16)$$

identifies a *rotation in the internal space of the doublets of $SU(2)$* , that is the reason for which under the transformations of the group \mathcal{G} it acts only on the doublets $\Psi_i(x)$. The scalar Y_i is a quantum number that characterize a given field $\Psi_i(x)$, and it is known that as *weak hypercharge* because, similarly to the case of the electric charge, this quantum number is the conserved Noether charge associated to the symmetry $U(1)_Y$ of the weak interaction.

Having determined the symmetry group characterizing the electroweak interactions, according to the gauge principle we have to impose that the lagrangian \mathcal{L}_0 given in Eq. (1.12) is invariant under the local transformation of the group symmetry \mathcal{G} . To implement this, as we know, we have to introduce a number of gauge field commensurate to the number of the generators of the group \mathcal{G} , and substitute to the usual derivatives the corresponding *covariant derivatives* [7, 16], defined through the introduced gauge fields:

$$D_\mu \Psi_1(x) = [\partial_\mu + ig\bar{W}_\mu(x) + ig'Y_1B_\mu(x)] \Psi_1(x) \quad (1.17)$$

$$D_\mu \Psi_2(x) = [\partial_\mu + ig'Y_2B_\mu(x)] \Psi_2(x) \quad (1.18)$$

$$D_\mu \Psi_3(x) = [\partial_\mu + ig'Y_3B_\mu(x)] \Psi_3(x) \quad (1.19)$$

where the coupling constant g and g' associated to the groups $SU(2)$ and $U(1)$ respectively are introduced, and we denote

$$\bar{W}_\mu(x) = \frac{\sigma_a}{2} W_\mu^a(x). \quad (1.20)$$

To be the symmetry defined from the group \mathcal{G} a local symmetry, it must occur that after the transformation U_j of the spinor $\Psi_j(x)$ the covariant derivative $D_\mu \Psi_j(x)$ is transformed as $\Psi_j(x)$:

$$\Psi_j(x) \xrightarrow{\mathcal{G}} U_j \Psi_j(x) \quad \wedge \quad D_\mu \Psi_j(x) \xrightarrow{\mathcal{G}} U_j D_\mu \Psi_j(x). \quad (1.21)$$

The condition introduced in Eq. (1.21) impose, for the gauge field $B_\mu(x)$ and $\bar{W}_\mu(x)$, the following transformation laws [6, 7, 10]

$$B_\mu(x) \xrightarrow{\mathcal{G}} B'_\mu(x) = B_\mu(x) - \frac{1}{g'} \partial_\mu \beta(x) \quad (1.22)$$

$$\bar{W}_\mu(x) \xrightarrow{\mathcal{G}} \bar{W}'_\mu(x) = U_L(x) \bar{W}_\mu(x) U_L^\dagger(x) + \frac{i}{g} [\partial_\mu U_L(x)] U_L^\dagger(x). \quad (1.23)$$

Substituting the covariant derivative defined in Eqs. (1.17), (1.18) and (1.19) to the usual derivative in the lagrangian \mathcal{L}_0 , we obtain the lagrangian

$$\begin{aligned} \mathcal{L} &= \sum_{j=1}^3 i \bar{\Psi}_j(x) \gamma^\mu D_\mu \Psi_j(x) \\ &= i \bar{\Psi}_1(x) \gamma^\mu [\partial_\mu + ig \bar{W}_\mu] \Psi_1(x) + \sum_{j=1}^3 i \bar{\Psi}_j(x) \gamma^\mu [\partial_\mu + ig' Y_j B_\mu] \Psi_j(x). \end{aligned} \quad (1.24)$$

To complete the lagrangian we have to insert the kinetic terms relative to the introduced gauge fields. To this end we define, according to the general prescription of the Yang-Mills theory, the tensors [6–8]:

$$B_{\mu\nu} = \partial_\mu B_\nu - \partial_\nu B_\mu, \quad (1.25)$$

$$W_{\mu\nu}^a = \partial_\mu W_\nu^a - \partial_\nu W_\mu^a - g f^{abc} W_\mu^b W_\nu^c. \quad (1.26)$$

Then the lagrangian that describes the free fields is:

$$\mathcal{L}_0^{tot} = \sum_{j=1}^3 i \bar{\Psi}_j(x) \gamma^\mu \partial_\mu \Psi_j(x) - \frac{1}{4} B_{\mu\nu} B^{\mu\nu} - \frac{1}{4} W_{\mu\nu}^a W_a^{\mu\nu}. \quad (1.27)$$

The interaction between the free fields is described by the *interaction lagrangian*:

$$\mathcal{L}_{int} = -g \bar{\Psi}_1(x) \gamma^\mu \bar{W}_\mu(x) \Psi_1(x) - g' B_\mu(x) \sum_{j=1}^3 Y_j \bar{\Psi}_j(x) \gamma^\mu \Psi_j(x). \quad (1.28)$$

In particular, using Eq. (1.20), we have

$$\bar{W}_\mu = \frac{1}{2} \begin{pmatrix} W_\mu^3 & W_\mu^1 - iW_\mu^2 \\ W_\mu^1 + iW_\mu^2 & -W_\mu^3 \end{pmatrix} = \frac{1}{2} \begin{pmatrix} W_\mu^3 & \sqrt{2} W_\mu^\dagger \\ \sqrt{2} W_\mu & -W_\mu^3 \end{pmatrix} \quad (1.29)$$

where we have introduced the bosonic field

$$W_\mu(x) = \frac{W_\mu^1(x) + iW_\mu^2(x)}{\sqrt{2}}. \quad (1.30)$$

Then, we obtain

$$\begin{aligned} &\bar{\Psi}_1 \gamma^\mu \bar{W}_\mu \Psi_1 \\ &= \frac{1}{\sqrt{2}} \left\{ \bar{\psi}_{\nu_l}^L \gamma^\mu W_\mu^\dagger \psi_l^L + \bar{\psi}_l^L \gamma^\mu W_\mu \psi_{\nu_l}^L \right\} + \frac{1}{2} \left\{ \bar{\psi}_{\nu_l}^L \gamma^\mu W_\mu^3 \psi_{\nu_l}^L - \bar{\psi}_l^L \gamma^\mu W_\mu^3 \psi_l^L \right\}. \end{aligned} \quad (1.31)$$

Since the weak interaction involving the charge currents provides the coupling of the charged bosons W^\pm with the left-handed fermions belonging to the same doublets, we can identify the field W_μ and his adjoint W_μ^\dagger as the bosonic fields of the vector bosons W^+ and W^- respectively, and then extrapolate for the interaction lagrangian (1.28) the part that describes the *weak coupling for the charged currents*:

$$\begin{aligned}\mathcal{L}_{CC} &= -\frac{g}{\sqrt{2}}\bar{\psi}_{\nu_l}^L(x)\gamma^\mu W_\mu^\dagger \psi_l^L(x) - \frac{g}{\sqrt{2}}\bar{\psi}_l^L(x)\gamma^\mu W_\mu \psi_{\nu_l}^L(x) \\ &= -\frac{g}{2\sqrt{2}}W_\mu^\dagger \bar{\psi}_{\nu_l}(x)\gamma^\mu(\mathbb{1} - \gamma_5)\psi_l(x) - \frac{g}{2\sqrt{2}}W_\mu \bar{\psi}_l(x)\gamma^\mu(\mathbb{1} - \gamma_5)\psi_{\nu_l}(x).\end{aligned}\quad (1.32)$$

The remaining part of the interaction lagrangian (1.28) describes the weak interactions with neutral currents, then the gauge fields $W_\mu^3(x)$ and $B_\mu(x)$ have to be related to the fields describing the bosons Z^0 and γ . However, it is worth to note that the gauge field $B_\mu(x)$, associated to the generator of the group $U(1)_Y$, can not be directly identified with the photon. In fact: i) the electromagnetic field couples with the left-handed and right-handed fermions in the same way, so that from Eq. (1.28) follows from the weak hypercharge Y_j have to be equal between them; ii) if we want to identify B_μ with the photonic field and then if we want to identify the second term of Eq. (1.28) with the interaction term of QED, then we have to impose that the constant factor of this term is the electric charge of the fermion. In conclusion, we have to impose the conditions:

$$Y_1 = Y_2 = Y_3 \quad g'Y_j = Q_j \quad \forall j.$$

Such conditions can not be satisfied at the same time, since the particles of the fermionic doublet would have the same electric charge. To remedy the problem, we introduce two vectorial field $A_\mu(x)$ and $Z_\mu(x)$ such that

$$\begin{pmatrix} W_\mu^3 \\ B_\mu \end{pmatrix} = \begin{pmatrix} \cos \theta_w & \sin \theta_w \\ -\sin \theta_w & \cos \theta_w \end{pmatrix} \begin{pmatrix} Z_\mu \\ A_\mu \end{pmatrix}, \quad (1.33)$$

where the introduced angle θ_w is known as *Weinberg angle* or electroweak mixing angle, because the vectorial fields $W_\mu^3(x)$ and $B_\mu(x)$ are related to the fields $A_\mu(x)$ and $Z_\mu(x)$ through of a rotation of an angle equal to an half of the Weinberg angle. The lagrangian describing the *weak coupling with neutral currents*, is then given by

$$\begin{aligned}\mathcal{L}_{NC} &= -\frac{g}{2}\bar{\Psi}_1(x)\gamma^\mu \sigma_3 \Psi_1(x)W_\mu^3(x) - g'B_\mu \sum_{j=1}^3 Y_j \bar{\Psi}_j(x)\gamma^\mu \Psi_j(x) \\ &= \left\{ -g \sin \theta_w \bar{\Psi}_1(x)\gamma^\mu \frac{\sigma_3}{2} \Psi_1(x) - g' \cos \theta_w \sum_{j=1}^3 \bar{\Psi}_j(x)\gamma^\mu Y_j \Psi_j(x) \right\} A_\mu(x) \\ &\quad + \left\{ -g \cos \theta_w \bar{\Psi}_1(x)\gamma^\mu \frac{\sigma_3}{2} \Psi_1(x) + g' \sin \theta_w \sum_{j=1}^3 \bar{\Psi}_j(x)\gamma^\mu Y_j \Psi_j(x) \right\} Z_\mu(x).\end{aligned}\quad (1.34)$$

At this point using the *Gell-Mann relation* [7, 18, 23]

$$Q = Y + T_3 \quad T_3 \equiv \frac{\sigma_3}{2} \quad (1.35)$$

we can identify the field $A_\mu(x)$ with the field that describes the photon if we impose

$$g \sin \theta_w = g' \cos \theta_w = e. \quad (1.36)$$

The relation (1.36) relates, through the Weinberg angle, the coupling constant of the weak and electromagnetic interactions, and thus states the *electroweak unification*. Using the aforementioned relation, we have:

$$\mathcal{L}_{NC} = \mathcal{L}_Z + \mathcal{L}_{QED},$$

i.e. the electroweak interaction lagrangian with neutral current has contributions from the interaction terms

$$\mathcal{L}_{QED} = -e A_\mu(x) \sum_{j=1}^3 Q_j \bar{\Psi}_j(x) \gamma^\mu \Psi_j(x) \quad (1.37)$$

$$\mathcal{L}_Z = -\frac{e}{2 \sin \theta_w \cos \theta_w} Z_\mu(x) [\bar{\psi}_{\nu_l} \gamma^\mu (v_\nu - a_\nu \gamma_5) \psi_{\nu_l} + \bar{\psi}_l \gamma^\mu (v_l - a_l \gamma_5) \psi_l] \quad (1.38)$$

where we have introduced the axial and vectorial coupling coefficients that depend from the Weinberg angle θ_w and, for a given Dirac field $\psi(x)$, from the eigenvalues t_3 of the third component of the isospin operator T_3 related to the eigenfunction $\psi(x)$

$$a = t_3 \quad v = t_3 - 2Q \sin^2 \theta_w. \quad (1.39)$$

The presence of such coefficients in Eq. (1.38) denotes, as just observed, that the Z^0 boson is coupled both to left-handed and to right-handed fermions, but with different weights. For instance, in the case of the neutrino $Q_\nu = 0 \Rightarrow a_\nu = v_\nu = 1/2$, and then the neutrino interaction with Z^0 can occur only through its left-handed component. Moreover, having no charge, a possible right-handed component of the neutrino can not interact with other particles not even through electromagnetic interaction. Finally, using Eqs. (1.25), (1.26), (1.30), (1.33) and (1.36), we obtain the Yang-Mills lagrangian which describes the free gauge fields and their self-interactions:

$$\begin{aligned} \mathcal{L}_{YM} &= -\frac{1}{4} B_{\mu\nu} B^{\mu\nu} - \frac{1}{4} W_{\mu\nu}^i W_i^{\mu\nu} \\ &= -\frac{1}{4} F_{\mu\nu} F^{\mu\nu} - \frac{1}{4} Z_{\mu\nu} Z^{\mu\nu} - \frac{1}{4} (W_{\mu\nu}^+ W_-^{\mu\nu} + W_{\mu\nu}^- W_+^{\mu\nu}) \\ &\quad + ie (W_{\mu\nu}^+ W_-^\mu A^\nu - W_{\mu\nu}^- W_+^\mu A^\nu + F_{\mu\nu} W_+^\mu W_-^\nu) \\ &\quad + ie \cot \theta_w (W_{\mu\nu}^+ W_-^\mu Z^\nu - W_{\mu\nu}^- W_+^\mu Z^\nu + Z_{\mu\nu} W_+^\mu W_-^\nu) \\ &\quad - e^2 \cot \theta_w (2W_\mu^- W_+^\mu Z_\nu A^\nu - W_\mu^- Z^\mu W_\nu^+ A^\nu - W_\mu^- A^\mu W_\nu^- Z^\nu) \\ &\quad - e^2 (W_\mu^- W_+^\mu A_\nu A^\nu - W_\mu^- A^\mu W_\nu^+ A^\nu) \\ &\quad - e^2 \cot^2 \theta_w (W_\mu^- W_+^\mu Z_\nu Z^\nu - W_\mu^- Z^\mu W_\nu^+ Z^\nu) \\ &\quad - \frac{e^2}{2 \sin^2 \theta_w} (W_\mu^- W_+^\mu W_\nu^- W_+^\nu + W_\mu^- W_-^\mu W_\nu^+ W_+^\nu), \end{aligned} \quad (1.40)$$

where we have defined the fields $W_\mu^+(x) \equiv W_\mu(x)$ and $W_\mu^-(x) \equiv W_\mu^\dagger(x)$, and we have introduced the tensors

$$\begin{aligned} F_{\mu\nu} &= \partial_\mu A_\nu - \partial_\nu A_\mu, & W_{\mu\nu}^+ &= \partial_\mu W_\nu^+ - \partial_\nu W_\mu^+, \\ Z_{\mu\nu} &= \partial_\mu Z_\nu - \partial_\nu Z_\mu, & W_{\mu\nu}^- &= \partial_\mu W_\nu^- - \partial_\nu W_\mu^-. \end{aligned}$$

This lagrangian, as prescribed from the Yang-Mills theory for the system with non-abelian symmetry, contains self-interaction terms between the fields of the gauge theory, i.e. the symmetry group $SU(2) \otimes U(1)$ does not give rise to any vertex with only the photon and Z^0 boson fields. The Yang-Mills lagrangian obtained in Eq. (1.40) describes the free gauge fields, but it presents a problem: gauge bosons that emerge from the theory are massless, since there are no terms of the kind $m^2 A_\mu^a A_\mu^a$. As is well known, the photon is a massless particle, but the W^\pm and Z^0 bosons, on the contrary, are extremely massive. However, the mass terms can not be directly added in the Yang-Mills lagrangian, since we would have an explicitly break of the gauge symmetry that we impose. Similarly, we can not consider an explicit fermionic mass term:

$$\mathcal{L}_m = -m\bar{\psi}\psi = -m(\bar{\psi}_L\psi_R + \bar{\psi}_R\psi_L).$$

Such a term is not allowed as it would break the chiral symmetry, reason for which we have supposed in the free lagrangian (1.12) that the fermions are massless. The solution to the mass problem lies in the *Higgs mechanism* [6–11, 26, 27].

1.3 The Higgs mechanism

1.3.1 Spontaneous breaking of the symmetry and Goldstone theorem

To understand how the gauge bosons acquires mass we have to introduce the *spontaneous symmetry breaking*. To this end we analyze the physical system described by a lagrangian that involves a set of N real scalar fields (from now on, if not strictly needed, we will use the convention to imply the sum over repeated Roman indices):

$$\mathcal{L} = \frac{1}{2}\partial_\mu\phi_i\partial^\mu\phi_i - \frac{1}{2}m^2\phi_i^2 - \frac{\lambda}{4}(\phi_i^2)^2. \quad (1.41)$$

This lagrangian has a continuous symmetry associated with the group $O(N)$, i.e. it is invariant under rotations in the hyperplane (ϕ_1, \dots, ϕ_N) :

$$\phi_i \rightarrow \phi'_i = R_{ij}\phi_j \quad R \in O(N).$$

We analyze the potential:

$$V(\phi) = \frac{1}{2}m^2\phi_i^2 + \frac{\lambda}{4}(\phi_i^2)^2. \quad (1.42)$$

To study the stationary points of the potential $V(\phi)$ and establish what is the absolute minimum, i.e. the ground state of the system, it is necessary to distinguish two cases:

- $m^2 > 0$: in this case the potential has a single minimum in $\Phi \equiv (0, 0, \dots, 0)$.
- $m^2 < 0$: if this condition is implemented, the potential $V(\phi)$ has a maximum in $\Phi \equiv (0, 0, \dots, 0)$, while the minima of the potential are given by the equation

$$\frac{\partial V}{\partial \phi_i} = \phi_i \left(m^2 + \lambda \sum_{j=1}^N \phi_j^2 \right) = 0 \quad \Rightarrow \quad \sum_{i=1}^N \phi_i^2 = -\frac{m^2}{\lambda}. \quad (1.43)$$

This relation describes a ring of minima in the hyperplane (ϕ_1, \dots, ϕ_N) , and then shows that the ground state of the system is degenerate, i.e. there are *infinite configurations that minimize the potential*: the choice of one of this configurations give rise to a *spontaneous symmetry breaking* (SSB), as the symmetry characterizing the lagrangian is not shared by the lowest energy state.

However, Eq. (1.43) determines only the length of the vector Φ_0 which identifies the minimum, but its direction is arbitrary. Conventionally, we choose the minimum so that it points to the N -th direction:

$$\Phi_0 \equiv (0, 0, \dots, 0, v) \quad v = \sqrt{-\frac{m^2}{\lambda}}. \quad (1.44)$$

Then we define $\sigma(x)$ and $\pi_k(x)$ expanding the field $\Phi(x) \equiv (\phi_1(x), \dots, \phi_N(x))$ around the minimum (1.44), i.e. they are the fields measuring the deviations of $\Phi(x)$ respect to the equilibrium ground state configuration $\Phi(x) = \Phi_0$:

$$\Phi(x) \equiv (\pi_1(x), \pi_2(x), \dots, \pi_{N-1}(x), v + \sigma(x)). \quad (1.45)$$

Substituting in Eq. (1.41) we obtain

$$\begin{aligned} \mathcal{L} = & \frac{1}{2} \partial_\mu \pi_k(x) \partial^\mu \pi_k(x) + \frac{1}{2} \partial_\mu \sigma(x) \partial^\mu \sigma(x) - \frac{1}{2} (-2m^2) \sigma^2(x) - \sqrt{-\lambda m^2} \sigma^3(x) \\ & - \left(\sqrt{-\lambda m^2} \pi_k^2(x) \sigma(x) + \frac{\lambda}{4} \sigma^4(x) + \frac{\lambda}{2} \pi_k^2(x) \sigma^2(x) + \frac{\lambda}{4} \pi_k^4(x) \right), \end{aligned} \quad (1.46)$$

where we have omitted constant term which is irrelevant. The Eqs. (1.41) and (1.46) are the same lagrangian density expressed in terms of different variables. Thus they are entirely equivalent and must lead to the same physical results.

Since by definition there are no particles in the vacuum, from Eqs. (1.44) and (1.45) we have that the *vacuum expectation value* (vev) of the field $\Phi(x)$ is given by:

$$\langle 0 | \Phi | 0 \rangle = |\Phi_0| = v. \quad (1.47)$$

This is the condition for spontaneous symmetry breaking in the quantized theory, analogous to Eq. (1.44) in the classical theory.

In Eq. (1.46) we have obtained a theory with a massive field $\sigma(x)$ and $N - 1$ massless fields: the $O(N)$ symmetry is broken and the new lagrangian has a residual $O(N - 1)$ symmetry. The massive field $\sigma(x)$ is associated to the radial oscillations of the field $\Phi(x)$ around the minimum Φ_0 (oscillations of the field along the direction in which the potential has non-zero second derivative), while the other $N - 1$ fields describe the tangential oscillations (oscillations that occur along the set of directions corresponding to a zero second derivative of the potential). These latter oscillations occur along the ring of minima, that is along the $N - 1$ -dimensional hypersurface where all the directions are equivalent: this correspond to the existence of the $O(N - 1)$ residual symmetry. It is worth to note that the difference between the number of initial and final independent continuous symmetries, i.e. the number of continuous symmetry spontaneously broken, is equal to $N - 1$ and then is equal to the number of massless fields $\pi_k(x)$. The appearance of massless particles in presence of the spontaneous breaking of a set of continuous symmetries is a general result known as *Goldstone theorem* [6–8, 28–30]: for each continuous symmetry spontaneously broken, the theory must predict a massless particle. The massless particles that emerge due to the SSB are known as *Goldstone bosons*.

1.3.2 Higgs mechanism. Spontaneous symmetry breaking of symmetry in the electroweak theory

The possibility to assign to the gauge bosons a mass term is related to the Higgs mechanism, which is originated by spontaneous symmetry breaking (SSB) of a system with a gauge symmetry [6–8]. In order to illustrate such a mechanism, we consider the general case of a physical system described by a set of N real scalar fields, whose lagrangian is characterized by a non-abelian symmetry gauge. Then the lagrangian is invariant under the fields transformations

$$\phi_i \rightarrow (\mathbb{1} - i\alpha_a t^a)_{ij} \phi_j$$

where the parameter α_a are the variables defining the transformation itself and t^a are the group generators of the lagrangian symmetry. In a Yang-Mills theory, the gauge principle impose that the global internal symmetry of the lagrangian is also a local symmetry. To this end we introduce the gauge fields A_μ^a and we perform the usual substitution

$$\partial_\mu \Phi \rightarrow D_\mu \Phi = (\partial_\mu + g T^a A_\mu^a) \Phi \quad \Phi \equiv (\phi_1, \dots, \phi_N) \quad (1.48)$$

where we have posed $T^a = -it^a$. Then, the kinetic term of the lagrangian becomes:

$$\frac{1}{2}(D_\mu \phi_i)^2 = \frac{1}{2}\partial_\mu \phi_i \partial^\mu \phi_i + g A_\mu^a (\partial^\mu \phi_i T_a^{ij} \phi_j) + \frac{1}{2}g^2 A_\mu^a A_b^\mu (T_a \Phi)_i (T^b \Phi)^i. \quad (1.49)$$

If the vev $\Phi_0 \equiv \langle 0|\Phi|0\rangle$ of the field Φ (that we remember is the classical value of the field minimizing the potential) is different from zero, then the ground state of the system is degenerate and to study the theory we have to choose a minimum of the potential and then study the oscillations around this minimum

$$\Phi(x) = \Phi_0 + \eta(x). \quad (1.50)$$

In particular the last term in Eq. (1.49) is quadratic in the gauge fields, then substituting Eq. (1.50) we obtain a sum of terms with the structure of mass terms for the gauge bosons:

$$\Delta\mathcal{L} = \frac{1}{2}m_{ab}^2[A_\mu(x)]^a[A^\mu(x)]^b \quad m_{ab}^2 = g^2(T_a\Phi_0)_i(T_b\Phi_0)^i. \quad (1.51)$$

The terms m_{ab} define the mass matrix, whose elements in the diagonal part are positive semi-definite

$$m_a^2 = g^2(T_a\Phi_0)^2 \geq 0. \quad (1.52)$$

Once fixed a , the quantity m_a^2 appears in the new lagrangian as a multiplicative factor in the term quadratic in the gauge field $A_\mu^a(x)$ that corresponds to the generator T^a , and then m_a can be interpreted as the mass of the gauge boson $A_\mu^a(x)$. This latter result summarize the *Higgs mechanism* [26, 27]. Finally, it is worth to note that in general the Higgs mechanism is such that all the gauge bosons of the theory acquires a mass, but if one of the generators \bar{T} of the symmetry group leaves the ground state unchanged, then

$$\Phi_0 \rightarrow \Phi'_0 = (\mathbb{1} + \alpha\bar{T})\Phi_0 \equiv \Phi_0 \Rightarrow \bar{T}\Phi_0 = 0 \Rightarrow \bar{m} = 0, \quad (1.53)$$

that is the gauge boson corresponding to the generator \bar{T} remains massless. Starting from these general results, we see how to apply the Higgs mechanism to the electroweak theory, in such a way to obtain mass terms for the gauge bosons that mediate the weak interaction, and then the correct description of the Weinberg, Salam and Glashow theory [26, 27, 31–33].

We introduce in the electroweak interaction the new term

$$\mathcal{L} = (D_\mu\Phi)^\dagger(D^\mu\Phi) - V(\Phi) \quad V(\Phi) = m^2\Phi^\dagger\Phi + \lambda(\Phi^\dagger\Phi)^2. \quad (1.54)$$

Since we want to break the $SU(2)$ symmetry, the field $\Phi(x)$ in Eq. (1.54) is a doublet of complex scalar fields:

$$\Phi \equiv \begin{pmatrix} \phi^+ \\ \phi^0 \end{pmatrix}. \quad (1.55)$$

If we assign hypercharge $Y = 1/2$ to the field $\Phi(x)$, then it follows from Eq. (1.35) that the lower component ϕ^0 is a neutral complex scalar field, while the upper component ϕ^+ is a charged complex scalar field. The scalar lagrangian \mathcal{L} introduced in Eq. (1.54) is by construction invariant for gauge transformation associated to the

group symmetry $SU(2) \otimes U(1)$ and in particular a possible choice for the generators of this group is:

$$\sigma_1 \quad \sigma_2 \quad \frac{\mathbb{1} - \sigma_3}{2} \quad \frac{\mathbb{1} + \sigma_3}{2}.$$

Minimizing the potential $V(\Phi)$ respect to the doublet Φ we obtain the condition

$$\langle 0|\Phi|0\rangle^2 = \Phi_0^\dagger \Phi_0 \equiv |\phi^0|^2 + |\phi^+|^2 = -\frac{m^2}{2\lambda}. \quad (1.56)$$

This relation defines a set of infinitely many minimum states and, taking into account the physics request that the vacuum charge is zero, Eq. (1.56) can be written in terms of two conditions for the complex scalars fields that constitute the doublets Φ :

$$|\phi^0|^2 = -\frac{m^2}{2\lambda} \equiv \frac{v^2}{2} \quad |\phi^+|^2 = 0. \quad (1.57)$$

In order to study the theory, we carry the following choice of vacuum state

$$\Phi_0 = \frac{1}{\sqrt{2}} \begin{pmatrix} 0 \\ v \end{pmatrix}, \quad (1.58)$$

so that the SSB occurs only in the electrically neutral component of the field $\Phi(x)$, and charge conservation holds exactly. In general, Φ_0 in (1.58) is not invariant under $SU(2) \otimes U(1)$ gauge transformations, but it is invariant under $U(1)$ electromagnetic gauge transformations, in order to ensure zero mass for the photon and conservation of the electric charge.

We observe that a linear combination of the generators σ_1 , σ_2 , $\frac{\mathbb{1} - \sigma_3}{2}$ if applied to the chosen minimum state Φ_0 gives a contribution different from zero, while the action of the remaining generator on Φ_0 gives zero contribution

$$\begin{cases} T\Phi_0 \neq 0 & \text{if } T = a\sigma_1 + b\sigma_2 + c\frac{\mathbb{1} - \sigma_3}{2} \\ T\Phi_0 = 0 & \text{if } T = \frac{\mathbb{1} + \sigma_3}{2} \end{cases}.$$

As we have seen, this implies that the theory has three massive gauge boson and a massless gauge boson. Having made these observations, we have to proceed with the determination of the masses of the gauge bosons W^\pm and Z^0 : to this end, it is necessary to study the oscillations of the field $\Phi(x)$ around the chosen minimum state Φ_0 in (1.58)

$$\Phi(x) = \frac{1}{\sqrt{2}} \begin{pmatrix} 0 \\ v + H(x) \end{pmatrix} \exp \left\{ i \frac{\sigma_i}{2} \theta^i(x) \right\} \quad (1.59)$$

where the new scalar field $H(x)$ is the *Higgs field*. To study the oscillations $H(x)$ around Φ_0 , the expression in Eq. (1.59) have to be substituted in the lagrangian in Eq. (1.54) and, to this end, is useful to carry out the gauge choice fixed by the

condition $\theta(x) = 0$, called *unitary gauge*. We start with the study of the kinetic term of the lagrangian: the covariant derivative $D_\mu \Phi$ in Eq. (1.54) is constructed through the gauge fields W_μ^i and B_μ associated to the symmetry group $SU(2) \otimes U(1)$ of the lagrangian

$$D_\mu \Phi = \left\{ (\mathbb{1}_{2 \times 2}) \partial_\mu + ig \frac{\sigma_i}{2} W_\mu^i + ig' \hat{Y}_\Phi B_\mu \right\} \Phi \quad (1.60)$$

where we have introduced the hypercharge matrix \hat{Y}_Φ that is a diagonal matrix, whose eigenvalues are the hypercharges associated to the complex scalar fields ϕ^+ and ϕ^0

$$\hat{Y}_\Phi = \begin{pmatrix} Y_{\phi^+} & 0 \\ 0 & Y_{\phi^0} \end{pmatrix} = \frac{1}{2} \begin{pmatrix} 1 & 0 \\ 0 & 1 \end{pmatrix}. \quad (1.61)$$

The covariant derivative, written in terms of the doublet Φ in Eq. (1.59) and of the fields $W_\mu^+ \equiv W_\mu$ and $W_\mu^- \equiv W_\mu^\dagger$, becomes

$$D_\mu \Phi(x) = \frac{1}{\sqrt{2}} \begin{pmatrix} 0 \\ \partial_\mu H(x) \end{pmatrix} + \frac{i}{2\sqrt{2}} [v + H(x)] \begin{pmatrix} g\sqrt{2}W_\mu^+(x) \\ g'B_\mu(x) - gW_\mu^3(x) \end{pmatrix}. \quad (1.62)$$

Correspondingly, the kinetic term of the scalar lagrangian becomes

$$(D^\mu \Phi)^\dagger (D_\mu \Phi) = \frac{1}{2} \partial_\mu H \partial^\mu H + \frac{1}{4} (v + H)^2 \left\{ g^2 W_\mu^+ W_\mu^- + \frac{1}{2} (gW_\mu^3 - g'B_\mu)^2 \right\}. \quad (1.63)$$

Then, using the electroweak unification relation in Eq. (1.36), and the relation defining the photon and Z^0 boson fields in Eq. (1.33), we obtain

$$(D^\mu \Phi)^\dagger (D_\mu \Phi) = \frac{1}{2} \partial_\mu H \partial^\mu H + \frac{1}{4} g^2 (v + H)^2 \left\{ W_\mu^+ W_\mu^- + \frac{1}{2 \cos^2 \theta_w} Z_\mu Z^\mu \right\}. \quad (1.64)$$

Thus the mass terms for the gauge bosons come from the kinetic part $(D^\mu \Phi)^\dagger (D_\mu \Phi)$ of the lagrangian in Eq. (1.54), and in particular we obtain:

$$W_\mu^\pm = \frac{1}{\sqrt{2}} (W_\mu^1 \mp iW_\mu^2) \quad \rightarrow \quad m_W = \frac{gv}{2}, \quad (1.65)$$

$$A_\mu = \sin \theta_w W_\mu^3 + \cos \theta_w B_\mu \quad \rightarrow \quad m_\gamma = 0, \quad (1.66)$$

$$Z_\mu = \cos \theta_w W_\mu^3 - \sin \theta_w B_\mu \quad \rightarrow \quad m_Z = \frac{gv}{2 \cos \theta_w}. \quad (1.67)$$

It is worth to note as Eqs. (1.65) and (1.67) put in evidence that the masses of the W^\pm and Z^0 bosons are related:

$$m_W = m_Z \cos \theta_w = \frac{1}{2} vg. \quad (1.68)$$

Measuring the masses of the electroweak interaction mediators bosons is then possible to determine the *vacuum expectation value* v of the field Φ , and it results to be $v \sim 246$ GeV. Having analyzed the kinetic term, we can now study the *Higgs potential*, that is obtained expanding the potential $V(\Phi)$ that appears in the lagrangian (1.54) around its minimum Φ_0 :

$$V(\Phi) = m^2 \Phi^\dagger \Phi + \lambda (\Phi^\dagger \Phi)^2 = \frac{1}{2} m^2 [v + H(x)]^2 + \frac{\lambda}{4} [v + H(x)]^4 \Rightarrow$$

$$V(\Phi) = V(\Phi_0) + \frac{1}{2}m_H^2 H^2 + \lambda v H^3 + \frac{\lambda}{4}H^4 \quad (1.69)$$

where $V(\Phi_0) = \frac{\lambda}{4}v^4$ is the value of the potential corresponding of its minimum Φ_0 and $m_H^2 = 2\lambda v^2$ is the mass of the Higgs boson. We observe that the theory does not provides any prediction of the Higgs boson mass, but only on the scale of the SSB v , that is related to the Fermi constant. Taking into account Eqs. (1.64) and (1.69), the scalar lagrangian can be written as $\mathcal{L} = -\lambda/4 v^4 + \mathcal{L}_H + \mathcal{L}_{GH}$, where \mathcal{L}_H is the total lagrangian of the Higgs field, while \mathcal{L}_{GH} is the lagrangian that describes the coupling of the Higgs boson with the gauge bosons, and then contains the mass terms of the W^\pm and Z^0 bosons generated from the Higgs mechanism:

$$\mathcal{L}_H = \frac{1}{2}\partial_\mu H \partial^\mu H - \frac{1}{2}m_H^2 H^2 - \frac{m_H^2}{2v}H^3 - \frac{m_H^2}{8v^2}H^4, \quad (1.70)$$

$$\mathcal{L}_{GH} = m_W^2 W_\mu^- W_+^\mu \left\{ 1 + \frac{2}{v}H + \frac{1}{v^2}H^2 \right\} + \frac{1}{2}m_Z^2 Z_\mu Z^\mu \left\{ 1 + \frac{2}{v}H + \frac{1}{v^2}H^2 \right\}. \quad (1.71)$$

We observe that the interaction with the Higgs have the characteristic of being proportional to the square of the coupled gauge bosons mass. In particular, from Eqs. (1.70) and (1.71) we obtain the Higgs boson self-interaction vertices and the interaction vertices for the coupling with the W and Z gauge bosons that are used in the computation of the Feynman diagrams.

The last property that we have to develop is the introduction of a mechanism that gives mass to fermions: we add to the electroweak lagrangian a Yukawa term in which there is a coupling of the fermionic spinors with the Higgs doublet. If we consider only a family of quark and a leptonic family, we can write this lagrangian as:

$$\mathcal{L}_Y = -c_1(\bar{u}, \bar{d})_L \begin{pmatrix} \phi^+ \\ \phi^0 \end{pmatrix} d_R - c_2(\bar{u}, \bar{d})_L \begin{pmatrix} \phi^{0*} \\ -\phi^- \end{pmatrix} u_R - c_3(\bar{\nu}, \bar{e})_L \begin{pmatrix} \phi^+ \\ \phi^0 \end{pmatrix} e_R + \text{h.c.} \quad (1.72)$$

where in the second term is present the C -conjugated field to the Higgs scalar doublet, $\Phi^c \equiv i\sigma_2\Phi^*$. In the unitary gauge, after the SSB, this lagrangian assumes the simplest form

$$\mathcal{L}_Y = -\frac{1}{\sqrt{2}}(v + H) \{ c_1 \bar{d}d + c_2 \bar{u}u + c_3 \bar{e}e \}. \quad (1.73)$$

Then we note that the SSB generates also the fermion masses:

$$m_d = c_1 \frac{v}{\sqrt{2}} \quad m_u = c_2 \frac{v}{\sqrt{2}} \quad m_e = c_3 \frac{v}{\sqrt{2}}. \quad (1.74)$$

Since we does not know the parameters c_i , the values of the fermionic masses remain arbitrary. Moreover, from Eq. (1.73), we can obtain the interaction vertices of the coupling between the Higgs boson and fermions.

In Eq. (1.72) it could be present a term for the neutrinos similar to the second term, that however we do not add in the Yukawa lagrangian because in the Standard

Model the neutrinos are described as massless particles: the presence of such a term, in fact, would produce a coupling of neutrinos with the Higgs field and then the generation of a mass term. From the lagrangian (1.73) we note that the coupling of the Higgs field with fermions depends by the masses of these latter and, in particular, is linear in m_f . Finally, when we consider the other fermionic generations, in the case of quarks we have to consider also the flavour mixing, described by the Cabibbo-Kobayashi-Maskawa (CKM) matrix, due to the fact that the mass eigenstates do not coincide with the weak ones: in conclusion, this generates an electroweak current that provide decays of the quarks between flavours via W^\pm bosons (while this mixing is not possible with the decay Z^0 boson). Instead, when we consider more leptonic families, this phenomenon is not present, always for the hypothesis of the Standard Model for which the neutrinos are massless. Anyhow, for the scopes of this thesis, it is not in our interest to go further into the details of this topic.

Chapter 2

Quantum correction to the Higgs potential

The *spontaneous symmetry breaking* determines the vacuum expectation value of a scalar field ϕ at the classical level, simply minimizing the potential $V(\phi)$. However, if we consider the perturbative loop corrections, the classical vev is modified. One of the aim of this Chapter is to find, in a quantum field theory, a function whose minimum gives us the exact vev: obviously, at the lowest order, the results obtained from this function have to bring back to the classical case, which is modified to higher orders by quantum corrections. Supposedly, these corrections will require a renormalization procedure to remove infinities. The function that respects these properties is the *effective potential* [8, 9]. Then, we will compute the effective potential of the Standard Model to show how we have the formation of a second minimum respect to the electroweak one.

2.1 Effective potential in scalar theories

We consider for the moment the simplest case of a single real scalar field ϕ , and we suppose that an external source $J(x)$ coupled to the field ϕ is added to the lagrangian. Then the vacuum-vacuum amplitude is given by the *functional generator* [7]

$$Z[J] = \langle \Omega | e^{-i\hat{H}T} | \Omega \rangle = \mathcal{N} \int \mathcal{D}\phi \exp \left(i \int d^4x [\mathcal{L}(\phi) + J(x)\phi(x)] \right), \quad (2.1)$$

where $|\Omega\rangle$ is the quantum vacuum state, while T is the time interval on which the functional integral is computed: in fact, the right hand side of Eq. (2.1) is precisely the path integral representation of the vacuum-vacuum amplitude in the presence of the source J . Instead \mathcal{N} is a normalization factor: being \mathcal{N} irrelevant for the computations of this paragraph, for the moment we put $\mathcal{N} = 1$ and we will restore it later. We define the functional $W[J]$ as

$$W[J] \equiv -i \ln Z[J]. \quad (2.2)$$

Expanding the amplitude in Eq. (2.1) in terms of the Hamiltonian eigenstates, and performing the Wick rotation (i.e. going to the euclidean signature) $\tau = it$, we can compute the limit $T \rightarrow \infty$ to obtain:

$$Z[J] = \langle \Omega | e^{-i\hat{H}T} | \Omega \rangle = \sum_n e^{-E_n T} |\langle n | \Omega \rangle|^2 \xrightarrow[T \rightarrow \infty]{} e^{-E_0 T} |\langle 0 | \Omega \rangle|^2.$$

Thus, going back to the minkowskian signature, and comparing the expression for $Z[J]$ obtained from Eq. (2.2), we have:

$$e^{-iE_0 T} = e^{iW[J]} \Rightarrow E_0[J] = -\frac{1}{T} W[J],$$

i.e. the functional $W[J]$ can be interpreted as the vacuum energy in the presence of the source $J(x)$ in the time interval T . In particular, for $J = 0$ we have the vacuum energy of the original theory [34]. We consider the functional derivative of $W[J]$ respect to $J(x)$

$$\frac{\delta W[J]}{\delta J(x)} = -\frac{i}{Z[J]} \frac{\delta Z[J]}{\delta J(x)} = \frac{\int \mathcal{D}\phi \phi(x) \exp[i \int (\mathcal{L} + J\phi)]}{\int \mathcal{D}\phi \exp[i \int (\mathcal{L} + J\phi)]} = \frac{\langle \Omega | \phi(x) | \Omega \rangle_J}{\langle \Omega | \Omega \rangle_J}, \quad (2.3)$$

where the subscript J denotes the presence of the external source. Setting $J = 0$ in Eq. (2.3), we obtain the one-point Green function, that is the vacuum expectation value of the field ϕ in the original theory:

$$\left. \frac{\delta W[J]}{\delta J(x)} \right|_{J=0} = \langle \phi(x) \rangle. \quad (2.4)$$

Instead, computing the second functional derivative of $W[J]$ we have:

$$\begin{aligned} \frac{\delta^2 W[J]}{\delta J(x) \delta J(y)} &= -\frac{i}{Z[J]} \frac{\delta^2 Z[J]}{\delta J(x) \delta J(y)} + \frac{i}{Z[J]^2} \frac{\delta Z[J]}{\delta J(x)} \frac{\delta Z[J]}{\delta J(y)} \\ &= i \left(\frac{\langle \Omega | \phi(x) \phi(y) | \Omega \rangle_J}{\langle \Omega | \Omega \rangle_J} - \frac{\langle \Omega | \phi(x) | \Omega \rangle_J \langle \Omega | \phi(y) | \Omega \rangle_J}{\langle \Omega | \Omega \rangle_J^2} \right). \end{aligned} \quad (2.5)$$

Setting $J = 0$ in Eq. (2.5) we obtain the connected two-point Green function, that is the full propagator of the field ϕ :

$$\left. \frac{\delta^2 W[J]}{\delta J(x) \delta J(y)} \right|_{J=0} = i(\langle \phi(x) \phi(y) \rangle - \langle \phi(x) \rangle \langle \phi(y) \rangle) = i \langle \phi(x) \phi(y) \rangle_{conn} = i D(x, y). \quad (2.6)$$

Proceeding in a similar way with the higher derivatives, we obtain that $W[J]$ can be identified with the functional generator of the connected Green functions [34]:

$$\langle \phi(x_1) \dots \phi(x_n) \rangle_{conn} = (-i)^{n+1} \left. \frac{\delta^n W[J]}{\delta J(x_1) \dots \delta J(x_n)} \right|_{J=0}. \quad (2.7)$$

We define the *classical field* ϕ_c as the vacuum expectation value of the field $\phi(x)$ in the presence of the source $J(x)$: thus, for Eq. (2.3), the classical field is given by

$$\phi_c(x) = \frac{\delta W[J]}{\delta J(x)}. \quad (2.8)$$

Now we define the *effective action* functional [8, 9] as the Legendre transform of $W[J]$:

$$\Gamma[\phi_c] = W[J] - \int d^4x J(x)\phi_c(x). \quad (2.9)$$

Then we compute its functional derivative respect to $\phi_c(x)$:

$$\begin{aligned} \frac{\delta\Gamma[\phi_c]}{\delta\phi_c(x)} &= \frac{\delta W[J]}{\delta\phi_c(x)} - \int d^4y \frac{\delta J(y)}{\delta\phi_c(x)}\phi_c(y) - J(x) \\ &= \int d^4y \frac{\delta J(y)}{\delta\phi_c(x)} \frac{\delta W[J]}{\delta J(y)} - \int d^4y \frac{\delta J(y)}{\delta\phi_c(x)}\phi_c(y) - J(x) = -J(x) \quad \Rightarrow \\ \frac{\delta\Gamma[\phi_c]}{\delta\phi_c(x)} &= -J(x) \end{aligned} \quad (2.10)$$

where in the last step we used Eq. (2.8). If we now put $J = 0$, Eqs. (2.4) and (2.8) tell us that $\phi_c = \langle\phi\rangle$, so that we deduce that the vacuum expectation value $\langle\phi\rangle$ is a stationary point of the effective action $\Gamma[\phi_c]$: in fact, from Eq. (2.10) for $J = 0$ and $\phi_c = \langle\phi\rangle$ we obtain:

$$\left. \frac{\delta\Gamma[\phi_c]}{\delta\phi_c(x)} \right|_{\phi_c=\langle\phi\rangle} = 0. \quad (2.11)$$

We can find a physical meaning also for the second functional derivative of $\Gamma[\phi_c]$. In fact:

$$\begin{aligned} \int d^4z \frac{\delta^2 W[J]}{\delta J(x)\delta J(z)} \frac{\delta^2\Gamma[\phi_c]}{\delta\phi_c(z)\delta\phi_c(y)} &= \int d^4z \frac{\delta\phi_c(z)}{\delta J(x)} \frac{\delta^2\Gamma[\phi_c]}{\delta\phi_c(z)\delta\phi_c(y)} = \\ &= \frac{\delta^2\Gamma[\phi_c]}{\delta J(x)\delta\phi_c(y)} = -\frac{\delta J(y)}{\delta J(x)} = -\delta^{(4)}(x-y). \end{aligned} \quad (2.12)$$

From Eq. (2.6) we know that for $J = 0$, and then for $\phi_c = \langle\phi\rangle$, the second functional derivative of $W[J]$, $\delta^2 W[J]/\delta J(x)\delta J(z)$, is the connected two-point Green function, i.e. the full propagator $iD(x, y)$. As a consequence, Eq. (2.12) becomes

$$\int d^4z D(x, z) \left. \frac{\delta^2\Gamma[\phi_c]}{\delta\phi_c(z)\delta\phi_c(y)} \right|_{\phi_c=\langle\phi\rangle} = i\delta^{(4)}(x-y). \quad (2.13)$$

This means that the second functional derivative of the effective action is the inverse of the propagator, and can be identified as the 1PI two-point Green function [34]

$$\left. \frac{\delta^2\Gamma[\phi_c]}{\delta\phi_c(z)\delta\phi_c(y)} \right|_{\phi_c=\langle\phi\rangle} = iD^{-1}(x, y). \quad (2.14)$$

Proceeding in a similar way with the higher derivatives, we conclude that the effective action $\Gamma[\phi_c]$ can be interpreted as the functional generator of 1PI Green function:

$$\langle \phi(x_1) \dots \phi(x_n) \rangle_{1PI} = i \frac{\delta^n \Gamma[\phi_c]}{\delta \phi_c(x_1) \dots \delta \phi_c(x_n)} \Bigg|_{\phi_c = \langle \phi \rangle}. \quad (2.15)$$

At this point we introduce the *effective potential*: the general form of the effective action is given by the standard kinetic term with the square of the derivative of the field, times a non trivial factor, a term that does not depend on the derivatives of the field, and an infinite series of corrective terms with higher order derivatives. In other words, we can write the effective action as an expansion in powers of derivatives of ϕ_c (*gradient expansion*) [35]:

$$\Gamma[\phi_c] = \int d^4x \left[-V_{eff}[\phi_c] + \frac{1}{2}(\partial_\mu \phi_c)^2 Z_{eff}[\phi_c] + \dots \right]. \quad (2.16)$$

The functional V_{eff} introduced in (2.16) is called *effective potential*. Since we want the vacuum state is invariant under Poincaré transformations, then we consider only solutions for which the vev of the field ϕ , and then ϕ_c , is independent from x . Thus, considering $\phi_c = cost.$, all the terms containing derivatives of ϕ_c in Eq. (2.16) vanish and we have only the term V_{eff} , that is however independent from x . As a consequence, the integral over x gives simply the 4-dimensional volume factor VT . In conclusion

$$\Gamma[\phi_c] = -VT V_{eff}(\phi_c), \quad (2.17)$$

so that, thermodynamically speaking, the effective action is an extensive quantity. Moreover, the condition in Eq. (2.11) for which $\langle \phi(x) \rangle = \phi_c$ minimize $\Gamma[\phi_c]$ for $J = 0$, with Eq. (2.17) is reduced to

$$\frac{d}{d\phi_c} V_{eff}(\phi_c) = 0. \quad (2.18)$$

Every solution of Eq. (2.18) gives us the vev of the field ϕ in a vacuum state invariant under translations, and then from such a relation we deduce that the effective potential is precisely the function that we proposed to find.

In general, the effective potential $V_{eff}(\phi_c)$ can have more stationary points: a maximum corresponds to an unstable configuration of the system; an absolute minimum is the state of minimal energy, also called *true vacuum*, that is a stable minimum state; a relative minimum is a metastable vacuum state, also called *false vacuum*, that can decay towards the true vacuum state of the system through quantum tunneling. In particular, in a system with spontaneous symmetry breaking, the vacuum state is degenerate, and then the effective potential will be stationary respect to all the minimum states.

At this point, we consider the expansion of the effective action $\Gamma[\phi_c]$ in powers of the classical field ϕ_c :

$$\Gamma[\phi_c] = \sum_{n=1}^{\infty} \frac{1}{n!} \int d^4x_1 \dots d^4x_n \Gamma^{(n)}(x_1, \dots, x_n) \phi_c(x_1) \dots \phi_c(x_n). \quad (2.19)$$

The coefficients of the expansion $\Gamma^{(n)}(x_1, \dots, x_n)$, according to Eq. (2.15), are the 1PI n -point Green function. Now we consider the Fourier transform of the coefficients $\Gamma^{(n)}(x_1, \dots, x_n)$:

$$\begin{aligned} \Gamma^{(n)}(x_1, \dots, x_n) &= \int \frac{d^4k_1}{(2\pi)^4} \dots \frac{d^4k_n}{(2\pi)^4} (2\pi)^4 \delta(k_1 + \dots + k_n) \\ &\times \Gamma^{(n)}(k_1, \dots, k_n) e^{i(k_1 \cdot x_1 + \dots + k_n \cdot x_n)}. \end{aligned}$$

Inserting this expression in Eq. (2.19) and expanding the $\Gamma^{(n)}$ in powers of momenta, we obtain

$$\begin{aligned} \Gamma[\phi_c] &= \sum_{n=1}^{\infty} \frac{1}{n!} \int d^4x_1 \dots d^4x_n \int \frac{d^4k_1}{(2\pi)^4} \dots \frac{d^4k_n}{(2\pi)^4} \\ &\times \int d^4x e^{-i(k_1 + \dots + k_n) \cdot x} e^{i(k_1 \cdot x_1 + \dots + k_n \cdot x_n)} \\ &\times \left[\Gamma^{(n)}(0, 0, \dots, 0) \phi_c(x_1) \dots \phi_c(x_n) + \dots \right] \\ &= \int d^4x \sum_{n=1}^{\infty} \frac{1}{n!} \left[\Gamma^{(n)}(0, 0, \dots, 0) \phi_c^n(x) \right]. \end{aligned}$$

In the first step we have used the integral representation of the Dirac delta $\delta(k_1 + \dots + k_n)$. In the second step we have recombined the factors $e^{-ik_i x}$ and $e^{ik_i x}$ in such a way to obtain the delta $\delta(x_i - x)$ using the integrals over k_i . Finally with these Dirac deltas we have solved the integrals over x_i . The higher order terms in the expansion in powers of momenta contribute with derivatives of the field, and then vanishes if we consider ϕ_c constant. Comparing this expression with Eq. (2.17) we obtain

$$V_{eff}(\phi_c) = - \sum_{n=1}^{\infty} \frac{1}{n!} \phi_c^n \Gamma^{(n)}(k_i = 0), \quad (2.20)$$

i.e. V_{eff} is given by the sum of all the 1PI diagrams with zero external momenta. If these diagrams involve integrations over the internal momenta, then in general they will be divergent, but if the theory is renormalizable these divergences can be absorbed in the physical parameters.

For instance, we consider the scalar theory described by the lagrangian:

$$\mathcal{L} = \frac{1}{2} \partial_\mu \phi \partial^\mu \phi - \frac{1}{2} m^2 \phi^2 - \frac{\lambda}{4} \phi^4.$$

All the divergences have to be absorbed by a redefinition of m^2 and λ and by the normalization of the field. A typical definition of the renormalized mass of a scalar

field is

$$m_R^2 \equiv \left. \frac{d^2 V}{d\phi_c^2} \right|_{\phi_c=0} = -\Gamma^{(2)}(k_i = 0) \quad (2.21)$$

i.e. using Eq. (2.20), we can define it as the opposite of the inverse of the propagator with zero external momenta. Similarly, always using Eq. (2.20), we can define the renormalized coupling constant as the 4-point 1PI correlation function with zero external momenta

$$\lambda_R \equiv \left. \frac{d^4 V}{d\phi_c^4} \right|_{\phi_c=0} = -\Gamma^{(4)}(k_i = 0). \quad (2.22)$$

Finally, the definition of the normalization factor of the field is usually given by

$$\left. \frac{\partial \Gamma^{(2)}}{\partial p^2} \right|_{p^2=m^2} = 1 \quad (2.23)$$

that, through Eq. (2.17), gives $Z(\phi_c = 0) = 1$.

In conclusion, from Eq. (2.20) we see that to compute the effective potential V_{eff} we have to sum all the 1PI diagrams, and apply renormalization conditions to cure the divergences of these diagrams [35]. Afterwards, from the effective potential V_{eff} we can obtain the vevs as its stationary points, and then compute the minima of the potential itself.

2.1.1 Computation of the effective action

The effective action $\Gamma[\phi_c]$ contains all the information about the quantum dynamics of the theory, so that it is important to understand the systematics of its explicit computation: the first step is to compute the functional $Z[J]$, from which we obtain $W[J]$ through Eq. (2.2), and afterwards we apply the Legendre transform respect to $\phi_c(x)$ in Eq. (2.9) to find $\Gamma[\phi_c]$ [7, 34]. The starting point is the classical lagrangian, rewritten in terms of the renormalized field ϕ_r : this can be divided in a renormalized part \mathcal{L}_r including the physical parameter, and a part $\delta\mathcal{L}$ that contains the counterterms:

$$\mathcal{L}[\phi_r] = \mathcal{L}_r[\phi_r] + \delta\mathcal{L}[\phi_r]. \quad (2.24)$$

Introducing the external source J , this can be divided similarly into a renormalized term J_r and an additional counterterm δJ :

$$J(x) = J_r(x) + \delta J(x). \quad (2.25)$$

The term J_r is defined imposing the definition of ϕ_c at the lowest order in perturbation theory:

$$\left. \frac{\delta S_r[\phi_r]}{\delta \phi_r(x)} \right|_{\phi_r=\phi_c} + J_r(x) = 0, \quad (2.26)$$

i.e. is defined as the term of J such that the first variation of the renormalized action with the inclusion of the external source vanishes. Then, Eq. (2.26) is the Euler-Lagrange equation of the renormalized part of the theory modified through the introduction of the source term $J\phi$. Instead, the term δJ is fixed imposing the definition of ϕ_c order by order in perturbation theory, i.e. $\phi_c(x) = \langle \phi(x) \rangle_{J_r + \delta J}$. At this point, we proceed considering the functional $Z[J]$ in Eq. (2.1) and writing it in terms of the decomposition in Eqs. (2.24) and (2.25):

$$\begin{aligned} Z[J] &= \int \mathcal{D}\phi \exp \left\{ i \int d^4x \left(\mathcal{L}_r[\phi_r(x)] + J_r(x)\phi_r(x) \right. \right. \\ &\quad \left. \left. + \delta\mathcal{L}[\phi_r(x)] + \delta J(x)\phi_r(x) \right) \right\} \\ &\equiv \int \mathcal{D}\phi \exp \left\{ i \left(S_r[\phi_r] + J_r.\phi_r + \delta S[\phi_r] + \delta J.\phi_r \right) \right\} \end{aligned} \quad (2.27)$$

where we have introduced the notation:

$$J.\phi = \int d^4x J(x)\phi(x). \quad (2.28)$$

The lowest contribution at this path integral comes from the classical configuration of the field $\phi_c(x)$. We can evaluate these integrals using the steepest descent approximation (that corresponds to a loop expansion in powers of \hbar), writing

$$\phi_r(x) = \phi_c(x) + \eta(x). \quad (2.29)$$

Now we can expand the action in the path integral in powers of the fluctuation $\eta(x)$. Concerning the first two terms in Eq. (2.27), we have

$$\begin{aligned} S_r[\phi_r] + J_r.\phi_r &= \int d^4x \left(\mathcal{L}_r[\phi_r(x)] + J_r(x)\phi_r(x) \right) \\ &= \int d^4x \left(\mathcal{L}_r[\phi_c(x)] + J_r(x)\phi_c(x) \right) + \int d^4x \left(\frac{\delta S_r[\phi_r]}{\delta \phi_r(x)} \Big|_{\phi_r=\phi_c} + J_r(x) \right) \eta(x) \\ &\quad + \frac{1}{2} \int d^4x \int d^4y \eta(x) \frac{\delta^2 S_r[\phi_r]}{\delta \phi_r(x) \delta \phi_r(y)} \Big|_{\phi_r=\phi_c} \eta(y) + \dots . \end{aligned} \quad (2.30)$$

The term linear in η vanishes for Eq. (2.26) and then we have only:

$$\begin{aligned} S_r[\phi_r] + J_r.\phi_r &= S_r[\phi_c] + J_r.\phi_c \\ &\quad + \frac{1}{2} \int d^4x \int d^4y \eta(x) \frac{\delta^2 S_r[\phi_r]}{\delta \phi_r(x) \delta \phi_r(y)} \Big|_{\phi_r=\phi_c} \eta(y) + \text{interaction vertices in } \eta. \end{aligned} \quad (2.31)$$

Concerning the last two terms in the action, that represent the counterterms, expanding the field ϕ_r around ϕ_c we obtain:

$$\delta S[\phi_r] + \delta J.\phi_r = (\delta S[\phi_c] + \delta J.\phi_c) + (\delta S[\phi_c + \eta] - \delta S[\phi_c] + \delta J.\eta). \quad (2.32)$$

The second term in Eq.(2.32) can be expanded in powers of η : we obtain the counterterms that have to be included in the Feynman diagrams corresponding to the self-interaction vertices in η due to the cubic and higher order terms in Eq.(2.31). The first term is a constant respect to the integration over η and thus gives an additional term in the exponential coming from the first term in Eq.(2.31) [7]. Putting together these terms we arrive to the expression for the functional generator $Z[J]$.

The higher order terms, that is the self-interaction terms together with their counterterms, can be combined to give the exponential of a sum of connected diagrams: then a part for these terms the functional $Z[J]$ is given by

$$Z[J] = \exp \left\{ i \left(S_r[\phi_c] + J_r \cdot \phi_c + \delta S[\phi_c] + \delta J \cdot \phi_c \right) \right\} \\ \times \int \mathcal{D}\eta \exp \left\{ \frac{i}{2} \int d^4x d^4y \eta(x) \frac{\delta^2 S_r[\phi_r]}{\delta \phi_r(x) \delta \phi_r(y)} \Big|_{\phi_r=\phi_c} \eta(y) \right\} + \dots \quad (2.33)$$

The inverse of the operator that appears in the quadratic term in η defines a propagator for the field η , that is given by:

$$D(x, y) = -i \left(\frac{\delta^2 S_r[\phi_c]}{\delta \phi_r(x) \delta \phi_r(y)} \right)^{-1}. \quad (2.34)$$

The functional integral in η can be computed with the Gaussian integral:

$$\int \mathcal{D}\eta \exp \left\{ \frac{i}{2} \int d^4x d^4y \eta(x) \frac{\delta^2 S_r[\phi_r]}{\delta \phi_r(x) \delta \phi_r(y)} \Big|_{\phi_r=\phi_c} \eta(y) \right\} = \det \left(-S_r^{(2)}[\phi_c] \right)^{-\frac{1}{2}}, \quad (2.35)$$

where $S_r^{(2)}[\phi_c]$ is the operator whose components are the second derivative of $S[\phi]$ respect to $\phi(x)$ and $\phi(y)$:

$$\frac{\delta^2 S[\phi]}{\delta \phi(x) \delta \phi(y)} \equiv \langle y | S^{(2)}[\phi] | x \rangle. \quad (2.36)$$

At this point, we use Eq.(2.2) to obtain $W[J]$: in particular, if O is a generic operator, we know that $\ln(\det O) = \text{Tr}(\ln O)$. In conclusion we find:

$$W[J] = S_r[\phi_c] + J_r \cdot \phi_c + \frac{i}{2} \text{Tr} \ln \left(-S_r^{(2)}[\phi_c] \right) \\ + \delta S[\phi_c] + \delta J \cdot \phi_c - i(\text{sum of connected diagrams}). \quad (2.37)$$

Finally, using Eq.(2.9), we compute the Legendre transform to obtain the effective action $\Gamma[\phi_c]$: reminding of Eq.(2.25), we obtain that all the terms depending explicitly form the external source J are cancelled. In conclusion

$$\Gamma[\phi_c] = S_r[\phi_c] + \frac{i}{2} \text{Tr} \ln \left(-S_r^{(2)}[\phi_c] \right) \\ + \delta S[\phi_c] - i(\text{sum of connected diagrams}). \quad (2.38)$$

As we expected, the effective action depends explicitly only by ϕ_c . Moreover, it is given by the sum of the classical action (first and third term), a one-loop correction written in closed form (second term), and a infinite series of higher-loop correction that can be computed diagrammatically using the vertices and the propagator deduced for the field fluctuation η .

Equivalently it is possible to compute the effective action in terms of the bare quantities. Following a computation similar to those of Eq. (2.38) we have:

$$\Gamma[\phi_c] = S[\phi_c] + \frac{i}{2} \text{Tr} \ln \left(-S^{(2)}[\phi_c] \right) + \mathcal{O}(\hbar^2). \quad (2.39)$$

In particular, in the next paragraph we will use precisely Eq. (2.39) in order to see explicitly the introduction of counterterms in scalar theories. It is worth to note as the $\text{Tr} \ln$ terms both in Eqs. (2.38) and (2.39) are $\mathcal{O}(\hbar)$ once we restore the dimensions.

2.1.2 Effective action for Linear Sigma Model

Using Eq. (2.39) we have find a complete way to compute the effective action $\Gamma[\phi_c]$, although not very useful for practical purposes. To better understand the meaning of this expression, we now see how to compute explicitly $\Gamma[\phi_c]$ in the *linear sigma model*, in which we have a N -uplet of scalar field $\Phi = (\phi^1, \phi^2, \dots, \phi^N)$ [7]. The lagrangian is

$$\mathcal{L} = \frac{1}{2} (\partial_\mu \phi^i)^2 - \frac{1}{2} m^2 (\phi^i)^2 - \frac{\lambda}{4} [(\phi^i)^2]^2. \quad (2.40)$$

We expand around the classical field $\phi^i = \phi_c^i + \eta^i$. Since we expect to find a vacuum state invariant under translation, we limit ourselves to study the simple case in which the classical field ϕ_c is *constant*. This condition simplifies considerably our computation: in particular, according to Eq. (2.17), the final result will be proportional to the 4-dimensional volume VT . At this point, inserting in the expansion of the fields in Eq. (2.40), we obtain

$$\begin{aligned} \mathcal{L} = & -\frac{1}{2} m^2 (\phi_c^i)^2 - \frac{\lambda}{4} [(\phi_c^i)^2]^2 - (m^2 + \lambda(\phi_c^i)^2) \phi_c^i \eta^i \\ & + \frac{1}{2} (\partial_\mu \eta^i)^2 - \frac{1}{2} m^2 (\eta^i)^2 - \frac{\lambda}{2} [(\phi_c^i)^2 (\eta^i)^2 + 2(\phi_c^i \eta^i)^2] + \dots \end{aligned} \quad (2.41)$$

According to Eq. (2.38), we can ignore the linear term in η , while from the quadratic term in η we obtain

$$\left. \frac{\delta^2 S[\Phi_c]}{\delta \phi^i(x) \delta \phi^j(y)} \right|_{\phi=\phi_c} = \left(-\partial^2 \delta^{ij} - m^2 \delta^{ij} - \lambda [(\phi_c^i)^2 \delta^{ij} + 2\phi_c^i \phi_c^j] \right) \delta^{(4)}(x-y). \quad (2.42)$$

We note that the operator in Eq. (2.42) has the form of a Klein-Gordon operator. To clarify this relation, we orientate the coordinates in such a way that Φ_c points towards the N -th direction:

$$\Phi_c = (0, 0, \dots, 0, \phi_c). \quad (2.43)$$

Therefore, the operator in Eq. (2.42) is properly equal to the Klein-Gordon operator $(-\partial^2 - M_i(\phi_c)^2)$, where

$$M_i(\phi_c)^2 = \begin{cases} \lambda\phi_c^2 + m^2 & \text{acting on } \eta^1, \dots, \eta^{N-1} \\ 3\lambda\phi_c^2 + m^2 & \text{acting on } \eta^N \end{cases}. \quad (2.44)$$

The functional determinant in Eq. (2.35) is the product of the determinants of these Klein-Gordon operators:

$$\det(-S^{(2)}[\phi_c]) = [\det(\partial^2 + (\lambda\phi_c^2 + m^2))]^{N-1} [\det(\partial^2 + (3\lambda\phi_c^2 + m^2))]. \quad (2.45)$$

We have already seen that for a generic operator we can convert the determinant in a trace, so that

$$\ln \det(\partial^2 + \mu^2) = \text{Tr} \ln(\partial^2 + \mu^2).$$

Applying to Eq. (2.45) we have:

$$\ln \det(-S^{(2)}[\phi_c]) = \text{Tr} \ln(\partial^2 + (3\lambda\phi_c^2 + m^2)) + (N-1) \text{Tr} \ln(\partial^2 + (\lambda\phi_c^2 + m^2)). \quad (2.46)$$

Then we compute the traces of the operators in Eq. (2.46) as the sum of their eigenvalues. It is easy to show that, being the Klein-Gordon operator diagonal, the operator $\ln(\partial^2 + \mu^2)$ is also diagonal, so that:

$$\begin{aligned} \text{Tr} \ln(\partial^2 + \mu^2) &= \int d^4x \langle x | \ln(\partial^2 + \mu^2) | x \rangle \\ &= \int d^4x \int \frac{d^4k}{(2\pi)^4} \langle x | \ln(\partial^2 + \mu^2) | p \rangle \langle p | x \rangle \\ &= \int d^4x \int \frac{d^4k}{(2\pi)^4} e^{-ikx} \ln(\partial^2 + \mu^2) e^{ikx} \\ &= VT \int \frac{d^4k}{(2\pi)^4} \ln(-k^2 + \mu^2). \end{aligned} \quad (2.47)$$

In the last step, once we apply the operator to e^{ikx} , the two exponentials cancel each other, so that the integral over x gives the factor VT of 4-dimensional volume: we note that this is exactly the factor that we expect to appear from $\Gamma[\phi_c]$.

Now we want to restore again the normalization factor \mathcal{N} using appropriate boundary condition on $\Gamma[\phi_c]$. For instance, to see the connection between the effective potential that we will extract from Eq. (2.39) and the one given by Eq. (2.20), we can choose $\Gamma[0] = 0$ to obtain:

$$\mathcal{N} = \det(-S_r^{(2)}[0])^{\frac{1}{2}}, \quad (2.48)$$

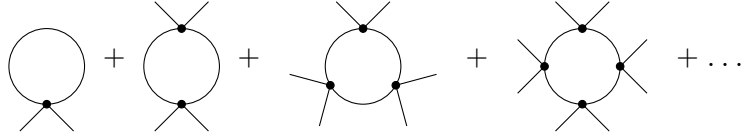
so that, in Eq. (2.39) we have the additional term $-\frac{i}{2} N \text{Tr} \ln(\partial^2 + m^2)$. Applying Eq. (2.47), we have:

$$\text{Tr} \ln(\partial^2 + M_i(\phi_c)^2) - \text{Tr} \ln(\partial^2 + m^2) = VT \int \frac{d^4k}{(2\pi)^4} \ln \left(\frac{-k^2 + M_i(\phi_c)^2}{-k^2 + m^2} \right). \quad (2.49)$$

In conclusion, from Eq.(2.39) with the additional term due to the normalization factor (2.48), we can extract the one-loop effective potential $V_{eff}(\phi_c)$ comparing the expression of $\Gamma[\phi]$ for ϕ_c constant with Eq.(2.17):

$$V_{eff}(\phi_c) = \frac{1}{2}m^2\phi_c^2 + \frac{1}{4}\lambda\phi_c^4 + \frac{i}{2} \int \frac{d^4k}{(2\pi)^4} \ln \left(\frac{-k^2 + m^2 + 3\lambda\phi_c^2}{-k^2 + m^2} \right) + (N-1)\frac{i}{2} \int \frac{d^4k}{(2\pi)^4} \ln \left(\frac{-k^2 + m^2 + \lambda\phi_c^2}{-k^2 + m^2} \right). \quad (2.50)$$

Obviously, the same result can be obtained from Eq.(2.20) where we have seen that the effective potential is given by the sum of the 1PI n -point Green function: in fact, up to the one-loop order $V_{eff}(\phi_c)$ is given by the tree level potential $V_0(\phi_c) = \frac{1}{2}m^2\phi_c^2 + \frac{1}{4}\lambda\phi_c^4$ with the resummation of the one-loop 1PI diagrams



so that, computing $i\Gamma^{(n)}(k_i = 0)$ with the usual Feynman rules, the resummation over n in (2.20) is the power expansion of logarithm, i.e. we obtain the last two terms in Eq.(2.50).

At this point, however, in order to simplify the computations of the loop integrals, it is convenient to normalize the effective action in a different way. In particular, we choose to normalize the effective action $\Gamma[\phi_c]$ to the massless theory one with a vacuum energy Ω . Then from the normalization factor \mathcal{N} we have an additional term $-N\frac{i}{2}\text{Tr}\ln(\partial^2) + \Omega$ in Eq.(2.39), where Ω is the bare vacuum energy constant that we have to renormalize together with the bare parameters m^2 and λ . With this choice of \mathcal{N} , instead of the expression in (2.50), for the effective potential we have:

$$V_{eff}(\phi_c) = \Omega + \frac{1}{2}m^2\phi_c^2 + \frac{1}{4}\lambda\phi_c^4 + \frac{i}{2} \int \frac{d^4k}{(2\pi)^4} \ln \left(1 - \frac{m^2 + 3\lambda\phi_c^2}{k^2} \right) + (N-1)\frac{i}{2} \int \frac{d^4k}{(2\pi)^4} \ln \left(1 - \frac{m^2 + \lambda\phi_c^2}{k^2} \right). \quad (2.51)$$

Then, we compute the following integral with momentum cut-off regularization after performing a Wick rotation:

$$\begin{aligned} \frac{i}{2} \int \frac{d^4k}{(2\pi)^4} \ln \left(1 - \frac{\mu^2}{k^2} \right) &= -\frac{1}{2} \int \frac{d^4k_E}{(2\pi)^4} \ln \left(1 + \frac{\mu^2}{k_E^2} \right) = -\frac{1}{32\pi^2} \int_0^{\Lambda^2} dk_E^2 \ln \left(1 + \frac{\mu^2}{k_E^2} \right) \\ &= -\frac{1}{32\pi^2} \left(\frac{(k_E^2)^2}{2} \ln \left(1 + \frac{\mu^2}{k_E^2} \right) \Big|_0^{\Lambda^2} + \frac{\mu^2}{2} \int_0^{\Lambda^2} dk_E^2 \frac{k_E^2}{k_E^2 + \mu^2} \right) \\ &= -\frac{1}{64\pi^2} \left[\Lambda^4 \ln \left(\frac{\Lambda^2 + \mu^2}{\Lambda^2} \right) + \mu^2 \Lambda^2 - (\mu^2)^2 \ln \left(\frac{\Lambda^2 + \mu^2}{\mu^2} \right) \right]. \end{aligned} \quad (2.52)$$

Expanding in powers of $m^2/\Lambda^2 \ll 1$, we obtain:

$$\frac{i}{2} \int \frac{d^4 k}{(2\pi)^4} \ln \left(1 - \frac{\mu^2}{k^2} \right) = -\frac{1}{64\pi^2} \left[2\mu^2 \Lambda^2 + (\mu^2)^2 \left(\ln \frac{\mu^2}{\Lambda^2} - \frac{1}{2} \right) \right] + \mathcal{O}(\Lambda^{-2}). \quad (2.53)$$

Now we want to express the effective potential in terms of the renormalized quantities. Then we write:

$$\begin{aligned} \Omega &= \Omega_R + \delta\Omega \\ m^2 &= m_R^2 + \delta m^2 \\ \lambda &= \lambda_R + \delta\lambda \end{aligned} \quad (2.54)$$

where $\delta\Omega$, δm^2 and $\delta\lambda$ are the counterterms that will absorb the divergent part of the effective potential and then are $\mathcal{O}(\hbar)$, as these comes from the $\mathcal{O}(\hbar)$ correction to the potential, i.e. the last two terms in (2.51). Then, if we insert the splitting in Eq. (2.54) in the effective potential, in the one-loop correction we can substitute simply m^2 and λ with m_R^2 and λ_R respectively, because the counterterms provide an $\mathcal{O}(\hbar^2)$ correction. Moreover, we can also choose $\Omega_R = 0$. Applying Eq. (2.53) to the effective potential, we can write:

$$\begin{aligned} V_{eff}(\phi_c) &= \frac{1}{2} m_R^2 \phi_c^2 + \frac{1}{4} \lambda_R \phi_c^4 + \delta\Omega + \frac{1}{2} \delta m^2 \phi_c^2 + \frac{1}{4} \delta\lambda \phi_c^4 \\ &+ \frac{1}{64\pi^2} \left[2(m_R^2 + 3\lambda_R \phi_c^2) \Lambda^2 + (m_R^2 + 3\lambda_R \phi_c^2)^2 \left(\ln \frac{m_R^2 + 3\lambda_R \phi_c^2}{\Lambda^2} - \frac{1}{2} \right) \right] \\ &+ \frac{N-1}{64\pi^2} \left[2(m_R^2 + \lambda_R \phi_c^2) \Lambda^2 + (m_R^2 + \lambda_R \phi_c^2)^2 \left(\ln \frac{m_R^2 + \lambda_R \phi_c^2}{\Lambda^2} - \frac{1}{2} \right) \right]. \end{aligned} \quad (2.55)$$

It is worth to note that this result is manifestly $O(N)$ symmetric: in fact Eq. (2.39) applied to the lagrangian in Eq. (2.40) is manifestly $O(N)$ invariant term by term. As a consequence, we had to arrive necessarily to a result for $V_{eff}(\phi_c)$ that is $O(N)$ invariant.

At this point, we have to apply renormalization conditions in order to determine the counterterms. We have seen in Eqs. (2.21), (2.22) and (2.23) a possible choice for the renormalization conditions at zero external momenta ($k_i = 0$). However, here we want to use a set of renormalization conditions with the introduction of an arbitrary scale μ . In particular, we require that the radiative correction to V_{eff} coming from the i -nth field vanish when $M_i(\phi_c)^2 = \mu^2$. It is easy to see that such property is implemented by the following renormalization conditions:

$$V_{eff}(\phi_c) \Big|_{\phi_c=0} = \frac{Nm_R^4}{64\pi^2} \ln \frac{m_R^2}{\mu^2}, \quad (2.56)$$

$$\frac{d^2 V_{eff}(\phi_c)}{d\phi_c^2} \Big|_{\phi_c=0} = m_R^2 + \frac{(N+2)\lambda_R m_R^2}{16\pi^2} \left(\ln \frac{m_R^2}{\mu^2} + \frac{1}{2} \right), \quad (2.57)$$

$$\frac{d^4 V_{eff}(\phi_c)}{d\phi_c^4} \Big|_{\phi_c=0} = 6 \left[\lambda_R + \frac{(N+8)\lambda_R^2}{16\pi^2} \left(\ln \frac{m_R^2}{\mu^2} + \frac{3}{2} \right) \right]. \quad (2.58)$$

Applying these renormalization conditions to Eq. (2.55), we obtain three equations for $\delta\Omega$, δm^2 and $\delta\lambda$:

$$\delta\Omega = -\frac{Nm_R^2\Lambda^2}{32\pi^2} + \frac{Nm_R^4}{64\pi^2} \left(\ln \frac{\Lambda^2}{\mu^2} + \frac{1}{2} \right), \quad (2.59)$$

$$\delta m^2 = -\frac{(N+2)\lambda_R\Lambda^2}{16\pi^2} + \frac{(N+2)\lambda_R m_R^2}{16\pi^2} \left(\ln \frac{\Lambda^2}{\mu^2} + \frac{1}{2} \right), \quad (2.60)$$

$$\delta\lambda = \frac{(N+8)\lambda_R^2}{16\pi^2} \left(\ln \frac{\Lambda^2}{\mu^2} + \frac{1}{2} \right). \quad (2.61)$$

From now on we will have only renormalized quantities, so that we will submit for notation simplicity the subscript R . Substituting Eqs. (2.59), (2.60) and (2.61) in Eq. (2.55) we obtain the renormalized effective potential:

$$\begin{aligned} V_{eff}(\phi_c) &= \frac{1}{2}m^2\phi_c^2 + \frac{1}{4}\lambda\phi_c^4 \\ &+ \frac{1}{64\pi^2} \left[(m^2 + 3\lambda\phi_c^2)^2 \ln \frac{m^2 + 3\lambda\phi_c^2}{\mu^2} \right. \\ &\left. + (N-1)(m^2 + \lambda\phi_c^2)^2 \ln \frac{m^2 + \lambda\phi_c^2}{\mu^2} \right]. \end{aligned} \quad (2.62)$$

Once we have obtained the expression of the effective potential in Eq. (2.62), as we know from Eq. (2.18), for every fixed value of m^2 , λ and μ we can determine the vacuum states of the system minimizing $V_{eff}(\phi_c)$ respect to ϕ_c .

The correction to $V(\phi)$ is not defined when the arguments of the logarithms become negative, but the minima of V_{eff} are located outside this region of values of ϕ_c [7, 35]. This problem is particularly clear in the limit $m^2 \rightarrow 0$: Eq. (2.62) acquires the form

$$V_{eff}(\phi_c) = \frac{1}{4}\phi_c^4 \left(\lambda + \frac{1}{4} \frac{\lambda^2}{(4\pi)^2} \phi_c^4 \left[(N+8) \left(\ln \frac{\lambda\phi_c^2}{\mu^2} - \frac{3}{2} \right) + 9\ln 3 \right] \right). \quad (2.63)$$

From this expression we can see that $V_{eff}(\phi_c)$ has a zero when ϕ_c is of order

$$\phi_c^2 \sim \frac{\mu^2}{\lambda} \exp \left[-\frac{(4\pi)^2}{(N+8)\lambda} \right]. \quad (2.64)$$

Near this point, we find a minimum corresponding to a non zero value of ϕ_c . However, this zero is present due to the "cancellation" of the term of lowest order quantum correction. In other words, the perturbation theory is completely "broken" before we can address the issue regarding a minimum of $V_{eff}(\phi_c)$ with $m^2 = 0$ due to SSB [7].

2.2 Standard Model one-loop effective potential

To compute the Higgs effective potential we have to extract the relevant part of the Standard Model lagrangian that we have seen in Chapter 1, i.e. the part containing

quadratic terms in the fields:

$$\begin{aligned}\mathcal{L} = & -\frac{1}{4}W_{\mu\nu}^a W_a^{\mu\nu} - \frac{1}{4}B_{\mu\nu} B^{\mu\nu} + (D_\mu \Phi)^\dagger (D^\mu \Phi) - m^2 \Phi^\dagger \Phi - \lambda (\Phi^\dagger \Phi)^2 \\ & - \frac{1}{2\xi} (\partial_\mu W_a^\mu)^2 - \frac{1}{2\xi} (\partial_\mu B^\mu)^2 + \mathcal{L}_{\text{ferm}} ,\end{aligned}\quad (2.65)$$

where the first two terms in the second line are the gauge fixing contribution, while $\mathcal{L}_{\text{ferm}}$ is the fermionic contribution that we will analyze in detail later. Moreover, the tensors $W_{\mu\nu}^a$ and $B_{\mu\nu}$ are given in (1.25) and (1.26), while Φ is the Higgs doublet in (1.55) and $D_\mu \Phi$ is given in (1.60).

2.2.1 Scalar contribution

We start with the computation of the contribution to the effective potential from the Higgs sector: it is worth to note that, if we write the scalar $SU(2)$ doublet explicitly

$$\Phi(x) = \begin{pmatrix} \frac{\phi_1 + i\phi_2}{\sqrt{2}} \\ \frac{\phi_3 + i\phi_4}{\sqrt{2}} \end{pmatrix} , \quad (2.66)$$

the tree level potential tree-level is

$$V(\Phi) = m^2 \Phi^\dagger \Phi + \lambda (\Phi^\dagger \Phi)^2 = \frac{1}{2} \mu^2 \phi_i^2 + \frac{\lambda}{4} (\phi_i^2)^2 \quad (2.67)$$

that is nothing but the Linear Sigma Model potential in Eq.(2.40) with $N = 4$, where we choose $\phi_3 \equiv H$ as the component of the doublet that acquires a non-zero classical value ϕ_c . Moreover, we want to renormalize the effective potential in such a way that the scalar radiative correction vanish for $M_i(\phi_c)^2 = \mu^2$ (with $M_i(\phi_c)^2$ given in (2.44)). Then, the scalar contributions to the counterterms are given in Eqs. (2.59)-(2.61), while the Higgs contribution to the renormalized effective potential is given by the first two lines of Eq. (2.62), and the Goldstone contributions are given by the third line with $N = 4$.

2.2.2 Gauge contribution

Once we choose $\phi_3 \equiv H$ in the doublet (2.66) as the only field that acquires a non-zero classical value ϕ_c , using Eqs. (1.33) and (1.36), we can write the relevant quadratic gauge part of Eq. (2.65) as:

$$\begin{aligned}\mathcal{L}_{\text{quadratic}} = & -\frac{1}{4} (W_{\mu\nu}^+ W_+^{\mu\nu} + W_{\mu\nu}^- W_-^{\mu\nu}) - \frac{1}{4} Z_{\mu\nu} Z^{\mu\nu} \\ & + \frac{1}{2} M_W(\phi_c)^2 (W_\mu^+ W_\mu^+ + W_\mu^- W_\mu^-) + \frac{1}{2} M_Z(\phi_c)^2 Z_\mu Z^\mu \\ & - \frac{1}{2\xi} [(\partial^\mu W_\mu^+)^2 + (\partial^\mu W_\mu^-)^2 + (\partial^\mu Z_\mu)^2] ,\end{aligned}\quad (2.68)$$

where the mass terms

$$M_W(\phi_c)^2 = \frac{1}{4}g^2\phi_c^2 \quad M_Z(\phi_c)^2 = \frac{1}{4}(g^2 + g'^2)\phi_c^2 \quad (2.69)$$

come from the kinetic part $D_\mu\Phi D^\mu\Phi$. Moreover, we will see that the contributions to the effective potential due to gauge bosons are of the form $M^4 \log M^2$ as for the scalar case, so that we have no contribution to the Higgs effective potential from the gauge field of the photon as $M_\gamma = 0$. This is the reason for which we do not include the photon kinetic term $-\frac{1}{4}F_{\mu\nu}F^{\mu\nu}$ in Eq. (2.68).

We start with the computation of the Z contribution. The first step is to rewrite the kinetic action:

$$\begin{aligned} S_{\text{kin}}[Z] &= -\frac{1}{4} \int d^4x Z^{\mu\nu} Z_{\mu\nu} = -\frac{1}{4} \int d^4x (\partial^\mu Z^\nu - \partial^\nu Z^\mu) (\partial_\mu Z_\nu - \partial_\nu Z_\mu) \\ &= -\frac{1}{2} \int d^4x (\partial^\mu Z^\nu \partial_\mu Z_\nu - \partial^\mu Z^\nu \partial_\nu Z_\mu). \end{aligned} \quad (2.70)$$

Then using the differentiation chain rule we have:

$$\partial^\mu Z^\nu \partial_\mu Z_\nu = \partial^\mu (Z^\nu \partial_\mu Z_\nu) - Z^\nu \partial^\mu \partial_\mu Z_\nu \quad (2.71)$$

$$\partial^\mu Z^\nu \partial_\nu Z_\mu = \partial^\mu (Z^\nu \partial_\nu Z_\mu) - Z^\nu \partial^\mu \partial_\nu Z_\mu \quad (2.72)$$

where the divergence terms in the integral give surface terms that vanish. Thus we write:

$$S_{\text{kin}}[Z] = \frac{1}{2} \int d^4x Z_\mu(x) (\partial^2 g^{\mu\nu} - \partial^\mu \partial^\nu) Z_\nu(x). \quad (2.73)$$

Then the action of the quadratic contribution can be written as:

$$\begin{aligned} S[Z] &= \frac{1}{2} \int d^4x Z_\mu(x) \left[\partial^2 g^{\mu\nu} - \left(1 - \frac{1}{\xi}\right) \partial^\mu \partial^\nu + g^{\mu\nu} M_Z(\phi_c)^2 \right] Z_\nu(x) \Rightarrow \\ S_{\mu\nu}^{(2)}[\phi_c] &= \partial^2 g_{\mu\nu} - \left(1 - \frac{1}{\xi}\right) \partial_\mu \partial_\nu + g_{\mu\nu} M_Z(\phi_c)^2. \end{aligned} \quad (2.74)$$

Since we want to compute the inverse operator $K_{\mu\nu}$ of $S_{\mu\nu}^{(2)}[Z]$, it is more convenient to write Eq. (2.74) in momentum space, so that we write the Fourier transform of the field $Z_\mu(x)$:

$$Z_\mu(x) = \int \frac{d^4k}{(2\pi)^4} Z_\mu(k) e^{-ikx}. \quad (2.75)$$

Then substituting in the action we obtain:

$$\begin{aligned} S[Z] &= \frac{1}{2} \int d^4x \int \frac{d^4k}{(2\pi)^4} Z_\mu(k) e^{-ikx} \\ &\times \left[\partial^2 g^{\mu\nu} - \left(1 - \frac{1}{\xi}\right) \partial^\mu \partial^\nu + g^{\mu\nu} M_Z(\phi_c)^2 \right] \int \frac{d^4k'}{(2\pi)^4} Z_\nu(k') e^{-ik'x} \\ &= \frac{1}{2} \int \frac{d^4k}{(2\pi)^4} \int \frac{d^4k'}{(2\pi)^4} Z_\mu(k) \\ &\times \left[-k^2 g^{\mu\nu} + \left(1 - \frac{1}{\xi}\right) k^\mu k^\nu + g^{\mu\nu} M_Z(\phi_c)^2 \right] Z_\nu(k') \int d^4x e^{-i(k+k')x}. \end{aligned} \quad (2.76)$$

We note that the integral over x gives $(2\pi)^4 \delta^{(4)}(k + k')$. In conclusion:

$$S[Z] = \frac{1}{2} \int \frac{d^4 k}{(2\pi)^4} Z_\mu(k) \left[-k^2 g^{\mu\nu} + \left(1 - \frac{1}{\xi}\right) k^\mu k^\nu + M_Z(\phi_c)^2 g^{\mu\nu} \right] Z_\nu(-k). \quad (2.77)$$

Then the operator (2.74) in momentum space is:

$$S_{\mu\nu}^{(2)}[\phi_c] = -k^2 g_{\mu\nu} + \left(1 - \frac{1}{\xi}\right) k_\mu k_\nu + M_Z(\phi_c)^2 g_{\mu\nu}. \quad (2.78)$$

The inverse operator $K_{\mu\nu}$ has the form

$$K_{\mu\nu} = A(k^2) g_{\mu\nu} + B(k^2) k_\mu k_\nu. \quad (2.79)$$

Using the condition $K^{\mu\rho} S_{\rho\nu}^{(2)}[Z] = \delta_\nu^\mu$, we can determine $A(k^2)$ and $B(k^2)$, so that:

$$K_{\mu\nu} = \frac{1}{k^2 - M_Z(\phi_c)^2} \left[-g_{\mu\nu} + (1 - \xi) \frac{k_\mu k_\nu}{k^2 - \xi M_Z(\phi_c)^2} \right]. \quad (2.80)$$

In the Landau gauge, for which $\xi = 0$, the numerator is the projector over the states satisfying the Lorentz condition:

$$P_{\mu\nu} = g_{\mu\nu} - \frac{k_\mu k_\nu}{k^2}. \quad (2.81)$$

With calculation similar to those seen in Section 2.1 for the scalar case, the one-loop contribution of the Z boson to $\Gamma[\phi_c]$ is given by $\frac{i}{2} \text{Tr} \ln \left(-S_{\mu\nu}^{(2)}[\phi_c] \right)$, that we want to write in terms of the operator $K_{\mu\nu}$ using the property of the logarithm:

$$\frac{i}{2} \text{Tr} \ln \left(-S_{\mu\nu}^{(2)}[\phi_c] \right) = -\frac{i}{2} \text{Tr} \ln (-K_{\mu\nu}), \quad (2.82)$$

where Tr denote also the trace over the Lorentz indices. We can exploit the following properties for an operator:

$$O = \sum_i \lambda_i \mathbb{P}_i \quad (2.83)$$

$$f(O) = \sum_i f(\lambda_i) \mathbb{P}_i \quad (2.84)$$

where λ_i are the eigenvalues of the matrix O and \mathbb{P}_i are the projectors over their relative eigenstate. In particular, considering the operator

$$O_{\mu\nu} = \int \frac{d^4 k}{(2\pi)^4} \frac{1}{k^2 - M_Z(\phi_c)^2} P_{\mu\nu} \quad (2.85)$$

it is clear from Eq. (2.83) that the (continuous) eigenvalues of $O_{\mu\nu}$ are $\frac{1}{k^2 - M_Z^2}$. Then, using Eq. (2.84)

$$\log(O_{\mu\nu}) = - \int \frac{d^4 k}{(2\pi)^4} \log(k^2 - M_Z(\phi_c)^2) P_{\mu\nu}. \quad (2.86)$$

We can express the trace over the continuum index k in Eq. (2.82) as an integral similarly to Eq. (2.47), and we can reduce the trace Tr over all the indices to a trace tr over only the Lorentz indices. In this way, we reduce the computation of Eq. (2.82) to the trace tr of an operator of the kind (2.86), so that:

$$\frac{i}{2} \text{Tr} \ln \left(-S_{\mu\nu}^{(2)}[\phi_c] \right) = \frac{i}{2} VT \int \frac{d^4 k}{(2\pi)^4} \log(k^2 - M_Z(\phi_c)^2) \text{tr} P_{\mu\nu}. \quad (2.87)$$

From Eq. (2.81) it is clear that $\text{tr} P_{\mu\nu} = 3$. Moreover, following Section 2.1.2, we normalize the effective action to the massless theory one, so that from \mathcal{N} we obtain the additional term $-\frac{i}{2} \text{Tr} \ln (\partial^2 g_{\mu\nu} - (1 - 1/\xi) \partial_\mu \partial_\nu)$. Clearly this term (in the Landau gauge) is equal to the right hand side of Eq. (2.87) with $M_Z(\phi_c)^2 = 0$. In conclusion, the radiative contribution to the Higgs effective potential coming from the Z boson is:

$$\tilde{V}_Z(\phi_c) = 3 \frac{i}{2} \int \frac{d^4 k}{(2\pi)^4} \log \left(1 - \frac{M_Z(\phi_c)^2}{k^2} \right). \quad (2.88)$$

Similarly we can compute the contribution of the W bosons, and it is easy to see that the result is given equal to Eq. (2.88) with the substitution $M_Z \rightarrow M_W$ and with a factor 2 that takes into account that there are two W bosons:

$$\tilde{V}_W(\phi_c) = 3i \int \frac{d^4 k}{(2\pi)^4} \log \left(1 - \frac{M_W(\phi_c)^2}{k^2} \right). \quad (2.89)$$

Using Eq. (2.53) we compute the integrals over k :

$$\tilde{V}_Z(\phi_c) = \frac{3}{64\pi^2} \left[2M_Z(\phi_c)^2 \Lambda^2 + (M_Z(\phi_c)^2)^2 \left(\ln \frac{M_Z(\phi_c)^2}{\Lambda^2} - \frac{1}{2} \right) \right], \quad (2.90)$$

$$\tilde{V}_W(\phi_c) = \frac{6}{64\pi^2} \left[2M_W(\phi_c)^2 \Lambda^2 + (M_W(\phi_c)^2)^2 \left(\ln \frac{M_W(\phi_c)^2}{\Lambda^2} - \frac{1}{2} \right) \right]. \quad (2.91)$$

In particular, as for the scalar contributions seen in Section 2.2.1, we require that the radiative contribution of the gauge boson Z to the effective potential vanishes when $M_Z(\phi_c)^2 = \mu^2$, and similarly for the gauge boson W when $M_W(\phi_c)^2 = \mu^2$. Then we cancel the divergences appearing in Eqs. (2.90) and (2.91) with the counterterms, considering additional terms in $\delta\Omega$, δm^2 and $\delta\lambda$ in order to take into account the gauge contributions. Finally, making explicit M_Z and M_W with Eqs. (2.69), the renormalized contributions to the Higgs potential coming from the gauge sector are:

$$V_Z(\phi_c) = \frac{3(g^2 + g'^2)^2 \phi_c^4}{1024\pi^2} \ln \frac{(g^2 + g'^2) \phi_c^2}{4\mu^2}, \quad (2.92)$$

$$V_W(\phi_c) = \frac{6g^4 \phi_c^4}{1024\pi^2} \ln \frac{g^2 \phi_c^2}{4\mu^2}. \quad (2.93)$$

2.2.3 Fermionic contribution

The fermionic contribution comes from the $\mathcal{L}_{\text{ferm}}$ in Eq. (2.65), that in principle contains for all the family of fermions (quarks and leptons) the corresponding kinetic

terms and the Yukawa term in Eq. (1.72). However, we will see that the fermionic contribution has again the form $M^4 \log M^2$, so that the dominant contribution comes from the quark top. Then the relevant fermionic contribution is:

$$\mathcal{L}_t = \bar{\psi}_a (\bar{i}\gamma^\mu \partial_\mu - M_t(\phi_c)) \psi_a, \quad (2.94)$$

where the mass term

$$M_t(\phi_c) = \frac{y_t}{\sqrt{2}} \phi_c \quad (2.95)$$

comes from the Yukawa term (1.72), using Eq. (2.66) for the Higgs doublet and choosing $\phi_3 \equiv H$ as the only field that acquires a non-zero classical value ϕ_c .

With calculation similar to those seen in Section 2.1 for the scalar case, the one-loop contribution of the top quark to $\Gamma[\phi_c]$ is given by

$$-\frac{i}{2} \text{Tr} \ln \left(-S_{ab}^{(2)}[\phi_c] \right) = -\frac{i}{2} \text{Tr} \ln \left[\delta_{ab} \left(-i\cancel{J} + M_t(\phi_c) \mathbb{1}_4 \right) \right], \quad (2.96)$$

where the minus sign overall comes from the anticommutation property of the top quark field $\psi(x)$. Then, proceeding as in Eq. (2.47):

$$-\frac{i}{2} \text{Tr} \ln \left(-S_{ab}^{(2)}[\phi_c] \right) = -\frac{i}{2} VT \text{tr} \int \frac{d^4 k}{(2\pi)^4} \ln \left[\delta_{ab} \left(-\cancel{k} + M_t(\phi_c) \mathbb{1}_4 \right) \right], \quad (2.97)$$

where here tr means the trace over the Lorentz indices and over the colour indices.

We use the fact that if O is diagonal, then also $f(O)$ is diagonal. In particular, the argument of the log is diagonal in the colour space due to δ_{ab} , so that:

$$\begin{aligned} \mathcal{T} \ln \left[\delta_{ab} \left(-\cancel{k} + M_t(\phi_c) \mathbb{1}_4 \right) \right] &= \mathcal{T} \left[\ln \left(-\cancel{k} + M_t(\phi_c) \mathbb{1}_4 \right) \delta_{ab} \right] \\ &= \ln \left(-\cancel{k} + M_t(\phi_c) \mathbb{1}_4 \right) \mathcal{T}(\delta_{ab}) = 3 \ln \left(-\cancel{k} + M_t(\phi_c) \mathbb{1}_4 \right), \end{aligned} \quad (2.98)$$

where \mathcal{T} means the trace over the colour indices and $\mathcal{T}(\delta_{ab}) = 3$. Then, from now on in this subsection tr means the trace over the Lorentz indices only. Moreover, using the property of the logarithm:

$$\begin{aligned} -\frac{i}{2} \text{Tr} \ln \left(-S_{ab}^{(2)}[\phi_c] \right) &= -3 \frac{i}{2} VT \text{tr} \int \frac{d^4 k}{(2\pi)^4} \ln \left(-\cancel{k} + M_t(\phi_c) \mathbb{1}_4 \right) \\ &= -3 \frac{i}{2} VT \text{tr} \int \frac{d^4 k}{(2\pi)^4} \left[\ln \left(-\cancel{k} + M_t(\phi_c) \mathbb{1}_4 \right) + \ln \left(\cancel{k} + M_t(\phi_c) \mathbb{1}_4 \right) \right] \\ &= -3 \frac{i}{2} VT \int \frac{d^4 k}{(2\pi)^4} \text{tr} \ln \left[\left(-k^2 + M_t(\phi_c)^2 \right) \mathbb{1}_4 \right], \end{aligned} \quad (2.99)$$

where in the last step we use $\cancel{k}^2 = k^2 \mathbb{1}_4$. The argument of the log is then diagonal also in the space of the Dirac matrices due to $\mathbb{1}_4$, and then:

$$\begin{aligned} \text{tr} \ln \left[\left(-k^2 + M_t(\phi_c)^2 \right) \mathbb{1}_4 \right] &= \text{tr} \left[\ln \left(-k^2 + M_t(\phi_c)^2 \right) \mathbb{1}_4 \right] \\ &= \ln \left(-k^2 + M_t(\phi_c)^2 \right) \text{tr}(\mathbb{1}_4) = 4 \ln \left(-k^2 + M_t(\phi_c)^2 \right), \end{aligned} \quad (2.100)$$

being $\text{tr}(\mathbb{1}_4) = 4$. In conclusion:

$$-\frac{i}{2}\text{Tr} \ln \left(-S_{ab}^{(2)}[\phi_c] \right) = -6i VT \int \frac{d^4 k}{(2\pi)^4} \ln \left(-k^2 + M_t(\phi_c)^2 \right). \quad (2.101)$$

Once we normalize the effective action to the massless theory one, as we done in the previous sections, from \mathcal{N} we obtain also the additional term $\frac{i}{2}\text{Tr} \ln (-i\mathcal{O})$, that is equal to Eq. (2.101) with $M_t(\phi_c) = 0$. In conclusion, the contribution to the Higgs effective potential of the quark top is:

$$\tilde{V}_t(\phi_c) = 6i \int \frac{d^4 k}{(2\pi)^4} \log \left(1 - \frac{M_t(\phi_c)^2}{k^2} \right). \quad (2.102)$$

Using Eq. (2.53) we compute the integral in k :

$$\tilde{V}_t(\phi_c) = \frac{12}{64\pi^2} \left[2M_t(\phi_c)^2 \Lambda^2 + (M_t(\phi_c)^2)^2 \left(\ln \frac{M_t(\phi_c)^2}{\Lambda^2} - \frac{1}{2} \right) \right], \quad (2.103)$$

and with Eq. (2.94) we explicit M_t . Requiring that this radiative contribution vanishes when $M_t(\phi_c)^2 = \mu^2$, we obtain the additional terms in the counterterms that take into account the quark top contribution. Finally, the renormalized contribution to the Higgs potential from the fermionic sector is:

$$V_t(\phi_c) = -\frac{3y_t^4 \phi_c^4}{64\pi^2} \ln \frac{y_t^2 \phi_c^2}{2\mu^2}. \quad (2.104)$$

2.3 Renormalization group improved effective Higgs potential

In conclusion, putting together the results of Eqs. (2.62), (2.93), (2.92) and (2.104) that give the one-loop effective potential correction to the classical Higgs potential Eq. (2.67) we get:

$$\begin{aligned} V_{eff}(\phi_c) &= V_0(\phi_c) + V_s(\phi_c) + V_g(\phi_c) + V_f(\phi_c) \\ &= \frac{1}{2}m^2 \phi_c^2 + \frac{\lambda}{4} \phi_c^4 \\ &+ \frac{(m^2 + 3\lambda\phi_c^2)^2}{64\pi^2} \ln \frac{m^2 + 3\lambda\phi_c^2}{\mu^2} + \frac{3(m^2 + \lambda\phi_c^2)^2}{64\pi^2} \ln \frac{m^2 + \lambda\phi_c^2}{\mu^2} \\ &+ \frac{6g^4 \phi_c^4}{1024\pi^2} \ln \frac{g^2 \phi_c^2}{4\mu^2} + \frac{3(g^2 + g'^2)^2 \phi_c^4}{1024\pi^2} \ln \frac{(g^2 + g'^2) \phi_c^2}{4\mu^2} \\ &- \frac{3y_t^4 \phi_c^4}{64\pi^2} \ln \frac{y_t^2 \phi_c^2}{2\mu^2}. \end{aligned} \quad (2.105)$$

The next step is the *Renormalization Group Improvement* (RGI) of the effective potential, that is an application of the renormalization group theory. We denote

with g_i a generic coupling constant of the Standard Model (despite of it is a scalar, gauge or Yukawa coupling). Being the loop expansion a coupling constants g_i power expansion, the n -loop effective potential will have terms of order g_i^{n+1} . Moreover, for every loop we have to consider a power of $\ln \phi_c^2/M^2$, such that the n -loop will have terms of the form

$$g_i^{n+1} \left(\ln \frac{\phi_c^2}{\mu^2} \right)^n.$$

Since we require that our expansion parameter is less than 1 in order for the perturbative expansion to be reliable, it is not sufficient to require that all the couplings be small, but that all the factor $g_i \ln(\phi_c^2/\mu^2)$ be small. In principle, it is always possible to choose μ in such a way that the logarithm is small, but it can only take a single value. If we are interested in the potential over a range from ϕ_1 and ϕ_2 , then we have to require that $g_i \ln(\phi_1^2/\phi_2^2)$ to be smaller than 1. However, in almost all the calculation in which the one-loop effective potential is needed, the region of field space over which we work is so large that $g_i \ln(\phi_1^2/\phi_2^2) \sim 1$. Then we need of a renormalization group improvement if we want that our loop expansion to remain valid. Such a potential generated with the renormalization group theory, is usually called *renormalization group improved effective potential* [36].

The renormalization scale μ in the expression of the effective potential (2.105) is arbitrary, and the effects of changing it can be absorbed into changes in the coupling constants and field, i.e. considering $g_i = g_i(\mu)$. The renormalization group equation for the effective potential is nothing but the statement that $V_{eff}(\phi_c)$ cannot be affected by the change in the arbitrary parameter μ :

$$\frac{dV}{d\mu} = 0. \quad (2.106)$$

Moreover, being the effective potential a function of the couplings g_i and of the field ϕ_c , we can explicit Eq. (2.106) using the chain rule, obtaining the *Callan-Symanzik equation*:

$$\left(\mu \frac{\partial}{\partial \mu} + \beta_{g_i} \frac{\partial}{\partial g_i} + m^2 \gamma_m \frac{\partial}{\partial m^2} + \phi_c \gamma \frac{\partial}{\partial \phi_c} \right) V_{eff}(\phi_c) = 0, \quad (2.107)$$

where we have defined

$$\beta_{g_i} = \mu \frac{dg_i(\mu)}{d\mu}. \quad (2.108)$$

The functions β_{g_i} are the *beta functions* that describe the changing of the couplings with the energy in a theory. We have also defined

$$\gamma \phi_c(\mu) = \mu \frac{d\phi_c(\mu)}{d\mu} \quad \gamma_m m^2(\mu) = \mu \frac{dm^2(\mu)}{d\mu} \quad (2.109)$$

where γ is called anomalous dimension. From Eq. (2.19) with $\phi_c = \text{const.}$ it is clear that computing the n -th derivative respect to ϕ_c of Eq. (2.107), it is reduced to the Callan-Symanzik equation for the 1PI Green's functions.

It is worth to note that the renormalization group equation is exact, and if we know β , γ e γ_m we can solve Eq. (2.107) exactly, and then if we known V_{eff} at a given value of ϕ_c , then we know it for all the value of ϕ_c . However, the functions β , γ and γ_m are known only perturbatively as a power series of the couplings g_i , and they do not require small logarithms. Thus, by only assuming that the couplings are small, the beta and gamma functions can be determined to the desired level of accuracy, and solving the Callan-Symanzik equation we obtain an expression for $V_{eff}(\phi_c)$ that is valid also if $g_i \ln(\phi_c^2/M^2)$ is not less than 1, then extending the region of validity of the potential.

Basing on dimensional grounds, we assume for the solution of Eq. (2.107) the following form:

$$V_{eff}(\phi_c) = \frac{1}{2} \tilde{m}^2(m^2, g_i; \phi_c, \mu) \phi_c^2 + \frac{1}{4} \tilde{\lambda}(m^2, g_i; \phi_c, \mu) \phi_c^4,$$

where \tilde{m}^2 has the dimension of a mass squared, while $\tilde{\lambda}$ is dimensionless: this fixes their dependence from the couplings m^2 and g_i . In fact, \tilde{m}^2 have to depend linearly on m^2 , so that it carries all the mass dimension and \tilde{m}^2 can depend on ϕ_c and μ only by the ratio ϕ_c/μ . Instead $\tilde{\lambda}$ can not depend on m^2 , and being dimensionless also it can depend on ϕ_c and μ only by the ratio ϕ_c/μ . Then it is useful to introduce the dimensionless variable

$$t = \ln \frac{\phi_c}{\mu} \quad (2.110)$$

and write the potential as:

$$V_{eff}(\phi_c) = \frac{1}{2} \tilde{m}^2(m^2, g_i; t) \phi_c^2 + \frac{1}{4} \tilde{\lambda}(g_i; t) \phi_c^4. \quad (2.111)$$

Inserting this solution in the Callan-Symanzik equation, and writing it in terms of the dimensionless variable t , we note that the ϕ_c^2 and ϕ_c^4 parts have to be separately zero, so that we obtain the two differential equations for \tilde{m}^2 and $\tilde{\lambda}$:

$$\left(-\frac{\partial}{\partial t} + \bar{\beta}_{g_i} \frac{\partial}{\partial g_i} + 4\bar{\gamma} \right) \tilde{\lambda}(g_i; t) = 0 \quad (2.112)$$

$$\left(-\frac{\partial}{\partial t} + \bar{\beta}_{g_i} \frac{\partial}{\partial g_i} + m^2 \bar{\gamma}_m \frac{\partial}{\partial m^2} + 2\bar{\gamma} \right) \tilde{m}^2(m^2, g_i; t) = 0, \quad (2.113)$$

where we have defined

$$\bar{\beta}_{g_i} = \frac{\beta_{g_i}}{1-\gamma} \quad \bar{\gamma}_m = \frac{\gamma_m}{1-\gamma} \quad \bar{\gamma} = \frac{\gamma}{1-\gamma}. \quad (2.114)$$

The Eqs. (2.112) and (2.113) can be solved using the method of characteristics, obtaining for the potential:

$$V_{eff}(\phi_c) = \frac{1}{2} m^2(t) G(t)^2 \phi_c^2 + \frac{1}{4} \lambda(t) G(t)^4 \phi_c^4, \quad (2.115)$$

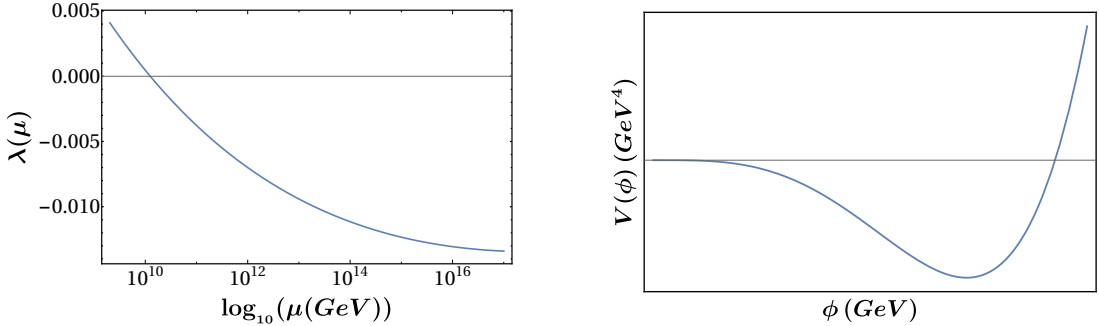


Figure 2.1: *Left panel:* Higgs running coupling constant, where we put in evidence that for $\mu \gtrsim 10^{11}$ we have negative values for $\lambda(\mu)$. *Right panel:* sketch of the RGI Higgs effective potential.

where

$$G(t) \equiv \exp \left(- \int_v^t dt' \bar{\gamma}(g_i(t')) \right), \quad (2.116)$$

while $g_i(t)$ and $m^2(t)$ are solutions of the differential equations

$$\frac{dg_i}{dt} = \bar{\beta}_{g_i}(g_i) \quad \frac{dm^2}{dt} = m^2(t) \bar{\gamma}_m(g_i) \quad (2.117)$$

with boundary conditions $g_i(v) = \bar{g}_i$ and $m^2(v) = m_H^2$ (for instance, the measured values of the Standard Model couplings and of the Higgs mass at the EW scale v). See Appendix A for the expression of β_{g_i} , γ_m and γ .

Once we know the beta and gamma function, we can solve (numerically) the set of differential equations (2.117), and we note an important characteristic of the running coupling constant $\lambda(\mu)$, i.e. at the scale $\mu_{\text{inst}} \sim 10^{11}$ GeV it becomes negative as we can see in Fig. 2.1. From the expression of the β_λ function in Appendix A it is clear that this behaviour is due to the quark top contribution that presents the fermionic characteristic opposite sign respect to the bosonic contributions. Moreover, being μ_{inst} the relevant scale of the problem and it is much larger than the EW scale $v \sim 246$ GeV, it is clear that we can neglect the ϕ^2 term in Eq. (2.115), and write the RG improved Higgs effective potential as:

$$V_{\text{RGI}}(\phi) \simeq \frac{1}{4} \lambda_{\text{eff}}(\phi) \phi^4. \quad (2.118)$$

In particular, this behaviour of the running coupling constant λ can be seen in Eq. (2.118) as an instability of the Higgs effective potential in μ_{inst} , and in the presence of a second minimum at a scale of $\phi \sim 10^{30}$ GeV. Then it is of the great importance to study the stability condition of the EW vacuum (where our Universe sits) respect to this second minimum. This topic will be the main argument of the next chapters.

Chapter 3

Instanton physics and vacuum decay

Many of the phenomena that we find in quantum field theory are related to the *tunnel effect*. The most known method for the study of the quantum tunneling is the *WKB method*, based on semiclassical approximations, while for the generalizations to the quantum field theories is useful to employ the path integral formalism. The approach to the quantum tunneling with functional formalism is the base of the *instanton method* [37–41] that is founded on searching the euclidean solution of the equation of motion. The elegance of this method lies in the fact that once the Euclidean formalism has been developed for systems with a finite number N of degrees of freedom, the generalization to the context of quantum field theory is immediate.

3.1 Tunneling in quantum mechanics

We consider a particle that moves in a one-dimensional space, subject to a potential $V(q)$ and having energy E , then described by the hamiltonian

$$\mathcal{H} = \frac{p^2}{2m} + V(q).$$

We denote with q_{max} the point in which V has a maximum, and with q_1 and q_2 the *classical inversion points*, that are the points in which the potential $V(q)$ is equal to the energy E of the particle, $E = V(q_j)$. Then in the region $q_1 < q < q_2$ we have $E < V(q)$ and such points define a region of the space in which the kinetic energy of the particle is negative, since the total energy E is less than the potential V

$$E_{cin}(q) = E - V(q) < 0 \quad \forall q \in [q_1, q_2].$$

The spatial interval $[q_1, q_2]$ then defines the *classical forbidden region*.

Quantum mechanics says us that exists a non zero probability that a particle which moves along a positive direction of the x axis, with energy E less than $V(q_{max})$, can cross the barrier. This classically forbidden motion is called *quantum tunneling*:

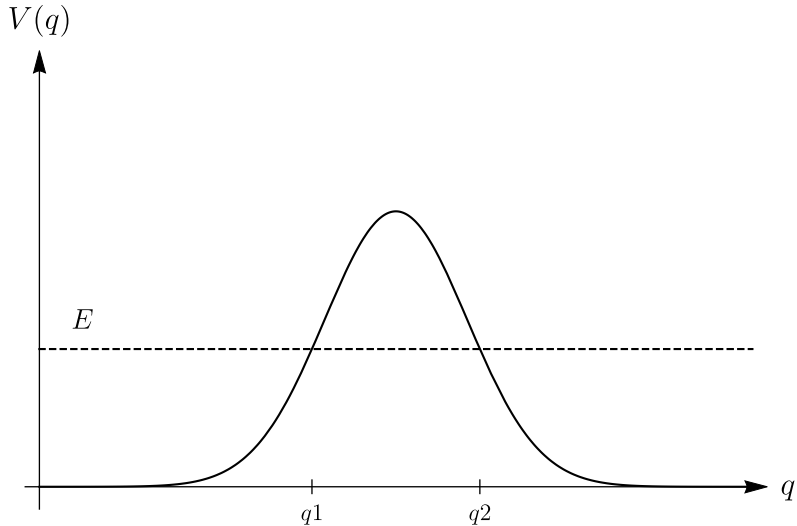


Figure 3.1: Potential energy barrier.

the probability amplitude relative to the possibility of transmission is given by the semiclassical approximation of the WKB method [37, 39–42]

$$|T(E)| = \exp \left\{ -\frac{1}{\hbar} \int_{q_1}^{q_2} \sqrt{2m[V(q) - E]} dq \right\} (1 + \mathcal{O}(\hbar)). \quad (3.1)$$

Then we can say that the tunneling probability at the lowest order is proportional to $e^{-\frac{B}{2\hbar}}$ where we have defined the transmission integral

$$B = 2 \int_{q_1}^{q_2} dq \sqrt{2m[V(q) - E]}. \quad (3.2)$$

Being the kinetic energy negative in the forbidden region, we have $\dot{q}^2(t) < 0$, i.e. the particle moves with a canonical velocity $\dot{q}(t)$ that is imaginary in the classically forbidden region. Such a velocity can be thought as the derivative of the canonical position $q(t)$ respect to an imaginary time $\tau = -it$. This observation suggests to adopt an euclidean analysis of the problem doing a Wick rotation of the t axis and identifying $t_E = \tau$. It is worth to study the tunneling phenomenon in the one dimensional case especially in two cases: the symmetric *double well potential* problem and the *metastable state* problem [38, 39].

In the first problem, for which the potential is shown in Fig. 3.2, the quantum states are degenerate. In fact the potential is characterized by two different ground states, $|L\rangle$ and $|R\rangle$, localized in correspondence of both the two degenerate minima. In quantum perturbation theory, this implies a spontaneous breaking of the parity symmetry, but this is not possible because the spectrum of the Schrödinger operator in this case is discrete and thus the ground state has to correspond to a *symmetric eigenfunction*. This apparent discrepancy is solved by the quantum tunneling that leads to a splitting of the energy level, and then the presence of a unique ground state given by the symmetric combination of $|L\rangle$ and $|R\rangle$.

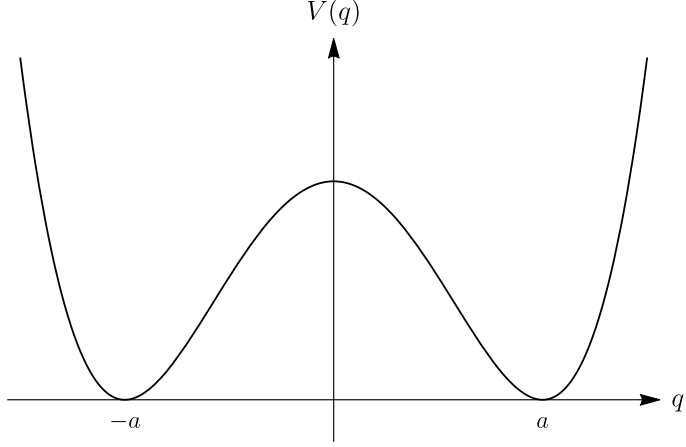


Figure 3.2: Double-well potential.

Referring to the situation shown in Fig. 3.2, where the minima are in $q = \pm a$ and the maximum is in $q = 0$, if the barrier is infinitely high $\lim_{q \rightarrow 0} V(q) = \infty$ (and then impenetrable), then the potential is equivalent to those of two decoupled harmonic oscillators with minima in $q = \pm a$. In this case there would be two possible set of harmonic oscillator eigenstates, localized in correspondence of the two minima and the two ground states would have the same energy E_0 .

Instead if the barrier is finite, as in Fig. 3.2, neither of the two ground states remain eigenstates of the hamiltonian because the possibility of tunneling couples the potentials of the harmonic oscillators and this perturbation alters the eigenstates of the system, creating a splitting of the energy levels. In particular, if $E_0 < V(0)$ then the symmetric and antisymmetric combinations of the two states $|L\rangle$ and $|R\rangle$ will give rise to the hamiltonian eigenstates:

$$|\pm\rangle = \frac{1}{\sqrt{2}} (|L\rangle \pm |R\rangle) \quad E_{\pm} = E_0 \mp \frac{\Delta}{2}, \quad (3.3)$$

where the factor that defines the splitting of the fundamental energy level is tied up to the tunneling probability through the relation

$$\frac{\Delta}{2} \propto \exp \left\{ -\frac{1}{\hbar} \int_{-a}^{+a} \sqrt{2m [V(q) - E]} dq \right\}. \quad (3.4)$$

The two states defined through Eq. (3.3) are then states of the system with energies more or less high compared to E_0 and in particular the ground state of the system is the state $|+\rangle$, i.e. it is the state given by the symmetric combination of the two original vacuum states. Now, if for $t = 0$ a particle is in the state $|L\rangle$, then at the generic time t

$$\begin{aligned} |\psi(t)\rangle &= e^{-\frac{i}{\hbar} \hat{H}t} \left[\frac{1}{\sqrt{2}} (|+\rangle + |-\rangle) \right] \\ &= \frac{1}{2} e^{-\frac{i}{\hbar} E_+ t} \left[(1 + e^{-\frac{i}{\hbar} \Delta t}) |L\rangle + (1 - e^{-\frac{i}{\hbar} \Delta t}) |R\rangle \right]. \end{aligned} \quad (3.5)$$

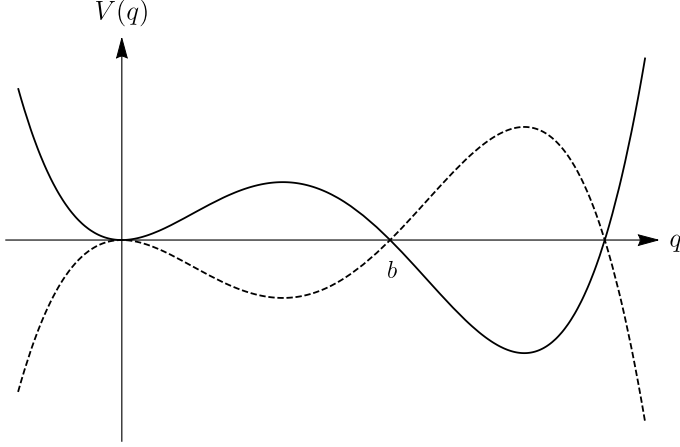


Figure 3.3: Potential with a metastable vacuum.

Then the system oscillates between the two states $|L\rangle$ and $|R\rangle$, and the oscillation occurs with a frequency Δ , i.e. it depends from the tunneling probability amplitude.

At this point, we study the problem of metastable state, a phenomenon that can occur when the potential describing a system presents one or more local minima in a side of the barrier and an absolute minimum from the other side, as in Fig. 3.3 [39]. If the barrier were infinite, i.e. if the tunneling probability vanish, there would be a set of discrete levels in a side of the barrier and a spectrum of energy levels thicker on the other side. In the case of a finite barrier, in which we suppose that the classical inversion points of motion are $q_i = a$ and $q_f = b$, the possibility of tunneling gives rise, as in the previous case, to a mixing of eigenstates of the hamiltonian, but in this case the tunneling probability is high as the system will tend to decay towards the absolute minimum, called *true vacuum*, of the potential. In the limit in which the width of the absolute minimum is infinity, it can be proved that if the system is initially in the state $|L\rangle$ (with reference to Fig. 3.3, the particle is located in the relative minimum $q = a$ with energy $E = 0$) the probability amplitude $\langle L|\psi(t)\rangle$ that, at the time t , the system is still in this state decays exponentially with the time, where the exponent is in turn proportional to $e^{-B/2\hbar}$. The state $|L\rangle$ is called *metastable state* and it is not an eigenstate of the hamiltonian. Moreover, it will have a complex energy E_0 whose imaginary part defines the *decay amplitude* of the state

$$\text{Im}[E_0] \equiv \frac{\Gamma}{2}. \quad (3.6)$$

In fact the potential analyzed can be seen as the analytic continuation of a potential with a single minimum in $q = a$ that constitutes the ground state of the system [39], and then the complex energy can be interpreted as the analytic continuation of the real energy associated to this state.

3.2 Tunneling with functional formalism

The WKB method turns out to be quite effective for the description of the phenomenon of tunneling in the context of quantum mechanics, but to extend the treatment to the context of quantum field theory it is easier to use the *functional formalism of the path integral* [43].

Let us see how to treat, in general, a one dimensional quantum system given by a particle with mass m , without spin and subject to a potential $V(q)$. Using the *path integral* formalism, the probability amplitude that the particle is in the position q_i at the initial time $t_i = -T/2$ and that it is revealed in the position q_f at the final instant $t_f = +T/2$, is given by the functional integral

$$\langle q_f; +T/2 | q_i; -T/2 \rangle \equiv \langle q_f | e^{-\frac{i}{\hbar} \hat{H} t} | q_i \rangle = \mathcal{N} \int \mathcal{D}q(t) \exp \left\{ \frac{i}{\hbar} S[q(t)] \right\} \quad (3.7)$$

where \mathcal{N} is a normalization factor. Performing the Wick rotation ($t = -i\tau$) the functional integral becomes

$$\langle q_f; +T/2 | q_i; -T/2 \rangle \equiv \langle q_f | e^{-\frac{1}{\hbar} \hat{H} \tau} | q_i \rangle = \mathcal{N} \int \mathcal{D}q(\tau) \exp \left\{ -\frac{1}{\hbar} S_E[q(\tau)] \right\} \quad (3.8)$$

where $S_E[q(\tau)]$ is the euclidean action, given by

$$S_E[q(\tau)] = \int_{-\frac{T}{2}}^{+\frac{T}{2}} \left[\frac{1}{2} m \dot{q}^2 + V(q) \right] d\tau, \quad (3.9)$$

and the dot denotes the derivative respect to τ . In other words, in Eq. (3.7) we do the substitutions $t \rightarrow -i\tau$ and $S[q(t)] \rightarrow iS_E[q(\tau)]$ with S_E defined by Eq. (3.9), to obtain Eq. (3.8). Moreover, Eq. (3.9) says that using the euclidean formalism is equivalent to study the motion of the particle in a potential $-V(q)$.

Since we want to determine the transition amplitude $\mathcal{A}(|q_i; -T/2\rangle \rightarrow |q_f; T/2\rangle)$, the path $q(\tau)$ which is followed by the particle will respect the conditions

$$q(-T/2) = q_i \quad q(+T/2) = q_f, \quad (3.10)$$

and then the functional integration in Eq. (3.8) have to be extended to the functions that respect such conditions.

Moreover, the euclidean formalism is useful also to obtain information on the ground state of the system: the matrix element in the left hand side of Eq. (3.8) can be expanded using the orthonormal complete set of eigenstates $|n\rangle$ of the hamiltonian \hat{H}

$$\langle q_f; +T/2 | q_i; -T/2 \rangle = \langle q_f | e^{-\frac{1}{\hbar} \hat{H} T} | q_i \rangle = \sum_{n=0}^{\infty} e^{-\frac{1}{\hbar} E_n T} \langle q_f | n \rangle \langle n | q_i \rangle. \quad (3.11)$$

In the limit $T \rightarrow \infty$ this amplitude is dominated by the terms corresponding to the energies E_n that are smaller. In particular, if E_0 is the energy of the ground state $|0\rangle$:

$$\langle q_f | e^{-\frac{1}{\hbar} \hat{H} T} | q_i \rangle \xrightarrow{T \gg 1} e^{-\frac{1}{\hbar} E_0 T} \langle q_f | 0 \rangle \langle 0 | q_i \rangle. \quad (3.12)$$

In other words, in this limit we can approximate

$$\langle q_f; +T/2 | q_i; -T/2 \rangle \sim \psi_0(q_f) \psi_0^*(q_i) e^{-\frac{E_0}{\hbar} T}. \quad (3.13)$$

In this way, determining the path integral in Eq. (3.8), we can obtain information on the energy of the ground state and on its corresponding wave function $\psi_0(q)$.

Now we see how to determine the path integral in Eq. (3.8) in the semiclassical limit, that is expanding the action around its minimum. We consider the “stationary path”, i.e. the path that minimizes the euclidean action (3.9), and that then is the classical solution $\bar{q}(\tau)$ of the euclidean equation of motion

$$\frac{\delta S_E[q]}{\delta q(\tau)} = 0 \quad \Rightarrow \quad -m\ddot{q}(\tau) + \frac{dV(q)}{dq} = 0. \quad (3.14)$$

The generic path is given by $q(\tau) = \bar{q}(\tau) + \eta(\tau)$, where $\eta(q)$ is the quantum fluctuation around $\bar{q}(\tau)$. Since all the paths must have the same extrema, it will be $\eta(\pm T/2) = 0$. At this point, we expand the euclidean action around the classical solution $\bar{q}(\tau)$:

$$S_E[q(\tau)] \sim S_E[\bar{q}(\tau)] + \frac{1}{2} \int \eta(\tau) \left[\frac{\delta^2 S_E[q]}{\delta q(\tau) \delta q(\tau')} \right]_{q(\tau)=\bar{q}(\tau)} \eta(\tau') d\tau d\tau'. \quad (3.15)$$

The term in square brackets in Eq. (3.15) is called *Quantum Fluctuation Operator* $S''_E[\bar{q}(\tau)]$, and it is obtained from the second variation of the euclidean action. To compute this operator we write the generic path as $q(\tau) = \bar{q}(\tau) + \lambda \eta(\tau)$ with η subject to the constraints seen above. Now we can see the action as a function of λ , $S_E = S_E(\lambda)$. Computing the second variation of the action around its minimum is now equivalent to compute the second derivative of $S_E(\lambda)$ in $\lambda = 0$. Then

$$\begin{aligned} \frac{dS_E}{d\lambda} &= \int_{-\frac{T}{2}}^{\frac{T}{2}} d\tau \left(\frac{\partial \mathcal{L}_E}{\partial q} \eta + \frac{\partial \mathcal{L}_E}{\partial \dot{q}} \dot{\eta} \right) \Big|_{\lambda=0} \Rightarrow \\ \frac{d^2 S_E}{d\lambda^2} &= \int_{-\frac{T}{2}}^{\frac{T}{2}} d\tau \left(\frac{\partial^2 \mathcal{L}_E}{\partial q^2} \eta^2 + 2 \frac{\partial^2 \mathcal{L}_E}{\partial q \partial \dot{q}} \eta \dot{\eta} + \frac{\partial^2 \mathcal{L}_E}{\partial \dot{q}^2} \dot{\eta}^2 \right) \Big|_{\lambda=0}. \end{aligned}$$

From now on we omit to specify that the partial derivative are computed in $\lambda = 0$ to lighten the notation. Integrating by parts:

$$\begin{aligned} \frac{d^2 S_E}{d\lambda^2} &= \int_{-\frac{T}{2}}^{\frac{T}{2}} d\tau \frac{\partial^2 \mathcal{L}_E}{\partial q^2} \eta^2 + \left[\frac{\partial^2 \mathcal{L}_E}{\partial q \partial \dot{q}} \eta^2 \right]_{-\frac{T}{2}}^{\frac{T}{2}} - \int_{-\frac{T}{2}}^{\frac{T}{2}} d\tau \frac{d}{d\tau} \left(\frac{\partial^2 \mathcal{L}_E}{\partial q \partial \dot{q}} \right) \eta^2 \\ &\quad + \left[\frac{\partial^2 \mathcal{L}_E}{\partial \dot{q}^2} \eta \dot{\eta} \right]_{-\frac{T}{2}}^{\frac{T}{2}} - \int_{-\frac{T}{2}}^{\frac{T}{2}} d\tau \eta \frac{d}{d\tau} \left(\frac{\partial^2 \mathcal{L}_E}{\partial q \partial \dot{q}} \dot{\eta} \right). \end{aligned}$$

Remembering that $\eta(\pm T/2) = 0$ and computing the derivatives of \mathcal{L}_E we obtain:

$$\frac{d^2 S_E}{d\lambda^2} \Big|_{\lambda=0} = \int_{-\frac{T}{2}}^{\frac{T}{2}} \eta \left(-m \frac{d^2}{d\tau^2} + \frac{d^2 V(q)}{dq^2} \right) \eta d\tau. \quad (3.16)$$

Then:

$$\begin{aligned} S_E''[\bar{q}(\tau)] &\equiv \left[\frac{\delta^2 S_E[q]}{\delta q(\tau) \delta q(\tau')} \right]_{q(\tau)=\bar{q}(\tau)} \delta(\tau - \tau') \\ &= \left[\left(-m \frac{d^2}{d\tau^2} + \frac{d^2 V(q)}{dq^2} \right) \delta(\tau - \tau') \right]_{q(\tau)=\bar{q}(\tau)}. \end{aligned} \quad (3.17)$$

In this approximation, i.e. up to $\mathcal{O}(\eta^2)$, being $\eta(\tau) = q(\tau) - \bar{q}(\tau)$, we have that the path integral in Eq. (3.8) is

$$\int \mathcal{D}q(\tau) e^{-\frac{1}{\hbar} S_E[q(\tau)]} \simeq e^{-\frac{1}{\hbar} S_E[\bar{q}(\tau)]} \int \mathcal{D}q(\tau) e^{-\frac{1}{2\hbar} \int d\tau \eta(\tau) \left(-m \frac{d^2}{d\tau^2} + \frac{d^2 V(q)}{dq^2} \right)_{\bar{q}} \eta(\tau)}. \quad (3.18)$$

Now we can do a change of variable $q(\tau) \rightarrow \eta(\tau)$ (with jacobian equal to 1)

$$\int \mathcal{D}q(\tau) e^{-\frac{1}{\hbar} S_E[q(\tau)]} \simeq e^{-\frac{1}{\hbar} S_E[\bar{q}(\tau)]} \int \mathcal{D}\eta(\tau) e^{-\frac{1}{2\hbar} \int d\tau \eta(\tau) \left(-m \frac{d^2}{d\tau^2} + \frac{d^2 V(q)}{dq^2} \right)_{\bar{q}} \eta(\tau)}. \quad (3.19)$$

To complete the computation of the path integral in Eq. (3.19), we have to find the eigenfunction $\psi_n(\tau)$ and the eigenvalues λ_n of the Quantum Fluctuation Operator solving the equation

$$\left(-m \frac{d^2}{d\tau^2} + \frac{d^2 V(q)}{dq^2} \right)_{\bar{q}} \psi_n(\tau) = \lambda_n \psi_n(\tau). \quad (3.20)$$

If we expand the quantum fluctuation $\eta(\tau)$ in terms of the eigenfunctions $\psi_n(\tau)$, we obtain

$$\eta(\tau) = \sum_n c_n \psi_n(\tau) \quad \Rightarrow \quad q(\tau) = \bar{q}(\tau) + \sum_n c_n \psi_n(\tau). \quad (3.21)$$

Obviously, the eigenfunctions $\psi_n(\tau)$ are a complete orthonormal set. Moreover, we know that the generic path $q(\tau)$ of the particle have to respect the boundary conditions in Eq. (3.10), and in particular the classical path, solution of the classical equation of motion (3.14), has to respect such conditions: as a consequence, from Eq. (3.21) we conclude that the eigenfunctions $\psi_n(\tau)$ of the Quantum Fluctuation Operator have to vanish in $\tau = \pm T/2$ [38, 39]. In conclusion, we have:

$$\psi_n(\pm T/2) = 0 \quad \int \psi_n(\tau) \psi_m(\tau) d\tau = \delta_{nm}. \quad (3.22)$$

Once we write the quantum fluctuation $\eta(\tau)$ as an expansion of the eigenfunctions in Eq. (3.21), we can substitute such expansion in the exponent of Eq. (3.19), obtaining

$$\begin{aligned} &\frac{1}{2\hbar} \int d\tau \eta(\tau) \left(-m \frac{d^2}{d\tau^2} + \frac{d^2 V(q)}{dq^2} \right)_{\bar{q}} \eta(\tau) = \\ &= \frac{1}{2\hbar} \int d\tau \left(\sum_m c_m \psi_m(\tau) \right) \left(\sum_n \lambda_n c_n \psi_n(\tau) \right) = \frac{1}{2\hbar} \sum_n \lambda_n c_n^2 \end{aligned} \quad (3.23)$$

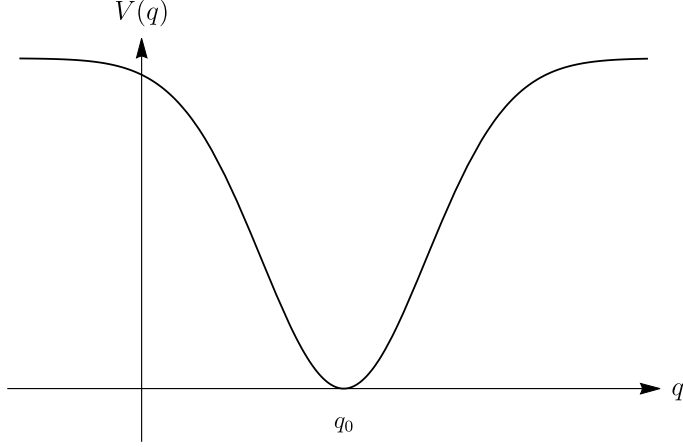


Figure 3.4: Potential of a single well.

where in the last step we have used the orthonormality of the eigenfunctions $\psi_n(\tau)$ given in Eq. (3.22).

Then, being $\eta(\tau) = \sum_n c_n \psi_n(\tau)$, we can do another change of variables: $\{\eta_i(\tau)\} \rightarrow \{\frac{c_n}{\sqrt{2\pi\hbar}}\}$, where the index i identifies the path $q_i(\tau)$. In conclusion (a part an irrelevant jacobian factor that can be included in the normalization factor \mathcal{N}), we obtain:

$$[\mathcal{D}q(\tau)] \equiv \prod_i dq_i(\tau) = \prod_n \frac{dc_n}{\sqrt{2\pi\hbar}}.$$

As a consequence, the path integral in Eq. (3.19) becomes:

$$\int \mathcal{D}\eta(\tau) e^{-\frac{1}{2\hbar} \int d\tau \eta(\tau) \left(-m \frac{d^2}{d\tau^2} + \frac{d^2 V(q)}{dq^2} \right)_{\bar{q}}} = \prod_n \int \frac{dc_n}{\sqrt{2\pi\hbar}} e^{-\frac{1}{2\hbar} \lambda_n c_n^2}. \quad (3.24)$$

Then if the eigenvalues λ_n are positive for all n , we have:

$$\int \mathcal{D}\eta(\tau) e^{-\frac{1}{2\hbar} \int d\tau \eta(\tau) \left(-m \frac{d^2}{d\tau^2} + \frac{d^2 V(q)}{dq^2} \right)_{\bar{q}}} = \prod_n \lambda_n^{-\frac{1}{2}} = [\det(S_E''(\bar{q}))]^{-\frac{1}{2}} \quad (3.25)$$

where in the first step we have used the gaussian integration. In conclusion, going up the chain of equality up to Eq. (3.8), we obtain the transition amplitude in the semiclassical approximation:

$$\langle q_f; +T/2 | q_i; -T/2 \rangle \equiv \langle q_f | e^{-\frac{i}{\hbar} \hat{H}T} | q_i \rangle = \mathcal{N} e^{-\frac{1}{\hbar} S_E[\bar{q}(\tau)]} [\det(S_E''(\bar{q}))]^{-\frac{1}{2}}. \quad (3.26)$$

A very simple case to study with the functional formalism is the potential with a single minimum in $q = q_0$, for which we suppose for simplicity $V(q_0) = 0$, as shown in Fig. 3.4. Taking the boundary conditions $q_i = q_f = q_0$, the unique solution of the equation of motion in Eq. (3.14) is the trivial solution $\bar{q}(\tau) = q_0$. For this solution it is obvious that $S_E = 0$. Thus, from Eqs. (3.26) and (3.17) we have that

$$\langle q_0 | e^{-\frac{1}{\hbar} \hat{H}T} | q_0 \rangle = \mathcal{N} [\det(-m \partial_\tau^2 + m\omega^2)]^{-\frac{1}{2}} \quad (3.27)$$

where we have denoted $\omega^2 = V''(q_0)/m$ (the prime denotes the derivative respect to q). For large values of T , it can be proved that [38]

$$\mathcal{N} \left[\det(-m\partial_\tau^2 + m\omega^2) \right]^{-\frac{1}{2}} = \sqrt{\frac{m\omega}{\pi\hbar}} e^{-\frac{1}{2}\omega T}. \quad (3.28)$$

Comparing Eq. (3.13) with Eq. (3.27) with the help of Eq. (3.28), we obtain that the energy of the ground state E_0 and the corresponding eigenfunction ψ_0 are exactly those of a one dimensional harmonic oscillator:

$$E_0 = \frac{1}{2}\hbar\omega \quad |\langle q_0 | 0 \rangle|^2 = \sqrt{\frac{m\omega}{\pi\hbar}}. \quad (3.29)$$

The detailed computation of Eq. (3.28) is referred to Appendix B.

In particular, in the case of the harmonic oscillator potential $\frac{1}{2}m\omega^2$, the parameter ω coincide with the frequency of the oscillator. Moreover, when we expand a generic potential $V(q)$ around its minimum q_0 , at the lowest order, this is reduced to the potential of an harmonic oscillator: this is the second order, since the zero order term $V(q_0)$ vanish by hypothesis, while the first order term $V'(q_0)$ vanish because q_0 is a stationary point.

3.2.1 Application to the double well potential and instantons

Let us apply the results seen in the previous subsection to the symmetric *double well* potential which was presented in the introduction of this chapter and shown in Fig. 3.2. In particular, we recall that if $q = \pm a$ are the minima of the potential then we assume $V(\pm a) = 0$ [38, 39].

Moreover, if we specify a shape for the double-well potential, we can also find a solution of the classical equation of motion (3.14):

$$V(q) = \lambda(q^2 - a^2)^2. \quad (3.30)$$

The vantage of using a specific expression for the potential as the one in Eq. (3.30) is that the determinant in Eq. (3.26) can be computed explicitly. With this potential we have

$$V''(q) = 4\lambda(3q^2 - a^2) \quad \Rightarrow \quad \frac{1}{m}V''(\pm a) = \frac{8\lambda a^2}{m} \equiv \omega^2.$$

Multiplying the classical equation of motion (3.14) for \dot{q} we obtain:

$$\begin{aligned} m\ddot{q} &= \frac{dV(q)}{dq} \quad \Rightarrow \quad m\dot{q}\ddot{q} = \frac{m}{2}\frac{d}{d\tau}\dot{q}^2 = \dot{q}\frac{dV(q)}{dq} = \frac{dq}{d\tau}\frac{dV(q)}{dq} = \frac{d}{d\tau}V(q) \quad \Rightarrow \\ \frac{m}{2}\frac{d}{d\tau}\dot{q}^2 &= \frac{d}{d\tau}V(q) \quad \Rightarrow \quad \frac{1}{2}m\dot{q}^2 = V(q) + c \end{aligned} \quad (3.31)$$

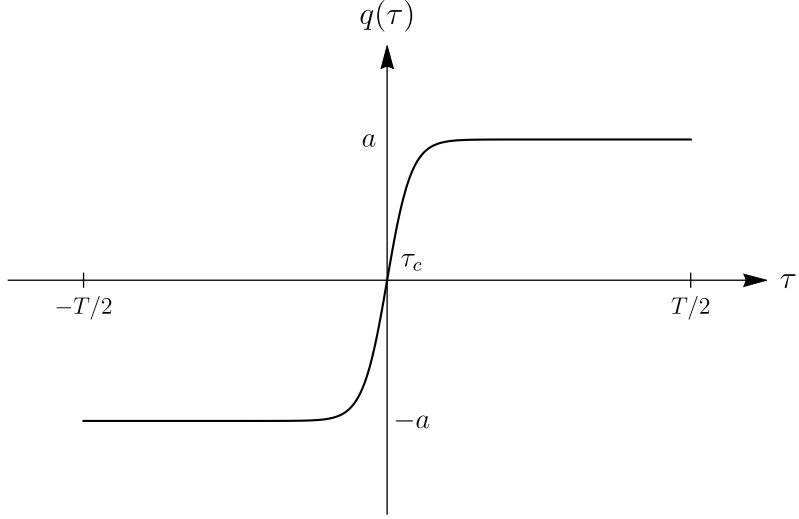


Figure 3.5: Instanton solution with centroid τ_c between the minima $-a$ and a . In the example shown in figure, the centroid is taken in $\tau_c = 0$.

In particular, with the boundary conditions that we will use, it is $c = 0$. Thus, the result of Eq. (3.31) says us that the solutions to the classical equation of motion correspond to solutions with vanishing energy:

$$E = \frac{1}{2}m\dot{q}^2 - V(q) = 0. \quad (3.32)$$

Substituting the expression (3.31) in the euclidean action (3.9), we obtain:

$$S_E[q] = \int_{-T/2}^{T/2} m\dot{q}^2 d\tau. \quad (3.33)$$

Solving explicitly the classical equation of motion with appropriate boundary conditions, we can have three kinds of solutions:

- the particles remains trapped in one of the two minima , so that the boundary conditions are $q(-T/2) = q(T/2) = a$ or $q(-T/2) = q(T/2) = -a$. In such a case, the solutions are respectively $q(\tau) = a$ and $q(\tau) = -a$ for every τ ;
- The particles leaves the minimum $-a$ to reach the minimum a , so that the boundary conditions are $q(-T/2) = -a$ and $q(T/2) = a$. In particular, this solution is called *instanton*. We can also have the situation in which the particles leaves the minimum a to reach the minimum $-a$. In such a case the boundary condition are $q(-T/2) = a$ and $q(T/2) = -a$, and the solution is called *anti-instanton*;
- the particles oscillates between the two minima.

To obtain the solution of (anti-) instanton, we insert the explicit expression of the potential in Eq. (3.32):

$$\dot{q} = \pm \sqrt{\frac{2\lambda}{m}}(a^2 - q^2) \quad q^2 \leq a^2 \quad \Rightarrow \quad \int_0^{q_f} \frac{dq}{a^2 - q^2} = \pm \sqrt{\frac{2\lambda}{m}} \int_{\tau_c}^{\tau} d\tau,$$

where q_I is the solution of (anti-) instanton, corresponding to the sign $(-)$ $+$, while τ_c is called *centroid of the instanton* and it is the point in which the instanton vanish. In conclusion, having defined $\omega^2 = 8\lambda a^2/m$, we obtain:

$$q_I(\tau) = \pm a \tanh \left[\frac{\omega}{2} (\tau - \tau_c) \right] \xrightarrow[\tau \rightarrow \infty]{} \pm a. \quad (3.34)$$

Let us compute the probability amplitudes using Eq. (3.8): first, we compute the *persistence amplitude* $\langle a | e^{-\frac{1}{\hbar} \hat{H}T} | a \rangle = \langle -a | e^{-\frac{1}{\hbar} \hat{H}T} | -a \rangle$, that is the probability amplitude that the particle, starting from a minimum, after a dynamical evolution in an euclidean time T continues to be found in the starting minimum:

$$I_0 = \langle a | e^{-\frac{1}{\hbar} \hat{H}T} | a \rangle = \mathcal{N} \int \mathcal{D}q(\tau) \exp \left\{ -\frac{1}{\hbar} S_E[q(\tau)] \right\}. \quad (3.35)$$

The boundary conditions will be $q(-T/2) = q(T/2) = a$: the only solution to the equation of motion (3.14) with these boundary conditions is the trivial solution $\bar{q}(\tau) = a$. Moreover, it is evident that $S_E[a] = 0$: in other words, we are in the same conditions of the single well potential and the amplitude (3.35), once defined $\omega^2 = V''(\pm a)/m$, is given by Eq. (3.28)

$$I_0 = \mathcal{N} [\det S''(a)]^{-\frac{1}{2}} = \left(\frac{m\omega}{\pi\hbar} \right)^{1/2} e^{-\frac{1}{2}\omega T}. \quad (3.36)$$

Now we compute the *transition amplitude* $\langle a | e^{-\frac{1}{\hbar} \hat{H}T} | -a \rangle = \langle -a | e^{-\frac{1}{\hbar} \hat{H}T} | a \rangle$, that is the probability amplitude that the particles steps from a minimum to another after a dynamical evolution in a time T :

$$I_{\text{inst}} = \langle a | e^{-\hat{H}T} | -a \rangle = \mathcal{N} \int \mathcal{D}q(\tau) \exp \left\{ -\frac{1}{\hbar} S_E[q(\tau)] \right\}. \quad (3.37)$$

In this case, the boundary conditions are given by $q(-T/2) = -a$ and $q(T/2) = a$. The euclidean action computed in the (anti-) instanton solution (3.34) is finite and it is given by Eq. (3.33):

$$S_I \equiv S[q_I] = \int_{-\frac{T}{2}}^{+\frac{T}{2}} m\dot{q}_I^2 d\tau = \frac{m\omega^3}{12\lambda}. \quad (3.38)$$

The detailed computation of Eq. (3.38) is referred to Appendix C. This result is particularly worth as it put in evidence the *translation invariance* of the action S_I , i.e. the fact that it is independent from the centroid τ_c of the instanton.

Applying Eq. (3.26) we obtain:

$$I_{\text{inst}} = \mathcal{N} e^{-\frac{1}{\hbar} S_I} [\det S''(q_I)]^{-\frac{1}{2}}. \quad (3.39)$$

However Eq. (3.26) was obtained in the hypothesis that the eigenvalues of the operator $S_E''(\bar{q})$ were all positive: in the double-well case it is possible to demonstrate that we have a zero mode, i.e. an eigenfunction of the operator with zero eigenvalue.

Then, the determinant gives a divergent factor and, in conclusion, this expression for I_{inst} is wrong.

We can easily demonstrate that the zero mode of the operator $S''_E(q_I)$ is given by

$$\psi_0(\tau) = N^{-1/2} \frac{dq_I(\tau)}{d\tau} \quad (3.40)$$

where N is a normalization factor. Being $\psi_0(\tau)$ a zero mode, it will be solution if the equation

$$\left[-m \frac{d^2}{d\tau^2} + V''(q_I) \right] \psi_0(\tau) = 0, \quad (3.41)$$

that is Eq. (3.20) with $\lambda_0 = 0$. To demonstrate that $\psi_0(\tau)$ in Eq. (3.40) is a zero mode of the Quantum Fluctuation Operator it is sufficient to see that \dot{q}_I is solution of Eq. (3.41):

$$m \frac{d^2}{d\tau^2} \dot{q}_I = \frac{d}{d\tau} m \ddot{q}_I = \left(\frac{dq_I}{d\tau} \frac{d}{dq_I} \right) V'(q_I) = \dot{q}_I V''(q_I), \quad (3.42)$$

where in the second step we have used the chain rule to write the derivative respect to τ as a derivative respect to q , and we have used the equation of motion $m \ddot{q}_I = V'(q_I)$. The factor N can be determined normalizing $\psi_0(\tau)$ to 1, and then computing the integral:

$$N = \int_{-T/2}^{T/2} \dot{q}_I^2 d\tau = \frac{S_I}{m}, \quad (3.43)$$

where in the last step we have used Eq. (3.38). In conclusion, the zero mode is given by

$$\psi_0(\tau) = \sqrt{\frac{m}{S_I}} \frac{dq_I}{d\tau}. \quad (3.44)$$

Now, we see how to treat this zero mode in the functional formalism: as in Eq. (3.21), we expand the quantum fluctuation in the base of the eigenfunctions of the Quantum Fluctuation Operator

$$q(\tau) = q_I(\tau) + \eta(\tau) = q_I(\tau) + \sum_n c_n \psi_n(\tau), \quad (3.45)$$

supposing (without lost of generality) that the zero mode is the eigenfunction with $n = 0$. Then, when we integrate over the corresponding c_0 , we do not have the gaussian factor in the integral: the axes c_0 in the space of the coefficients c_n is called *flat direction*.

If we vary the coefficient c_0 , we have a variation of $q(\tau)$ given by:

$$\delta q = \psi_0(\tau) \delta c_0.$$

On the other hand, a variation of the centroid τ_c induces a variation on $q(\tau)$:

$$\delta q = \frac{\delta q}{\delta \tau_c} \delta \tau_c = -\frac{\delta q_I}{\delta \tau} \delta \tau_c = -\sqrt{\frac{S_I}{m}} \psi_0(\tau) \delta \tau_c$$

where in the last step we used Eq. (3.44). Comparing the two expressions for δq , we obtain the jacobian factor for the change of variables $c_0 \rightarrow \tau_c$ in the integration over the flat direction, $|dc_0/d\tau_c| = \sqrt{S_I/m}$, that is:

$$\frac{dc_0}{\sqrt{2\pi\hbar}} = \sqrt{\frac{S_I}{2\pi\hbar m}} d\tau_c. \quad (3.46)$$

In this way, the integration over the zero mode is substituted by an integration over the centroid τ_c : in other words, τ_c is promoted to dynamical variable, called *collective coordinate*, over which we integrate. Regarding the other directions c_1, c_2, c_3, \dots , called *gaussian directions*, these do not cause problems and then the integration over these variables continues to give the product of the eigenvalues λ_n for $n \geq 1$.

In conclusion, the integration over the flat direction gives a factor T times for the pre-factor in Eq. (3.46), while the integration over the gaussian directions gives a factor $[\det' S''(q_I)]^{-\frac{1}{2}}$, where the prime in the determinant denotes that this is computed excluding the zero eigenvalue λ_0 from the product of the λ_n . With this treatment of the zero modes, Eq. (3.39) becomes

$$I_{\text{inst}} = \mathcal{N} T \left(\frac{S_I}{2\pi\hbar m} \right)^{1/2} e^{-\frac{1}{\hbar} S_I} [\det' S''(q_I)]^{-\frac{1}{2}}.$$

If we now define

$$K = \left(\frac{S_I}{2\pi\hbar m} \right)^{1/2} \left[\frac{\det' S''(q_I)}{\det S''(a)} \right]^{-\frac{1}{2}}, \quad (3.47)$$

the transition amplitude becomes

$$I_{\text{inst}} = \mathcal{N} K T e^{-\frac{1}{\hbar} S_I} [\det S''(a)]^{-1/2}. \quad (3.48)$$

Obviously, the factor $\mathcal{N}[\det S''(a)]^{-1/2}$ is still the determinant of the one-well potential, and then is given by Eq. (3.28).

In addition to the contribution in Eq. (3.48), we have to consider also the contributions of the quasi-solutions given by the multi-instantons, i.e. by configurations in which we have n alternating solutions of instanton and anti-instanton well distinct from each other, as shown in Fig. 3.6. To obtain these conditions we have to apply the *dilute gas approximation*. For large values of τ the instanton $q_I(\tau)$ tends to a : then, the instanton equation (3.31)

$$\frac{dq}{d\tau} = \sqrt{\frac{2V(q)}{m}}$$

can be approximated expanding the potential $V(q)$

$$\frac{dq}{d\tau} = \sqrt{\frac{V''(a)}{m}} (q(\tau) - a). \quad (3.49)$$

Being $\omega^2 = V''(\pm a)/m$, we can solve the differential equation obtaining:

$$q(\tau) \sim a - e^{-\omega\tau}. \quad (3.50)$$

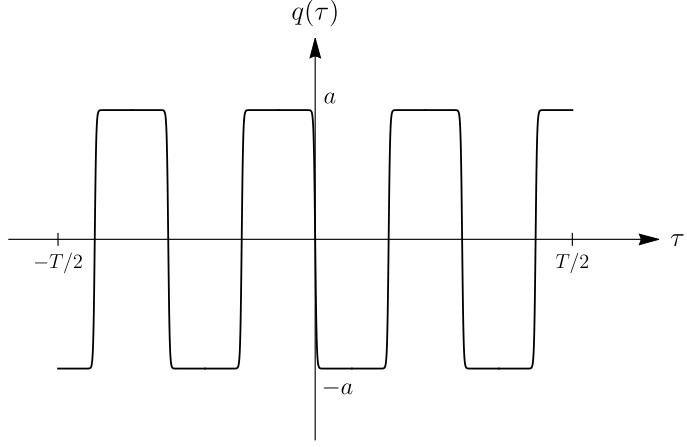


Figure 3.6: Multi-instanton solution, in which we have n instantons and anti-instantons alternating and distinct between them, as established by the *dilute instanton gas approximation*.

Such a behaviour shows that the size of the instanton is of order ω^{-1} . Then, to have an instanton/anti-instanton solution as the one shown in Fig. 3.6 it has to verify that $\omega^{-1} \ll T$. In particular, once we compute the contribution to the amplitudes that comes from the quasi-solutions of the dilute instanton gas approximation, we will see that such a contribution is even the dominant one, although it comes from approximate solutions.

In this configuration with n alternating instantons and anti-instantons, we denote with $q_n(\tau)$ the corresponding quasi-solution: the action is simply given by n times the action S_I of the single instanton $S(q_n) = nS_I$. Concerning the determinant, we consider the time evolution operator $e^{-\frac{1}{\hbar}HT}$ as the product of operators describing the evolution of the system in time intervals of the order ω^{-1} centered in τ_i , i.e. in the centroids of the instantons/anti-instantons: if it were not for these small intervals around the centers of (anti-) instantons, V'' would be always equal to ω^2 , and the result for the determinant would be given directly from Eq. (3.28), that is it would be as if the system were trapped in a single minimum [38]. On the other hand, each of these intervals containing an (anti-) instanton involves a correction by a factor K to the contribution of Eq. (3.28): then, we have

$$[\det' S''(q_n)]^{-1/2} = \left(\frac{m\omega}{\pi\hbar}\right)^{\frac{1}{2}} e^{-\frac{\omega}{2}T} K^n. \quad (3.51)$$

Also in this case, the prime denotes a reduced determinant computed only on the non-zero eigenvalues. In fact, every (anti-) instanton, in addition to contributing to the K correction, contributes to the calculation of the amplitude also with a zero mode: we can introduce a collective coordinate τ_i for each (anti-) instanton

$$-\frac{T}{2} < \tau_1 < \tau_2 < \dots < \tau_n < \frac{T}{2}.$$

Finally, integrating over all the collective coordinates τ_i , we obtain the factor:

$$\int_{-T/2}^{T/2} d\tau_1 \int_{\tau_1}^{-T/2} d\tau_2 \dots \int_{\tau_{n-1}}^{T/2} d\tau_n = \frac{T^n}{n!}. \quad (3.52)$$

Putting together all these factors, we obtain that the contribution of the configuration $q_n(\tau)$ with n alternating instantons and anti-instantons is given by:

$$I_n = \left(\frac{m\omega}{\pi\hbar} \right)^{\frac{1}{2}} e^{-\frac{\omega}{2}T} e^{-\frac{1}{\hbar}nS_I} K^n \frac{T^n}{n!}. \quad (3.53)$$

Since for $n = 1$ Eq. (3.53) has to reduce to Eq. (3.48), we conclude that the correction factor K is exactly given by Eq. (3.47).

Now we can compute the total contribution to the amplitudes $\langle a | e^{-\frac{1}{\hbar}\hat{H}T} | a \rangle$ and $\langle a | e^{-\frac{1}{\hbar}\hat{H}T} | -a \rangle$. To this end, it is important to remember that an instanton describes the transition from the minimum $-a$ to the minimum a , while an anti-instanton describes the opposite transition, from a to $-a$: it is then clear that to have an effective transition from a minimum to the other, we need to consider a configuration with an odd number n of (anti-) instantons, while to have a permanence in the starting minimum, we need to consider a configuration with an even number of (anti-) instantons. In other words, the *transition amplitude* is given by the sum over all the odd n of the contribution I_n , while the *persistence amplitude* is given by the sum of all the even n of I_n :

$$\begin{aligned} \langle a | e^{-\frac{1}{\hbar}\hat{H}T} | -a \rangle &= \langle -a | e^{-\frac{1}{\hbar}\hat{H}T} | a \rangle = \sum_{\text{odd } n} I_n = \\ &= \left(\frac{m\omega}{\pi\hbar} \right)^{\frac{1}{2}} e^{-\frac{\omega}{2}T} \sum_{\text{odd } n} \frac{1}{n!} \left(e^{-\frac{1}{\hbar}S_I} KT \right)^n = \left(\frac{m\omega}{\pi\hbar} \right)^{\frac{1}{2}} e^{-\frac{\omega}{2}T} \sinh \left(e^{-\frac{1}{\hbar}S_I} KT \right) \end{aligned} \quad (3.54)$$

$$\begin{aligned} \langle a | e^{-\frac{1}{\hbar}\hat{H}T} | a \rangle &= \langle -a | e^{-\frac{1}{\hbar}\hat{H}T} | -a \rangle = \sum_{\text{even } n} I_n = \\ &= \left(\frac{m\omega}{\pi\hbar} \right)^{\frac{1}{2}} e^{-\frac{\omega}{2}T} \sum_{\text{even } n} \frac{1}{n!} \left(e^{-\frac{1}{\hbar}S_I} KT \right)^n = \left(\frac{m\omega}{\pi\hbar} \right)^{\frac{1}{2}} e^{-\frac{\omega}{2}T} \cosh \left(e^{-\frac{1}{\hbar}S_I} KT \right) \end{aligned} \quad (3.55)$$

where in the sums over n we have simply recognised the Taylor expansion of the hyperbolic functions.

Let us see that the contribution to the probability amplitudes that arises from the diluted instanton gas approximation is the dominant one: in fact, this approximation is valid only where the density of the instantons n/T is sufficiently low. In an exponential sum $\sum y^n/n!$, the dominant contribution comes from the terms $n \sim y$, so that the dominant contribution in Eqs. (3.54) and (3.55) comes from the terms

$$\frac{n}{T} \sim Ke^{-\frac{1}{\hbar}S_I} \quad \Rightarrow \quad n \lesssim KTe^{-\frac{1}{\hbar}S_I}.$$

This expression says us that, for small \hbar , the dominant terms are those for which the density of (anti-) instantons n/T is exponentially small, and then when their average

separation is very large. We note as this average separation between the (anti-) instantons is independent from T : the dilute instanton gas approximation is then a good approximation for small \hbar and the condition for its validity is independent from T , as long as T is large enough [38].

To conclude the study of the double-well, we now see how to apply the probability amplitude computed in this subsection to obtain the ground state of the system and its first excited state. To this end, it is useful to write Eqs. (3.54) and (3.55) in a unique equation:

$$\langle \pm a | e^{-\frac{1}{\hbar} \hat{H}T} | -a \rangle = \left(\frac{m\omega}{\pi\hbar} \right)^{\frac{1}{2}} e^{-\frac{\omega}{2}T} \frac{1}{2} \left[\exp \left(+KT e^{-\frac{1}{\hbar} S_I} \right) \mp \exp \left(-KT e^{-\frac{1}{\hbar} S_I} \right) \right]. \quad (3.56)$$

We denote with $|+\rangle$ e $|-\rangle$ the combinations, respectively, symmetric and e anti-symmetric of the two states of harmonic oscillators $|L\rangle$ and $|R\rangle$ localized at the two minima: as we know, $|+\rangle$ and $|-\rangle$ are eigenstate of the hamiltonian, on the contrary of the two state $|L\rangle$ and $|R\rangle$. In particular, they are the two eigenstates with the lowest energy levels (ignoring that without the penetration barrier they becomes degenerate):

$$|\pm\rangle = \frac{1}{\sqrt{2}} (|L\rangle \pm |R\rangle). \quad (3.57)$$

For T sufficiently large, we can neglect all the contributions that come from the eigenstates with higher energy, and then we can write:

$$\langle \pm a | e^{-\frac{1}{\hbar} \hat{H}T} | -a \rangle = \langle \pm a | + \rangle \langle + | -a \rangle e^{-\frac{1}{\hbar} E_+ T} + \langle \pm a | - \rangle \langle - | -a \rangle e^{-\frac{1}{\hbar} E_- T}. \quad (3.58)$$

Clearly $\langle a | \pm \rangle = \pm \langle -a | \pm \rangle$, and we have also $|\langle a | + \rangle| = |\langle a | - \rangle|$ for very large T . Then:

$$\langle \pm a | e^{-\frac{1}{\hbar} \hat{H}T} | -a \rangle = |\langle a | + \rangle|^2 \left(e^{-\frac{1}{\hbar} E_+ T} \mp e^{-\frac{1}{\hbar} E_- T} \right). \quad (3.59)$$

Comparing Eqs. (3.56) and (3.59) we find the lowest energy levels E_{\pm} :

$$E_{\pm} = \frac{\hbar\omega}{2} \mp \hbar K e^{-\frac{1}{\hbar} S_I}. \quad (3.60)$$

that, once we compute the determinant in K (see Appendix C) is the same result in Eq. (3.3) that is obtained with the WKB method.

3.2.2 Application to the decay of a metastable state and bounce solutions

Let us study the decay of a *metastable state*, that is the state of a system in which we have a potential $V(q)$ that presents a local minimum in $q = a$, as those shown in Fig. 3.7. We suppose also in this case that $V(a) = 0$. If we consider a dynamical evolution in a time T , most of the results obtained in the previous subsection can

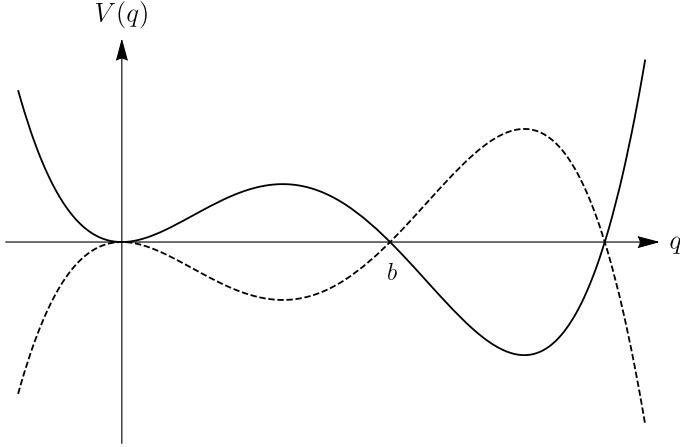


Figure 3.7: Potential with a metastable vacuum. In the example shown in the figure we have $a = 0$. In addition to the minimum a , we have another point b in which the potential is zero, called *classical motion inversion point*. The dashed potential corresponds to the euclidean potential $-V(q)$.

be immediately reapplied: for instance, the classical euclidean equation of motion is still given by

$$m\ddot{q} = \frac{dV(q)}{dq}. \quad (3.61)$$

Again, from the equation of motion we obtain that their solutions corresponds to solutions with vanishing energy $E = 1/2 m\dot{q}^2 - V(q) = 0$, from which it follows that the euclidean action is given by:

$$S_E[q] = \int_{-T/2}^{T/2} m\dot{q}^2 d\tau. \quad (3.62)$$

This time, solving the classical equations of motion with the boundary conditions, we have two kind of solutions:

- the particle remains trapped into the metastable minimum, so that the boundary conditions are $q(-T/2) = q(T/2) = a$. In this case, the solution is given by $q(\tau) = a$ for every time τ ;
- The particle leaves the minimum a to reach the classical motion inversion point b , also called *turning point*. Since in a we have $E = 0$ and in b we have $V(b) = 0$, for the conservation of energy it is clear that in b it is $\dot{q} = 0$. As a consequence, once the particle reaches the turning point b it can only return in the metastable minimum a . Then the boundary conditions are again $q(-T/2) = q(T/2) = a$, so that to these boundary conditions correspond another classical solution in addition to the trivial one, contrary to what happens with the double-well. This solution is called *bounce solution* $q_b(\tau)$ and is shown in Fig. 7.1.

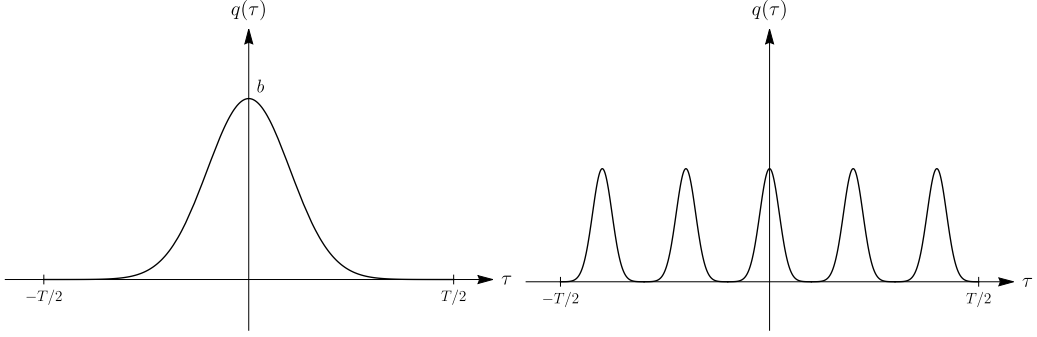


Figure 3.8: Left panel: bounce solution. Right panel: multi-bounce solution.

Then, this analysis allows us to conclude that the only probability amplitude that we have to compute is given by:

$$\langle a | e^{-\frac{1}{\hbar} \hat{H} T} | a \rangle = \mathcal{N} \int \mathcal{D}q(\tau) e^{-\frac{1}{\hbar} S_E[q]} \quad (3.63)$$

with boundary conditions $q(-T/2) = q(T/2) = a$. The amplitude in Eq. (3.63), in addition to consider the contribution to the classical solutions, also takes into account the *multi-bounce* solution shown in Fig. 7.1. In this case, we do not have restrictions on the number n of bounce, so that summing over all the contributions we obtain an exponential rather than an hyperbolic function:

$$\begin{aligned} \langle a | e^{-\frac{1}{\hbar} \hat{H} T} | a \rangle &= \mathcal{N} [\det S''(a)]^{-\frac{1}{2}} \exp \left[K T e^{-\frac{1}{\hbar} S_E[q_b]} \right] = \\ &= \left(\frac{m\omega}{\pi\hbar} \right)^{\frac{1}{2}} e^{-\frac{\omega}{2} T} \exp \left[K T e^{-\frac{1}{\hbar} S_E[q_b]} \right] \end{aligned} \quad (3.64)$$

since the determinant computed in the trivial solution is still given by Eq. (3.28), and also in this case we define $\omega^2 = V''(a)/m$.

In the limit $\omega T \gg 1$, in a similar way to the case of the double well, it is possible to extract the value of the ground state energy E_0 : in fact in this limit we have

$$\langle a | e^{-\frac{1}{\hbar} \hat{H} T} | a \rangle = \langle a | \psi_0 \rangle \langle \psi_0 | a \rangle e^{-\frac{1}{\hbar} E_0 T}. \quad (3.65)$$

In conclusion, comparing Eqs. (3.64) and (3.65), we have:

$$E_0 = \frac{1}{2} \hbar \omega - \hbar K e^{-\frac{1}{\hbar} S_E[q_b]}. \quad (3.66)$$

However this time the corrective factor K due to every bounce is not given by Eq. (3.47). In fact, first of all we note that, respect to the result obtained with the WKB method, we lost a factor $1/2$ in the second term of Eq. (3.66). Moreover, it would not be possible to have a decay: since in the case of a metastable state the *decay rate* is given by $\Gamma = 2 \text{Im} E_0$, if the expression of K were given by Eq. (3.47), then E_0 would be real and therefore $\Gamma = 0$.

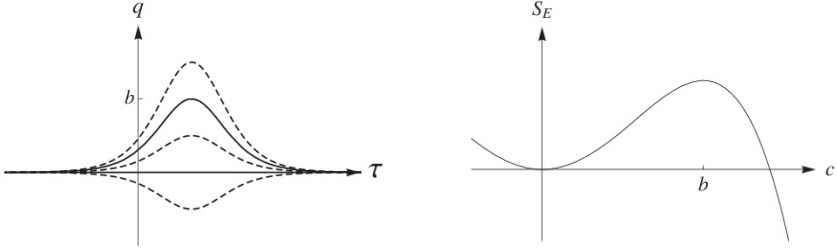


Figure 3.9: Left panel: family of functions parametrized by their stationary point c . Right panel: behaviour of the action in function of c [39].

In fact, for a potential which presents a metastable vacuum it is necessary to take into account some devices regarding the factor K , which will be a pure imaginary quantity. First of all, following the same argument that gives Eq. (3.44), we have to note that the Quantum Fluctuation Operator has still a zero mode:

$$\psi_0(\tau) = \sqrt{\frac{m}{S_b}} \dot{q}_b(\tau), \quad (3.67)$$

where S_b is the action in Eq. (3.62) computed in the bounce solution $q_b(\tau)$. We denote with $\bar{\tau}$ the euclidean instant of time in which the particle reaches the turning point b . Having found that $dq_b/d\tau = 0$ in the turning point b , i.e. for $\tau = \bar{\tau}$, we conclude that correspondingly the bounce solution has a maximum. However, precisely because the bounce solution has a maximum in the turning point $dq_b/d\tau = 0$, from Eq. (3.67) we conclude that the zero mode $\psi_0(\tau)$ has instead a node corresponding to this point.

Now, for the operator $S''_E[q_b]$ the lowest eigenvalues corresponds to an eigenfunction without nodes, the successive eigenvalues corresponds to an eigenfunction with a node, and so on [39]. This property, precisely because the zero mode has a node, allows us to conclude that there must be an eigenfunction without nodes, with an eigenvalue lower than $\lambda_0 = 0$, that is a negative eigenvalues [44].

To understand the origin of these negative modes in a qualitative way, we consider the family of configurations shown in the left panel of Fig. 3.9. We parametrize these configurations through their stationary point (maximum) c . The path with $c = b$ corresponds to the bounce solution, while the one with $c = a$ corresponds to the trivial solution $q(\tau) = a$.

The trivial solution and the bounce solution, being the only solutions to the equations of motion, are the only configurations of this paths family that are stationary for the action $S_E[q]$: the trivial solution is a local minimum for $S_E(c)$, since for a small variation $\delta q(\tau)$ the kinetic energy, as well as the potential one, acquires a positive increment. Then, when c increases from 0 to one of the values corresponding to these variations, the total action can only increase monotonically until it reach the bounce. Since this is the only other stationary point, then it have to be a maximum for the action $S_E(c)$. Thus, when c further increases, the configurations

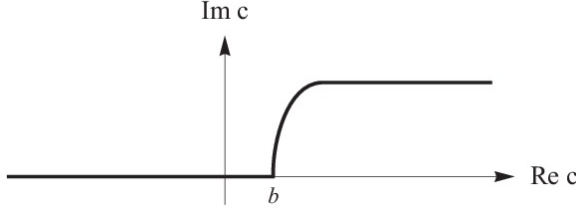


Figure 3.10: Contour in the complex plane over which we solve the integral over the negative mode [39].

begin to stay "for more time" in the region with negative potential energy, so that the action decreases monotonically.

As we know, our path integral is an integral over infinite dimensions, but the only problematic integration is the one over the coefficient of the negative mode. We can see how to treat this integration considering the similar integral

$$J = \int_{-\infty}^{+\infty} \frac{dc}{\sqrt{2\pi\hbar}} e^{-\frac{1}{\hbar}S_c}, \quad (3.68)$$

where $S(c)$ is the function just described and is shown in the right panel of Fig. 3.9. When $c \rightarrow -\infty$ the action increases and the integral converges. On the other hand, when $c \rightarrow \infty$ we have that $S(c) \rightarrow -\infty$ and then the integral diverges. The solution consists in using the analytic continuation to the complex plane: the key observation is the fact that the potential with a metastable state in $q = a$ can be seen as the analytic continuation of a potential with a global minimum in $q = a$. For this last potential, the minimum corresponds to a stable state with a well defined real energy, and the integration over c gives a finite integral. In our case, there are no stable states localized around $q = a$ and the integral over c is not well defined. It becomes well defined when we deform the integration contour for the variable c from the real axes to the complex plane, as shown in Fig. 3.10.

The integration from $-\infty$ to b is clearly real. The imaginary part comes from the remain contour: using the *steepest descent approximation* we obtain

$$\begin{aligned} \text{Im}J &= \text{Im} \left(\int \exp \left\{ - \left[\frac{1}{\hbar}S_b + \frac{1}{2\hbar}S''_E[q_b](c-b)^2 \right] \right\} \frac{dc}{\sqrt{2\pi\hbar}} \right) \\ &= \frac{1}{2} e^{-\frac{1}{\hbar}S_b} [\det S''_E[q_b]]^{-\frac{1}{2}}, \end{aligned} \quad (3.69)$$

where the factor $1/2$ is due to the fact that the contour involves only half of the gaussian peak. Taking into account this factor, the new factor K is given by:

$$K = \frac{i}{2} \sqrt{\frac{S_b}{2\pi\hbar m}} \left[\frac{\det' S''_E[q_b]}{\det S''_E[a]} \right]^{-\frac{1}{2}}. \quad (3.70)$$

Then, from Eq. (3.66) we obtain the decay rate:

$$\Gamma = 2 \text{Im}E_0 = \sqrt{\frac{S_b}{2\pi\hbar m}} \left[\frac{\det' S''_E[q_b]}{\det S''_E[a]} \right]^{-\frac{1}{2}} e^{-\frac{1}{\hbar}S_b}. \quad (3.71)$$

We note that this result is obtained supposing that $V(a) = 0$. In general case in which $V(a) \neq 0$, defining $B = S_b - S(a)$, we obtain

$$\Gamma = \sqrt{\frac{B}{2\pi\hbar m}} \left[\frac{\det' S_E''[q_b]}{\det S_E''[a]} \right]^{-\frac{1}{2}} e^{-\frac{1}{\hbar}B}. \quad (3.72)$$

Specifying the potential $V(q)$ we can also compute the determinant factor in a way similar to the one seen for the double well case.

3.3 Quantum tunnelling in systems with N degrees of freedom

Let us generalize the results seen in the previous subsection to a discrete dynamical system with N degrees of freedom. We introduce the N -dimensional vector $\mathbf{q} \equiv (q_1, \dots, q_N)$ which has as components the generalized coordinates q_i associated to every degree of freedom of the system. The lagrangian describing this system can be written in a compact way as:

$$\mathcal{L} = \frac{1}{2} \sum_{i=1}^N m\dot{q}_i^2 - V(q_1, \dots, q_N) = \frac{1}{2} m\dot{\mathbf{q}}^2 - V(\mathbf{q}). \quad (3.73)$$

The extension of the WKB method to the case of a system with N degrees of freedom is based on the search of the *most probable escape path* (MPEP) [39, 45, 46]: in fact, to study the tunnelling from a local minimum of the potential, it is not sufficient to know the probability amplitude to pass through the barrier, but also the preferential point in which the particle emerges from the barrier in the classically permitted region. In fact the barrier, being multidimensional, can be crossed in any direction.

Every possible *path* through the barrier can be parametrized by a curve $\mathbf{q}(s)$, where the parameter s is defined by the relation:

$$(ds)^2 = \sum_{i=1}^N \left(\frac{\partial q_i}{\partial s} ds \right)^2 = (d\mathbf{q})^2. \quad (3.74)$$

If we choose $s_i = 0$, the initial condition for the path $\mathbf{q}(s)$ is given by $\mathbf{q}(0) = \mathbf{q}_0$: in this point, the potential $V(\mathbf{q})$ is equal to the energy of the particle $E \equiv V(\mathbf{q}_0)$. Instead the final point $\mathbf{q}_f = \mathbf{q}(s_f)$ is not univocal, since it depends from the particular path. The generic $\mathcal{P}(q_0 \rightarrow q_f) \equiv \mathbf{q}(s)$, once parametrized in this way, constitutes a one-dimensional trajectory for which the correspondent *transmission integral* can be defined, similarly to the one dimensional case:

$$\begin{aligned} B[\mathcal{P}] &= 2 \int_{\mathbf{q}_0}^{\mathbf{q}_f} \sqrt{2m[V(\mathbf{q}) - E]} d\mathbf{q} \quad \Rightarrow \\ B[\mathcal{P}] &= 2 \int_0^{s_f} \sqrt{2m[V[\mathbf{q}(s)] - E]} ds \end{aligned} \quad (3.75)$$

where we have used Eq. (3.74). Then the MPEP is the path that minimizes the transmission integral $B[\mathcal{P}]$ in Eq. (3.75). In conclusion, following the WKB approximation, the tunneling amplitude will be given by $Ae^{-\frac{B}{2\hbar}}$, where B is precisely the transmission integral (3.75), while A is a parameter to be determined.

In particular, to minimize the integral $B[\mathcal{P}]$ it is useful to use the lagrangian formalism. According to the *Jacobi principle* of classical mechanics, assigned a physical system described by the lagrangian \mathcal{L} introduced in Eq. (3.73), the path $\mathbf{q}(s) : \mathbf{q}_0 \rightarrow \mathbf{q}_f$ that minimizes the integral

$$I = \int_0^{s_f} \sqrt{2m [E - V(\mathbf{q}(s))] } \, ds$$

provides the solution to the equations of motion

$$\frac{1}{2}m\dot{\mathbf{q}}^2 + V(\mathbf{q}) = E. \quad (3.76)$$

Instead, according to the *Hamilton principle*, the same solution can be found minimizing the action that describes the system:

$$S[q] = \int_{t_0}^{t_f} \mathcal{L}(\mathbf{q}, \dot{\mathbf{q}}) dt = \int_{t_0}^{t_f} \left[\frac{1}{2}m\dot{\mathbf{q}}^2 - V(\mathbf{q}) \right] dt \quad (3.77)$$

with the boundary conditions $\mathbf{q}(t_0) = \mathbf{q}_0$ e $\mathbf{q}(t_f) = \mathbf{q}_f$.

This result suggests that the path which minimizes the transmission integral $B[\mathcal{P}]$ given in Eq. (3.75) can be obtained as solution that minimizes the following action:

$$S_E[q] = \int_{\tau_0}^{\tau_f} \left[\frac{1}{2}m\dot{\mathbf{q}}^2 + V(\mathbf{q}) \right] d\tau \quad (3.78)$$

which is nothing but the euclidean action obtained performing a Wick rotation $\tau = it$ (from now on, the point denotes a derivative respect to τ , and not respect to t). Applying the Hamilton principle to Eq. (3.78), i.e. finding the stationary points of the action S_E , we obtain *the euclidean equation of motion*:

$$m\ddot{\mathbf{q}}(\tau) = \nabla V(\mathbf{q}). \quad (3.79)$$

If $\bar{\mathbf{q}}(\tau)$ is the general solution of Eq. (3.79), multiplying for $\dot{\mathbf{q}}$ and following a similar argument to the one of Eq. (3.32) (this time we have $E = V(\mathbf{q}) \neq 0$), we obtain:

$$\frac{1}{2}m\dot{\mathbf{q}}^2 = V(\bar{\mathbf{q}}) - E = V(\bar{\mathbf{q}}) - V(\mathbf{q}_0). \quad (3.80)$$

Then, we can compute the euclidean action in the solution $\bar{\mathbf{q}}(\tau)$ of the equation of motion:

$$\begin{aligned} S_E[\bar{\mathbf{q}}] &= \int_{\tau_0}^{\tau_f} 2[V(\bar{\mathbf{q}}) - V(\mathbf{q}_0)] d\tau + \int_{\tau_0}^{\tau_f} V(\mathbf{q}_0) d\tau = \\ &= \int_{\tau_0}^{\tau_f} (m\dot{\mathbf{q}}^2)^{\frac{1}{2}} \sqrt{2[V(\bar{\mathbf{q}}) - V(\mathbf{q}_0)]} d\tau + \int_{\tau_0}^{\tau_f} V(\mathbf{q}_0) d\tau = \\ &= \int_0^{s_f} \sqrt{2m[V(\bar{\mathbf{q}}(s)) - V(\mathbf{q}_0)]} ds + \int_{\tau_0}^{\tau_f} V(\mathbf{q}_0) d\tau, \end{aligned} \quad (3.81)$$

where in the last step we have used Eq. (3.74) for the change of variable in the first integral. This equation put in evidence the relation between the euclidean action (3.78) and the transmission integral (3.75):

$$S_E[\bar{\mathbf{q}}] = \frac{1}{2}B[\bar{\mathcal{P}}] + \int_{\tau_0}^{\tau_f} V(\mathbf{q}_0)d\tau. \quad (3.82)$$

In the case of a double well potential, as we know, the *transition amplitudes* are characterized by an *instanton* solution, whose transmission integral according to Eq. (3.82) is given by:

$$\frac{1}{2}B[\bar{\mathcal{P}}] = S_E[\bar{\mathbf{q}}] - S_E[\mathbf{q}_0]. \quad (3.83)$$

In the case in which we have a tunneling between a local minimum \mathbf{q}_0 and a *turning point* \mathbf{q}_f that is not a minimum of the potential, the turning point $\mathbf{q}_f \equiv \bar{\mathbf{q}}(\bar{\tau})$ is reached in the time interval $[-\infty, \bar{\tau}]$, where $\bar{\tau}$ is the euclidean time for which the first derivative of the solution vanish, $\dot{\mathbf{q}}(\bar{\tau}) = 0$, as the velocity of the particle vanish in the turning point (classical inversion point of the motion). Since the lagrangian is invariant under *time reversal* transformations, the solution can be continued in such a way that the path ends in $\bar{\mathbf{q}}(\infty) = \mathbf{q}_0$, and correspondingly the euclidean action is doubled. Then to the solution to the equation of motion, i.e. the *bounce solution*, corresponds the transmission integral

$$B[\bar{\mathcal{P}}] = S_E[\bar{\mathbf{q}}] - S_E[\mathbf{q}_0]. \quad (3.84)$$

In conclusion, the *bounce* corresponds to a path that origins in the local minimum \mathbf{q}_0 , continues to the turning point $\mathbf{q}_f \equiv \bar{\mathbf{q}}(\bar{\tau})$, and ends in \mathbf{q}_0 .

3.4 Quantum tunneling in QFT

The description of the quantum tunneling through functional formalism is useful because it can be easily generalized to the case of continuous dynamical system, i.e. a system with *infinity degrees of freedom*, and then in the contest of a *quantum field theory*.

In the transition to the continuum limit, the N -dimensional configuration space of the generalized coordinate $q_i(t)$ is substituted by an ∞ -dimensional configuration space, and then the generalized coordinates $q_i(t)$ become continuous functions $\phi_a(x)$ in space and time.

The transition to the continuum limit, as we will see, implies the presence of additional *zero modes*. Regarding the *negative modes* we have seen that in the instanton case (double well problem) there are no negative modes, while in the case of the bounce solution (decay of a metastable state) the presence of a negative mode is related to the fact the path is extended to the classically permitted region, and this is due to the instability of the local minimum state in $q = a$. The instability of

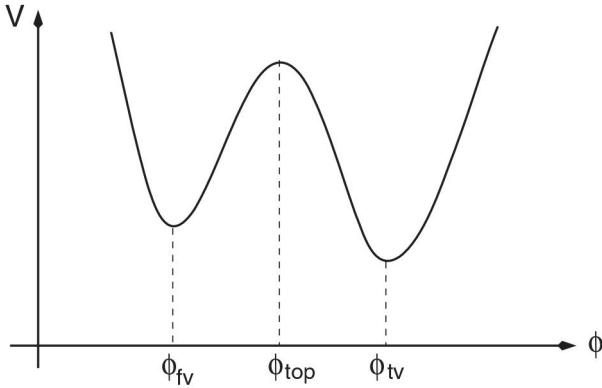


Figure 3.11: Scalar potential with two non-degenerate minima [39].

the local minimum state is independent on the number of degrees of freedom of the system, so that the argument that we have seen in quantum mechanics is valid also in the case of the bounce solution in quantum field theory [38, 39], i.e. there is no appearance of additional negative modes.

As a consequence, in the generalization to a quantum field theory the divergences emerge both in the computation of the functional determinants [47] and in the counterterms of the euclidean action: these latter are removed by renormalization. From now on, we will work in natural units $\hbar = c = 1$.

3.4.1 Bounce in QFT: vacuum decay

Let us consider a scalar theory, described by the lagrangian density

$$\mathcal{L} = \frac{1}{2} \partial_\mu \phi \partial^\mu \phi - V(\phi), \quad (3.85)$$

where the potential $V(\phi)$, shown in Fig. 3.11, presents two non-degenerate minima: the minimum ϕ_{fv} is a local minimum and represents a state of *false vacuum* [40, 41], while the minimum ϕ_{tv} is an absolute minimum, i.e. it is the ground state of the theory, called *true vacuum*. Classically the state ϕ_{fv} is stable, while from the quantum point of view it can decay through *quantum tunneling* in the state ϕ_{tv} [48]. The potential $V(\phi)$ is a density of potential energy, therefore what actually needs to be analyzed is the integral of $V(\phi)$ over all the space \mathbb{R}^3

$$U[\phi(\mathbf{x})] = \int d^3\mathbf{x} \left[\frac{1}{2} (\nabla \phi)^2 + V(\phi) \right]. \quad (3.86)$$

If the false vacuum decays following a series of configurations spatially homogeneous, this would require the tunneling through an infinite potential energy barrier: the tunneling amplitude in this case would vanish. Instead, the false vacuum decays through a tunneling process, which starts from a spatially homogeneous state, in

a state with a region in which there is a bubble of true vacuum immersed in a background of false vacuum. In this case the tunneling, that is the nucleation of a bubble, can originate at any point $\mathbf{x} \in \mathbb{R}^3$ and then the *decay rate* Γ , that depends from the volume of the physical space, is formally infinite; the quantity physically relevant is then the *decay rate for volume unity* Γ/V [38, 39].

A continuous dynamical system is a system with infinite degrees of freedom, so that the possible path that connects ϕ_{fv} and ϕ_{tv} are infinite. Every path is defined by a succession of field configurations, constitutes a transversal section of the potential barrier, and it has to conclude in an *end-point* which is at the same energy of the starting potential, $V_{fv} \equiv V(\phi_{fv})$. As we know, the path effectively followed by the system is obtained minimizing the classical euclidean action and constitutes the *bounce solution* of the euclidean equation of motion. The equation of dynamical evolution of the scalar $\phi(x)$ are obtained from the Euler-Lagrange equations:

$$\frac{\partial \mathcal{L}}{\partial \phi} = \partial_\mu \frac{\partial \mathcal{L}}{\partial (\partial_\mu \phi)} \quad \Rightarrow \quad \frac{\partial^2}{\partial t^2} \phi - \nabla^2 \phi + \frac{dV}{d\phi} = 0. \quad (3.87)$$

Then, passing to the euclidean formalism, the equations of motion become:

$$\frac{\partial^2}{\partial \tau^2} \phi + \nabla^2 \phi = \frac{dV}{d\phi} \quad (3.88)$$

which are obtained starting from the Euclidean action

$$S_E[\phi] = \int d\tau d^3\mathbf{x} \left[\frac{1}{2} \dot{\phi}^2 + \frac{1}{2} (\nabla \phi)^2 + V(\phi) \right]. \quad (3.89)$$

With the appropriate boundary conditions, that we will see later, from this equation we obtain the *bounce solution* $\phi_b(\mathbf{x}, t)$. The decay rate for volume units has the following form [39]

$$\frac{\Gamma}{\mathcal{V}} = A e^{-B} \quad \text{con } B = S_E[\phi_b] - S_E[\phi_{fv}], \quad (3.90)$$

where $S_E[\phi_b]$ is the euclidean action computed in the bounce solution, while

$$S_E[\phi_{fv}] = \int d\tau d^3\mathbf{x} V_{fv}$$

is the euclidean action computed in the homogeneous solution of false vacuum. Instead, the factor A comes from a computation of functional determinants [47]. Although both of these actions are infinite, their difference is finite.

Solving Eq. (3.88) is equivalent to find a static solution in four spatial dimensions: apparently, this is forbidden by the Derrick theorem [39, 49]. However, in the demonstration of the Derrick theorem we assume that ϕ reaches the absolute minimum of V at infinity, and this does not happen for the bounce solution. Now, for a theory in D spatial dimensions we can define:

$$I_K = \frac{1}{2} \int d\tau d^D x (\partial_\mu \phi_b)^2 \quad I_V = \int d\tau d^D x [V(\phi_b) - V_{fv}].$$

With a manipulation similar to the one of the Derrick theorem, we obtain

$$I_V = \frac{1-D}{1+D} I_K. \quad (3.91)$$

As a consequence, we conclude that

$$B = S_E[\phi_b] - S_E[\phi_{fv}] = I_K + I_V = \frac{2}{1+D} I_K. \quad (3.92)$$

In our case, $D = 3$ so that we obtain:

$$B = \frac{1}{2} \int \left\{ \frac{1}{2} \partial_\mu \phi_b(x) \partial^\mu \phi_b(x) \right\} d^3 \mathbf{x} d\tau = \frac{1}{2} I_K. \quad (3.93)$$

Let us determine the boundary conditions for Eq. (3.88) needed to obtain the bounce solution: such conditions are obtained from the fact that the bounce represents a path through the configurations space that starts from the state ϕ_{fv} at the time instant $\tau_{in} = -\infty$, reaches the *turning point* in the opposite side of the barrier at a time instant $\bar{\tau}$, and then returns in the initial configuration at $\tau_{fin} = +\infty$ [38, 39]

$$\phi(\mathbf{x}, \pm\infty) = \phi_{fv} \quad \forall \mathbf{x} \in \mathbb{R}^3. \quad (3.94)$$

We note that it must be $\partial\phi/\partial\tau = 0$ everywhere along the hypersurfaces $\tau = \tau_{ini}$ and $\tau = \bar{\tau}$, since these are the hypersurfaces of the turning point where the kinetic energy is zero. Moreover, we have to require that all the configurations along the *tunneling path* have finite potential energy, comparable to $V(\phi_{fv})$, so that:

$$\phi(|\mathbf{x}| = \infty, \tau) = \phi_{fv} \quad \forall t \in \mathbb{R}. \quad (3.95)$$

Now we note that the euclidean equation of motion in Eq. (3.88) and the boundary conditions in Eqs. (3.94) and (3.95) show a symmetry respect to the transformations defined by the group $O(4)$, i.e. respect to the rotations in the 4-dimensional euclidean space. Then we can fix $\bar{\tau} = 0$, that is we choose the origin as the centre of symmetry and use the $O(4)$ invariance to find the bounce. In fact the bounce, being a non-trivial solution of the PDEs invariant under the $O(4)$ group transformations, it must also be invariant with respect to these transformations. In order to exploit the $O(4)$ invariance, we define

$$r = \sqrt{\tau^2 + \mathbf{x}^2}. \quad (3.96)$$

This quantity represents the distance of the generic point (τ, \mathbf{x}) of the euclidean space from the origin, that is the *radial coordinate*. Since the *bounce solution* $\phi_b(x)$ is invariant respect to the $O(4)$ symmetry, we can suppose that it depends exclusively from the distance r of the generic point (τ, \mathbf{x}) from the origin of the euclidean space, that is $\phi_b(\tau, \mathbf{x}) \equiv \phi_b(r)$. Taking into account the definition in Eq. (3.96), the euclidean equations of motion (3.88) become

$$\ddot{\phi}(r) + \frac{3}{r} \dot{\phi}(r) = \frac{dV(\phi)}{d\phi} \quad (3.97)$$

where the dots denote the derivatives of the field $\phi(r)$ respect to the variable r . The boundary conditions in Eqs. (3.94) and (3.95) become a single condition for Eq. (3.97):

$$\lim_{r \rightarrow \infty} \phi(r) = \phi_{fv}. \quad (3.98)$$

Moreover, we have to require that the solution is not singular in the origin. In particular, for the condition of regularity in the origin we have

$$\dot{\phi}(0) = 0. \quad (3.99)$$

Having the $O(4)$ symmetry, the *tunneling exponent* in Eq. (4.15) becomes

$$B = 2\pi^2 \int_0^\infty dr r^3 \left\{ \frac{1}{2} \dot{\phi}_b^2(r) + V(\phi_b) - V_{fv} \right\}. \quad (3.100)$$

In conclusion, taking into account of the $O(4)$ symmetry, we have reduced a problem with infinite degrees of freedom to the study of a simple differential equation. The existence of a bounce solution for the equation of motion in Eq. (3.88), i.e. a solution compatible with the boundary conditions (3.94) and (3.95) was demonstrated by Coleman using his argument of the *overshoot-undershoot method* [39].

At this point we proceed to the determination of the decay rate for volume units [38, 39]. To determine Γ/\mathcal{V} it is sufficient to take into account the changing that we encounter in the passage to the continuum limit, and then modifying appropriately the relation of Eq. (3.72) for the decay width obtained in the context of quantum mechanics. Since the bounce solution, in the context of the quantum field theory, is not spatially homogeneous, in addition to the zero mode corresponding to the invariance under time translations, there are other three zero modes corresponding to the invariance under space translations, i.e. a zero mode for each of the three generators of the spatial translations in \mathbb{R}^3 . Moreover, as we have just explained, the passage to the continuum limit can not give rise to new negative modes. Another point of fundamental importance in the study of the decay rate is its renormalization: some divergences are cancelled by ratio of determinants [47], the other divergences have to be treated and in particular we can use the method of counterterms of the renormalized perturbation theory.

In conclusion, the *decay width for volume units* is

$$\frac{\Gamma}{\mathcal{V}} = \left\{ \prod_{a=0}^4 \sqrt{\frac{N_a}{2\pi}} \right\} \left| \frac{\det' S_E''[\phi_b]}{\det S_E''[\phi_{fv}]} \right|^{-\frac{1}{2}} \exp \left\{ - (S_E[\phi_b] - S_E[\phi_{fv}]) \right\}, \quad (3.101)$$

where the euclidean actions that appear in the previous equation are written in terms of the renormalized parameters and of the counterterms. The factor N_a is the normalization factor of the zero mode corresponding to the translations along the direction x_a of the Minkowski space: for the $O(4)$ symmetry of the bounce, these factors have to be equal and, using Eq. (3.92), they are given by

$$N_a = \int d^4x (\partial_a \phi)^2 = \frac{1}{4} \int d^4x (\partial_\mu \phi)^2 = \frac{1}{2} I_K = B.$$

As a consequence, we have

$$\frac{\Gamma}{\mathcal{V}} = \left(\frac{B}{2\pi} \right)^2 \left| \frac{\det' S_E''[\phi_b]}{\det S_E''[\phi_{fv}]} \right|^{-\frac{1}{2}} e^{-\{S_{ct}[\phi_b] - S_{ct}[\phi_{fv}]\}} e^{-B} \quad (3.102)$$

where the action S_{ct} that appears in Eq. (3.102) is the action of the counterterms. In conclusion, we observe that once the *decay width* Γ is determined we can obtain the *tunneling time* $\tau \sim \Gamma^{-1}$ associated to the decay of the vacuum.

3.4.2 Bounce in QFT: inclusion of gravity

Now we want to include the effect of gravity in the study of the stability problem in QFT. In fact, there are many cases in which gravity becomes important: the most obvious case is the one in which we have a transition involving a mass scale close to the Planck scale. Gravitational effects can also come into play at lower mass scales if the "true vacuum bubble" is formed with a size large enough to be sensitive to the curvature of spacetime (*strong gravity regime*).

Let us start with a brief description of the initial state of false vacuum, which requires some observations when gravity is included. The scalar field is obviously uniform, equal to ϕ_{fv} everywhere. The nature of spacetime depends on the value of the potential in the false vacuum. If $V_{fv} \equiv V(\phi_{fv}) = 0$, the *false vacuum spacetime* is simply a Minkowski flat spacetime. If, on the other hand, V_{fv} is not zero, then it will be equal to a non-zero cosmological constant and the false vacuum will be either a de Sitter spacetime or an anti-de Sitter spacetime, depending on whether V_{fv} is either positive or negative, respectively [39]. Regarding the tunneling problem, Coleman and de Luccia have shown that including gravity the nucleation rate will still be obtained from a bounce solution, but with a Euclidean action that now includes gravitational contribution. In other words

$$\frac{\Gamma}{\mathcal{V}} = A e^{-B} = A e^{-\{S[\phi_b] - S[\phi_{fv}]\}} \quad (3.103)$$

where ϕ_b is a bounce solution of the Euler-Lagrange equations obtained from the gravitational action [50].

To obtain the equations of motion with the inclusion of gravity, we consider the minimal action that is obtained including the Einstein-Hilbert term:

$$S[\phi, g_{\mu\nu}] = \int d^4x \sqrt{g} \left[-\frac{R}{16\pi G} + \frac{1}{2} g^{\mu\nu} \nabla_\mu \phi \nabla_\nu \phi + V(\phi) \right] \quad (3.104)$$

where R is the Ricci scalar and G is the Newton gravitational constant. The potential $V(\phi)$, as in the case of flat spacetime, presents a local minimum (*false vacuum*) at $\phi = \phi_{fv}$, and a global minimum (*true vacuum*) at $\phi = \phi_{tv}$.

We know that in flat spacetime, for a theory with a single scalar field, the bounce solution that minimizes the action has an $O(4)$ symmetry. Since there is no reason

why gravitational effects can break this symmetry, we can assume that even in the presence of gravity the bounce is invariant under 4-dimensional rotations. Basing on this assumption, we can determine an euclidean metric that is invariant by rotations: we start from the 3-dimensional case, in which the generic metric invariant under rotations is the one of the 3-sphere. On each sphere we can introduce the angular coordinates in the usual way and therefore we define a radial curve as the curve obtained for fixed angular coordinates. For the rotational invariance, the radial curve has to be perpendicular to the intersecting 3-spheres: we choose our radial coordinate r to measure the distance along these radial curves. As a result, the metric we are looking for can be written in the form

$$ds^2 = dr^2 + \rho^2(r)d\Omega_3^2 \quad (3.105)$$

where $d\Omega_3^2$ is the metric of the unitary 3-sphere, while ρ is the curvature radius for each 3-sphere at fixed r coordinate.

From the action in Eq. (3.104), we obtain the Euler-Lagrange and Einstein field equations ($\kappa = 8\pi G$):

$$R_{\mu\nu} - \frac{1}{2}g_{\mu\nu}R = \kappa T_{\mu\nu} \quad (3.106)$$

$$T_{\mu\nu} = \partial_\mu\phi\partial_\nu\phi - g_{\mu\nu}\left[\frac{1}{2}\partial_\mu\phi\partial^\mu\phi + V(\phi)\right] \quad (3.107)$$

$$\partial_\mu\partial^\mu\phi = \frac{dV(\phi)}{d\phi}. \quad (3.108)$$

Using the metric given in Eq. (3.105), the equations in (3.106) and (3.108) become:

$$\ddot{\rho} + 3\frac{\dot{\rho}}{\rho}\dot{\phi} = \frac{dV}{d\phi} \quad \dot{\rho}^2 = 1 - \frac{\kappa}{3}\rho^2\left(-\frac{1}{2}\dot{\phi}^2 + V(\phi)\right) \quad (3.109)$$

where the dots denotes the differentiation respect to the radial coordinate r . The bounce solution needed to compute the false vacuum transition rate is now given by the field solution and the metric solution, respectively $\phi_b(r)$ and $\rho_b(r)$, of these coupled differential equations, once we have identified the appropriate boundary conditions. Differentiating Eq. (3.109-b) with respect to r , we obtain another useful equation which, in particular, is more stable for numerical analysis:

$$\ddot{\rho} = -\frac{\kappa}{3}\rho\left(\dot{\phi}^2 + V(\phi)\right). \quad (3.110)$$

In the derivation of Eqs. (3.109) from Einstein equations, we can also compute the Ricci scalar using the metric in Eq. (3.105):

$$R = -\frac{6}{\rho^2}(\rho\ddot{\rho} + \dot{\rho}^2 - 1). \quad (3.111)$$

However, this expression is not useful to compute numerically the tunneling exponent B . To obtain an expression numerically more stable, computing the trace in

Eq. (3.106), we have the following general expression:

$$\frac{R}{\kappa} = \partial_\mu \phi \partial^\mu \phi + 4V(\phi). \quad (3.112)$$

We will use soon this last expression in the action to explicit the Einstein-Hilbert term.

The boundary conditions for the field equations depend on the topology of the solution which, as often happens in general relativity, cannot be specified in advance. In particular, they depend on the asymptotic behavior of ρ : in the case of our interest, i.e. the one in which the spacetime of the false vacuum is a Minkowski spacetime, we have that $V_{fv} = 0$. Then, Eq. (3.109-b) calculated in the false vacuum solution reduces to $\dot{\rho}^2 = 1$, since ϕ_{fv} is uniform and therefore $\dot{\phi}$ vanishes. Consequently, the curvature ρ is given by $\rho(r) = r + c$, where c is an integration constant: this straight line is therefore the straight line to which the solution ρ of the equations of motion tends asymptotically. In other words, as anticipated at the beginning of this subsection, if $V_{fv} = 0$ the spacetime is reduced to simple flat Minkowski spacetime in the false vacuum, and the solution has the topology of \mathbb{R}^4 . Given the $O(4)$ invariance of the spacetime, we can take the boundary condition $\rho(0) = 0$, and this will be the only zero for the curvature ρ . Finally, as regards the ϕ field, the boundary conditions will always be given by Eqs. (3.98) and (3.99). Summing up, the boundary conditions for the bounce solution of Eq. (3.109) are:

$$\phi(\infty) = 0 \quad \dot{\phi}(0) = 0 \quad \rho(0) = 0. \quad (3.113)$$

Finally, let us compute the tunneling exponent B using Eq. (3.112) to obtain a general expression for the action. Inserting Eq. (3.112) in the action (3.104) to explicit the term that contain the Ricci scalar R , after simple manipulations we get:

$$S[\phi, g_{\mu\nu}] = - \int d^4x \sqrt{g} V(\phi). \quad (3.114)$$

Using the $O(4)$ symmetry, Eq. (3.114) becomes:

$$S[\phi, \rho] = -2\pi^2 \int_0^\infty dr \rho^3 V(\phi). \quad (3.115)$$

The integration extremes in Eq. (3.115) are due to the fact that we are in a curved background with the topology of \mathbb{R}^4 , so that $r \in [0, \infty]$. It is worth to note that if we compute the action in the false vacuum trivial solution of the equations (3.109), we obtain $S_{fv} \equiv S[\phi_{fv}, \rho_{fv}] = 0$, since in our topology $V(\phi_{fv}) = 0$. In conclusion, from Eq. (3.115) we obtain that the tunneling exponent is simply given by $B = S[\phi_b, \rho_b]$.

Chapter 4

New solutions in the presence of New Physics beyond the Standard Model

In Chapter 2 we have seen how the radiative corrections to the Higgs potential introduce the problem of the *stability of the electroweak vacuum*, since we have the formation of a second minimum in addition to the EW one, where our Universe sits. In this Chapter we present a brief overview of the state of art of this problem up to the results presented in [51]. Then, using the tools introduced in Chapter 3, we move on to the computation of the bounce solution needed to obtain the decay rate of the EW vacuum in presence of gravity. In particular, the new results obtained in [51] with the introduction of New Physics (NP) in the Standard Model (SM) are illustrated.

4.1 Stability problem of the electroweak vacuum in Standard Model

The discovery of the Higgs boson, theoretically postulated as a fundamental ingredient of the electroweak theory to introduce the masses of the SM particles, by the ATLAS and CMS collaborations of the *Large Hadron Collider* [52, 53] led to results that proved to be perfectly consistent with the theoretical predictions of the Standard Model. Moreover, one of the most important goals of present theoretical and experimental particle physics is the search for New Physics (NP) beyond the Standard Model (BSM), even though direct experimental searches up to now have not revealed any sign of it. These results have revived a great interest in the idea that New Physics can only manifest at very high energy scales, and in particular at the *Planck scale* M_P .

In this context, the study of the stability of the electroweak vacuum can give an important boost, as we will see. For this study, as we have seen in Chapter 2, it is needed to know the Higgs effective potential $V_{eff}(\phi)$ up to very high values

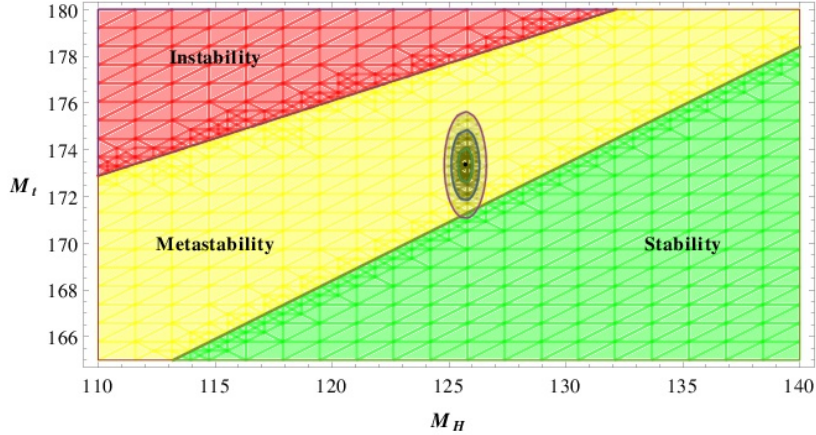


Figure 4.1: Phase diagram in the plane (m_H, m_t) that is obtained with the standard analysis of the stability problem, i.e. considering the Standard Model alone. The determination of the stability and instability lines allows to divide the (m_H, m_t) plane into three regions, and in particular the point (m_H^{exp}, m_t^{exp}) , identified by the current experimental values of the masses of the Higgs boson and the top quark, is in the region of metastability and is close to the stability line [54].

of the Higgs field $\phi(x) \equiv H(x)$. If we denote with v the point in which the Higgs potential has a minimum, i.e. where we have the *electroweak minimum* $v \sim 246$ GeV, the effective potential $V_{eff}(\phi)$ due to the *loop corrections* associated to quark top, has a maximum for $\phi > v$, and subsequently decreases forming a new minimum in $\phi = \phi_{min} \gg v$. For simplicity we can normalize the potential $V_{eff}(\phi)$ in such a way that $V_{eff}(v) = 0$, and with this normalization choice the *instability scale*, $\phi_{inst} \gg v$, is determined by the following condition

$$V_{eff}(\phi_{inst}) = 0, \quad (4.1)$$

i.e. ϕ_{inst} is a zero of the Higgs effective potential immediately following the electroweak minimum v . The instability scale is mainly determined by the values of the masses of the Higgs boson and the top quark. The experimental values [55–60] for these values are:

$$m_H^{exp} = 125.7 \pm 0.25 \text{ GeV} \quad m_t^{exp} = 173.34 \pm 1.3 \text{ GeV} \quad (4.2)$$

and considering their central values, we find:

$$\phi_{inst} \sim 10^{11} \text{ GeV}.$$

For $\phi > \phi_{inst}$ the Higgs effective potential becomes negative and for $\phi \gg v$ it forms the second minimum ϕ_{min} . The *condition of stability* depends on the specific values of the parameters of the Standard Model, and in particular on the values of the

mass of the Higgs boson m_H and on the mass of the top quark m_t . If the minimum is higher than the electroweak vacuum, then the latter is *absolutely stable*, otherwise the electroweak vacuum is a state of *false vacuum*, i.e. it is a *metastable state* which decays through *quantum tunneling* towards the state ϕ_{min} of *true vacuum*. In the latter case it is necessary to compare the average life τ of the electroweak vacuum with the age of the Universe T_U . Summing up:

- The electroweak vacuum v is stable, i.e. it is a state of *true vacuum*, if we have that $V_{eff}(\phi_{min}) > V_{eff}(v)$. This condition defines, in the space of parameters (m_H, m_t) , the *region of absolute stability*.
- The electroweak vacuum v is unstable, i.e. it is a state of *false vacuum*, if we have that $V_{eff}(\phi_{min}) < V_{eff}(v)$ and that the average life τ of the vacuum is $\tau < T_U$. In the (m_H, m_t) plane these conditions identify the *region of absolute instability*.
- The electroweak vacuum v is metastable if we have that $V_{eff}(\phi_{min}) < V_{eff}(v)$ and that the average life of the vacuum is $\tau > T_U$. This case, which is what is realized considering the current experimental values for m_H and m_t , is usually called *metastability scenario*.

To study the stability of the electroweak vacuum we have first to determine the functional form of the Higgs effective potential $V_{eff}(\phi)$ (see Chapter 2). In general, the condition of stability of the electroweak vacuum is studied varying the masses m_H and m_t and the results are presented through *phase diagrams* of stability in the plane (m_H, m_t) . This plane is thus divided into the regions of stability, metastability and instability, and the straight lines that separate these regions are defined by the conditions [61–64]

$$V_{eff}(v) = V_{eff}(\phi_{min}) \quad \text{Stability line} \quad (4.3)$$

$$V_{eff}(v) > V_{eff}(\phi_{min}) \quad \text{and} \quad \tau = T_U \quad \text{Instability line.} \quad (4.4)$$

According to this analysis, when the central values for the masses of the Higgs boson and the top quark are considered, the electroweak minimum is in the region of metastability and the average life of the electroweak vacuum is enormously greater than the life of the Universe. As is clear from Fig. 4.1 [65], the current experimental values for the masses of the Higgs boson and the top quark [55–60] are compatible with a metastable universe, very close to the region of stability.

The EW vacuum stability condition was first studied in a flat spacetime background, and the interesting possibility that the SM is valid all the way up to the Planck scale M_P , meaning that NP shows up only at this scale, was investigated. In such a scenario, naturally prompted by the lack of direct observation of hints of new physics, the analysis was performed under the assumption [66] that the presence of NP at M_P could be neglected for the computation of the tunneling time τ from the

false to the true vacuum of the SM, so that τ was calculated by considering SM interactions only [62–64, 66–70]. In particular, in [67] it was argued that the reason why NP at M_P (even if present) can be neglected in the calculation of the tunneling rate is due to the fact that the instability scale $\phi_{\text{inst}} \sim 10^{11}$ GeV is sufficiently smaller than M_P , i.e. a decoupling effect was expected.

However, it was later realized that the EW vacuum is very sensitive to unknown NP even if it lives at scales far away from ϕ_{inst} , and the decay rate of the EW vacuum can be strongly modified by its presence [54, 65, 71, 72]. The reason why the decoupling theorem does not hold in this case is that tunneling is a non-perturbative phenomenon [72], while the former applies when calculating scattering amplitudes in perturbation theory at energies E much lower than M_{cut} , the physical cut-off scale of the theory under investigation (M_P , M_{GUT} , ...). In this case the contributions to scattering amplitudes from physics that lives at M_{cut} is suppressed by factors of E/M_{cut} to the appropriate power, and this is how physics at the scale M_{cut} is decoupled from physics at the scale E .

Instead, as we have seen in Chapter 3, for the tunneling phenomena the bulk of the contribution to τ comes from the exponential of the (Euclidean) action calculated at the saddle point of the path integral for the tunneling rate, i.e. the *bounce solution* to the (Euclidean) Euler-Lagrange equation [38], and for this tree level contribution no suppression factors of the kind $(E/M_P)^n$ can ever appear. If the Higgs potential is modified by the presence of NP at M_P , the new bounce is certainly different from the one obtained when these terms are neglected. The action calculated for this new bounce solution is also modified and (once exponentiated) it can give rise to a value of τ enormously different from the one obtained when the NP terms are neglected.

As we have said in Section 3.4.2, the inclusion of gravity in the vacuum stability analysis was pioneered in [50] by Coleman and de Luccia. For the transition from a false Minkowski vacuum to a true Anti-de Sitter (AdS) vacuum, it was shown that, when the size of the Schwarzschild radius of the true vacuum bubble is much smaller than its size, i.e. when gravitational effects are weak, the probability of materialization of such a bubble is close to the flat spacetime result, while when the Schwarzschild radius becomes comparable to the bubble size, i.e. in a strong gravitational regime, the presence of gravity stabilizes the false vacuum, preventing the materialization of a true vacuum bubble. In other words, gravity tends to stabilize the false vacuum, and in a strong gravity regime the materialization of bubbles of true vacuum is quenched. Coleman and collaborators considered a scalar theory where the potential $V(\phi)$ has an energy density difference $V(\phi_{\text{fv}}) - V(\phi_{\text{tv}})$ much smaller than the height of the “potential barrier”, $V(\phi_{\text{top}}) - V(\phi_{\text{fv}})$, where $V(\phi_{\text{top}})$ is the maximum of the potential between the two minima. Given this condition, the true vacuum bubble is separated from the false vacuum sea by a “thin wall”, and this allows to treat the problem analytically, within the so-called *thin-wall*

approximation.

However, the SM case is very far from the "thin wall regime" analyzed in [50]. In order to get close to the SM case, but still keeping a simple model as in [50], a scalar theory with a potential whose parameters can be adjusted to explore cases far from the thin wall regime was considered in [73], and a numerical analysis of the false vacuum stability condition was performed. The main result is that for the potential that well approximates the SM case, the stabilizing effect of gravity is hardly seen even in very strong gravity regimes. As suggested in [74–76], the total quenching of the vacuum decay rate can eventually be reached at some very high scale. As shown in [73] however, for the SM case such an effect takes place in a far transplanckian regime where the theory has already lost its validity. The results obtained with the simple model considered in [73] were later confirmed in [77], where a bona fide SM Higgs effective potential was used.

In order to complete the stability analysis of the EW vacuum when gravity is taken into account, it is of the greatest importance to understand to which extent the presence of gravity can counteract the NP destabilizing effect discussed in [54, 65, 71, 72]. In the present Chapter we address these issues, that are very important for current studies and for model building of BSM physics, where we are often confronted with the possibility of considering NP at Planckian and/or trans-Planckian scales. Anticipating on the results of the following sections, we will see that the tunneling time from the false to the true vacuum is still strongly dependent on NP even if it lives at very high ($\gg \phi_{\text{inst}}$) scales, thus confirming the results of the analysis performed in the flat spacetime background [54, 65, 71, 72].

Summing up the theory presented in Chapter 3, the computation of the decay time of the state of our Universe is reduced to the computation of the bounce solution of the equation of motion of a scalar field ϕ with the appropriate boundary conditions, that are Eqs. (3.97)–(3.99) for the *flat spacetime* case, and Eqs. (3.109) and (3.113) for the *curved spacetime* case. In both cases, the decay rate Γ of the false vacuum is given by:

$$\Gamma = D e^{-(S[\phi_b] - S[\phi_{\text{fv}}])} \equiv D e^{-B} \quad (4.5)$$

where $B \equiv S[\phi_b] - S[\phi_{\text{fv}}]$ is the *tunneling exponent* and the exponential of $-B$ gives the "tree-level" contribution to the decay rate, while D is the quantum fluctuation determinant. If $V(\phi_{\text{fv}}) = 0$, the action $S[\phi_{\text{fv}}]$ vanishes, and the tunneling exponent is simply $B = S[\phi_b]$. In particular these equations, a part for very special cases, can not be solved analytically and then is necessary to solve them numerically, and this is the case for the Standard Model. For this purpose, we have developed a new numerical method to find the bounce solution, whose details are presented in Appendix D.

Since we are interested in the stability analysis of the EW vacuum, in our case the scalar field ϕ is the Higgs field, and the potential $V(\phi)$ is the renormalization

group improved Higgs effective potential that we have written in Eq. (2.118) as:

$$V_{\text{SM}}(\phi) \sim \frac{1}{4} \lambda_{\text{SM}}(\phi) \phi^4, \quad (4.6)$$

where $\lambda_{\text{SM}}(\phi)$ is the quartic running coupling $\lambda_{\text{SM}}(\mu)$ (μ is the running scale) with $\mu = \phi$ [71, 78].

However, the purpose of the present Chapter is to study the impact that NP at high energies can have on the stability condition of the EW vacuum when the SM coupling to gravity is taken into account. We are then not interested in precision measurements and/or refinements of previous analyses. We can then leave aside these questions and work in a simplified yet very robust framework, by using a good approximation of the SM effective potential that was obtained in [79] by fitting the two-loops improved Higgs potential with the three parameter function [79]:

$$\lambda_{\text{SM}}(\phi) = \lambda_* + \alpha \left(\ln \frac{\phi}{M_P} \right)^2 + \beta \left(\ln \frac{\phi}{M_P} \right)^4, \quad (4.7)$$

where $M_P = 1/\sqrt{G}$ is the Planck mass. The fit gives:

$$\lambda_* = -0.013 \quad \alpha = 1.4 \times 10^{-5} \quad \beta = 6.3 \times 10^{-8}. \quad (4.8)$$

In the following we work with the Higgs potential (4.6) with $\lambda_{\text{SM}}(\phi)$ given by (4.7) and (4.8).

Moreover, both in the flat and curved spacetime cases, an important parameter is the size \mathcal{R} of the bounce, defined as the value of r such that

$$\phi_b(\mathcal{R}) = \frac{1}{2} \phi_b(0). \quad (4.9)$$

Going back to (4.5) for the vacuum decay rate, a good approximation to the prefactor for the case that we are considering is given in terms of the bounce size \mathcal{R} and of T_U , the age of the Universe, and the EW vacuum tunneling time $\tau = \Gamma^{-1}$ turns out to be [71]:

$$\tau \simeq \left(\frac{\mathcal{R}^4}{T_U^3} \right) e^B. \quad (4.10)$$

In the following we use (4.10) to calculate the false vacuum lifetime.

Before ending this Section and moving to the study of the impact of NP on the EW vacuum stability, we would like to test our tools starting with the known cases of the flat and curved spacetime backgrounds in the absence of NP (i.e. considering the SM alone), and briefly sketch the analysis for these cases.

Flat spacetime. In order to proceed with the numerical solution of the bounce equation (3.97), we begin by scaling the dimensionful field ϕ and the radial coordinate r to dimensionless quantities, $\varphi(x)$ and x respectively, by using Planck units:

$$x \equiv M_P r \quad \varphi(x) \equiv \frac{\phi(r)}{M_P}. \quad (4.11)$$

Then Eq. (3.97), the boundary conditions (3.98)-(3.99) and the potential (4.6) become:

$$\varphi''(x) + \frac{3}{x}\varphi'(x) = \frac{dU}{d\varphi} \quad (4.12)$$

$$\varphi(\infty) = 0 \quad \varphi'(0) = 0 \quad (4.13)$$

$$U(\varphi) = \frac{1}{4}\varphi^4 (\lambda_* + \alpha \ln^2 \varphi + \beta \ln^4 \varphi), \quad (4.14)$$

where the prime denotes the derivative respect to x . After the scaling (4.11), the tunneling exponent (3.100) becomes:

$$B = 2\pi^2 \int_0^\infty dx x^3 \left[\frac{1}{2}\varphi'_b(x) + U(\varphi_b) \right]. \quad (4.15)$$

Solving numerically the bounce equation (4.12), with the Higgs potential given by (4.14) and (4.8), and inserting the result for $\varphi_b(x)$ in (4.15), after using the values found for B and \mathcal{R} , namely $B = 2025.27$ and $\mathcal{R} = 10.7597$, we finally get for the lifetime τ of the EW vacuum:

$$\tau_{\text{flat}} \sim 10^{639} T_U, \quad (4.16)$$

in very good agreement with the results known in the literature. This is the first test of our numerical method (see Appendix D), and also shows that we are considering a good approximation for the Higgs potential.

Curved spacetime. As in the case of flat spacetime, we move to dimensionless quantities. Defining the dimensionless curvature $a(x) = M_P \rho(r)$, Eqs. (3.109-a) and (3.110) (that will be used in the following numerical integration) become:

$$\varphi'' + 3 \frac{a'}{a} \varphi' = \frac{dU}{d\varphi} \quad a'' = -\frac{8\pi}{3}a (\varphi'^2 + U), \quad (4.17)$$

where the potential $U(\varphi)$ is the same as in (4.14). The corresponding boundary conditions are:

$$\varphi(\infty) = 0 \quad \varphi'(0) = 0 \quad a(0) = 0 \quad a'(0) = 1. \quad (4.18)$$

As we have already said, $\rho(r) \sim r$ for $r \rightarrow \infty$, and the asymptotic ($x \rightarrow \infty$) behavior of the bounce solution in the presence of gravity is the same as in the flat spacetime case.

In terms of dimensionless quantities, from (3.115) we find for the tunneling exponent:

$$B = -2\pi^2 \int_0^\infty dx a_b^3 U(\varphi_b) \quad (4.19)$$

where (φ_b, a_b) is the bounce solution to the system (4.17).

In the left panel of Fig. 4.2 the bounce profile $\varphi_b(x)$ is plotted. The right panel shows the difference $a_b(x) - x$: we clearly see how $a_b(x)$ reaches asymptotically the

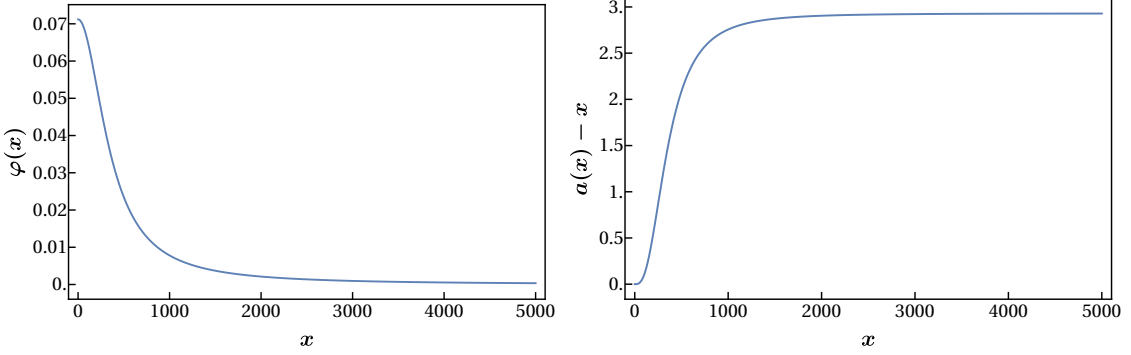


Figure 4.2: *Left panel:* Profile of the bounce solution $\varphi(x)$ in the presence of gravity. It is obtained for the potential (4.14) with the parameters λ_*, α, β given in (4.8). The center of the bounce is at $\varphi(0) = 0.0712$, its size is $\mathcal{R} = 350.2996$ and the tunneling exponent is $B = 2062.5836$. *Right panel:* Difference between the curvature radius and its asymptotic value, $a(x) - x$, for the same parameters as in the left panel.

Minkowskian behavior $a(x) \sim x + c$. Finally, with the help of (4.10), we obtain the tunneling time in the presence of gravity:

$$\tau_{\text{grav}} \sim 10^{661} T_U. \quad (4.20)$$

Once again we observe that the above result is in good agreement with known results [77]. Moreover, comparing (4.20) with the corresponding flat spacetime tunneling time (4.16), we see that gravity (as expected) tends to stabilize the EW vacuum.

4.2 New physics: Higher order operators

The results briefly presented in Section 4.1 are known and concern the stability analysis under the assumption that new physics at M_P is decoupled from the physics that triggers the EW vacuum decay, and that it should be possible to calculate the tunneling rate ignoring these terms.

The analysis of the previous section is essential to set the proper framework where the effects of the presence of NP at M_P can be properly investigated. We parametrize NP as in [54, 65, 71] with the help of higher powers of ϕ added to the Higgs potential:

$$V_{\text{NP}}(\phi) = \frac{\lambda_6}{6} \frac{\phi^6}{M_P^2} + \frac{\lambda_8}{8} \frac{\phi^8}{M_P^4}. \quad (4.21)$$

It was shown in [54, 65, 71] for the flat spacetime case that when $\lambda_6 < 0$ and $\lambda_8 > 0$ the potential (4.21) destabilizes the EW vacuum. In other words, these NP terms favor the nucleation of true vacuum bubbles and, depending on the specific values of λ_6 and λ_8 , this destabilization effect could dramatically reduce the EW

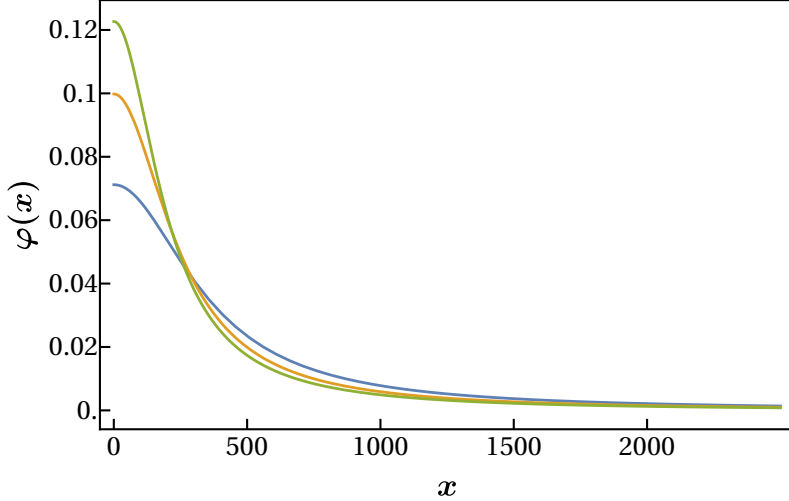


Figure 4.3: The blue curve is the profile of the bounce solution obtained for the potential (4.22) with $\lambda_6 = 0$ and $\lambda_8 = 0$, i.e. in the absence of new physics. The yellow curve is the profile of the bounce solution for $\lambda_6 = -0.03$ and $\lambda_8 = 0.03$, while the green one is the profile of the bounce obtained for $\lambda_6 = -0.04$ and $\lambda_8 = 0.04$. Note that with increasing values of the couplings the center of the bounce $\varphi(0)$ becomes larger while the size diminishes.

vacuum lifetime τ in (4.16) and make it even shorter than the age of the Universe T_U . We now consider the same kind of analysis in the presence of gravity.

Adding the NP terms (4.21) to the SM Higgs potential (4.6), and moving again to dimensionless quantities, the new dimensionless potential $U(\varphi)$ becomes:

$$U(\varphi) = \frac{1}{4}\varphi^4 \left(\lambda_* + \alpha \ln^2 \varphi + \beta \ln^4 \varphi + \frac{2}{3}\lambda_6\varphi^2 + \frac{1}{2}\lambda_8\varphi^4 \right). \quad (4.22)$$

A first important result of our analysis is that for each value of the couple (λ_6, λ_8) there is a different bounce solution to Eqs. (4.17), all of them being different from the solution obtained for the SM alone, i.e. the case $\lambda_6 = 0, \lambda_8 = 0$. Therefore, the “new” bounce solutions related to the presence of new physics, here parametrized in terms a given couple (λ_6, λ_8) , is still present even when in the stability analysis gravity is explicitly taken into account.

In order to illustrate these results, in Fig. 4.3 we show bounce solutions to Eqs. (4.17) for $\lambda_6 = -0.03, \lambda_8 = 0.03$ (yellow curve), $\lambda_6 = -0.04, \lambda_8 = 0.04$ (green curve) and compare them with the corresponding $\lambda_6 = 0, \lambda_8 = 0$ (blue curve) case. The profiles obtained are definitely *new solutions* to these equations related to the specific values of λ_6 and λ_8 , clearly different from the bounce (blue curve) obtained for the SM alone ($\lambda_6 = 0$ and $\lambda_8 = 0$).

With the help of (4.10) we now calculate the EW vacuum lifetime for different values of the NP couplings λ_6 and λ_8 . The fourth column of Tab. 4.1 contains different values of the tunneling time obtained for different couples (λ_6, λ_8) . For

λ_6	λ_8	τ_{flat}/T_U	τ_{grav}/T_U
0	0	10^{639}	10^{661}
-0.05	0.1	10^{446}	10^{653}
-0.1	0.2	10^{317}	10^{598}
-0.15	0.25	10^{186}	10^{512}
-0.3	0.3	10^{-52}	10^{287}
-0.45	0.5	10^{-93}	10^{173}
-0.7	0.6	10^{-162}	10^{47}
-1.2	1.0	10^{-195}	10^{-58}
-1.7	1.5	10^{-206}	10^{-106}
-2.0	2.1	10^{-206}	10^{-121}

Table 4.1: Tunneling time for different values of λ_6 and λ_8 , both for the flat and curved spacetime cases. We note that although gravity tends to stabilize the EW vacuum (the tunneling time τ_{grav} is always higher than the corresponding one in flat spacetime τ_{flat}), new physics has always a strong impact.

comparison, the third column contains the corresponding values of τ for the flat spacetime analysis. First of all we note that the effect already seen in the previous section for the SM alone (also reported in the first line of the table, the case $\lambda_6 = 0$, $\lambda_8 = 0$), namely that the presence of gravity tends to stabilize the EW vacuum, is maintained even in the presence of new physics.

However, a simple inspection of this table shows that even though the presence of gravity tends to stabilize the EW vacuum as compared to the corresponding flat spacetime case, still for $O(1)$ values of the new physics couplings λ_6 and λ_8 the tunneling time can be made smaller than the age of the Universe T_U . Let us consider just a couple of examples. For $\lambda_6 = -0.3$ and $\lambda_8 = 0.3$ for instance, the EW vacuum in the flat spacetime background is unstable, being $\tau \sim 10^{-52}T_U$, but for the corresponding case with gravity included we observe a stabilization of the EW vacuum: $\tau \sim 10^{287}T_U$. There is a competition between the destabilizing effect of NP and the stabilizing effect of gravity. In this example, gravity takes over new physics and as a result the EW vacuum turns out to be stable. However for larger (absolute) values of the NP couplings, the destabilizing effect of NP takes over the stabilizing effect of gravity. For instance, for $\lambda_6 = -1.2$ and $\lambda_8 = 1.0$, despite the stabilizing effect of gravity ($\tau_{\text{grav}} \gg \tau_{\text{flat}}$), the EW vacuum turns out to be unstable: $\tau_{\text{grav}} \sim 10^{-58}T_U$.

The results discussed above with the help of Table 4.1 are better summarized in Fig. 4.4 where the stability diagram in the (λ_6, λ_8) plane is presented for the range of values $-1.5 < \lambda_6 < -0.4$ and $0.4 < \lambda_8 < 1.5$. We see that, when the analysis is performed in the flat spacetime case (i.e. when we ignore the presence of gravity), the stability region ($\tau > T_U$, blue area) is confined to the upper right corner of

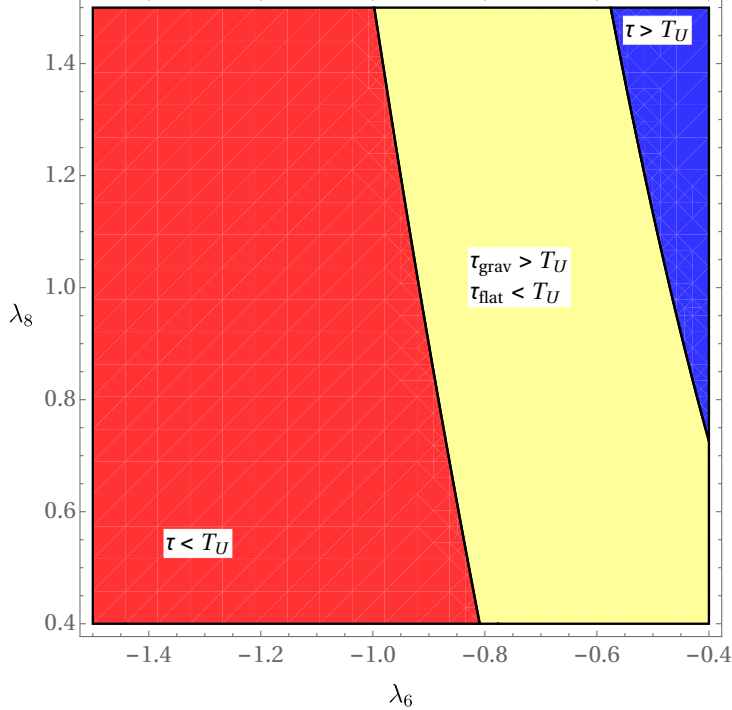


Figure 4.4: Stability diagram in the (λ_6, λ_8) plane showing three separate regions where: (i) $\tau_{flat}, \tau_{grav} > T_U$ (blue region); (ii) $\tau_{flat} < T_U, \tau_{grav} > T_U$ (yellow region); (iii) $\tau_{flat}, \tau_{grav} < T_U$ (red region). Note that, as in the blue (red) area τ_{flat} and τ_{grav} are both larger (smaller) than T_U , in these regions we wrote $\tau > T_U$ ($\tau < T_U$) with no further specification. The potential of (4.14) and parameters λ_*, α, β given in (4.8) are used. Note that although the inclusion of gravity induces an enlargement of the region with EW vacuum lifetime larger than T_U , for a large portion of the phase diagram we have $\tau < T_U$, even when gravity is taken into account.

this figure. When the presence of gravity is taken into account, the stability region ($\tau > T_U$) broadens (blue + yellow area), and this shows the tendency of gravity toward stabilization. Yet, for a large portion of the parameter space the EW vacuum is still unstable, thus showing that the potential stabilization that should be induced by gravity is not sufficient to counteract against the destabilization mechanism due to the presence of high energy NP. In this respect, it is important to note that this destabilization occurs for physical $O(1)$ values of the coupling constants λ_6 and λ_8 . In Fig. 4.5 we show some more quantitative details of the phase diagram drawn in Fig. 4.4, presenting the flat spacetime case (left panel) separately from the case when gravity is taken into account (right panel).

Let us summarize the results of the present Section. We have seen that the stability condition of the EW vacuum is the result of a competition between the destabilizing effect of NP and the stabilizing tendency of gravity. However, even keeping the values of the coupling constants in the natural $O(1)$ range, for a large portion of the parameter space the destabilization induced by Planckian NP largely

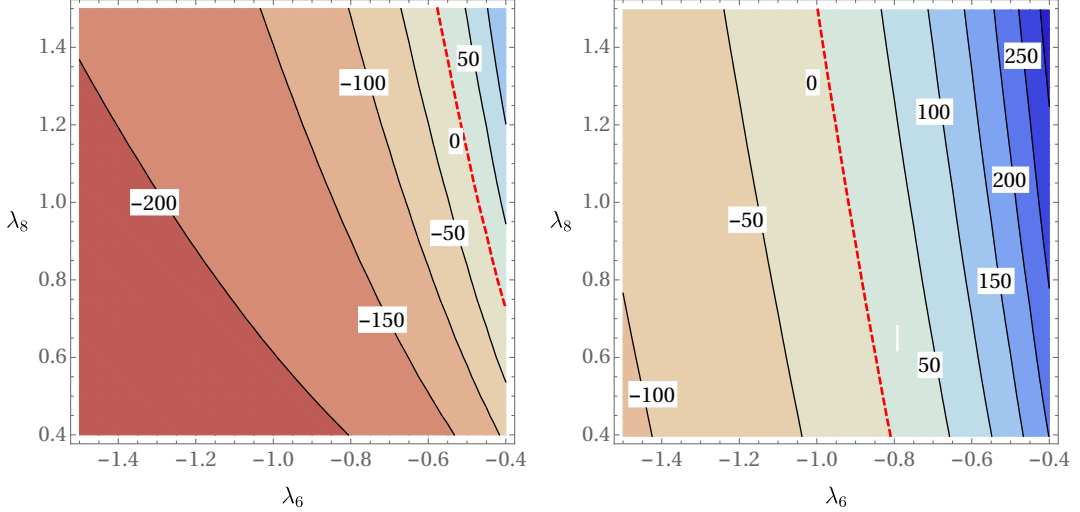


Figure 4.5: Stability diagrams in the (λ_6, λ_8) plane for $\log_{10}(\tau/T_U)$ with the potential of (4.14) and parameters λ_* , α , β given in (4.8). *Left panel:* flat spacetime case. *Right panel:* curved spacetime case. In each of the two panels, the black lines are curves with fixed values of $\log_{10}(\tau/T_U)$ (reported on it), while the thick red dashed line indicates the points where $\tau = T_U$. Colors serve as a guidance, indicating the decreasing of $\log_{10}(\tau/T_U)$ from the right to the left. Note that the inclusion of gravity induces a broad enlargement of the region where the EW vacuum is stable ($\log_{10}(\tau/T_U) > 0$).

overwhelms the tendency of gravity toward stabilizing the EW vacuum: the contribution to the decay rate through the new bounce solution by far dominates the contribution coming from the bounce solution obtained by considering SM only.

4.3 New physics: large mass particles

In the present Section the stability analysis of the EW vacuum will be performed by considering a different parametrization for NP at high energy scales. Actually in [54, 65, 71] and in the previous section the analysis was performed by parametrizing NP at the Planck scale in terms of few higher order (non-renormalizable) operators. This is just a convenient and efficient way of mimicking the presence of new physics, clearly not an (illegitimate) truncation of the UV completion of the SM. However, it was expressed a certain skepticism on these results, suggesting that this effect should disappear when the infinite tower higher dimensional operators of the renormalizable UV completion of the SM is taken into account, so that the expected decoupling of very high energy physics from the mechanism that triggers the decay of the false vacuum should be recovered. It was actually suspected that this effect takes place above the physical cutoff, where the control of the theory is lost [80].

Although it is understandable that the parametrization of NP in terms of higher

order operators could be the source of a certain confusion, the destabilizing effect has nothing to do with this parametrization. For the case of a flat spacetime background in [72] the stability analysis was performed by parametrizing NP in terms of renormalizable additional terms, with a fermion and a boson with very high masses that interact with the Higgs field, and it was shown that the destabilizing effect found in [54, 65, 71] is still present.

In this Section we present the same kind of analysis of [72] taking into account the presence of gravity (i.e. considering the case of a curved spacetime background), and show that as for the case of the parametrization used in the previous section, gravity does not produce any washing out of the destabilizing effect of new physics, although it slightly mitigates it. In order to illustrate the destabilization phenomenon we consider as in [72] a renormalizable model that is not a realistic high energy UV-completion of the SM but is very appropriate to the purposes of the this Section. New Physics that lives at very high energy scales is then parametrized by adding to the SM a scalar field S and a fermion field ψ that interact in a simple way with the Higgs field ϕ , with very large masses (see below) M_S and M_f of the scalar and fermion respectively.

Apart from the kinetic terms, the additional terms in the Lagrangian are:

$$\Delta \mathcal{L} = \frac{M_S^2}{2} S^2 + \frac{\lambda_S}{4} S^4 + g_S \phi^2 S^2 + M_f \bar{\psi} \psi + g_f \phi \bar{\psi} \psi. \quad (4.23)$$

To understand how a NP Lagrangian of this kind can arise in a physical setup, we note that the large mass term M_f can be thought as a sort of heavy right handed “neutrino” in the framework of a see-saw mechanism. While the corresponding light “neutrino” is totally harmless for the stability of the EW vacuum, the heavy “neutrino” can play an important role in destabilizing the vacuum. The scalar field S counterbalances the destabilizing effect of ψ . Note that models with new scalar fields coupled to the Higgs (although admittedly unrealistic) have already been used to provide a stabilization mechanism for the Higgs effective potential [81, 82].

For the purposes of the present Chapter, it is sufficient to consider the impact of the additional terms (4.23) on the Higgs effective potential $V(\phi)$ at the one-loop level only. In fact we do not need a better level of precision as we are not interested in extracting precise numbers but we only want to illustrate the destabilization effect that arises from very high energy physics (see also the considerations developed below Eq. (4.6)). The one-loop contribution to $V(\phi)$ from these terms is:

$$V_1(\phi) = \frac{(M_S^2 + 2g_S\phi^2)^2}{64\pi^2} \left[\ln \left(\frac{M_S^2 + 2g_S\phi^2}{M_S^2} \right) - \frac{3}{2} \right] - \frac{(M_f^2 + g_f^2\phi^2)^2}{16\pi^2} \left[\ln \left(\frac{M_f^2 + g_f^2\phi^2}{M_S^2} \right) - \frac{3}{2} \right], \quad (4.24)$$

where the renormalization scale μ is taken as $\mu = M_S$. In this respect we note that at very high values of the running scale the SM quartic coupling reaches a

plateau: $\lambda_{\text{SM}}(\mu)$ has practically the same value in the whole range $[M_f, M_S]$, and this is why we can use $\lambda_{\text{SM}}(M_S)$ as the threshold value for the coupling (even though strictly speaking we should use $\lambda_{\text{SM}}(M_f)$ (see below)), and can choose $\mu = M_S$ as the renormalization (threshold) scale.

The presence of the high energy NP of (4.23) is then taken into account by adding to the SM potential $V_{\text{SM}}(\phi)$ in (4.6) and (4.7) the contribution coming from $V_1(\phi)$. To this end we have to implement the matching conditions described below. First of all we expand the potential $V_1(\phi)$ in powers of ϕ and isolate the constant, the ϕ^2 and the ϕ^4 terms. Then at the threshold scale M_f we require that: (i) the renormalized cosmological constant Λ , given by the sum of all the constant terms (those coming from the SM potential and those coming from $V_1(\phi)$) vanishes, $\Lambda(\mu = M_f) \sim 0$; (ii) the renormalized mass term, given by the sum of all the coefficients of ϕ^2 , and identified with the SM mass parameter $m_{\text{SM}}^2(\mu = M_f)$ at the scale M_f , vanishes: $m_{\text{SM}}^2(\mu = M_f) \sim 0$ (more precisely we neglect this term to a very high degree of accuracy for the large values of ϕ considered); (iii) the renormalized quartic coupling, given by the sum of all the coefficients of ϕ^4 , is identified with the SM quartic coupling at the scale M_f , $\lambda_{\text{SM}}(\mu = M_f)$. In other words, at the scale M_f this coefficient is matched with the value of the quartic coupling obtained by considering the running of the renormalization group equations for the SM couplings alone.

The above requirements for the renormalized cosmological constant and mass are well known features. For the renormalized Λ (apart from the fine tuning problem) we can practically consider that $\Lambda(\mu = 0) \sim \Lambda(\mu = M_f) \sim 0$. The same is true for the renormalized mass, for which we take $m^2(\mu = 0) \sim m^2(\mu = M_f) \sim 0$, meaning that we neglect the ϕ^2 term as compared to the ϕ^4 and other terms for these large values of ϕ , and that the running of the renormalized mass is totally harmless in this respect. For the quartic coupling we have a true matching condition. In fact we require that at the threshold scale $\mu = M_f$ the quartic coupling coincides with $\lambda_{\text{SM}}(\mu = M_f)$, that is obtained by running the renormalization group equations for the SM couplings only. Practically starting from the scale M_f , the potential is given by the SM contribution $V_{\text{SM}}(\phi)$ plus the contribution of $V_1(\phi)$ subtracted of its constant, quadratic and quartic powers of ϕ , that we call $\bar{V}_1(\phi)$ from now on:

$$V_{\text{tot}}(\phi) = \frac{1}{4} \lambda_{\text{SM}}(\phi) \phi^4 + \bar{V}_1(\phi). \quad (4.25)$$

We are now ready to use our model of high energy NP to calculate the EW vacuum lifetime for different values of the masses M_f and M_S of ψ and S , and for different values of the coupling constants. For our illustrative purposes we have chosen to consider the four following examples: (i) $M_S = 2.5 \times 10^{-1}$, $M_f = 3 \times 10^{-4}$, $g_S = 0.96$, $g_f^2 = 0.5$; (ii) $M_S = 2.0 \times 10^{-1}$, $M_f = 10^{-4}$, $g_S = 0.9$, $g_f^2 = 0.5$; (iii) $M_S = 2.0 \times 10^{-1}$, $M_f = 10^{-3}$, $g_S = 0.95$, $g_f^2 = 0.4$; (iv) $M_S = 1.5 \times 10^{-1}$,

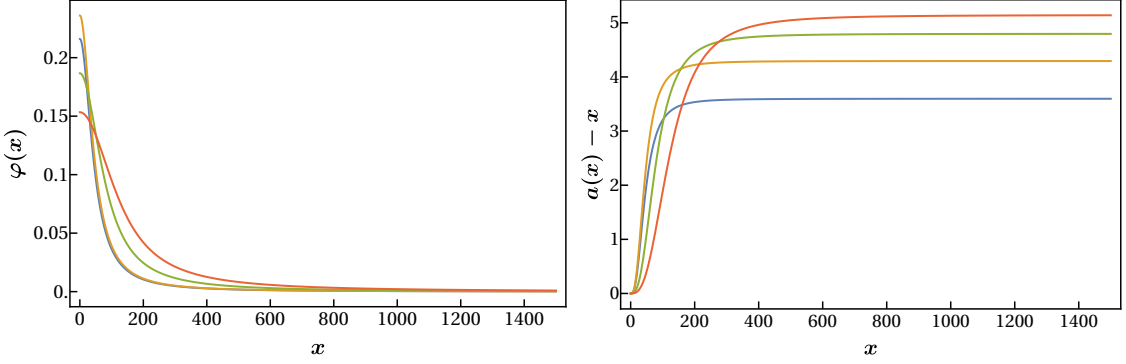


Figure 4.6: *Left panel:* Profile of the bounce solutions $\varphi(x)$ for the potential (4.25) relative to the four cases considered in the text: $M_S = 2.5 \times 10^{-1}$, $M_f = 3 \times 10^{-4}$, $g_S = 0.96$, $g_f^2 = 0.5$ (yellow); $M_S = 2.0 \times 10^{-1}$, $M_f = 10^{-4}$, $g_S = 0.9$, $g_f^2 = 0.5$ (blue); $M_S = 2.0 \times 10^{-1}$, $M_f = 10^{-3}$, $g_S = 0.95$, $g_f^2 = 0.4$ (green); $M_S = 1.5 \times 10^{-1}$, $M_f = 5 \times 10^{-3}$, $g_S = 0.92$, $g_f^2 = 0.4$ (red). *Right panel:* the corresponding difference between the curvature radius and its asymptotic value, $a(x) - x$, for the same parameters as in the left panel.

$M_f = 5 \times 10^{-3}$, $g_S = 0.92$, $g_f^2 = 0.4$. First of all we have to solve the bounce equations (4.17) for $\varphi(x)$ and $a(x)$. In Fig. 4.6 the profiles of the bounce solutions $\varphi_b(x)$ for the four different cases (i), (ii), (iii) and (iv) and the corresponding plots of $a_b(x) - x$ are presented, with colors yellow, blue, green and red respectively.

These are the first relevant results of the present Section: in the presence of NP at very high energies, new bounce solutions exist not only when the analysis is carried in the flat spacetime background [72] but also when we take into account the presence of gravity. These results reinforce those of the previous section, where high energy NP was parametrized in terms of higher order operators, and show that the appearance of new bounce solutions is not an artifact of the specific parametrization used in Section 4.2.

Using (4.10) to calculate the vacuum lifetime, for the examples considered above we find in units of T_U (going from (i) to (iv)):

$$\tau = 10^{-65}, \tau = 10^{-93}, \tau = 10^{94}, \tau = 10^{307}, \quad (4.26)$$

to be compared with the corresponding results for the tunneling time obtained from the analysis performed in a flat spacetime background, where we have:

$$\tau = 10^{-80}, \tau = 10^{-103}, \tau = 10^{80}, \tau = 10^{293}. \quad (4.27)$$

Eqs. (4.26) and (4.27) together with Fig. 4.6 contain the main lesson of the present Section. They definitely show that, even when gravity is included in the analysis, the presence of NP at high energy scales can have an enormous impact on the vacuum lifetime. It is worth to remind here that when the calculation is performed in the

curved spacetime background and the presence of high energy new physics is not considered, the tunneling time is given by (4.20) ($\tau \sim 10^{661} T_U$), while from (4.26) we see that τ strongly depends on the parameters of new physics, and can turn out to be even shorter than the age of the Universe.

Moreover, by comparing (4.26) and (4.27) we see that gravity, while still showing a slight tendency toward stabilization (which is what we observe in the absence of NP when comparing (4.16) with (4.20)), only produces a “tiny” effect, that qualitatively does not modify significantly the stability condition of the EW vacuum. Despite the fact that in our toy model NP lives at very high energy scales, the expectation that the tunneling time should be insensitive to it, in other words that the result shown in (4.20) should not be modified by the presence of NP at high energies, is not fulfilled. These results confirm the analysis of the previous section. Here, with the help of a fully renormalizable toy UV completion of the SM, we have shown that the EW vacuum lifetime strongly depends on NP even if the latter lives at very high energy scales. These findings are at odds with a widely diffused expectation, based on a naive application of the decoupling argument, and show that the fact that the vacuum stability condition depends on physics that lives at very high energy scales is not due to an illegitimate extrapolation of the theory beyond its validity, as it was previously thought [80]. On the contrary, that expectation was based on an illegitimate application of the decoupling theorem to a phenomenon (the tunneling of the EW vacuum) to which it cannot be applied. Before ending this Section, we would like to stress once again that with respect to the previous section, where NP interactions were parametrized with the help of higher order non-renormalizable operators, here NP is given in terms of a fully renormalizable theory, thus showing that the effect that we present is a genuine physical effect and has nothing to do with the specific parametrization of NP.

Chapter 5

Direct Higgs-gravity interaction and stability of our Universe

In the previous chapter we have seen that the tunneling time τ of the EW vacuum is extremely sensitive to the presence of unknown New Physics, and the latter can enormously lower τ . This poses a serious problem for the stability of our universe, demanding for a physical mechanism that protects it from a disastrous decay. In this Chapter we will see that there exists an universal stabilizing mechanism that naturally originates from the non-minimal coupling between gravity and the Higgs boson. This Higgs-gravity interaction necessarily arises from the quantum dynamics of the Higgs field in a gravitational background. Then such a stabilizing mechanism is certainly present, and it is not related to any specific model, being rather *natural* and *universal* as it comes from fundamental pillars of our physical world: gravity, the Higgs field, the quantum nature of physical laws [83].

5.1 Non-minimal coupling of Higgs field to gravity

In Section 3.4.2 we have seen how to include gravity in the analysis of the stability problem of a false vacuum for a scalar field theory. In particular, we have considered a maximally symmetric spacetime, i.e. a spacetime with $O(4)$ symmetry described by the metric (3.105), and the scalar field was minimally coupled to gravity, i.e. we have considered only the Einstein-Hilbert term in the action (3.104) as interaction terms of gravity.

Instead, in Chapter 4 we have applied such a theory to the study of the stability problem of the EW vacuum, and in particular considering the SM alone we find that

$$\tau_{\text{SM}} \sim 10^{661} T_U , \quad (5.1)$$

i.e. the tunneling time τ_{SM} is much larger than the age of the Universe T_U . However, considering New Physics at the Planck scale M_P , the tunneling time τ can become less than T_U also in the presence of gravity, as we have seen in Table 4.1.

In this Chapter we want to study the effect of destabilizing New Physics on the EW vacuum lifetime when we consider a more general gravitational setup. In fact, the quantum dynamics of the Higgs field ϕ in a gravitational background *imposes* a direct interaction between ϕ and gravity [84, 85]. Then, the action that describes the dynamics of the field ϕ is [77]

$$S[\phi, g_{\mu\nu}] = \int d^4x \sqrt{g} \left[-\frac{R}{16\pi G} + \frac{1}{2}g^{\mu\nu}\partial_\mu\phi \partial_\nu\phi + V(\phi) + \frac{1}{2}\xi\phi^2R \right] \quad (5.2)$$

where R is the Ricci scalar and G is the Newton gravitational constant. Instead, ξ is the coupling constant of the direct coupling between gravity and the scalar field ϕ . The potential $V(\phi)$, as in the minimal coupling case $\xi = 0$, has a local minimum (*false vacuum*) in $\phi = \phi_{fv}$, and an absolute minimum (*true vacuum*) in $\phi = \phi_{tv}$. Moreover, $\phi = \phi_{fv}$ is a Minkowskian false vacuum $V(\phi_{fv}) = 0$.

As in the minimal coupling case, there are no reasons for which gravitational effects can break the $O(4)$ symmetry of the flat spacetime case, so that we can assume that also in the presence of non-minimally coupled gravity the bounce solution is invariant under 4 dimensional rotations. Basing on this assumption, the curved spacetime is still described by the metric

$$ds^2 = dr^2 + \rho^2(r)d\Omega_3^2 \quad (5.3)$$

where $d\Omega_3^2$ is the metric of the unitary 3-sphere, while ρ is the curvature radius of each 3-sphere at fixed r .

From the action in Eq. (5.2), we obtain the Euler-Lagrange and the Einstein field equations ($\kappa = 8\pi G$):

$$R_{\mu\nu} - \frac{1}{2}g_{\mu\nu}R = \kappa \frac{T_{\mu\nu} + 2\xi \left[\partial_\mu(\phi \partial_\nu\phi) - g_{\mu\nu}\partial_\lambda(\phi \partial^\lambda\phi) \right]}{1 - \kappa\xi\phi^2} \quad (5.4)$$

$$T_{\mu\nu} = \partial_\mu\phi \partial_\nu\phi - g_{\mu\nu} \left[\frac{1}{2}\partial_\mu\phi \partial^\mu\phi + V(\phi) \right] \quad (5.5)$$

$$\partial_\mu\partial^\mu\phi = \frac{dV(\phi)}{d\phi} + \xi R\phi. \quad (5.6)$$

Using the metric given in Eq. (5.3), the equations in (5.4) and (5.6) become:

$$\ddot{\phi} + 3\frac{\dot{\rho}}{\rho}\dot{\phi} = \frac{dV}{d\phi} + \xi\phi R \quad \dot{\rho}^2 = 1 - \frac{\kappa}{3}\rho^2 \frac{-\frac{1}{2}\dot{\phi}^2 + V(\phi) - 6\xi\dot{\rho}\phi\dot{\phi}}{1 - \kappa\xi\phi^2}, \quad (5.7)$$

where the dots denotes the differentiation respect to the radial coordinate r . The bounce solution needed to compute the transition rate from the false vacuum is again given by the field and metric solutions, respectively $\phi_b(r)$ and $\rho_b(r)$, of these coupled differential equations, once we have the appropriate boundary conditions (3.113):

$$\phi(\infty) = 0 \quad \dot{\phi}(0) = 0 \quad \rho(0) = 0. \quad (5.8)$$

For numerical computation is useful to differentiate Eq. (5.7-b) respect to r , obtaining the equation:

$$\ddot{\rho} = -\frac{\kappa}{3\rho} \frac{\dot{\phi}^2 + V(\phi) - 3\xi \left(\dot{\phi}^2 + \phi \ddot{\phi} + \frac{\dot{\rho}}{\rho} \phi \dot{\phi} \right)}{1 - \kappa \xi \phi^2}, \quad (5.9)$$

and the boundary condition $\dot{\rho}(0) = 1$. In fact, as in the minimal coupling case the equations (5.7-a) and (5.9), once we use the scaling to M_P to obtain their dimensionless version, are more stable for a numerical analysis. It is worth to note as for $\xi = 0$ the Eqs. (5.7) and (5.9) are reduce to the Eqs. (3.109) and (3.110), i.e. the equations of motion for ϕ and ρ in a curved spacetime background with a minimal coupling of gravity and matter, the case studied in Chapter 4 [50].

In the derivation of Eq. (5.7) from the Einstein equation, we can compute the Ricci scalar using the metric in Eq. (5.3):

$$R = -\frac{6}{\rho^2} (\rho \ddot{\rho} + \dot{\rho}^2 - 1). \quad (5.10)$$

However, this expression is not useful to numerically solve the equations of motion. To obtain a numerically stable expression, we compute the trace of Eq. (5.4) obtaining the following general expression:

$$(1 - \kappa \xi \phi^2) \frac{R}{\kappa} = (1 - 6\xi) \partial_\mu \phi \partial^\mu \phi + 4V(\phi) - 6\xi \phi \partial_\mu \partial^\mu \phi. \quad (5.11)$$

Then, we can use Eq. (5.6) to explicit $\partial_\mu \partial^\mu \phi$ in Eq. (5.11): in this way, using the $O(4)$ symmetry, we obtain an expression for R in terms of the scalar field ϕ and its derivatives:

$$R = \kappa \frac{\dot{\phi}^2 (1 - 6\xi) + 4V(\phi) - 6\xi \phi dV/d\phi}{1 - \kappa \xi (1 - 6\xi) \phi^2}. \quad (5.12)$$

The Eq. (5.12), contrary to Eq. (5.10), is not a general expression for R since, having used the equation of motion Eq. (5.6), it is valid only for the solution of Eq. (5.7). However, as anticipated, it is useful to explicit R in Eq. (5.7-a) just using Eq. (5.12) to numerically solve this equation together with Eq. (5.9).

Finally, we compute the tunneling exponent B , using Eq. (5.11) to obtain a general expression for the action. Inserting Eq. (5.11) in Eq. (5.2) to explicit the terms that contains the Ricci scalar R , after simple steps we obtain:

$$S[\phi, g_{\mu\nu}] = \int d^4x \sqrt{g} \left[-V(\phi) + 3\xi \partial_\mu (\phi \partial^\mu \phi) \right]. \quad (5.13)$$

The second term in this expression, after integration, is reduced to a boundary term that vanish at infinity. Then, using the $O(4)$ symmetry, the Eq. (5.13) becomes:

$$S[\phi, \rho] = -2\pi^2 \int_0^\infty dr \rho^3 V(\phi). \quad (5.14)$$

At this point, we must note some important properties concerning Eq. (5.14): (i) there is no explicit dependence of the action on coupling ξ , and therefore the action will depend on this parameter only through a possible implicit dependence of the scalar field $\phi(r)$ and of the curvature $\rho(r)$; (ii) if we compute the action in the trivial solution of false vacuum of Eq. (5.7), we get $S_{fv} \equiv S[\phi_{fv}, \rho_{fv}] = 0$, since in our topology $V(\phi_{fv}) = 0$. Finally, from Eq. (5.14), we get that tunneling exponent is given by $B = S[\phi_b, \rho_b]$.

5.2 Effect of Planck scale New Physics

Once we have computed the bounce solution from Eq. (5.7) with the boundaries (5.8), we can compute the decay rate $\Gamma (= 1/\tau)$ from the false to the true vacuum, that is still given by [40, 41, 50]:

$$\Gamma = D e^{-[S_b - S_{fv}]}, \quad (5.15)$$

where $S_b \equiv S[\phi_b, \rho_b]$, S_{fv} is the action calculated at the trivial false vacuum solution (ϕ_{fv}, ρ_{fv}) , and D is the quantum fluctuation determinant.

As for the minimal coupling case $\xi = 0$, we can define the size \mathcal{R} of the bounce as the value of the radial coordinate r such that $\phi_b(\mathcal{R}) = \frac{1}{2}\phi_b(0)$, so that the prefactor D in Eq. (5.15) can be estimated to a good approximation [86] as $D \simeq T_U^3 \mathcal{R}^{-4}$, and τ then becomes:

$$\tau \simeq \left(\frac{\mathcal{R}^4}{T_U^3} \right) e^{S_b} = \left(\frac{\mathcal{R}^4}{T_U^4} \right) e^{S_b} T_U. \quad (5.16)$$

In calculating the EW vacuum lifetime τ , in the bounce equations (5.7) we have to use the appropriate potential $V(\phi)$. If we consider the Standard Model only, i.e. assuming that NP has no impact on τ [63, 64, 66, 67], we have to consider the SM (renormalization group improved) Higgs potential $V_{\text{SM}}(\phi)$ [35, 87, 88], still given by:

$$V_{\text{SM}}(\phi) = \frac{1}{4}\lambda_{\text{SM}}(\phi)\phi^4, \quad (5.17)$$

where $\lambda_{\text{SM}}(\phi)$ is the quartic running coupling $\lambda_{\text{eff}}(\mu)$ with $\mu = \phi$ [68–70, 89]. In particular, we use the fit given in Eqs. (4.7) and (4.8) for the running coupling constant, as we have done in Chapter 4. As long as the NP terms are neglected, the inclusion of $\frac{1}{2}\xi\phi^2R$ in the action does not change the stability condition of the universe, as τ still remains much larger than T_U (see the blue line of Fig. 5.2) [77].

However, as we have seen in the previous chapter, we know that the necessarily present NP terms can have an enormous impact on τ [51, 54, 65, 71–73]. For the New Physics at high (Planckian) energies we use the parametrization in Eq. (4.21), i.e. we add to the SM Higgs potential $V_{\text{SM}}(\phi)$ higher powers of ϕ :

$$V_{\text{NP}}(\phi) = \alpha_1 \frac{\phi^6}{M_P^2} + \alpha_2 \frac{\phi^8}{M_P^4}, \quad (5.18)$$

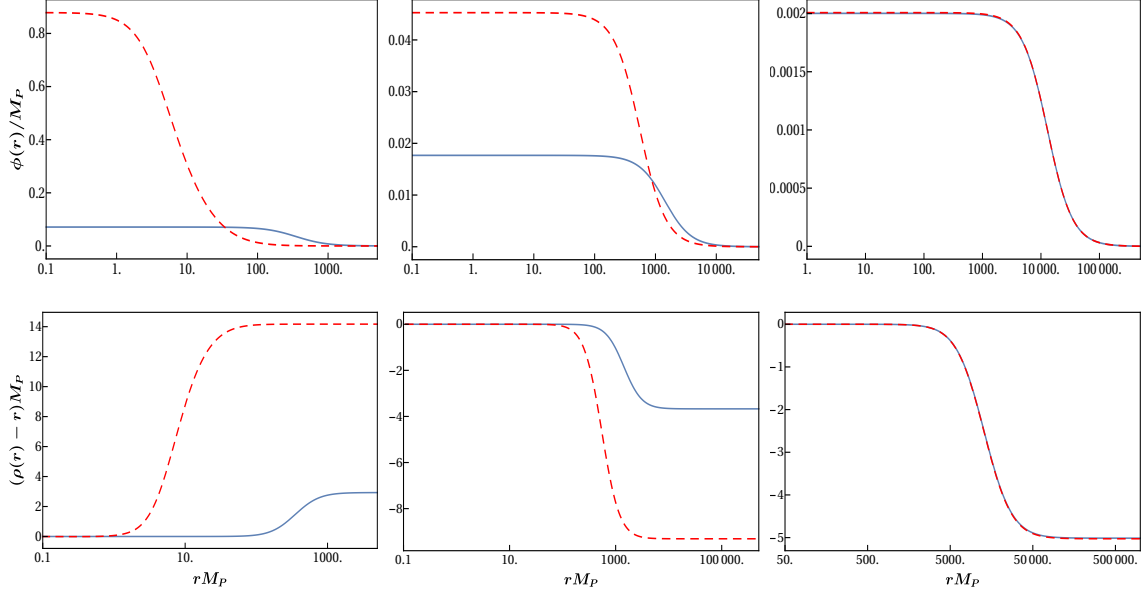


Figure 5.1: *Left column.* - *Upper panel:* bounce solution $\phi_{\text{NP}}(r)$ (red dashed line) for the action in (5.2), with potential $V(\phi) = V_{\text{SM}}(\phi) + V_{\text{NP}}(\phi)$, where $\alpha_1 = -0.2$ and $\alpha_2 = 0.125$. The bounce $\phi_{\text{SM}}(r)$ (blue solid line) for the SM potential $V_{\text{SM}}(\phi)$ alone is also plotted. *Lower panel:* the same for $\rho(r) - r$. *Middle and right columns:* the same as for the left column for the action with the additional term $\frac{1}{2}\xi\phi^2R$ with $\xi = 1, 10$ respectively.

where we have defined $\alpha_1 = \lambda_6/6$ and $\alpha_2 = \lambda_8/8$, so that we now take

$$V(\phi) = V_{\text{SM}}(\phi) + V_{\text{NP}}(\phi). \quad (5.19)$$

As an illustrative example, we consider for the (dimensionless) couplings α_1 and α_2 specific values, $\alpha_1 = -0.2$ and $\alpha_2 = 0.125$, and for the EW vacuum lifetime in the presence of NP with $\xi = 0$ we find (see the eighth row of Tab 4.1):

$$\tau_{\text{NP}} = 10^{-58} T_U. \quad (5.20)$$

In fact, as we know the presence of these NP terms can enormously lower τ [51, 54, 65, 71–73], to the point that we can get $\tau \ll T_U$. In particular, the huge difference between τ_{SM} and τ_{NP} is due to a big difference between the bounces in the two cases considered, as can be seen from the left column of Fig. 5.1.

From the results presented in Chapter 4 we conclude that there must be a mechanism that protects our universe from a disastrous decay. In this Chapter we show that there exists a *universal* stabilizing mechanism that arises from the combination of three basic pillars of our physical world: (i) gravity; (ii) the Higgs boson; (iii) the quantum nature of physical laws. In fact we show that turning on (as we must) the interaction $\xi\phi^2R$, with the exception of a tiny range of values of ξ , the EW vacuum lifetime τ is enormously enhanced and becomes much larger than T_U , even in the

ξ	τ_{SM}	τ_{NP}
-15	10^{736}	10^{736}
-10	10^{726}	10^{726}
-5	10^{710}	10^{710}
-1	10^{684}	10^{680}
-0.5	10^{677}	10^{600}
-0.3	10^{672}	10^{358}
-0.1	10^{666}	10^{65}
0	10^{661}	10^{-58}
0.3	10^{660}	10^{-167}
0.5	10^{668}	10^{23}
0.7	10^{674}	10^{346}
0.8	10^{676}	10^{512}
1	10^{679}	10^{666}
5	10^{709}	10^{709}
10	10^{725}	10^{725}
15	10^{735}	10^{735}

Table 5.1: Values of τ_{SM} (second column) and τ_{NP} (third column) in T_U units for different values of ξ (first column). For τ_{SM} , only the SM potential $V_{\text{SM}}(\phi)$ is considered. For τ_{NP} , the potential $V_{\text{NP}}(\phi)$ of Eq. (4.21) is added to $V_{\text{SM}}(\phi)$, with coupling constants: $\alpha_1 = -0.2$ and $\alpha_2 = 0.125$.

presence of Planckian NP. We can see such effect in the result presented in Tab. 5.1, where we shows the tunneling time τ_{NP} (and for comparison τ_{SM}) for different ξ , taking $\alpha_1 = -0.2$ and $\alpha_2 = 0.125$ in $V_{\text{NP}}(\phi)$.

A graphical representation of the results of Tab. 5.1 is given in Fig. 5.2, where the decay time τ (more precisely $\log_{10}(\tau/T_U)$) as a function of ξ is plotted in the interval $-1.5 \leq \xi \leq 1.8$. The range of ξ where τ is lower than T_U is very tiny ($-0.05 \lesssim \xi \lesssim 0.5$), and centered around its minimal value $\xi_{\min} \sim 0.22$. We observe that, for increasing values of $|\xi|$, τ_{NP} tends towards τ_{SM} : this means that the interaction $\frac{1}{2}\xi\phi^2R$ is so strong to *wash out* the destabilizing effect of the NP potential (5.18).

The coincidence between τ_{NP} and τ_{SM} is due to the fact that with increasing $|\xi|$ the bounces obtained with the Higgs potential $V(\phi) = V_{\text{SM}}(\phi) + V_{\text{NP}}(\phi)$ tend towards the SM ones, as can be seen from Fig. 5.1. In fact, actually $\phi_{\text{SM}}(0)$ and $\phi_{\text{NP}}(0)$ both decrease with increasing ξ , and reach the value $\phi(0) \sim 0.002$ for $\xi = 10$. For further increasing values of ξ , not presented in the figure, $\phi_{\text{SM}}(0)$ and $\phi_{\text{NP}}(0)$ still coincide and take lower and lower values. For negative ξ , the same trend is observed for increasing $|\xi|$.

To better appreciate the impact of this mechanism, we estimate (for these sufficiently large values of $|\xi|$) the relative weight in the equations of motion (5.7-a) and (5.9) of the two terms ϕ^4 and ϕ^6 in the potential $V(\phi) = V_{\text{SM}}(\phi) + V_{\text{NP}}(\phi)$ by considering the ratio:

$$A(\phi) = \frac{\alpha_1\phi^6}{(\lambda/4)\phi^4} = \frac{4\alpha_1}{\lambda}\phi^2. \quad (5.21)$$

Being $\phi(0) = \max \phi_b(r)$ and $\phi(0) \ll 1$, we find $A(\phi) \ll 1$ (Planck units), so that

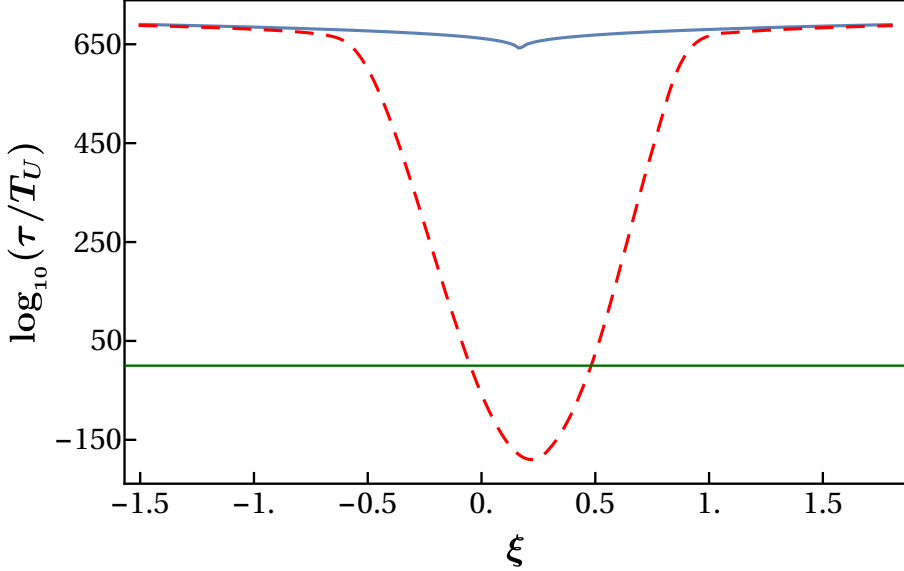


Figure 5.2: The red dashed line is the $\log_{10}(\tau/T_U)$ as a function of ξ for the Higgs potential $V(\phi) = V_{\text{eff}}(\phi) + V_{\text{NP}}(\phi)$, where: $\alpha_1 = -0.2$ and $\alpha_2 = 0.125$. The blue line is the $\log_{10}(\tau/T_U)$ for the SM potential $V_{\text{eff}}(\phi)$ alone. The green horizontal line separates the region $\tau < T_U$ (lower one) from the region $\tau > T_U$ (upper one).

the (potentially destabilizing) ϕ^6 term is very much suppressed as compared to the standard ϕ^4 term. It is then not surprising that the bounce solution for the potential $V_{\text{SM}}(\phi) + V_{\text{NP}}(\phi)$ converges to the corresponding bounce for $V_{\text{SM}}(\phi)$ alone.

A direct consequence of the coincidence of $(\phi_{\text{SM}}(r), \rho_{\text{SM}}(r))$ and $(\phi_{\text{NP}}(r), \rho_{\text{NP}}(r))$ is properly the coincidence of τ_{NP} and τ_{SM} , i.e. the washing out of the NP destabilization. In fact, from (5.14) we see that S_b at the bounce $(\phi_{\text{NP}}(r), \rho_{\text{NP}}(r))$ is:

$$S_{\text{NP}} = -2\pi^2 \int_0^\infty dr \rho_{\text{NP}}^3 [V_{\text{eff}}(\phi_{\text{NP}}) + V_{\text{NP}}(\phi_{\text{NP}})]. \quad (5.22)$$

As for sufficiently large values of $|\xi|$ we have $(\phi_{\text{NP}}(r), \rho_{\text{NP}}(r)) \rightarrow (\phi_{\text{SM}}(r), \rho_{\text{SM}}(r))$, Eq. (5.22) can be replaced with:

$$S_{\text{NP}} = -2\pi^2 \int_0^\infty dr \rho_{\text{SM}}^3 [V_{\text{eff}}(\phi_{\text{SM}}) + V_{\text{NP}}(\phi_{\text{SM}})]. \quad (5.23)$$

For the argument given above, the second term in the r.h.s. of Eq. (5.23) is negligible as compared to the first one, i.e. $S_{\text{NP}} \rightarrow S_{\text{SM}}$. In conclusion, having $\phi_{\text{SM}}(r)$ and $\phi_{\text{NP}}(r)$ practically the same size \mathcal{R} , from Eq. (5.16) it follows that τ_{NP} and τ_{SM} coincide.

The enormous stabilizing effect of the Higgs-gravity interaction can be further illustrated by comparing values of τ calculated at different values of ξ (e.g. $\xi = 0$, $\xi = 0.9$) in a region of the parameter space (α_1, α_2) where in the $\xi = 0$ case τ is always lower than T_U . For α_1 and α_2 we chose the ranges: $-0.25 \leq \alpha_1 \leq -0.16$;

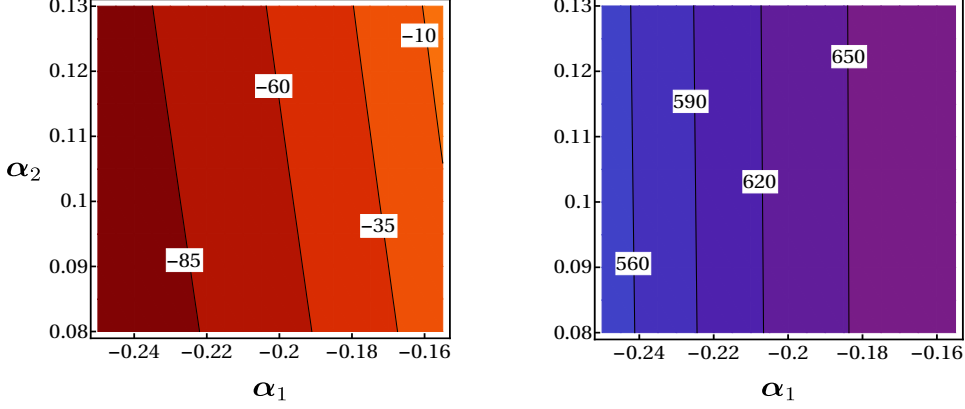


Figure 5.3: *Left panel.* Stability diagram in the (α_1, α_2) plane for the range $-0.25 \leq \alpha_1 \leq -0.16$, $0.08 \leq \alpha_2 \leq 0.13$, when $\xi = 0$. *Right panel.* Stability diagram for $\xi = 0.9$ in the same region of the (α_1, α_2) plane.

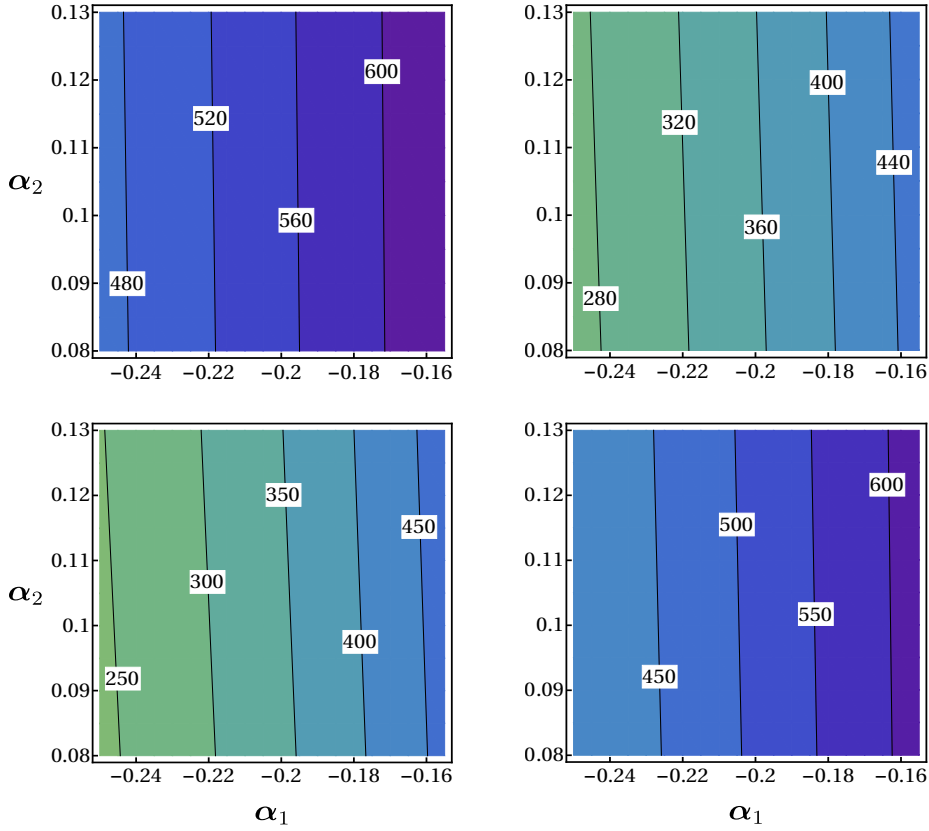


Figure 5.4: Stability diagrams in the (α_1, α_2) plane for the potential $V(\phi) = V_{\text{eff}}(\phi) + V_{\text{NP}}(\phi)$, with α_1 and α_2 in the same ranges as in Fig. 5.3. From left to right, from top to bottom: $\xi = -0.4, -0.3, 0.7, 0.8$. The first two values of ξ are on the left of ξ_{\min} (the value of ξ where τ reaches its minimal value), the last two ones on the right side.

$0.08 \leq \alpha_2 \leq 0.13$. The results are shown in Fig. 5.3: the left panel is the stability diagram for the $\xi = 0$ case (it is a zoom in the dangerous parameter region of the

right panel of Fig. 4.5, plotted in terms of α_1 and α_2), the right one for $\xi = 0.9$. The black lines are level curves with the same value of τ , and the numbers on the top of them are $\log_{10}(\tau/T_U)$. The red color scale of the left panel, ranging from darker to lighter (left to right), indicates increasing values of τ ; as said above, $\tau < T_U$ in the whole region. The right panel is the stability diagram for $\xi = 0.9$. The blue color scale again indicates increasing values τ going from left to right. The values of τ have enormously increased, and in the same region of the (α_1, α_2) plane they turn out to be much larger than T_U . The destabilizing effect of the NP terms is entirely *washed out* by the direct coupling between the Higgs field and gravity. In Fig. 5.4 we consider other values of ξ ($\xi = -0.4, -0.3, 0.7, 0.8$) that confirm these results.

The results shown in these stability diagram suggest an important conclusion. If we do not take into account the direct Higgs-gravity interaction, NP terms can strongly destabilize the EW vacuum, and without a knowledge of high energy New Physics, in particular without a complete theory of Quantum Gravity, we cannot draw any conclusion on the ultimate fate of our universe. The Higgs-gravity interaction term, whose presence is guaranteed by exceptionally well known experimental facts (gravity, the Higgs boson, the quantum nature of physical laws), acts as a *universal stabilizing mechanism*, that washes out any potentially destabilizing effect from high energy New Physics (for instance from unknown Quantum Gravity), protecting our universe from a disastrous decay.

Chapter 6

Stability of the EW Vacuum in SUGRA frameworks

In the previous chapters we have seen that the problem of stability of the EW vacuum [35, 66, 67, 87–98] has been central not only in our understanding of the Standard Model, but also in demystifying the very nature of possible New Physics. In particular, we have shown that Planckian NP can strongly affect the stability of the EW vacuum and the presence of possible harmful Planck-scale-suppressed operators of the form ϕ^{2n}/M_P^{2n-4} can no longer be ignored in the computation [51].

Although we may not be able to exclude *a priori* such harmful operators, one may still wonder whether a mechanism exists in order to protect the EW vacuum from a disastrous decay. In Chapter 4 we have seen that the direct interaction between the Higgs boson and gravity can provide such a mechanism. We can also require whether a protective symmetry can be invented in order to postpone the appearance of these harmful Planck-scale-suppressed operators ϕ^{2n}/M_P^{2n-4} to arbitrarily high orders n , so as to render their destabilising effect on the EW vacuum harmless.

In this Chapter we will show how supergravity (SUGRA) embeddings of the SM [99] could be sufficient to protect the stability of the EW vacuum up to very large values of the soft supersymmetry (SUSY) breaking scale M_S , above the SM instability scale of 10^{11} GeV. Moreover, we will explicitly demonstrate how discrete R symmetries could be used in order to restrict the form of the holomorphic superpotential \mathcal{W} , and so suppress the appearance of the harmful Planck-scale operators of the type ϕ^{2n}/M_P^{2n-4} to arbitrary higher powers of n [100].

6.1 Theoretical background

In this Chapter we will refer to many equations of the previous chapters which we will report here for the sake of simplicity. In particular, we will consider both the

flat spacetime background, described by the action (3.89)

$$S[\phi] = \int d^4x \left(\frac{1}{2} \partial_\mu \phi \partial_\mu \phi + V(\phi) \right), \quad (6.1)$$

and the curved spacetime background, described by the action (3.104)

$$S[\phi, g_{\mu\nu}] = \int d^4x \sqrt{g} \left(-\frac{1}{2} M_{\text{Pl}}^2 R + \frac{1}{2} g^{\mu\nu} \partial_\mu \phi \partial_\nu \phi + V(\phi) \right), \quad (6.2)$$

where M_{Pl} is the *reduced* Planck mass. The latter is related to the ordinary Planck mass $M_P \approx 1.9 \times 10^{19}$ GeV and the Newton's constant G_N as follows:

$$M_{\text{Pl}}^2 \equiv \frac{M_P^2}{8\pi} = (8\pi G_N)^{-1}. \quad (6.3)$$

In Eqs. (6.1) and (6.2), $g_{\mu\nu}$ is the $O(4)$ symmetric metric given in Eq. (3.105), while $V(\phi)$ is the potential with a metastable state that is given by Eqs. (4.6), (4.7) and (4.8) in the Standard Model case.

As in the previous chapters, we will compute the bounce solutions relative to the potential taken into account using Eqs. (3.97), (3.98) and (3.99) for the flat spacetime background, and Eqs. (3.109) and (3.113) for the curved spacetime background. Then, the tunneling time $\tau = \Gamma^{-1}$ is computed in the usual way:

$$\Gamma = D e^{-\left(S[\phi_b] - S[\phi_{\text{fvl}}]\right)} \equiv D e^{-B} \Rightarrow \tau \simeq \left(\frac{\mathcal{R}^4}{T_U^4}\right) e^{S_b} T_U, \quad (6.4)$$

where \mathcal{R} is the size of the bounce solution. The tunneling exponent B in the flat space time case is given by:

$$B = 2\pi^2 \int_0^\infty dr r^3 \left(\frac{1}{2} \dot{\phi}_b^2 + V(\phi_b) \right) = -2\pi^2 \int_0^\infty dr r^3 V(\phi_b), \quad (6.5)$$

where in the left hand side, following steps similar to those of Derrick's theorem, the kinetic term $\frac{1}{2} \dot{\phi}_b^2$ in (6.5) may effectively be replaced with $-2V(\phi_b)$. Instead, in the curved spacetime case the tunneling exponent B is given by:

$$B = -2\pi^2 \int_0^\infty dr \rho^3 V(\phi). \quad (6.6)$$

6.2 Planckian New Physics Effects

In this Section we consider the presence of Planck-scale suppressed operators of the type ϕ^{2n}/M^{2n-4} in addition to the SM effective potential $V_{\text{SM}}(\phi)$, where M is of order M_P . Such operators could in principle be generated by quantum gravity effects and as such, they cannot be excluded *a priori* from $V_{\text{SM}}(\phi)$. If their contribution to the SM potential becomes negative, they may have a dramatic destabilizing effect on our EW vacuum, as extensively discussed in Chapter 4 for $n = 3$ [54, 65, 71, 72].

As we will show below this destabilizing effect may be present also for $n > 3$: for these reasons we call such operators that contribute with a *negative* sign to $V_{\text{SM}}(\phi)$ as *harmful* operators.

Let us consider a set of distinct ϕ^{2n} -models that could effectively describe unknown Planckian NP effects. To this end, we extend the SM effective potential as follows:

$$V_{2n}(\phi) = V_{\text{SM}}(\phi) + V_{\text{NP}}^{(2n)}(\phi), \quad (6.7)$$

where $n \geq 3$, and

$$V_{\text{NP}}^{(2n)}(\phi) = \frac{c_1}{2n} \frac{\phi^{2n}}{M^{2n-4}} + \frac{c_2}{2(n+1)} \frac{\phi^{2(n+1)}}{M^{2n-2}}. \quad (6.8)$$

It is worth to note that all potentials $V_{2n}(\phi)$ in (6.7) reduce to $V_{\text{SM}}(\phi)$ for $\phi \ll M$, as its NP part, $V_{\text{NP}}^{(2n)}(\phi)$, becomes subdominant in this small-field regime. For all the NP effective potentials $V_{\text{NP}}^{(2n)}(\phi)$, we will assume that c_1 is negative, but c_2 is positive, so as to ensure the convexity of the potential at high field values of $\phi \gg M$. Thus, the first term ϕ^{2n}/M^{2n-4} in (6.8) represents a harmful operator, which we will use from now on to characterize both the ϕ^{2n} -model and its effective potential $V_{2n}(\phi)$.

In the following, we will analyze numerically the impact of the harmful Planck-scale NP operators ϕ^{2n}/M^{2n-4} on the tunnelling time τ of the EW vacuum, for *all* $n \geq 3$. To better assess the relevance of these operators, we will simply set $c_1 = -2$ and $c_2 = 2$. Moreover, we will investigate two Planck-scale scenarios with: (i) $M = M_{\text{P}}$ and (ii) $M = M_{\text{P}}/10$, for both a flat and a curved background metric.

6.2.1 Planck-Scale Scenarios with $M = M_{\text{P}}$

We first consider a class of ϕ^{2n} -scenarios with scalar potentials $V_{2n}(\phi)$ given by (6.7), where the Planckian NP scale M is set equal to M_{P} . As can be seen from the upper panel of Fig. 6.1 and presented by dashed lines in multiple colours, the negative contribution of the harmful Planck-scale operators $\phi^{2n}/M_{\text{P}}^{2n-4}$ in (6.8) produces a second minimum in their respective effective potentials at $\phi \sim M_{\text{P}}$. For comparison, in the same panel we display with a solid blue line the SM effective potential $V_{\text{SM}}(\phi)$ given in (4.6).

As we know from the previous chapters, a key quantity that determines the tunnelling decay time τ of the EW vacuum is the actual profile of the bounce solutions $\phi(r) \equiv \phi_b(r)$. These are depicted by dashed lines in multiple colours on the lower panel of Fig. 6.1 for a flat background metric, where the solid line in blue corresponds to the SM bounce. Note that all the bounces $\phi(r)$ reach their highest value close to $r = 0$, thereby giving the largest support to the tunnelling exponent B in (6.4). When normalising the effect of the harmful NP operators to the

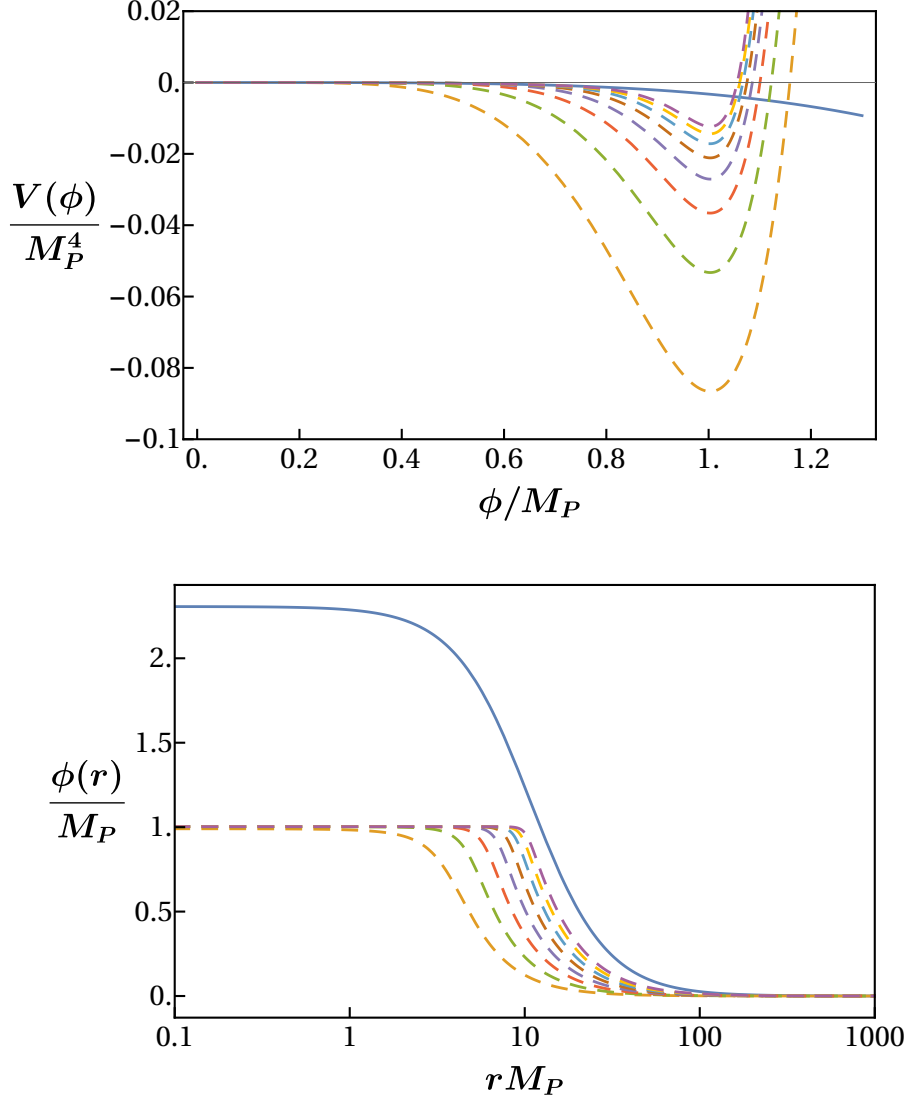


Figure 6.1: *Upper panel.* Scalar potentials $V_{2n}(\phi)$ [cf. (6.7)], for $3 \leq n \leq 10$, as functions of ϕ (dashed lines), with $c_1 = -c_2 = -2$ and $M = M_P$. The blue line corresponds to the SM potential $V_{\text{SM}}(\phi)$ given in (5.17). *Lower panel.* Radial profiles of bounce solutions $\phi(r) \equiv \phi_b(r)$ (dashed lines) for the same class of Planck-scale scenarios evaluated for a flat spacetime metric. The solid (blue) line refers to the respective SM bounce.

one originating from the SM potential term $\frac{1}{4}\lambda\phi^4$, we get the ratio

$$R_{2n} = \frac{2c_1}{n\lambda} \left(\frac{\phi(0)}{M_P} \right)^{2n-4}. \quad (6.9)$$

Since $\phi(0)/M_P \sim 1$ for all $n \geq 3$, we expect that as n increases, R_{2n} will decrease and the predictions for the EW vacuum lifetime τ will get closer to the SM value τ_{SM} . Indeed, this property is observed in Tab. 6.1 for the flat spacetime case. In order to get a lifetime τ much larger than the age of the Universe T_U , we need to suppress all potentially harmful operators ϕ^{2n}/M_P^{2n-4} up to $n = 6$, while one gets $\tau \sim \tau_{\text{SM}}$

$\frac{\phi^{2n}}{M^{2n-4}}$	τ/T_U (flat)	τ/T_U (curved)	$\frac{\phi^{2n}}{M^{2n-4}}$	τ/T_U (flat)	τ/T_U (curved)
$n = 3$	10^{-208}	10^{-122}	$n = 7$	10^7	8.8×10^{661}
$n = 4$	10^{-166}	3.4×10^{661}	$n = 8$	10^{71}	8.8×10^{661}
$n = 5$	10^{-114}	8.8×10^{661}	$n = 9$	10^{133}	8.8×10^{661}
$n = 6$	10^{-55}	8.8×10^{661}	$n = 10$	10^{193}	8.8×10^{661}

Table 6.1: Lifetime τ of the EW vacuum for a class of Planck-scale scenarios with harmful operators ϕ^{2n}/M^{2n-4} , evaluated for a flat and a curved background metric. As input values for the NP parameters, we set $c_1 = -c_2 = -2$ and $M = M_P$.

when $n \geq 50$. In the next section, we will outline a protective mechanism within a SUGRA framework, which can in principle give rise to such a suppression.

Let us now investigate the effect of a curved background metric on the EW vacuum lifetime τ . Unlike in the flat spacetime, an important novel aspect of the curved metric is that for increasing n , the bounce solutions $\phi(r)$ and $\rho(r)$ rapidly tend to the corresponding SM bounces, as shown in Fig. 6.2. As exhibited in Tab. 6.1, we obtain $\tau \sim \tau_{\text{SM}} \sim 10^{661} T_U$ (cf. Eq. (4.20)), for all Planck-scale scenarios with $n \geq 4$. This stabilizing effect of gravity on the EW vacuum may also be attributed to the fact that for $n \geq 4$, one finds $\phi(0) \sim 0.07$ which is smaller by more than one order of magnitude from the corresponding value in the flat spacetime. As a result, the size of NP contributions as represented by R_{2n} in (6.9) will decrease more drastically as n grows, for a curved spacetime metric. In the next section, we will explore whether this feature will persist for Planck-scale scenarios with a lower quantum gravity scale M .

6.2.2 Planck-Scale Scenarios with $M = M_P/10$

Proceeding as in the previous section, we will analyze a similar class of ϕ^{2n} -models, by assuming that the Planckian NP scale M is now one order of magnitude smaller, i.e. $M = M_P/10$. Such a choice may be motivated by the fact that the relevant energy scale of quantum gravity that enters Einstein's equation is the reduced Planck mass M_{Pl} (cf. Eq. (6.3)), rather than the ordinary Planck mass M_P .

From the upper panel of Fig. 6.3, we observe that the minimum of the potentials V_{2n} is now located to a smaller value at $\phi_{\min} \sim M_P/10$. The profiles of the bounces $\phi(r)$ for a flat spacetime metric are presented by dashed lines in various colours in the lower panel of Fig. 6.3, while the solid (blue) line stands for the SM bounce. In order to assess the impact of gravity, we give in Tab. 6.2 the lifetime τ of

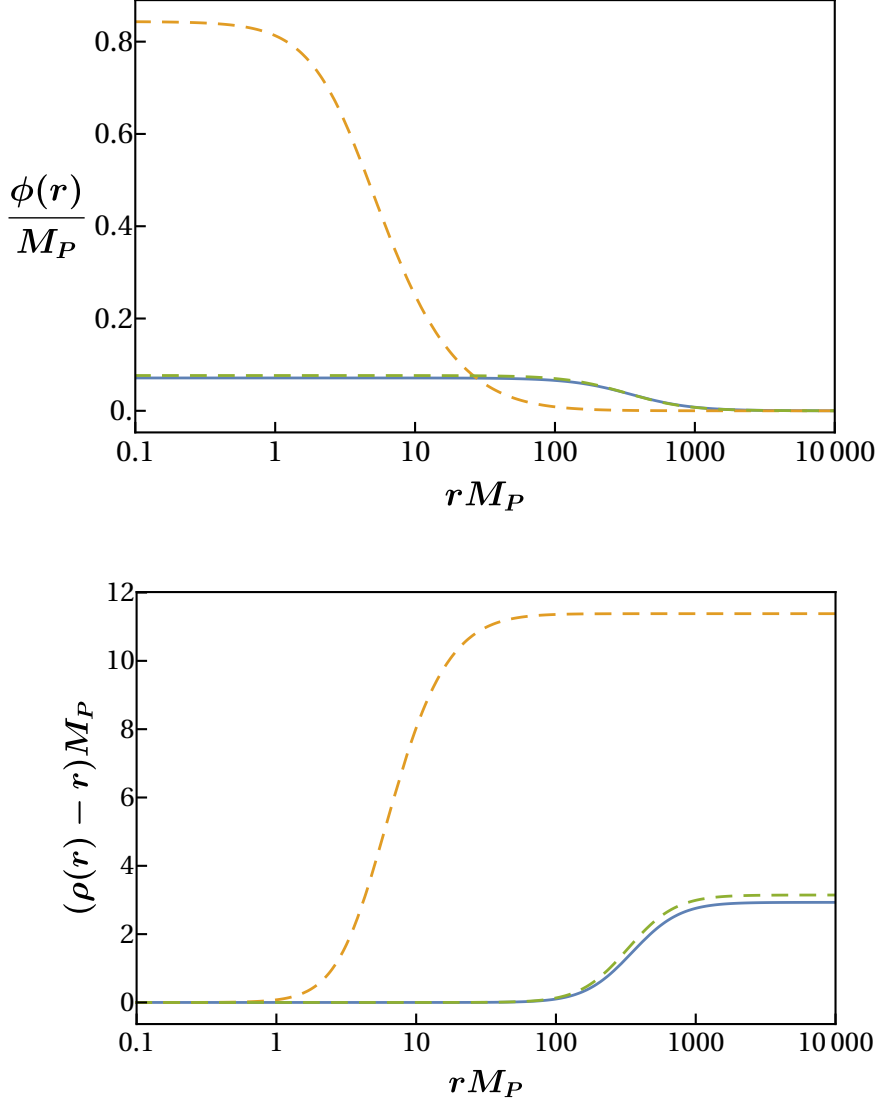


Figure 6.2: *Upper panel.* Radial dependence of the bounce solutions $\phi(r)$ (dashed lines) for the Planck-scale scenarios, with $n = 3, 4$ and $M = M_P$, evaluated for a curved spacetime metric. *Lower panel.* Radial profiles for $\rho(r) - r$ (dashed lines) for the same scenarios and background metric. The solid (blue) lines in the two panels show the bounce profiles in the SM.

the EW vacuum, for both a flat and a curved spacetime background. As opposed to the previous scenarios, we now observe that the impact of gravity is less significant, and restoration of the SM prediction for τ takes place for $n \geq 41$.

Comparing the flat-spacetime results exhibited in Tabs. 6.2 and 6.1, we notice that the predicted values for the tunnelling times τ for each n turn out to be close. As before, we may understand this result by looking at the ratios,

$$R_{2n} = \frac{2c_1}{n\lambda} \left(\frac{\phi(0)}{M} \right)^{2n-4} = \frac{2c_1}{n\lambda} \left(\frac{10\phi(0)}{M_P} \right)^{2n-4}. \quad (6.10)$$

Unlike the previous case $M = M_P$, an extra factor 10^{2n-4} now appears, because we

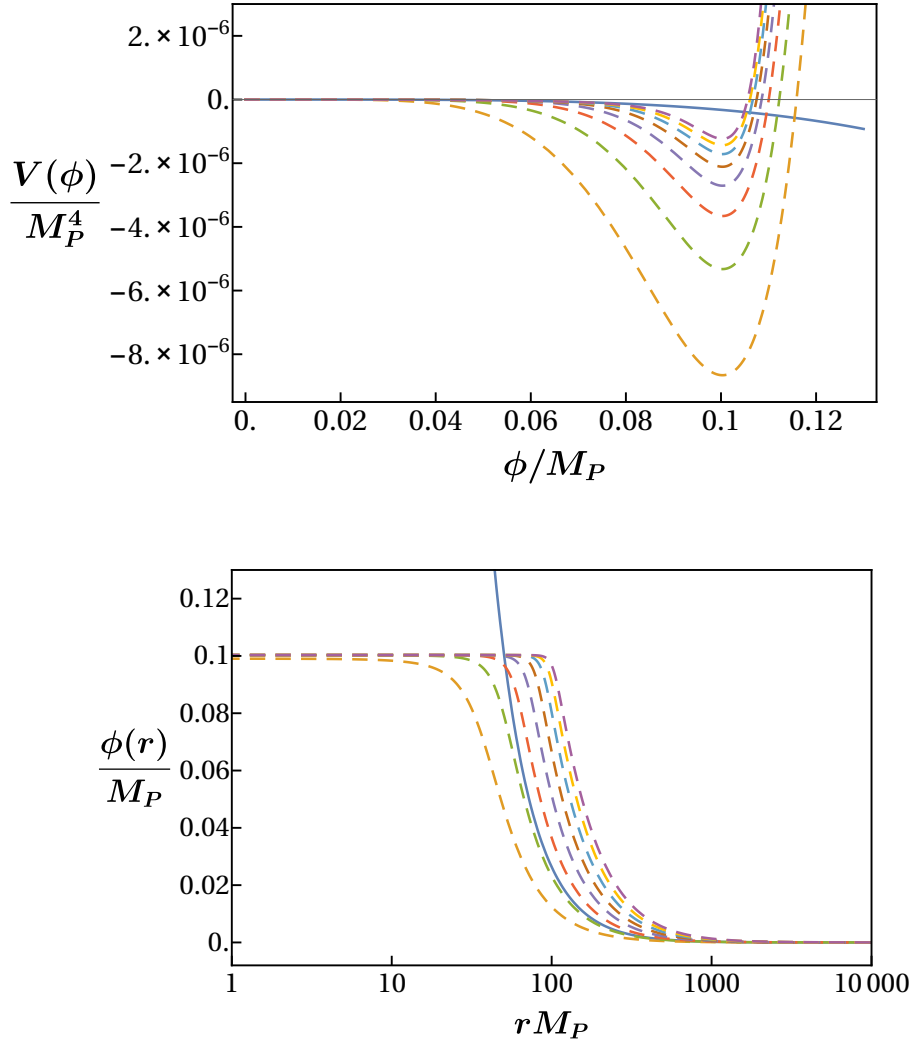


Figure 6.3: The same as in Fig. 6.1, but setting instead $M = M_P/10$.

$\frac{\phi^{2n}}{M^{2n-4}}$	τ/T_U (flat)	τ/T_U (curved)	$\frac{\phi^{2n}}{M^{2n-4}}$	τ/T_U (flat)	τ/T_U (curved)
3	10^{-204}	10^{-203}	7	10^{12}	10^{21}
4	10^{-162}	10^{-160}	8	10^{76}	10^{87}
5	10^{-110}	10^{-106}	9	10^{138}	10^{152}
6	10^{-51}	10^{-44}	10	10^{198}	10^{214}

Table 6.2: Lifetime τ of the EW vacuum for a class of Planck-scale scenarios that include harmful operators ϕ^{2n}/M^{2n-4} , with $M = M_P/10$, evaluated for both a flat and a curved background metric.

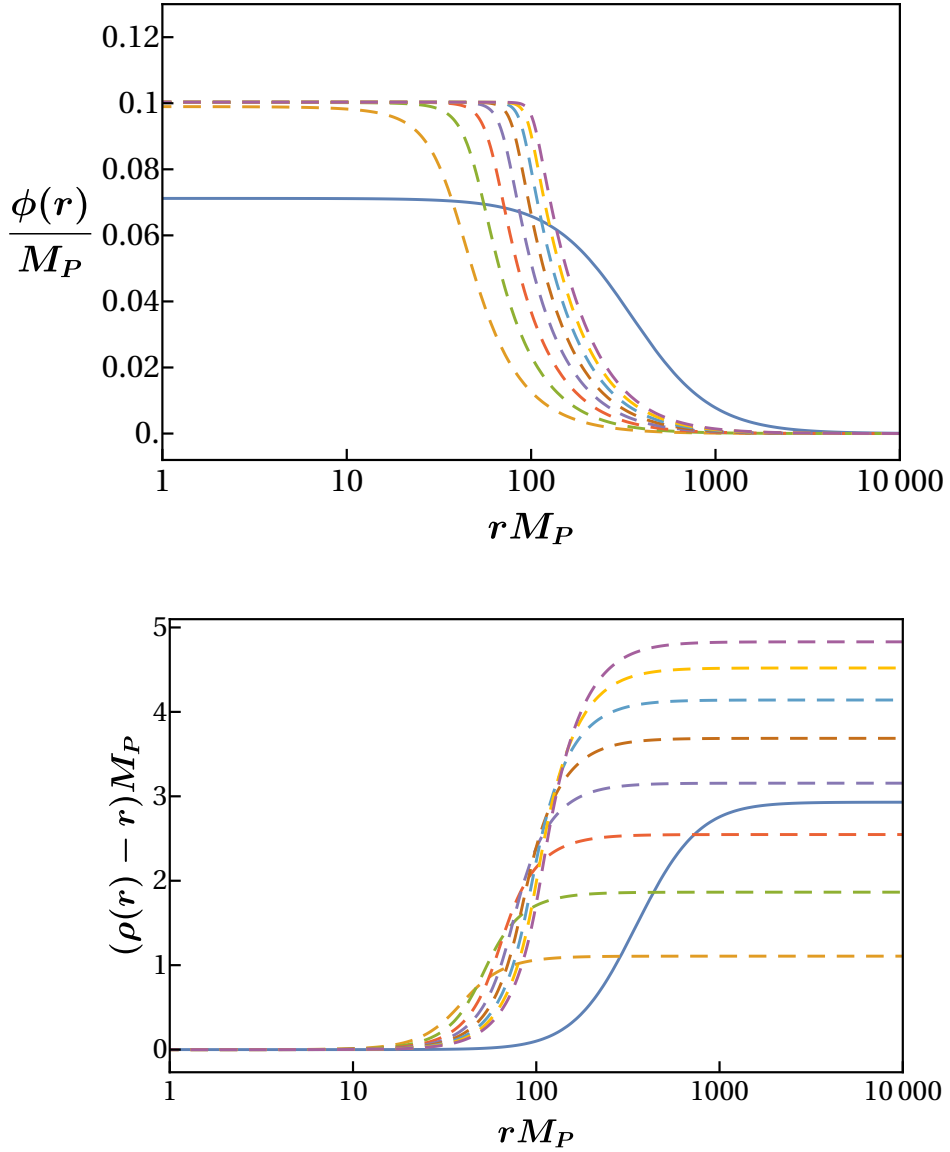


Figure 6.4: The same as in Fig. 6.2, for scenarios with $3 \leq n \leq 10$ and $M = M_P/10$.

have $M = M_P/10$. As can be seen from the lower panel of Fig. 6.3, the maximum of all bounces reached at their origin ($r = 0$) approaches the value: $\phi(0)/M_P \sim 0.1$. Hence, the enhancement factor 10^{2n-4} in (6.10) gets compensated by a corresponding factor $(\phi(0)/M_P)^{2n-4} \sim 10^{-(2n-4)}$. As a consequence of this cancellation, the order-of-magnitude estimates of the tunnelling time τ for the two Planck-scale scenarios, with $M = M_P$ and $M = M_P/10$, will be comparable.

Let us now turn our attention to the curved spacetime analysis and the numerical estimates of the EW vacuum lifetime τ given in Tab. 6.2. As mentioned earlier, the impact of gravity on τ is minimal in this case. This can be better understood by analysing the profile for the bounce solutions $\phi(r)$ and $\rho(r)$, for $n \geq 3$. As shown in Fig. 6.4, the bounces $\phi(r)$ quickly approach the ones found above in Fig. 6.3 (lower panel) for the flat spacetime metric. Hence, we expect for the EW vacuum lifetime τ

to be less affected by the presence of gravity, becoming independent of the radial coordinate $\rho(r)$.

The above exercise illustrates how the occurrence of harmful operators in Planckian NP theories that happen to realise a relatively low scale of quantum gravity M face a serious destabilization problem of the EW vacuum. In the next section, we will discuss mechanisms that can naturally suppress the presence of leading harmful operators to sufficiently higher powers of n , within a minimal SUGRA framework.

6.3 Protective Mechanisms in SUGRA

Given our ignorance of a UV-complete theory of quantum gravity, Planck-scale gravitational effects are usually treated within the context of a low-energy effective field theory by considering *all* possible gauge-invariant non-renormalizable operators suppressed by inverse powers of a high-scale mass M , which is typically of the order of the *reduced* Planck mass $M_{\text{Pl}} \approx 2.4 \times 10^{18}$ GeV. Specifically, gravitational effects on the SM scalar potential $V_{\text{SM}}(\phi)$ along the gauge-invariant field direction $\phi = \sqrt{2}(\Phi^\dagger\Phi)^{1/2} \geq 0$, where Φ is the SM Higgs doublet, may be described by the effective potential

$$V(\phi) = V_{\text{SM}}(\phi) + \sum_{n=3}^{\infty} \frac{\lambda_{2n}}{2n} \frac{\phi^{2n}}{M^{2n-4}}, \quad (6.1)$$

with $V_{\text{SM}}(\phi) = -m^2\phi^2/2 + \lambda\phi^4/4$. Depending on the sign and size of the coefficient λ_6 for the leading Planck-scale suppressed operator ϕ^6/M^2 , the lifetime of the EW vacuum can vary by many orders of magnitude [54]. In particular, if λ_6 is negative and $|\lambda_6|$ large, the operator ϕ^6/M^2 then becomes *harmful* and could lead to a dramatic destabilization of the EW vacuum, for both flat and curved spacetime backgrounds [51]. In the following, we will show how SUGRA embeddings of the SM [99] could protect the EW vacuum from rapid decay up to very large values of the soft SUSY-breaking scale M_S , above the so-called SM metastability scale of 10^{11} GeV.

To start with, let us first consider the Minimal Supersymmetric extension of the Standard Model (MSSM), in which only Planck-mass suppressed non-renormalizable operators involving the Higgs chiral superfields $\hat{H}_{1,2}$ are considered. In other words, we ignore for simplicity non-renormalizable operators of all other chiral superfields in the effective superpotential $\widehat{\mathcal{W}}$. In a SUGRA framework, $\widehat{\mathcal{W}}$ will then be given by

$$\widehat{\mathcal{W}} = \widehat{\mathcal{W}}_0 + \mu \hat{H}_1 \hat{H}_2 + \sum_{n=2}^{\infty} \frac{\rho_{2n}}{2n} \frac{(\hat{H}_1 \hat{H}_2)^n}{M^{2n-3}}, \quad (6.2)$$

where

$$\widehat{\mathcal{W}}_0 = h_l \hat{H}_1 \hat{L} \hat{E} + h_d \hat{H}_1 \hat{Q} \hat{D} + h_u \hat{H}_2 \hat{Q} \hat{U} \quad (6.3)$$

is the usual MSSM superpotential without the μ term, and \hat{H}_1 , \hat{H}_2 are the chiral superfields for the two Higgs doublets, \hat{Q} , \hat{L} are the chiral superfields for the quark and lepton left-handed iso-doublets, and \hat{U} , \hat{D} , \hat{E} are their respective right-handed iso-singlet counterparts¹. Note that in writing (6.3), we have suppressed all flavour indices from the lepton and quark Yukawa couplings h_l , h_d and h_u .

To simplify matters, we consider that all our SUGRA embeddings are based on a minimal Kaehler potential $\hat{\mathcal{K}}$ given by

$$\hat{\mathcal{K}} \equiv \mathcal{K}(\hat{\varphi}_i^*, \hat{\varphi}_i) = \hat{H}_1^\dagger \hat{H}_1 + \hat{H}_2^\dagger \hat{H}_2 + \dots, \quad (6.4)$$

where $\hat{\varphi}_i$ is a generic chiral superfield and contributions from $SU(2)_L$ and $U(1)_Y$ vector superfields are not shown. At the tree level, the scalar SUGRA potential V may be written as a sum of three terms: $V = V_F + V_D + V_{\text{br}}$, since it receives three contributions from: (i) F -terms (V_F), (ii) D -terms (V_D), and (iii) the so-called SUSY-breaking terms (V_{br}) induced by spontaneous breakdown of SUGRA that may occur in the so-called hidden sector of the theory [99]. In particular, the F - and D -terms of the potential V may be calculated from the general expressions:

$$V_F = e^{\mathcal{K}/M_{\text{Pl}}^2} \left[\left(\mathcal{W}_{,i} + \frac{\mathcal{K}_{,i}}{M_{\text{Pl}}^2} \mathcal{W} \right) G^{-1,ij} \left(\mathcal{W}_{,j} + \frac{\mathcal{K}_{,j}}{M_{\text{Pl}}^2} \mathcal{W}^* \right) - 3 \frac{|\mathcal{W}|^2}{M_{\text{Pl}}^2} \right] \quad (6.5)$$

$$V_D = \frac{g^2}{2} f_{ab}^{-1} D^a D^b, \quad (6.6)$$

where $\mathcal{W} \equiv \mathcal{W}(\varphi_i)$, $\mathcal{K} \equiv \mathcal{K}(\varphi_i^*, \varphi_i)$, $\mathcal{W}_{,i} \equiv \partial \mathcal{W} / \partial \varphi_i$, $\mathcal{K}_{,i} \equiv \partial \mathcal{K} / \partial \varphi_i$, $\mathcal{K}_{,\bar{i}} \equiv \mathcal{K}_{,i}^*$ etc, for a generic scalar field φ_i , and $G^{-1,ij}$ is the inverse of the Kaehler-manifold metric: $G_{ij} = \mathcal{K}_{,ij} = \partial^2 \mathcal{K} / (\partial \varphi_i \partial \varphi_j)$. In addition, g is a generic gauge coupling, e.g. of $SU(2)_L$, f_{ab} is the gauge kinetic function taken to be minimal, i.e. $f_{ab} = \delta_{ab}$, and $D^a = \mathcal{K}_{,\varphi} T^a \varphi$ are the so-called D -terms, where T^a are the generators of the gauge group. Finally, the SUSY-breaking Higgs potential V_{br}^H generated from the effective superpotential in (6.2) is given by

$$V_{\text{br}}^H = m_1^2 |H_1|^2 + m_2^2 |H_2|^2 + \left(B\mu H_1 H_2 + \sum_{n=2}^{\infty} A_{2n} \frac{(H_1 H_2)^n}{M^{2n-3}} + \text{H.c.} \right). \quad (6.7)$$

For the purpose of this Chapter, we will assume that the μ -term and the soft mass parameters $m_{1,2}^2$ and $B\mu$ are of order M_S , but all other SUSY-breaking A -terms A_{2n} could be as large as M . Although such an unusual assumption does not sizeably destabilize the gauge hierarchy for $M_S \lesssim 10$ TeV, it can still significantly affect the predictions for the Higgs-boson mass spectrum. Here, we will not address the mechanism causing this large hierarchy between the soft parameters and the higher order A -terms, as it strongly depends on the details of the hidden sector in which SUSY gets spontaneously broken [99].

¹Here we follow the conventions of [101]. A comprehensive review of the EW sector of the MSSM is given in [102]

Let us for the moment consider the SUSY limit of the MSSM, by ignoring the induced SUSY-breaking terms V_{br}^H in the scalar potential V . Assuming that the μ -term is of order M_S and so negligible when compared to M_{Pl} , the renormalizable part of the MSSM potential, denoted by V_0 , has an F - and D -flat direction associated with the gauge-invariant operator $\hat{H}_1 \hat{H}_2$. In the absence of the μ -term, the scalar field configuration:

$$H_1 = \frac{1}{\sqrt{2}} \begin{pmatrix} \phi \\ 0 \end{pmatrix}, \quad H_2 = \frac{e^{i\xi}}{\sqrt{2}} \begin{pmatrix} 0 \\ \phi \end{pmatrix}, \quad (6.8)$$

with $\xi \in [0, 2\pi)$ and all other scalar fields taken at the origin, gives rise to an exact flat direction for V_0 , i.e. $\partial V_0 / \partial \phi = 0$. Here ϕ is a *positive* scalar field background with canonical kinetic term that parameterizes the D -flat direction. The CP-odd angle ξ indicates that the flat directions for H_1 and H_2 may also differ by an arbitrary relative phase ξ . Hence, the parameters (ϕ, ξ) describe fully the D -flat direction of interest. Now, in the flat-space limit $M_{\text{Pl}} \rightarrow \infty$, V_{0F} is positive, implying that $V_0 = V_{0F} + V_{0D} \geq 0$, where the equality sign holds along a flat direction, such as the ϕ -direction.

The above property of a non-negative potential will generically persist in the minimal SUGRA for the full observable-sector potential V , namely upon the inclusion of gauge-invariant non-renormalizable operators consisting only of MSSM fields. To see this, we first write the MSSM superpotential $\widehat{\mathcal{W}}$ as the sum: $\widehat{\mathcal{W}} = \sum_a \widehat{\mathcal{W}}^a$, where $\widehat{\mathcal{W}}^a$ is an arbitrary superpotential term labelled by the index a . Then, we notice that the only negative contribution to V can potentially come from both the cross terms and the last term that occur in V_F given in (6.5). In particular, up to an overall positive factor $e^{\mathcal{K}/M_{\text{Pl}}^2}$, we have

$$V_F \supset \sum_{a,b} \left[\left(\frac{\mathcal{K}_{,\bar{i}}}{M_{\text{Pl}}^2} \mathcal{W}_{,i}^a \mathcal{W}^{b*} + \text{H.c.} \right) - 3 \frac{\mathcal{W}^a \mathcal{W}^{b*}}{M_{\text{Pl}}^2} \right] = \sum_{a,b} (N_a + N_b - 3) \frac{\mathcal{W}^a \mathcal{W}^{b*}}{M_{\text{Pl}}^2}. \quad (6.9)$$

In arriving at the last equality in (6.9), we used the fact that $\mathcal{K}_{,\bar{i}} \mathcal{W}_{,i}^a = N_a \mathcal{W}^a$ in minimal SUGRA, where N_a is the number of scalar fields φ_i present in $\widehat{\mathcal{W}}^a$. Given that $N_{a,b} \geq 2$ for all superpotential terms in the MSSM, the last expression on the RHS of (6.9) will be non-negative, with a possible exception specific field configurations for which $N_a \neq N_b$. Thus, barring fine-tuning, the F -term potential V_F of the observable sector in (6.5) will be non-negative². Since $V_D \geq 0$ as well, the complete MSSM scalar potential, including the infinite series of the non-renormalizable operators, will generically be non-negative.

²Instead, hidden-sector chiral superfields \hat{Z} can lead to a negative contribution to V_F via SUSY-breaking effects from a Polonyi-type superpotential $\widehat{\mathcal{W}}_{\text{hidden}} = m^2 (\hat{Z} + \beta)$, for which $N_{a,b} \leq 1$. This negative contribution is even desirable, as it can be used to fine-tune the cosmological constant to its observed small value. Similarly, non-minimal Kaehler potential may also lead to negative contributions to V_F . A more detailed discussion is given in [99].

The above situation changes drastically, if the SUSY-breaking A -terms as given in (6.7) are added to the scalar potential V . For illustration, let us consider the minimally extended MSSM superpotential

$$\widehat{\mathcal{W}} = \widehat{\mathcal{W}}_0 + \mu \widehat{H}_1 \widehat{H}_2 + \frac{\rho_4}{4} \frac{(\widehat{H}_1 \widehat{H}_2)^2}{M}, \quad (6.10)$$

which induces the SUSY-breaking potential

$$V_{4,\text{br}}^H = m_1^2 |H_1|^2 + m_2^2 |H_2|^2 + \left(B\mu H_1 H_2 + A_4 \frac{(H_1 H_2)^2}{M} + \text{H.c.} \right), \quad (6.11)$$

for the Higgs sector. For simplicity, we envisage a scenario for which $m_{1,2}^2 \ll B\mu$. Moving along the D -flat direction as stated in (6.8), and upon ignoring radiative corrections for field values $\phi > M_S$, the leading part of the scalar potential takes on the simple form:

$$V_4(\phi) = e^{\phi^2/M_{\text{Pl}}^2} \left[-\frac{m^2}{2} \phi^2 + \frac{\text{Re}(e^{2i\xi} A_4)}{2M} \phi^4 + \frac{|\rho_4|^2}{8} \frac{\phi^6}{M^2} \left(1 + \frac{5}{32} \frac{\phi^2}{M_{\text{Pl}}^2} + \frac{1}{32} \frac{\phi^4}{M_{\text{Pl}}^4} \right) \right], \quad (6.12)$$

where higher-order terms proportional to $|\mu|/M \lesssim M_S/M \ll 1$ were neglected and $m^2 = |e^{i\xi} B\mu - |\mu|^2|$ is arranged to be of the required EW order. Note that even if $A_4 > 0$, the field direction (6.8) with $\xi = \pi/2$ will make the coefficient $\text{Re}(e^{2i\xi} A_4)$ entering the potential V_4 in (6.12) negative. If A_4 is comparable to M , the quartic coupling ϕ^4 can become both sizeable and negative, giving rise to a potential V_4 that develops a new minimum of order $M/|\rho_4|$, far away from its SM value. On the other hand, the higher powers ϕ^6 , ϕ^8 and ϕ^{10} are all proportional to the positive coefficient $|\rho_4|^2$, thereby ensuring the convexity of the potential V_4 . Clearly, this exercise shows that SUSY is rather effective in protecting the stability of the EW vacuum from *unknown* Planck-scale gravitational effects, unless the induced SUSY-breaking coupling A_4 happens to be of order $M \sim M_{\text{Pl}}$.

In the following, we will see that SUSY may still be effective for protecting the stability of our EW vacuum, even for extreme scenarios with $A_{2n} \sim M_{\text{Pl}}$ and M_S above the metastability scale of order 10^{11} GeV, along the lines of split-SUSY [103, 104]. To this end, let us first consider the following discrete symmetry transformations on the chiral superfields:

$$(\widehat{H}_1, \widehat{H}_2, \widehat{Q}, \widehat{L}) \rightarrow \omega (\widehat{H}_1, \widehat{H}_2, \widehat{Q}, \widehat{L}), \quad (6.13)$$

whereas the remaining iso-singlet chiral superfields, \widehat{U} , \widehat{D} and \widehat{E} , do not transform. Equation (6.13) implies: $\widehat{\mathcal{W}} \rightarrow \omega^2 \widehat{\mathcal{W}}$. If $\omega^2 = 1$, the discrete transformations stated in (6.13) give rise to a global Z_2 symmetry, which is automatically satisfied by the complete effective superpotential \mathcal{W}_{eff} in (6.2) and the minimal Kaehler potential \mathcal{K} in (6.4). For $\omega^2 \neq 1$, however, the superpotential \mathcal{W} is charged and (6.13) represents

a non-trivial discrete R -symmetry, which is maintained by an appropriate rotation of the Grassmann-valued coordinates of the SUSY space.

We may now exploit this discrete R -symmetry in order to suppress lower powers of the non-renormalizable operators in the effective superpotential $\widehat{\mathcal{W}}$ given in (6.2), as well as the respective A_{2n} terms induced by $\widehat{\mathcal{W}}$. Given that $\widehat{H}_1 \widehat{H}_2 \rightarrow \omega^2 \widehat{H}_1 \widehat{H}_2$ under the discrete R -symmetry transformations in (6.13), we may now require that

$$\omega^{2n} = \omega^2, \quad (6.14)$$

for $n > 2$. Note that for $n = 1, 2$, no non-trivial restrictions on the form of $\widehat{\mathcal{W}}$ will arise.

Let us therefore turn our attention to the case with $n = 3$ in (6.14). This leads to a scenario realizing the discrete R -symmetry Z_4^R , with $\omega^4 = 1$ and $\omega^2 = -1 \neq 1$. In this case, $\widehat{\mathcal{W}}$ takes on the form:

$$\widehat{\mathcal{W}} = \widehat{\mathcal{W}}_0 + \mu \widehat{H}_1 \widehat{H}_2 + \frac{\rho_6}{6} \frac{(\widehat{H}_1 \widehat{H}_2)^3}{M^3} + \frac{\rho_{10}}{10} \frac{(\widehat{H}_1 \widehat{H}_2)^5}{M^7} + \dots \quad (6.15)$$

In such a minimal SUGRA framework with R -symmetry, the induced SUSY-breaking potential for the Higgs sector is expected to be of the form [99]:

$$V_{6,\text{br}}^H = \left(B\mu H_1 H_2 + A_6 \frac{(H_1 H_2)^3}{M^3} + A_{10} \frac{(H_1 H_2)^5}{M^7} + \dots \right) + \text{H.c.} \quad (6.16)$$

As before, we assume for simplicity that the soft SUSY-breaking mass parameters $m_{1,2}^2$ are small, i.e. $m_{1,2}^2 \ll B\mu$, so that they can be ignored. Likewise, we assume that only the leading ρ_6 -coupling and the A_6 term are sizeable and so relevant. In this case, along the D -flat direction (6.8), the scalar potential for $\phi > M_S$ will acquire the simple form

$$V_6(\phi) = e^{\phi^2/M_{\text{Pl}}^2} \left[-\frac{m^2}{2} \phi^2 + \frac{\text{Re}(e^{3i\xi} A_6)}{4M} \frac{\phi^6}{M^2} + \frac{|\rho_6|^2}{32} \frac{\phi^{10}}{M^6} \left(1 + \frac{9}{72} \frac{\phi^2}{M_{\text{Pl}}^2} + \frac{1}{72} \frac{\phi^4}{M_{\text{Pl}}^4} \right) \right]. \quad (6.17)$$

In fact, this last result can be generalized to a discrete R -symmetry Z_{2n-2}^R , with $\omega^{2(n-1)} = 1$ and $n \geq 3$. In this case, the leading form of the scalar potential V_{2n} for $\phi > M_S$ becomes

$$\begin{aligned} V_{2n}(\phi > M_S) = & e^{\phi^2/M_{\text{Pl}}^2} \left[-\frac{m^2}{2} \phi^2 + \frac{\text{Re}(e^{n i \xi} A_{2n})}{2^{n-1} M} \frac{\phi^{2n}}{M^{2(n-2)}} \right. \\ & \left. + \frac{|\rho_{2n}|^2}{2^{2n-1}} \frac{\phi^{2(2n-1)}}{M^{2(2n-3)}} \left(1 + \frac{4n-3}{2(2n)^2} \frac{\phi^2}{M_{\text{Pl}}^2} + \frac{1}{2(2n)^2} \frac{\phi^4}{M_{\text{Pl}}^4} \right) \right]. \end{aligned} \quad (6.18)$$

In the above, we have also neglected all small terms that are proportional to $|\mu|/M$. If $A_{2n} > 0$, the proper harmful D -flat direction is obtained for $\xi = \pi/n$, leading to the smallest negative coefficient for the ϕ^{2n} operator in (6.18), since $\text{Re}(e^{n i \xi} A_{2n}) = -A_{2n} < 0$.

In the next section, we will use the leading form of the SUGRA-derived potential $V_{2n}(\phi)$ in (6.18), for field values $\phi > M_S$, in order to assess the stability of the EW vacuum against the presence of harmful Planck-scale suppressed operators.

6.4 EW Vacuum Stability in SUGRA Models

In this Section, we will analyze the stability of the EW vacuum, upon minimally embedding the SM into an effective SUGRA theory that happens to predict the leading form of Planckian NP. We will consider a SUGRA-derived extension of the SM effective potential $V_{2n}(\phi)$ for Higgs field values ϕ above the soft SUSY-breaking scale M_S . This means that for $\phi > M_S$, we will adopt the leading form of the SUGRA potential $V_{2n}(\phi)$ of (6.18). Instead, for $\phi < M_S$, the SM effective potential $V_{\text{SM}}(\phi)$ given in (5.17) will be regarded to be an accurate approximation of the theory, i.e. $V_{2n}(\phi < M_S) = V_{\text{SM}}(\phi)$. Given that the reduced Planck mass M_{Pl} (cf. (6.3)) becomes the relevant mass scale in SUGRA, all mass parameters will be given in M_{Pl} units. To simplify further our analysis, we identify the scale M in (6.18) with M_{Pl} , i.e. $M = M_{\text{Pl}}$.

As for the soft SUSY-breaking scale M_S , we consider two different scenarios that realize: (i) a very large $M_S = 10^9$ TeV; (ii) a relatively low $M_S = 10$ TeV. In all scalar potentials $V_{2n}(\phi)$, we select the flat direction for which the CP-odd phase ξ in (6.8) is given by $\xi = \pi/n$. This gives rise to a harmful operator $\phi^{2n}/M_{\text{Pl}}^{2n-4}$ which has the largest negative contribution to $V_{2n}(\phi)$. Furthermore, for the induced SUSY-breaking trilinears A_{2n} , we assume that they take the following four discrete values:

$$A_{2n} = M_{\text{Pl}}, \quad M_{\text{Pl}}/5, \quad M_{\text{Pl}}/10, \quad M_{\text{Pl}}/50. \quad (6.19)$$

Finally, we set all superpotential couplings $\rho_{2n} = 1$, for simplicity.

6.4.1 SUGRA Scenarios with $M_S = 10^9$ TeV

We will first consider a minimal SUGRA scenario with $M_S = 10^9$ TeV. The results of our analysis are exhibited in Tab. 6.3, for different values of n corresponding to the SUGRA potentials $V_{2n}(\phi)$ (cf. (6.18)). In detail, Tab. 6.3 shows the value of the AdS vacuum energy $V_{\min} \equiv V_{2n}(\phi_{\min})$ at the Planckian AdS vacuum ϕ_{\min} , the field values, ϕ_0^{flat} and ϕ_0^{curved} , as determined at the center of the bounce (with $\phi_0 \equiv \phi_b(r=0)$), as well as the EW vacuum lifetimes τ^{flat} and τ^{curved} (in T_U units) for a flat and a curved spacetime background, respectively. A key theoretical parameter in our analysis is the SUSY-breaking trilinear coupling A_{2n} , which takes four representative values as stated in (6.19).

From Tab. 6.3, we observe that for $A_{2n} = M_{\text{Pl}}$, no noticeable stabilizing effect on the EW vacuum was found, notwithstanding the presence of gravity and the induced curved background metric. In fact, we have checked that $\tau^{\text{flat}} \sim \tau^{\text{curved}}$, for very high values of n as well. Although this result may seem counter-intuitive, it certainly implies that the protective mechanism presented in Section 6.3 appears to be ineffective to assure the stability of our EW vacuum in this case.

n	A_{2n}	V_{\min}	ϕ_{\min}	ϕ_0^{flat}	ϕ_0^{curved}	τ^{flat}	τ^{curved}
2	1	-4.1791	1.4310	1.4281	1.4253	10^{-238}	10^{-238}
	1	-5.1768	1.4308	1.4308	1.4308	10^{-238}	10^{-237}
	1	-5.6986	1.4264	1.4264	1.4264	10^{-238}	10^{-236}
3	1/5	-0.0133	0.7161	0.0021	0.0019	10^{-200}	10^{-200}
	1/5	-0.0401	0.9790	0.9787	0.9786	10^{-146}	10^{-135}
	1/5	-0.0669	1.0991	1.0991	1.0991	10^{-129}	10^{-104}
4	1/10	-0.0014	0.5122	0.0013	0.0013	10^{-170}	10^{-170}
	1/10	-0.0057	0.8268	0.8262	0.8261	10^{75}	10^{100}
	1/10	-0.0108	0.9809	0.9809	0.9809	10^{193}	10^{260}
2	1/50	-9.8×10^{-6}	0.2307	0.0008	0.0008	10^{61}	10^{61}
	1/50	-0.00007	0.5554	0.5543	0.5543	10^{4205}	10^{4354}
	1/50	-0.00018	0.7519	0.7519	0.7519	10^{8317}	10^{9056}

Table 6.3: Numerical estimates of the AdS vacuum energy V_{\min} at the AdS vacuum ϕ_{\min} , the field values $\phi_0 \equiv \phi_b(0)$ at the center of the bounce, the EW vacuum lifetimes τ (in T_U units) for a flat and a curved spacetime background, in SUGRA scenarios with harmful operators ϕ^{2n}/M^{2n-4} (cf. (6.18)). The input parameters for such scenarios are: $M_S = 10^9$ TeV, $M = M_{\text{Pl}}$, $\rho_{2n} = 1$, while A_{2n} takes the four discrete values given in (6.19). All energy scales are given in units of the reduced Planck mass M_{Pl} .

As A_{2n} assumes smaller values as shown in Tab. 6.3, e.g. $A_{2n} = M_{\text{Pl}}/5$, we notice that unlike $n = 2$, the lifetime of the EW vacuum, τ^{flat} and τ^{curved} evaluated separately for a flat and a curved spacetime metric, gets prolonged, as expected. For all the scenarios with $n = 2$, the destabilizing effect of the negative ϕ^4 potential term is so strong that even the inclusion of gravity can no longer alter the value of τ . Otherwise, we anticipate on general grounds that the inclusion of gravity will increase the stability of the EW vacuum for all scenarios $n \geq 3$. However, for the scenario with $A_{2n} = M_{\text{Pl}}/5$, all low order harmful operators with $n = 2, 3, 4$ lead to lifetimes $\tau \ll T_U$, as can be seen from Tab. 6.3. When A_{2n} becomes even smaller, i.e. $A_{2n} = M_{\text{Pl}}/10$ and $A_{2n} = M_{\text{Pl}}/50$, a quicker stabilization of the EW vacuum is achieved and the predicted tunnelling time τ becomes much larger than the age of the Universe T_U , for all scenarios with $n \geq 3$ and $n \geq 2$, respectively. This result is

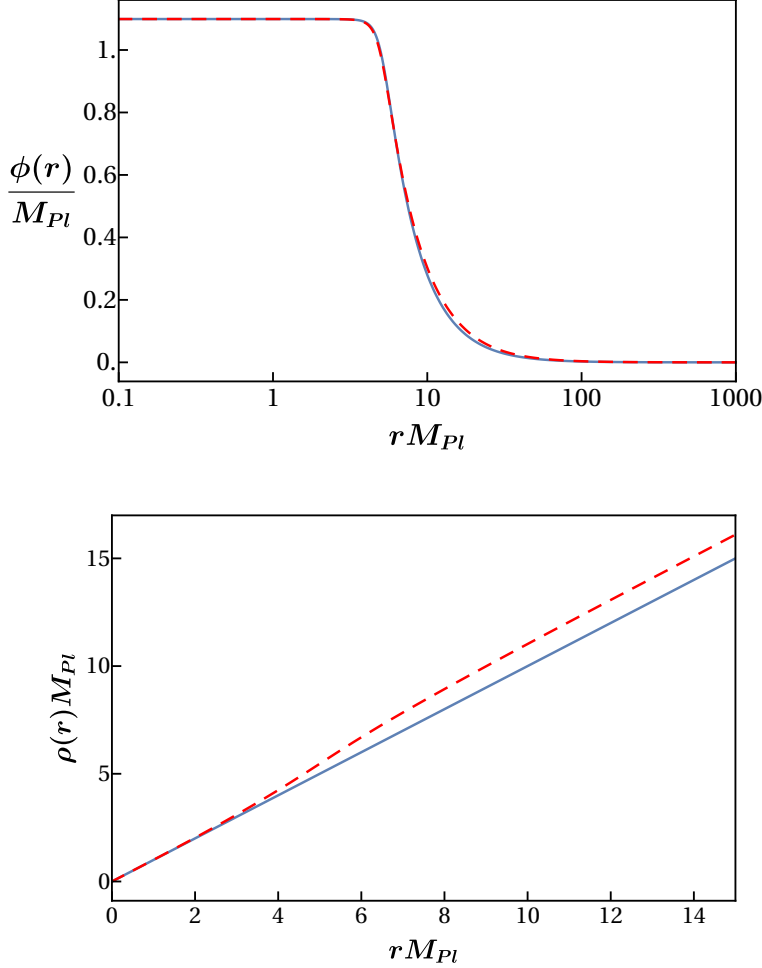


Figure 6.5: The bounces $\phi(r)$ (upper panel) and the curvatures $\rho(r)$ (lower panel) for the potential (6.18) with $A_{2n} = M_{Pl}/5$ and $n = 4$, for a flat (solid blue) and a curved (dashed red) spacetime.

in agreement with the discussion presented in Section 6.2, since the negative A_{2n} -dependent contribution of the harmful operators to the potentials V_{2n} becomes less significant for scenarios with lower values A_{2n} .

Finally, it is interesting to observe that as n increases, the AdS vacuum ϕ_{\min} and the bounces, ϕ_0^{flat} and ϕ_0^{curved} at $r = 0$, all start to converge towards the same value: $\phi_{\min} = \phi_0^{\text{flat}} = \phi_0^{\text{curved}}$. In the same context, we have verified that the whole radial profile $\phi^{\text{flat}}(r)$ will start to coincide with that of $\phi^{\text{curved}}(r)$. In fact, the difference between τ^{flat} and τ^{curved} found in Tab. 6.3 will result from the two actions of the bounce solutions (cf. (6.5) and (6.6)),

$$S_b^{\text{flat}} = -2\pi^2 \int_0^\infty dr r^3 V(\phi^{\text{flat}}) \quad \text{and} \quad S_b^{\text{curved}} = -2\pi^2 \int_0^\infty dr \rho^3 V(\phi^{\text{curved}}),$$

which determine the tunnelling exponent B in (6.4). Hence, the deviation of the curvature of the metric, $\rho = \rho(r)$ (curved spacetime), from the respective flat one, $\rho^{\text{flat}}(r) = r$, will control the difference in the predictions for τ^{flat} versus τ^{curved} .

n	A_{2n}	V_{\min}	ϕ_{\min}	ϕ_0^{flat}	ϕ_0^{curved}	τ^{flat}	τ^{curved}
2	1	-4.1791	1.4310	1.4281	1.4253	10^{-238}	10^{-238}
3	1	-5.1768	1.4308	1.4308	1.4308	10^{-238}	10^{-237}
4	1	-5.6986	1.4264	1.4264	1.4264	10^{-238}	10^{-236}
2	1/5	-0.0133	0.7161	2.24×10^{-7}	2.04×10^{-7}	10^{-184}	10^{-184}
3	1/5	-0.0401	0.9790	0.9787	0.9786	10^{-146}	10^{-135}
4	1/5	-0.0669	1.0991	1.0991	1.0991	10^{-129}	10^{-104}
2	1/10	-0.0014	0.5123	1.49×10^{-7}	1.47×10^{-7}	10^{-154}	10^{-154}
3	1/10	-0.0057	0.8268	0.8262	0.8261	10^{76}	10^{100}
4	1/10	-0.0108	0.9809	0.9809	0.9809	10^{218}	10^{260}
2	1/50	-9.8×10^{-6}	0.2307	1.10×10^{-7}	1.10×10^{-7}	10^{76}	10^{76}
3	1/50	-0.00008	0.5554	0.5543	0.5543	10^{4196}	10^{4354}
4	1/50	-0.00018	0.7519	0.7519	0.7519	10^{8006}	10^{9056}

Table 6.4: The same as in Tab. 6.3, but with $M_S = 10$ TeV.

In Fig. 6.5, we give a concrete example, where we plot the bounces $\phi(r)$ (upper panel) and the curvatures $\rho(r)$ (lower panel) for the potential (6.18) with $n = 4$ and $A_{2n} = M_{\text{Pl}}/5$, for a flat (solid blue line) and a curved (dashed red line) background metric. We see that while the two bounce solutions for $\phi(r)$ practically coincide, the corresponding ones for $\rho(r)$ differ from one another, thereby causing the prediction for τ^{flat} to significantly deviate from that for τ^{curved} .

6.4.2 SUGRA Scenarios with $M_S = 10$ TeV

We will now study a class of minimal SUGRA scenarios with a soft SUSY-breaking scale $M_S = 10$ TeV. Such scenarios are better motivated, in the sense that they require a much smaller degree of fine tuning for solving the infamous gauge hierarchy problem. Otherwise, all other theoretical parameters take the same values as before. This exercise will allow us to probe the sensitivity of our results to M_S . Tab. 6.4 summarizes the findings of our analysis.

As was the case for the SUGRA scenarios with $M_S = 10^9$ TeV, we find similar features for those with $M_S = 10$ TeV. As before, we obtain that for any fixed value of A_{2n} , the EW vacuum lifetime τ will increase with n . Likewise, τ will also increase,

as A_{2n} decreases. Similarly, we notice that for $n = 2$, the destabilizing effect of the negative ϕ^4 potential term is strong enough to counter-act the respective stabilising effect thanks to gravity. As a consequence, the predictions for τ turn out not to depend on the choice of the background metric. As before, we observe that for $A_{2n} = M_P/50$, the EW vacuum lifetime gets adequately prolonged, becoming much larger than T_U , already from $n = 2$ and on.

If we compare the results presented in Tab. 6.4 to those in Tab. 6.3, we will observe that the tunnelling times τ^{flat} and τ^{curved} are rather comparable, especially when $n \geq 3$. Evidently, this suggests that even if gravity is taken into account, the bounce solutions seem to be insensitive to the matching of the SM effective potential $V_{\text{SM}}(\phi)$ to the SUGRA potential $V_{2n}(\phi)$ for a wide range of ϕ values: $\phi = 10 - 10^9$ TeV.

In order to gain further insight into this point, we consider a variant effective scalar potential $\tilde{V}_{2n}(\phi)$. To be precise, for $\phi < 10$ TeV, we set $\tilde{V}_{2n}(\phi) = V_{\text{SM}}(\phi)$, and for $\phi > 10^9$ TeV, $\tilde{V}_{2n}(\phi) = V_{2n}(\phi)$. However, between the field values $\phi = 10$ TeV and $\phi = 10^9$ TeV, the new potential $\tilde{V}_{2n}(\phi)$ is assumed to follow an interpolating straight line. Interestingly enough, the tunnelling times τ , as well as the other parameters shown in Tab. 6.4, come out to be close to the corresponding ones obtained when $V_{\text{SM}}(\phi)$ or $V_{2n}(\phi)$ are used as an interpolation from 10 to 10^9 TeV. Consequently, the bounce solutions turn out to be insensitive to the shape of the potential in the above range of ϕ . This observation explains the robustness and the independence of these results for a wide range of soft SUSY-breaking scales: $M_S = 10 - 10^9$ TeV.

Chapter 7

Electroweak vacuum lifetime in two Higgs doublet models

The two-Higgs doublet model (2HDM) [105, 106] is arguably the simplest SM extension, in which the particle content of the SM is complemented by a second Higgs doublet. The model boasts a rich phenomenology, with a larger scalar sector, including two CP-even scalars, a pseudoscalar and a charged scalar, and may have spontaneous CP breaking for certain choices of its parameters, thus offering an additional source of CP violation. Obviously, the additional scalars predicted in 2HDM are not yet discovered, and the model must also be in agreement with current experimental searches for BSM particles. Even after demanding that the 125 GeV scalar be SM-like, there remains a large 2HDM parameter space available to comply with those experimental results.

An interesting property of the 2HDM strictly related to the scope of this thesis is that already at the classical level it has a richer vacuum structure. Whereas in the classical SM potential there can only be one type of minimum, the 2HDM has the possibility of *three* physically different kinds of minima: an electroweak-breaking but CP-and-charge preserving (we call it “normal” minimum), analogous to the SM; a minimum which spontaneously breaks both the electroweak and CP symmetries; and a minimum where the vacuum expectation value (vev) of the scalar doublets carries electric charge, and electric charge conservation no longer holds. However, the scalar potential of the model is such that, at least at tree level, minima of a different nature cannot simultaneously coexist [107–110]. The stability of a 2HDM vacuum against tunneling to another vacuum of a different nature is therefore ensured by the theory itself, at least at tree level.

Moreover, there is a very crucial property concerning 2HDM normal vacua: for certain regions of the parameter space, there may exist *two* non-degenerate vacua of this type [109–111], both of them CP and charge preserving, but having vevs which break the electroweak symmetry. However, the vevs of the doublets, v_i , are such that in “our” minimum they satisfy $v_1^2 + v_2^2 = 246 \text{ GeV}^2$ (thus in “our” minimum

all elementary particles have their well-known masses), whereas a different mass spectrum holds for the second minimum. If the EW vacuum which the universe currently occupies is not the absolute minimum of the potential, it will sooner or later tunnel to a deeper minimum that breaks the same symmetries, then ensuring a situation similar to those of Higgs effective potential in SM. The fundamental difference between the 2HDM and the SM is that in the latter case the EW vacuum shows its instability (metastability) only once radiative corrections are taken into account, and this is mainly due to the negative contribution to the potential coming from the top quark (see Chapter 2). Instead in the 2HDM the coexistence of two minima in the potential already occurs at tree-level, and the analysis of the stability of the false vacuum (the EW minimum in our case) can be already undertaken at this level (i.e. prior to the study of the loop corrected potential). The conditions under which a second 2HDM minimum may exist, and the condition which discriminates whether “our” minimum is the global one were established in refs. [109, 110, 112, 113], and we will summarize them in Section 7.2. The deeper vacuum, different from the “standard” EW breaking one, was usually dubbed *panic vacuum* in the context of the 2HDM [112, 113]: in fact, as we know a transition from the EW minimum to the deeper one would be disastrous, as such a transition would release a colossal amount of energy and, since the fields in the two minima have different vevs, all elementary particles would change their masses upon transition to the deeper vacuum.

However, the mere existence of a “panic” vacuum is not sufficient to exclude the parameters of the potential which yield such a possibility. In fact, if the tunneling time τ from the false to the true vacuum is larger than the age of the universe, the existence of the deeper vacuum would have no impact whatsoever in the phenomenology observed while the universe lies in the upper minimum. Thus the computation of τ becomes a fundamental tool to distinguish between those regions of the parameter space which yield dangerous panic vacua, and those for which the deeper vacua exist but are practically harmless. In this Chapter, we will undertake a thorough analysis of the tunneling between neutral vacua in the 2HDM by calculating the EW vacuum lifetime. To this end, we have to look for the bounce solutions to the Euclidean Euler-Lagrange equations that have $O(4)$ symmetry [114]. It is worth to note that here we limit ourselves to compute the EW vacuum lifetime in the flat spacetime background, while the inclusion of gravity is postponed to future studies.

7.1 The Two-Higgs Doublet Model potential

The 2HDM is perhaps the simplest extension of the SM since the particle content of the 2HDM is enlarged by a second $SU(2)_W \times U(1)_Y$ doublet, but the gauge and fermion content of the model is the same as the SM’s [105, 106]. The model therefore contains two hypercharge 1 doublets, Φ_1 and Φ_2 , in terms of which the most general

renormalizable 2HDM scalar potential is written as

$$\begin{aligned} V = & m_{11}^2 |\Phi_1|^2 + m_{22}^2 |\Phi_2|^2 - \left(m_{12}^2 \Phi_1^\dagger \Phi_2 + h.c. \right) \\ & + \frac{1}{2} \lambda_1 |\Phi_1|^4 + \frac{1}{2} \lambda_2 |\Phi_2|^4 + \lambda_3 |\Phi_1|^2 |\Phi_2|^2 + \lambda_4 |\Phi_1^\dagger \Phi_2|^2 \\ & + \left[\frac{1}{2} \lambda_5 (\Phi_1^\dagger \Phi_2)^2 + \lambda_6 |\Phi_1|^2 (\Phi_1^\dagger \Phi_2) + \lambda_7 |\Phi_2|^2 (\Phi_1^\dagger \Phi_2) + h.c. \right], \end{aligned} \quad (7.1)$$

where the coefficients m_{12}^2 , $\lambda_{5,6,7}$ can be complex. The doublets Φ_1 and Φ_2 are not physical fields: the mass eigenstates which arise from them are physical, but the doublets themselves are not. This means that any linear combination of the doublets which preserves the form of the model's kinetic terms provides an equally valid physical description of physics. This corresponds to an invariance of the model under fields redefinitions, so called *basis changes* of the form $\Phi'_i = U_{ij} \Phi_j$, where U is a 2×2 unitary matrix. Though the potential of Eq. (7.1) seemingly has 14 independent real parameters, the freedom to redefine the doublets means that in fact one can eliminate three of those parameters, and thus the most general 2HDM scalar potential has 11 independent real parameters [115].

Considering the whole theory we must include the Yukawa sector, i.e. the scalar-fermion interactions, but this makes us fall into a problem: if we build the most general lagrangian with two Higgs doublets, the Yukawa sector will include tree-level flavour changing neutral currents (FCNC) mediated by neutral scalars. This happens because the most general Yukawa terms of the 2HDM include interactions of both doublets with all fermions. However, these FCNC are very tightly constrained by experimental data and they should be avoided. The most studied model eliminates tree-level scalar-mediated FCNC by imposing a \mathbb{Z}_2 discrete symmetry upon the model. The discrete symmetry usually considered demands that the lagrangian be invariant under a transformation on the doublets of the form $\Phi_1 \rightarrow \Phi_1$ and $\Phi_2 \rightarrow -\Phi_2$ [116, 117]. As a consequence, the parameters m_{12}^2 , λ_6 and λ_7 vanish from the potential, though m_{12}^2 is reintroduced as a (real) soft-breaking term, to enlarge the allowed parameter space and, among other things, allow the theory to have a *decoupling limit* [115] where the masses of all scalars other than the SM-like one can be made very large. The final potential with which we will be working is thus

$$\begin{aligned} V = & m_{11}^2 |\Phi_1|^2 + m_{22}^2 |\Phi_2|^2 - m_{12}^2 (\Phi_1^\dagger \Phi_2 + h.c.) \\ & + \frac{1}{2} \lambda_1 |\Phi_1|^4 + \frac{1}{2} \lambda_2 |\Phi_2|^4 + \lambda_3 |\Phi_1|^2 |\Phi_2|^2 + \lambda_4 |\Phi_1^\dagger \Phi_2|^2 + \frac{1}{2} \lambda_5 \left[(\Phi_1^\dagger \Phi_2)^2 + h.c. \right], \end{aligned} \quad (7.2)$$

where now all parameters are real (we have further imposed CP conservation on the potential, which makes all possible complex phases vanish).

The 2HDM, of course, is not only a theory of the scalar sector, it includes also gauge bosons and three generations of fermions, as does the SM. The most general

Yukawa sector of the model, as mentioned above, will generate tree-level FCNC which are strongly disfavoured by experimental results. These are eliminated imposing, on the full lagrangian, the discrete symmetry $\Phi_1 \rightarrow \Phi_1$ and $\Phi_2 \rightarrow -\Phi_2$ and we have already explained the impact of this symmetry on the scalar sector; on the Yukawa sector, it forces only one of the doublets to couple (and thus give mass) to each generation of like-charged fermions. Depending on how the fermionic fields (both the left doublets and right singlets) transform under the \mathbb{Z}_2 symmetry, there are then several possible types of 2HDM, with different phenomenologies and classified according to their scalar-fermion interactions. Usually, one considers four different types¹:

- Model Type I, where all fermions couple to a single Higgs doublet, chosen as Φ_2 per convention.
- Model Type II, where all right-handed up-type quarks couple to Φ_2 , but right-handed down-type quarks and charged leptons couple to Φ_1 . This type of couplings is analogous to what happens in SUSY models.
- The Lepton-specific model, in which all quarks couple to Φ_2 , but right-handed charged leptons couple to Φ_1 .
- The Flipped model, in which right handed up quarks and charged leptons couple to Φ_2 , but right-handed down quarks couple to Φ_1 .

Thus for each model each same-charge type of fermions may gain their masses from different Higgs doublets. The fact that only one Higgs doublet couples to fermions of the same electric charge eliminates tree-level FCNC, as the couplings between the physical scalar particles and the fermions will be described by diagonal matrices [106]. As already mentioned, each of these models has different phenomenologies, a subject we will address in Section 7.1.3.

7.1.1 Theoretical constraints on quartic couplings

The quartic couplings of (7.2) are not completely unconstrained. In order to ensure that the potential is bounded from below (BFB), meaning, no directions in field space along which the potential can tend to minus-infinity, the couplings need to obey [118]

$$\begin{aligned} \lambda_1 &> 0 \quad , \quad \lambda_2 > 0 \, , \\ \lambda_3 &> -\sqrt{\lambda_1 \lambda_2} \quad , \quad \lambda_3 + \lambda_4 - |\lambda_5| > -\sqrt{\lambda_1 \lambda_2} \, . \end{aligned} \tag{7.3}$$

¹The number of possible models would increase if one were to consider also the possible interaction terms between the scalar doublets and neutrinos, which we will not do in the current work.

It has been proven that these (tree-level) conditions are both necessary and sufficient [109, 110]. Another set of constraints upon the potential’s parameters arises from requiring that the theory be unitary. This translates into further constraints upon the quartic couplings of the potential, which may be reduced to [119–121]

$$\begin{aligned} |\lambda_3 - \lambda_4| &< 8\pi \\ |\lambda_3 + 2\lambda_4 \pm 3\lambda_5| &< 8\pi \\ \left| \frac{1}{2} \left(\lambda_1 + \lambda_2 + \sqrt{(\lambda_1 - \lambda_2)^2 + 4\lambda_4^2} \right) \right| &< 8\pi \\ \left| \frac{1}{2} \left(\lambda_1 + \lambda_2 + \sqrt{(\lambda_1 - \lambda_2)^2 + 4\lambda_5^2} \right) \right| &< 8\pi. \end{aligned} \quad (7.4)$$

Here we will consider these tree-level constraints, though one-loop contributions have been considered [122–131].

7.1.2 The electroweak-breaking minimum

The potential described by Eq. (7.2) can yield, depending of the values of the parameters, different types of minima. The scalar fields can acquire vacuum expectation values (vevs) and break the symmetries of the model in different ways. We call “normal vacuum” the case where both doublets acquire real and neutral vevs,

$$\langle \Phi_1 \rangle_N = \frac{1}{\sqrt{2}} \begin{pmatrix} 0 \\ v_1 \end{pmatrix}, \langle \Phi_2 \rangle_N = \frac{1}{\sqrt{2}} \begin{pmatrix} 0 \\ v_2 \end{pmatrix}. \quad (7.5)$$

These normal minima are similar to the SM vacuum: they break the same gauge symmetries and preserve CP, and constitute the focus of this Chapter (we will briefly discuss other types of possible 2HDM minima in Section 7.2). Let us now define the (real) components of the doublets Φ_1 and Φ_2 as

$$\Phi_1 = \frac{1}{\sqrt{2}} \begin{pmatrix} \varphi_{c1} + i\varphi_{c2} \\ \varphi_{r1} + i\varphi_{i1} \end{pmatrix}, \quad \Phi_2 = \frac{1}{\sqrt{2}} \begin{pmatrix} \varphi_{c3} + i\varphi_{c4} \\ \varphi_{r2} + i\varphi_{i2} \end{pmatrix}, \quad (7.6)$$

where the upper components correspond to charged (+1) fields and the lower components, to neutral ones. When the potential develops a normal minimum, the real neutral components, φ_{r1} and φ_{r2} , give rise to two mass eigenstates which correspond to CP-even scalars, dubbed h and H . On the other hand, the imaginary components, φ_{i1} and φ_{i2} , originate a pseudoscalar particle, A , and the neutral Goldstone boson G^0 which provides the Z boson with its mass. Finally, the upper, charged components φ_{ci} yield a charged Higgs scalar, H^\pm and the charged Goldstone boson G^\pm which gives mass to the W gauge bosons. For such normal minima it is also customary to define two angles: the ratio of the vevs v_1 and v_2 defines the angle β , such that

$$\tan \beta = \frac{v_2}{v_1}. \quad (7.7)$$

β is the angle which diagonalizes both the charged and pseudoscalar squared scalar mass matrices, and can be considered to only take values between 0 and $\pi/2$ without loss of generality². On the other hand, the CP-even squared scalar mass matrix is diagonalized by a different angle, α , defined such that the two physical eigenstates, h and H , are related to the neutral real components of the doublets as

$$\begin{aligned} h &= \sin \alpha \varphi_{r1} - \cos \alpha \varphi_{r2} \\ H &= -\cos \alpha \varphi_{r1} - \sin \alpha \varphi_{r2}. \end{aligned} \quad (7.8)$$

Again without loss of generality, this angle can be chosen such that $-\pi/2 \leq \alpha \leq \pi/2$. The minimization conditions relate the vevs of Eq. (7.5) to the parameters of the potential, such that

$$\begin{aligned} m_{11}^2 v_1 - m_{12}^2 v_2 + \frac{\lambda_1}{2} v_1^3 + \frac{\lambda_{345}}{2} v_2^2 v_1 &= 0 \\ m_{22}^2 v_2 - m_{12}^2 v_1 + \frac{\lambda_2}{2} v_2^3 + \frac{\lambda_{345}}{2} v_1^2 v_2 &= 0, \end{aligned} \quad (7.9)$$

where we have defined

$$\lambda_{345} \equiv \lambda_3 + \lambda_4 + \lambda_5. \quad (7.10)$$

Notice that, since the potential is invariant under a sign change for both doublets, if Eqs. (7.9) admit a solution $\{v_1, v_2\}$ obviously $\{-v_1, -v_2\}$ will also be a solution. Also obviously, this second solution will be physically indistinguishable from the first one. This seemingly trivial point will be extremely important later on, and we will show in Section 7.4 that it can have a stunning impact on the tunneling rates between vacua.

Instead of the potential's couplings, we can choose to describe the model in terms of the four physical masses, $m_h = 125$ GeV, m_H , m_A and m_{H^\pm} , the angles β and α , the vev $v = 246$ GeV and a further parameter, for instance the soft breaking term m_{12}^2 : a total of eight parameters, just as the potential of Eq. (7.2). The quartic couplings of the model can then be expressed as

$$\begin{aligned} \lambda_1 &= \frac{1}{v^2 c_\beta^2} \left(c_\alpha^2 m_H^2 + s_\alpha^2 m_h^2 - m_{12}^2 \frac{s_\beta}{c_\beta} \right), \\ \lambda_2 &= \frac{1}{v^2 s_\beta^2} \left(s_\alpha^2 m_H^2 + c_\alpha^2 m_h^2 - m_{12}^2 \frac{c_\beta}{s_\beta} \right), \\ \lambda_3 &= \frac{1}{v^2} \left[2m_{H^\pm}^2 + \frac{s_{2\alpha}(m_H^2 - m_h^2)}{s_{2\beta}} - \frac{m_{12}^2}{s_\beta c_\beta} \right], \\ \lambda_4 &= \frac{1}{v^2} \left(m_A^2 - 2m_{H^\pm}^2 + \frac{m_{12}^2}{s_\beta c_\beta} \right), \\ \lambda_5 &= \frac{1}{v^2} \left(\frac{m_{12}^2}{s_\beta c_\beta} - m_A^2 \right), \end{aligned} \quad (7.11)$$

where for simplification we defined $s_\theta = \sin \theta$ and $c_\theta = \cos \theta$.

²This choice is valid for one specific vacuum, other vacua may have vevs of different signs.

7.1.3 Experimental constraints on the 2HDM

The larger scalar content of the 2HDM, compared with the SM, leads to measurable impacts on several experimental observables. So far no scalars other than the 125 GeV one have been discovered, and therefore BSM searches at the LHC and elsewhere impose bounds on the masses and couplings of the extra scalars of the 2HDM. Further, even before the discovery of the Higgs boson, electroweak precision studies from LEP and other accelerators were used to curtail the values of BSM models, including the 2HDM. A charged scalar such as the one predicted by the 2HDM has considerable contributions to several B-meson observables, and data from B-physics measurements constitute some of the model’s most stringent constraints. In this Chapter we incorporated a wealth of experimental constraints in the parameter scans used in Section 7.5.

In general, BSM physics may have substantial contributions to Electroweak Precision Constraints (EWPC), namely the oblique S , T and U parameters [132–134]. These constraints may, for instance, force the charged Higgs mass and the pseudoscalar one to be very close in value. We computed these oblique parameters and used the most recent fit [135] to constrain the 2HDM parameter space. Direct searches from LEP, using the channel $e^+ e^- \rightarrow H^+ H^-$ [136], impose a lower bound on the charged Higgs mass of roughly 100 GeV, which we also implemented. Moreover, the 2HDM contributions to B-physics observables, such as the values of the $b \rightarrow s\gamma$ decay rate [137–141] and the $Z \rightarrow b\bar{b}$ width [137, 142], impose considerable constraints, usually expressed as exclusions on the m_{H^\pm} – $\tan\beta$ plane. Roughly speaking, these constraints translate as requiring that $\tan\beta$ be above 1 for most of the parameter space in all model types, and an almost $\tan\beta$ -independent lower bound on the charged Higgs mass for model type II (and Flipped), of roughly ~ 580 GeV [141]. Other flavour constraints, such as those arising from $B \rightarrow \tau\nu$, $\Delta M_{B_{s,d}}$, etc. [143], were also taken into account.

The Higgs boson discovery at the LHC has been followed by many measurements of this particle’s properties, which have been seen to be very much in agreement with what one could expect for a SM-like scalar. The experimental results are thus pushing the 2HDM into the so-called “alignment limit”, wherein the 125 GeV state is almost “aligned” with one of the doublets (this in practice corresponds to values of $\sin(\beta - \alpha)$ very close to 1), and the remaining scalars sufficient massive, or with sufficiently weak interactions, to have eluded detection thus far. In practical terms, the LHC constraints are obtained from the μ ratios between the observed number of events in some Higgs-mediated channel, and the SM expected value for the same quantity. Then, for the 2HDM the quantities to compare with experimental results such as those from [144] are

$$\mu_X = \frac{\sigma^{2HDM}(pp \rightarrow h)}{\sigma^{SM}(pp \rightarrow h)} \frac{BR^{2HDM}(h \rightarrow X)}{BR^{SM}(h \rightarrow X)}, \quad (7.12)$$

where σ stands for the production cross section of h in proton-proton collisions at the LHC and BR for the decay branching ratios of h to some final state X , such as ZZ , WW , $\gamma\gamma$, $b\bar{b}$, The fact that h is behaving in a SM-like manner means that the measured values for these μ_X are close to one, but the current experimental uncertainties still allow values with deviations larger than 30% from unity. In our calculations we will consider mostly scalars produced via the main channel of gluon-gluon fusion, the cross sections of such processes being obtained by **SusHiv1.6.0** [145, 146], at NNLO QCD. Other production channels (such as VBF, $b\bar{b}h$ or $t\bar{t}h$) could also have been used, but for the purposes of the work presented in this Chapter they would be an unnecessary complication. As for the branching ratios, all decay widths were computed at leading order, with the necessary NLO QCD corrections to the $b\bar{b}$ width taken into account. In fact, requiring that μ_{ZZ} , $\mu_{\gamma\gamma}$, $\mu_{b\bar{b}}$ and $\mu_{\tau\bar{\tau}}$ be within 30% of their SM value (*i.e.*, all μ 's having values in the interval 0.7 to 1.3) is more than enough to ensure compliance with the $2 \times 1\sigma$ experimental precision from [144], and even with current run-II results.

Finally, there is a wealth of results on searches for the extra scalars predicted in the 2HDM (see ref. [147] and references therein, for a review of the status of the diverse search channels), with measurements imposing exclusion regions in the parameter space of the model. By and large, requiring that the 125 GeV state h be very SM-like is sufficient to comply with most exclusion bounds for other scalar searches, even though there are exceptions [148], like pseudoscalar production and decay to Zh in the wrong sign limit in the 2HDM [149–155]. For the purposes of this Chapter, in which we wish to show the possible importance of the tunneling time calculations in 2HDM parameter space, it was verified that in regions of parameters analysed the 30% bound on the several μ_X was sufficient to comply with extra scalar search results.

7.2 Coexisting minima in the 2HDM

Since the 2HDM has a scalar potential much more elaborate than the SM one, it possesses therefore a richer vacuum structure. In fact, in the 2HDM *three* classes of vacua may occur, depending on the parameters of the model. The first corresponds to normal vacua, wherein the doublets have vevs such as those described by Eq. (7.5). This kind of vacuum therefore breaks $SU(2)_L \times U(1)_Y$ down to $U(1)_{em}$, just as the EW vacuum in the SM, therefore preserving both CP and the electromagnetic symmetry.

Vacua with a spontaneous breaking of CP are also possible, and in fact their existence is the main reason the model was created by T.D. Lee [105]. Such vacua occur when the doublets have neutral vevs, but now, unlike Eq. (7.5), a relative

complex phase between them appears, *i.e.* the vevs are of the form

$$\langle \Phi_1 \rangle_{CP} = \frac{1}{\sqrt{2}} \begin{pmatrix} 0 \\ \bar{v}_1 \end{pmatrix}, \quad \langle \Phi_2 \rangle_{CP} = \frac{1}{\sqrt{2}} \begin{pmatrix} 0 \\ \bar{v}_2 \exp^{i\theta} \end{pmatrix}, \quad (7.13)$$

with $\theta \neq n\pi$, for any integer n . The complex phase induces spontaneous CP breaking and the resulting scalar mass eigenstates have no definite CP quantum numbers: they are neither CP-even nor CP-odd. As a consequence, the neutral mass matrix in such minima is more complex than the analogous matrix in normal vacua: in the latter, a 4×4 matrix breaks into two 2×2 blocks, one having two non-zero eigenvalues, corresponding to the masses of the CP-even states h and H , the other having a zero eigenvalue (the Goldstone boson G^0) and the pseudoscalar mass of A ; in the former case, the 4×4 matrix does not reduce to two blocks, it possesses a zero eigenvalue (again the neutral Goldstone) and three eigenstates with interactions such that they are neither scalars nor pseudoscalars.

Charge breaking vacua are also a possibility, where the upper components of the doublets also acquire vevs, *i.e.* we will have

$$\langle \Phi_1 \rangle_{CB} = \frac{1}{\sqrt{2}} \begin{pmatrix} 0 \\ v'_1 \end{pmatrix}, \quad \langle \Phi_2 \rangle_{CB} = \frac{1}{\sqrt{2}} \begin{pmatrix} v'_3 \\ v'_2 \end{pmatrix}. \quad (7.14)$$

These minima, of course, are to be avoided: the charged vev v'_3 above will break the electromagnetic symmetry and give the photon a mass. In the scalar mass matrix, the neutral (lower) components of the doublets now appear mixed with the charged ones (upper), the resulting 8×8 mass matrix having a total of four zero eigenvalues, corresponding to the expected four Goldstone bosons arising from the full breaking of the gauge symmetry group.

The existence of a diverse number of minima in the potential raises the possibility of tunneling between different vacua, and certainly the hypothetical existence of, for instance, a CB minimum deeper than a EW or CP one, could constitute a problem for the model. However, it has been shown that if a normal minimum exists, any CP or charge breaking solutions of the minimisation equations are necessarily saddle points which lie above the normal minimum [107–110]. In fact, it was possible to show that the value of the potential at normal vacua (V_N), CP stationary points (V_{CP}) or CB ones (V_{CB}) can be related to one another, for coexisting tree-level stationary points of these types. The following formulae have been established:

$$V_{CB} - V_N = \left(\frac{m_{H^\pm}^2}{4v^2} \right)_N \left[(v_1 v'_2 - v_2 v'_1)^2 + v_1^2 v'_3^2 \right] \quad (7.15)$$

$$V_{CP} - V_N = \left(\frac{m_A^2}{4v^2} \right)_N \left[(v_1 \bar{v}_2 \cos \theta - v_2 \bar{v}_1)^2 + v_1^2 \bar{v}_2^2 \sin^2 \theta \right], \quad (7.16)$$

with the vevs for each possible stationary points defined in Eqs. (7.5), (7.13) and (7.14), and the subscript “ N ” refers that the masses m_{H^\pm} , m_A and the vev v are

computed at the normal stationary point. The terms within the square brackets are obviously positive thus, if N is a minimum, its squared scalar masses will all be positive, and hence these expressions show that $V_{CB} > V_N$ and $V_{CP} > V_N$ when N is a minimum. It is also easy to show that in that case both CP and CB stationary points would necessarily be saddle points. Analogously, if the potential is such that a CP (CB) minimum occurs, any eventual normal or CB (CP) stationary points would live above the minimum and be saddle points. Thus tunneling to deeper minima of a different nature is impossible in the 2HDM.

There is however another aspect of the 2HDM vacuum structure which sets it apart from the SM, to wit, in certain situations the minimization conditions allow for several non-equivalent normal stationary points [111]. Therefore, already at tree-level, *there is the possibility of two (no more than two) normal minima coexisting in the potential, at different depths* [109, 110]. In other words, other than the normal vacuum with vevs given by Eq. (7.5), for which one has $v_1^2 + v_2^2 = v^2 = (246 \text{ GeV})^2$, there may exist a second normal vacuum N' , with different vevs $\{v'_1, v'_2\}$. For this second minimum of the potential, the sum of the squared vevs takes a different value, smaller or larger than $(246 \text{ GeV})^2$. The two minima are not degenerate, in fact they verify [112, 113]

$$V_{N'} - V_N = \frac{1}{4} \left[\left(\frac{m_{H^\pm}^2}{v^2} \right)_N - \left(\frac{m_{H^\pm}^2}{v^2} \right)_{N'} \right] (v_1 v'_2 - v_2 v'_1)^2, \quad (7.17)$$

where the quantity $(m_{H^\pm}^2/v^2)$ is evaluated at each of the minima, N and N' . This raises the possibility that our vacuum, with $v = 246 \text{ GeV}$, is not the deepest one: there is nothing, in Eq. (7.17), which privileges the minimum N over N' , unlike what happened in Eqs. (7.15) or (7.16). In fact, for certain regions of the 2HDM potential, N' may be found to be the global minimum of the model, and a minimum where the exact same symmetries have been broken, but where *all elementary particles have different masses*. In that situation our universe could tunnel to this deeper minimum, with obvious catastrophic consequences.

The conditions under which this rather intriguing possibility arises were established in literature [109, 110, 112, 113]. Defining the quantity

$$k = \sqrt[4]{\frac{\lambda_1}{\lambda_2}}, \quad (7.18)$$

the necessary (but not sufficient) conditions for the softly broken \mathbb{Z}_2 2HDM potential to have two minima are

$$m_{11}^2 + k^2 m_{22}^2 < 0, \quad (7.19)$$

$$\sqrt[3]{x^2} + \sqrt[3]{y^2} \leq 1, \quad (7.20)$$

where we have defined the variables x and y as

$$\begin{aligned} x &= \frac{4 k m_{12}^2}{m_{11}^2 + k^2 m_{22}^2} \frac{\sqrt{\lambda_1 \lambda_2}}{\lambda_{345} - \sqrt{\lambda_1 \lambda_2}}, \\ y &= \frac{m_{11}^2 - k^2 m_{22}^2}{m_{11}^2 + k^2 m_{22}^2} \frac{\sqrt{\lambda_1 \lambda_2} + \lambda_{345}}{\sqrt{\lambda_1 \lambda_2} - \lambda_{345}}. \end{aligned} \quad (7.21)$$

It was demonstrated [113] that *the EW vacuum “N” (“our” minimum) is the global, true, minimum of the theory if and only if $D > 0$* , where the discriminant D is a quantity given by

$$D = m_{12}^2(m_{11}^2 - k^2 m_{22}^2)(\tan \beta - k). \quad (7.22)$$

Notice how, remarkably, the value of D can, in principle, be obtained by experiments performed on “our” minimum, without any knowledge of the existence of N' .

Let us again recall (see the discussion following Eq. (7.9)) that if the minimisation conditions yield the solutions $N = \{v_1, v_2\}$ and $N' = \{v'_1, v'_2\}$, they also include other “mirror” solutions, $\bar{N} = \{-v_1, -v_2\}$ and $\bar{N}' = \{-v'_1, -v'_2\}$. This is a trivial consequence of the fact that the potential is invariant under a sign change of both doublets, $V(\Phi_1, \Phi_2) = V(-\Phi_1, -\Phi_2)$, and *apparently* this has no physical consequences: the potential is degenerate at N and \bar{N} (N' and \bar{N}'), and physics at these two minima is entirely identical. No physical differences whatsoever may arise from being at N or \bar{N} (N' or \bar{N}'), because the only difference between both minima is the overall sign of *both* fields: no interference effects, for instance, will be sensitive to the sign change. The SM minimum of the Higgs potential, of course, is also degenerate with a continuum of other possible solutions: recall the shape of the tree-level SM Higgs potential, where infinitely many degenerate minima lie in a full circle. This is due to the fact that the SM minimum is determined by the equation $\langle |\Phi| \rangle = v/\sqrt{2}$, which yields a continuum of possible solutions, corresponding to different gauge choices for the Higgs doublet Φ . However, for the 2HDM potential, each of the minima N and N' is not degenerate with a continuum of other minima, but rather with another separate isolated minimum, \bar{N} and \bar{N}' respectively. We emphasize these seemingly trivial aspects of the minimisation solutions because they may have dramatic consequences in the computation of tunneling rates, as will be discussed below in Section 7.4.

7.3 Tunneling and bounces

In Chapters 3 - 6 we have developed and used the theoretical tools needed to compute the tunneling time τ for the decay of a false vacuum toward a true vacuum in the case of a single scalar theory. In particular, we know that the tunneling time is given by the decay rate, $\tau = \Gamma^{-1}$, computed via the bounce solution related to the potential under consideration. However, in the case of the 2HDM (i.e. with the

potential (7.2)) we are studying the stability of the EW vacuum in a theory with more than one scalar field.

The extension of the theoretical tools of the bounce equations to the case with N real fields ϕ_i , $i = 1, \dots, N$ is straightforward. If we denote the fields with $\boldsymbol{\phi} = (\phi_1, \phi_2, \dots, \phi_N)$ and the potential as $V(\boldsymbol{\phi})$, the bounce configuration is a non-trivial solution of the coupled system of N ordinary differential equation:

$$\frac{d^2\phi_i}{dr^2} + \frac{3}{r} \frac{d\phi_i}{dr} = \frac{\partial V(\boldsymbol{\phi})}{\partial \phi_i} \quad (7.23)$$

with boundary conditions

$$\left. \frac{d\phi_i}{dr} \right|_{r=0} = 0 \quad \lim_{r \rightarrow \infty} \phi_i = \phi_i^{\text{fv}}, \quad (7.24)$$

where $\phi_i = \phi_i^{\text{fv}}$ are the values of the fields ϕ_i at the false vacuum. Following the same steps of the $N = 1$ case, the action calculated at the bounce solution $\boldsymbol{\phi}_b(r) = (\phi_1(r), \dots, \phi_N(r))_{\text{bounce}}$ for the N field case takes the form:

$$B = -\frac{\pi^2}{2} \int_0^\infty dr r^3 \left[\frac{dV(\boldsymbol{\phi})}{d\phi_i} \phi_i \right]_{\boldsymbol{\phi}_b}, \quad (7.25)$$

where a sum over i is implied.

Apart from very simple cases, the system (7.23) cannot be solved analytically and we have to rely on numerical methods to evaluate the bounce configurations. To this end, we used the public Wolfram Mathematica code developed in [156]. The latter solves the system (7.23) with the help of a multiple shooting method, exploiting the asymptotic behavior of the bounce solution for $r \rightarrow 0$ and $r \rightarrow \infty$ (that is known in both cases analytically). Finally, the tunneling rate is given by:

$$\Gamma = T_U^3 \left[\sum_i \phi_i^2(0) \right]^2 e^{-B}. \quad (7.26)$$

In general, if the false vacuum can decay towards more than one state, Γ is obtained by calculating the different rates Γ_i : $\Gamma = \sum_i \Gamma_i$ and $\tau = \Gamma^{-1}$.

For the 2HDM case, the two doublets have a total of eight real components, as seen in Eq. (7.6). Therefore, in principle, the calculation of the bounce solution should involve all eight fields, which should contribute to the tunneling time shown in Eq. (7.26). However, the gauge structure of the model allows a considerable simplification of this procedure. In fact, since the model has a $SU(2) \times U(1)$ gauge invariance, we can choose a specific gauge in order to remove several of the real components of the doublets. This is a well-known feature of the 2HDM [106] which, in passing, is also the reason why the most generic vacua of the model can be cast into the form of eqs. (7.5), (7.13) and (7.14). In the end, we can choose to eliminate two of the upper components of the doublets (two charged fields) and one of the

imaginary components of the lower part of the doublets, so that we are left with simplified doublets given by

$$\Phi_1 = \frac{1}{\sqrt{2}} \begin{pmatrix} 0 \\ \phi_1 \end{pmatrix}, \quad \Phi_2 = \frac{1}{\sqrt{2}} \begin{pmatrix} \phi_4 + i\phi_5 \\ \phi_2 + i\phi_3 \end{pmatrix}, \quad (7.27)$$

where for convenience we have renamed the real component fields.

For the CP-conserving potential of Eq. (7.1) that we have been studying, the bounce equation (7.23) will allow a further simplification, involving only two of the above component fields, namely ϕ_1 and ϕ_2 . In fact, let us consider the derivatives of the potential with respect to each of the ϕ_i that appear in the right-hand side of the bounce equation (7.23). These are given by

$$\frac{\partial V}{\partial \phi_1} = \frac{1}{2} [2m_{11}^2 + \lambda_1 \phi_1^2 + \lambda_3(\phi_2^2 + \phi_3^2 + \phi_4^2 + \phi_5^2) + \lambda_4(\phi_2^2 + \phi_3^2) + \lambda_5(\phi_2^2 - \phi_3^2)] \phi_1 - m_{12}^2 \phi_2 \quad (7.28)$$

$$\frac{\partial V}{\partial \phi_2} = \frac{1}{2} [2m_{22}^2 + \lambda_2(\phi_2^2 + \phi_3^2 + \phi_4^2 + \phi_5^2) + (\lambda_3 + \lambda_4 + \lambda_5)\phi_1^2] \phi_2 - m_{12}^2 \phi_1 \quad (7.29)$$

$$\frac{\partial V}{\partial \phi_3} = \frac{1}{2} [2m_{22}^2 + \lambda_2(\phi_2^2 + \phi_3^2 + \phi_4^2 + \phi_5^2) + (\lambda_3 + \lambda_4 - \lambda_5)\phi_1^2] \phi_3 \quad (7.30)$$

$$\frac{\partial V}{\partial \phi_4} = \frac{1}{2} [2m_{22}^2 + \lambda_2(\phi_2^2 + \phi_3^2 + \phi_4^2 + \phi_5^2) + \lambda_3\phi_1^2] \phi_4 \quad (7.31)$$

$$\frac{\partial V}{\partial \phi_5} = \frac{1}{2} [2m_{22}^2 + \lambda_2(\phi_2^2 + \phi_3^2 + \phi_4^2 + \phi_5^2) + \lambda_3\phi_1^2] \phi_5. \quad (7.32)$$

Notice how in the three last equations the fields ϕ_3 , ϕ_4 and ϕ_5 factorize, and how that does not occur for the derivatives of the potential with respect to ϕ_1 and ϕ_2 . This leads to bounce equations for each of the ϕ_i of the following form:

$$\frac{d^2 \phi_1}{dr^2} + \frac{3}{r} \frac{d\phi_1}{dr} = f_1(\phi_1, \dots, \phi_5) \phi_1 - m_{12}^2 \phi_2 \quad (7.33)$$

$$\frac{d^2 \phi_2}{dr^2} + \frac{3}{r} \frac{d\phi_2}{dr} = f_2(\phi_1, \dots, \phi_5) \phi_2 - m_{12}^2 \phi_1 \quad (7.34)$$

$$\frac{d^2 \phi_3}{dr^2} + \frac{3}{r} \frac{d\phi_3}{dr} = f_3(\phi_1, \dots, \phi_5) \phi_3 \quad (7.35)$$

$$\frac{d^2 \phi_4}{dr^2} + \frac{3}{r} \frac{d\phi_4}{dr} = f_4(\phi_1, \dots, \phi_5) \phi_4 \quad (7.36)$$

$$\frac{d^2 \phi_5}{dr^2} + \frac{3}{r} \frac{d\phi_5}{dr} = f_5(\phi_1, \dots, \phi_5) \phi_5, \quad (7.37)$$

where the functions f_i can be read from Eqs. (7.28)-(7.32). These equations must be solved with the boundary conditions (7.24). In our case, for which both the true and false vacua of the CP conserving potential are themselves CP and charge conserving, the boundary condition (7.24) always implies $\phi_3(\infty) = \phi_4(\infty) = \phi_5(\infty) = 0$ at any vacua.

We observe that there is a fundamental difference between the bounce equations for $\{\phi_1, \phi_2\}$ and those for $\{\phi_3, \phi_4, \phi_5\}$. Namely, in the right-hand side of the latter equations the factorization of the fields ϕ_3 , ϕ_4 and ϕ_5 implies that the trivial solutions $\phi_3(r) = 0$, $\phi_4(r) = 0$ and $\phi_5(r) = 0$ exist. Moreover, they respect the above-mentioned boundary conditions, and thus are acceptable bounce solutions. On the contrary, in the right-hand side of the first two equations there is an extra term linear in the fields ϕ_1 and ϕ_2 . And, though the trivial solutions $\phi_1(r) = 0$ and $\phi_2(r) = 0$ also satisfy eqs. (7.33) and (7.34), they do not comply with the boundary conditions at infinity for these two fields, which are of the form $\phi_1(\infty) = v_1$ and $\phi_2(\infty) = v_2$ with non-zero values for the false vacua vevs v_1 and v_2 ³: thus they are not bounce solutions.

This strongly suggests that the bounce solutions connecting the true and false vacua have the profiles $\phi_3(r)$, $\phi_4(r)$ and $\phi_5(r)$ identically vanishing in the whole range for r , from 0 to ∞ . This would imply that the original 2HDM 8-field bounce calculation reduces to a 2-field problem. In fact, in all the hundreds of thousands of cases that we have studied numerically (see Section 7.5), we have always verified that only $\phi_1(r)$ and $\phi_2(r)$ have non-trivial profiles, while $\phi_3(r)$, $\phi_4(r)$ and $\phi_5(r)$ always vanish⁴.

This is not merely a mathematical property of the bounce equations (7.23), but rather it is dictated by the physics of the model. To illustrate this point, let us consider for the moment the Complex 2HDM (C2HDM) [157–165], where no CP symmetry is imposed on the potential of Eq. (7.2). In this generalisation, both parameters m_{12}^2 and λ_5 can be complex although one of these phases can always be absorbed into one of the fields. We are then left with a single complex parameter in the potential, which we choose as the soft breaking term. Let us then write $m_{12}^2 = |m_{12}^2| \exp^{i\theta_{12}}$. This potential may have coexisting minima as well [111]. However, there is the possibility that in one of these minima the vevs of the doublets are real (as in Eq. (7.5)) and in the other the vevs have a relative complex phase (as in Eq. (7.13)). But since the potential explicitly breaks the CP symmetry due to the presence of the phase θ_{12} , *both* of these vacua are CP breaking, even if the vevs are real. For the C2HDM potential with complex m_{12}^2 , then, the derivatives of the potential with respect to ϕ_i are slightly modified, and the bounce equations (7.33)–(7.37) become

$$\frac{d^2\phi_1}{dr^2} + \frac{3}{r} \frac{d\phi_1}{dr} = f_1(\phi_1, \dots, \phi_5) \phi_1 - |m_{12}^2| (\phi_2 \cos \theta_{12} - \phi_3 \sin \theta_{12}) \quad (7.38)$$

$$\frac{d^2\phi_2}{dr^2} + \frac{3}{r} \frac{d\phi_2}{dr} = f_2(\phi_1, \dots, \phi_5) \phi_2 - \phi_1 |m_{12}^2| \cos \theta_{12} \quad (7.39)$$

³Notice how the soft breaking term m_{12}^2 in the potential prevents solutions of the minimisation conditions of Eq. (7.9) with any of the vevs equal to zero.

⁴Notice however that we do not possess a full analytical demonstration of this property.

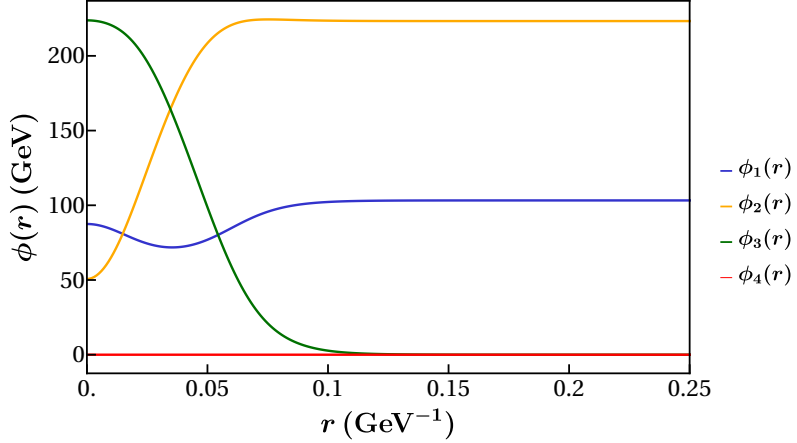


Figure 7.1: Bounce solution ($\phi_1, \phi_2, \phi_3, \phi_4$) for the C2HDM. The fifth bounce for ϕ_5 is identical to that for ϕ_4 .

$$\frac{d^2\phi_3}{dr^2} + \frac{3}{r} \frac{d\phi_3}{dr} = f_3(\phi_1, \dots, \phi_5) \phi_3 + \phi_1 |m_{12}^2| \sin \theta_{12} \quad (7.40)$$

$$\frac{d^2\phi_4}{dr^2} + \frac{3}{r} \frac{d\phi_4}{dr} = f_4(\phi_1, \dots, \phi_5) \phi_4 \quad (7.41)$$

$$\frac{d^2\phi_5}{dr^2} + \frac{3}{r} \frac{d\phi_5}{dr} = f_5(\phi_1, \dots, \phi_5) \phi_5. \quad (7.42)$$

Comparing the system of equations (7.33)-(7.37) with the corresponding system (7.38)-(7.42) we observe that, while the two last equations remain unchanged, the right hand side of the third equation contains an additional term that does not factorize ϕ_3 (further, the non-factorized terms in Eqs. (7.38)-(7.39) have also changed). Thus, we no longer expect a trivial profile for the bounce solution $\phi_3(r)$. Clearly, the appearance of the additional term in the bounce equation for ϕ_3 , which we recall is the complex neutral component of the second doublet, depends on the presence of the explicitly CP breaking phase θ_{12} : the different physics described by the C2HDM induces a different structure in the bounce equations. At this point, we consider many different choices for the parameters of the C2HDM potential in which coexisting minima occur. These points are chosen such that the false vacuum has real vevs, while the vevs of the true minimum have a relative complex phase. Computing the bounce solution for this parameter space, our expectation for the bounce profiles is fully confirmed: for this new model, ϕ_1, ϕ_2 and ϕ_3 are non trivial profiles, while ϕ_4 and ϕ_5 vanish as before. We see a particular example of this behaviour in Fig. 7.1, where we plot the different fields of the bounce solution ϕ_i as a function of r . We remind that in this plot the fields tend at $r \rightarrow \infty$ to the false vacua vevs, and thus ϕ_3 in that limit vanishes, as expected. As opposed to what happened in the CP conserving potential, however, $\phi_3(r)$ is no longer vanishing everywhere. In particular, we observe that at $r = 0$ it is taking a non-zero value, thus contributing (as well as the other non-zero components of the bounce) to the evaluation of the

tunneling time in Eq. (7.26).

It is worth stressing at this stage that this change in the behaviour of $\phi_3(r)$ is due to the different physics described by the two potentials. Only due to the explicit CP violation of the C2HDM can ϕ_3 have a non-trivial profile, while explicit CP conservation forces this component of the bounce to vanish for all values of r . Further, we have to note that for both potentials ϕ_4 and ϕ_5 are always vanishing, which is to be expected on physical grounds, since no charge breaking can occur in either of the models when a normal minimum exists.

7.4 Tunneling to degenerate vacua

At this stage, and before we embark on scans of the 2HDM parameter space, let us discuss a novel aspect of the tunneling calculations which arise in this model. As we have emphasised previously, if the minimisations conditions (7.9) have a solution of the form $\{v_1, v_2\}$, they also include the solutions $\{-v_1, -v_2\}$. The same happens for the second, non degenerate minimum N' , which corresponds to vevs of the form $\{v'_1, v'_2\}$.

Let now $N \equiv \{v_1, v_2\}$ and $\bar{N} \equiv \{-v_1, -v_2\}$ be the false vacua of the model, and assume that “our” vacuum corresponds to N . The universe may now tunnel to *two* degenerate true vacua, $N' = \{v'_1, v'_2\}$ and $\bar{N}' = \{-v'_1, -v'_2\}$. Since N' and \bar{N}' describe exactly the same physics, but (as we will see soon) there are crucial differences between the tunneling rates from N to either N' or \bar{N}' .

In order to understand this critical point, let us consider a specific example, for which the parameters of the 2HDM potential (7.2) are chosen to be

$$\begin{aligned} m_{11}^2 &= -12305.9, \quad m_{22}^2 = -7932.3, \quad m_{12}^2 = -1047.5 \text{ (GeV}^2\text{)} \\ \lambda_1 &= 2.07544, \quad \lambda_2 = 0.377709, \quad \lambda_3 = 1.8562, \\ \lambda_4 &= -1.7028, \quad \lambda_5 = -0.345453. \end{aligned} \tag{7.43}$$

This choice of parameters yields a maximum M at field values $M \equiv \{\phi_1, \phi_2\} = \{0, 0\}$ and the following minima (all vevs in GeV),

$$\begin{aligned} N &\equiv \{97.3767, 225.907\}, \quad \bar{N} \equiv \{-97.3767, -225.907\} \\ N' &\equiv \{162.491, -319.463\}, \quad \bar{N}' \equiv \{-162.491, 319.463\}. \end{aligned} \tag{7.44}$$

We also have two couples of saddle points,

$$\begin{aligned} S_1 &\equiv \{43.6574, 221.06\}, \quad \bar{S}_1 \equiv \{-43.6574, -221.06\} \\ S_2 &\equiv \{95.5578, 48.8458\}, \quad \bar{S}_2 \equiv \{-95.5578, -48.8458\}. \end{aligned} \tag{7.45}$$

If we now calculate the bounce solutions for the transitions from N to N' and from N to \bar{N}' , and assuming for the sake of argument that only one of these tran-

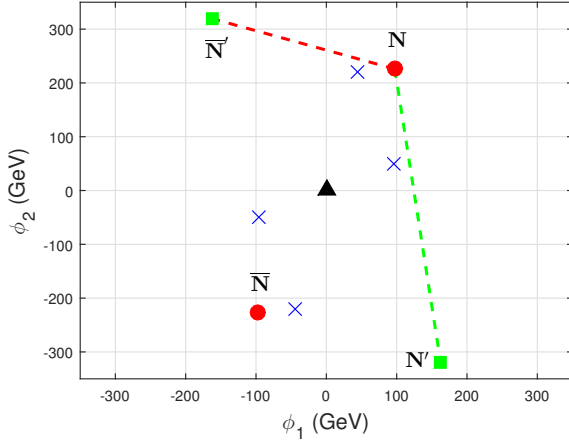


Figure 7.2: Location of all extrema of the 2HDM potential for the choice of parameters in (7.43). Saddle points are marked with “ \times ”, the maximum of the potential, at $(0, 0)$, with a black triangle. The false minima are marked with red circles, the true ones with green squares. The lines connecting N to N' and \bar{N}' illustrate how different the paths between these minima may be.

sitions was possible, we would obtain the following tunneling times (see Eq. (7.26)),

$$\begin{aligned}\tau(N \rightarrow N') &\simeq 8 \times 10^{2131} T_U, \\ \tau(N \rightarrow \bar{N}') &\simeq 2 \times 10^{-113} T_U,\end{aligned}\quad (7.46)$$

where T_U is the current age of the universe. If one were to only consider the transition $N \rightarrow N'$ one would conclude that the false vacuum N was absolutely stable, whereas the second transition, $N \rightarrow \bar{N}'$, instead shows N to be incredibly unstable, having decayed to \bar{N}' almost immediately after the Big Bang. The discrepancy between the tunneling times for both transitions is astonishing, all the more so because the lower minima N' and \bar{N}' are degenerate and describe exactly the same physics. Thus one might naively expect that there should be no difference in the tunneling rate from N to either of them: after all the difference in the value of the potential between N and N' or between N and \bar{N}' is exactly the same, and given by Eq. (7.17). The fundamental reason of this difference is extremely simple to understand, and lies in the landscape of minima and saddle points yielding very different possible paths for tunneling between N and N' or \bar{N}' . This may be seen in Fig. 7.2, where it is illustrated, in the $\{\phi_1, \phi_2\}$ plane, the locations of all extrema of the potential listed above. Notice how N is *not* equally distant from N' and \bar{N}' ; notice also, and perhaps even more importantly, that the path from N to both of the lower minima passes close to a different landscape of saddle points. Instead, from N to N' there is a saddle point almost at the beginning, to \bar{N}' the first saddle point is further away. Also, the steepest descent from N to N' is possibly “deviated” by the several remaining saddle points and the maximum along the way, which would

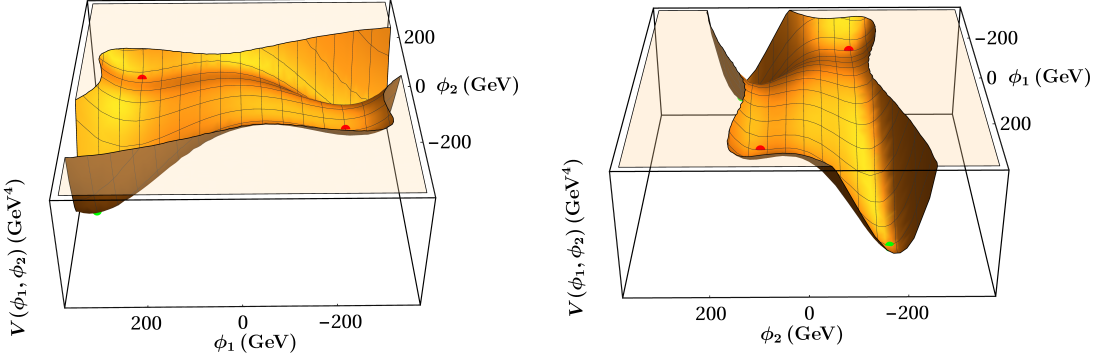


Figure 7.3: Left panel: Plot of the potential $V(\phi_1, \phi_2)$ of Eq. (7.2) for the parameters given of Eq. (7.43). Right panel: The same potential rotated anticlockwise by 90 degrees. The left panel better shows the decay path from N to N' ; the right panel from N to \bar{N}' . The path connecting N while N' is longer than the path connecting N with \bar{N}' .

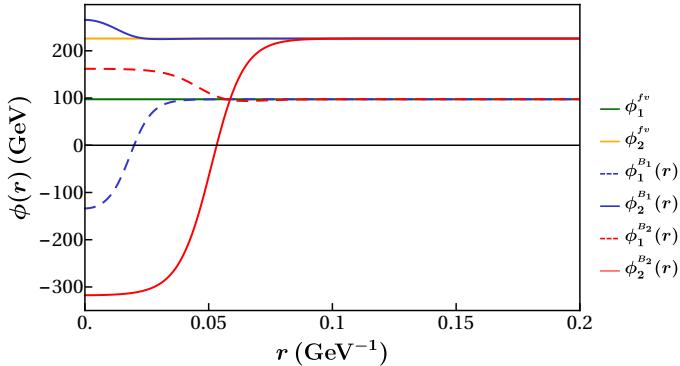


Figure 7.4: Bounce solutions for fields ϕ_1 and ϕ_2 for the transitions from N to N' ($B1$) and from N to \bar{N}' ($B2$). In both cases the fields ϕ_i tend to the same values at $r \rightarrow \infty$, *i.e.* the values of the fields at the false vacuum N , ϕ_1^{fv} e ϕ_2^{fv} . But at $r = 0$ the fields assume different values, close to the vevs at each of the degenerate true vacua.

explain the much larger tunneling time found, whereas the path to \bar{N}' seems much more “direct”. To further drive in this point, consider Fig. 7.3, where we show 3D plots illustrating the shape of the potential along the (seemingly) shortest path from N to both N' and \bar{N}' : these images show that, even though the difference in depth of the potential is exactly the same between N and N' or between N and \bar{N}' , it is quite clearly easier for the latter transition to occur than the former. In fact the bounce solutions obtained in the transition from N to N' (which we now call “ $B1$ ”) and from N to \bar{N}' (“ $B2$ ”) are quite different, as can be appreciated in Fig. 7.4. In this plot it is presented the evolution with the radial coordinate r of the two bounce profiles for the fields ϕ_1 and ϕ_2 found for the specific example we have been considering. Notice how the solutions, $B1$ and $B2$, converge for large values of r to the same values, which are the values of the vevs at the false vacuum N , as was

to be expected. However, the values of the fields ϕ_i at $r = 0$ diverge significantly, assuming even opposite signs. Recall that at $r = 0$ the bounce solution is found for values of the fields “close” to the true vacuum of the theory. Hence we find that, for the bounce $B1$, ϕ_1 assumes a large negative value, $\simeq -130$ GeV and ϕ_2 a large positive one, $\simeq 260$ GeV. It is worth to note how these values for the bounce are close to the vevs of the true vacuum \bar{N}' (~ -162 , ~ 320 GeV). Likewise, the values found for the bounce solution $B2$ are close to the vevs found for the other lower vacuum, N' . Thus, despite the fact that both N' and \bar{N}' are degenerate and at the same relative depth to N , the bounce solutions for the two possible transitions are very different, and in fact lead to very different values for the bounce action $S[\phi_b]$ from Eq. (7.25), and hence to the two extremely different lifetime values found.

If the potential has, from N , two possible “decay channels”, then its decay rate, Γ , will be given by

$$\Gamma = \Gamma(N \rightarrow N') + \Gamma(N \rightarrow \bar{N}') = \frac{1}{\tau(N \rightarrow N')} + \frac{1}{\tau(N \rightarrow \bar{N}')} \quad (7.47)$$

with the “partial” tunneling times from Eq. (7.46). Thus, the lifetime τ of the false vacuum N will obviously be

$$\tau = \frac{1}{\Gamma} = \left(\frac{1}{\tau(N \rightarrow N')} + \frac{1}{\tau(N \rightarrow \bar{N}')} \right)^{-1} \simeq 2 \times 10^{-113} T_U \quad (7.48)$$

where in analogy with nuclear decays, when one of the decay channels is much faster than the other, it dominates over the total lifetime. The conclusion to draw from this particular example is simple: both degenerate lower vacua must be considered for the calculation of the tunneling time, and the stability of the false vacuum may depend crucially on which of the true vacua it is decaying into. It was verified that differences in tunneling times to true degenerate vacua can be as extreme as those presented in Eq. (7.46) for many choices of parameters in the potential, though not always. For many other regions of parameter space, though the two possible decay rates may differ, they do not affect qualitatively the overall stability of the false vacuum. Meaning, in many cases, if the tunneling time to one of the lower vacua is, say, much larger (smaller) than T_U , the other tunneling time, while possibly very different, will also be much larger (smaller) than T_U . Nonetheless, as we will shortly see, for certain regions the computation of τ taking into account the existence of both possible true vacua increased the number of dangerous false vacua by as much as 50%.

7.5 2HDM Numerical Scans

The physics arguments of Section 7.3 show that the tunneling rate calculation can be reduced, for the CP conserving potential of Eq. (7.2), to a two-field problem.

Nonetheless extensive numerical checks were performed, comparing eight-field calculations with two-field ones, and no differences were ever found. Also, in Section 7.4 it was shown the importance of computing the tunneling rates to *both* degenerate true vacua. Armed with these two important theoretical insights, we can proceed to an extensive scan of the 2HDM parameter space. The goal of this Section is to ascertain how much of that parameter space should be avoided due to tunneling times shorter than the age of the universe.

It was chosen to work in models type I and II (for the remaining types of Yukawa interactions the conclusions reached would certainly be very similar). All parameter scans presented in this Section are such that:

- They include at least one (CP conserving) minimum with $v = 246$ GeV and $m_h = 125$ GeV.
- All theoretical and experimental results mentioned in Section 7.1.3 are satisfied. In particular, we demanded that all μ_X ratios (defined in Eq. (7.12)) be within 30% of their expected SM value of 1, which reproduces quite satisfactorily the current status of LHC results.
- $1 \leq \tan \beta \leq 30$ and $-\pi/2 \leq \alpha \leq \pi/2$.
- The mass of the heavier CP-even scalar H is chosen in the interval between 130 and 1000 GeV. The mass of the pseudoscalar A is chosen between 100 and 1000 GeV. For the charged mass, its lower bound is 100 GeV for model type I and 580 GeV for model type II (the difference due to flavour physics constraints described in Section 7.1.3). The upper bound for the charged mass is again 1000 GeV.
- The soft breaking parameter m_{12}^2 is taken with both signs, and magnitude below roughly 500 GeV 2 .

These parameter scans are not meant to be exhaustive: representative regions of the 2HDM parameter space were merely sampled to illustrate the possible impact that tunneling times to deeper vacua lower than the age of the universe may have. We now consider different scenarios.

7.5.1 General scans for type I and II models

To illustrate the possible relevance of false vacua exclusion (due to low tunneling times) in general, “blind”, scans of parameter space, we generated large datasets (over 100000 different combinations of parameters) for models type I and II.

In Fig. 7.5 it is shown the result of the analysis, by plotting the values of λ_5 *vs* the pseudoscalar mass m_A . The colour code in these plots is such that:

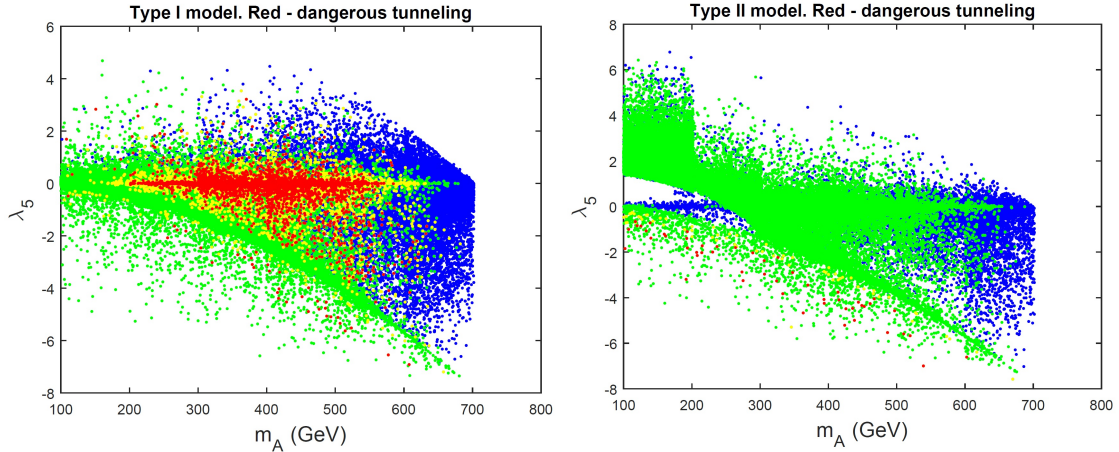


Figure 7.5: Scatter plot of λ_5 vs. m_A for general scan on the parameter space of a type I (left) and type II (right) 2HDM. In blue, all points generated which conform to theoretical and experimental constraints; in green, the subset of those for which two normal vacua are possible; in yellow, the subset of those for which $D < 0$ and thus the EW vacuum may be the false one; and in red, those points for which the tunneling time to the true vacuum is smaller than the age of the universe.

- In blue we present all points generated which satisfy the theoretical and experimental constraints explained above. The other colours are superimposed on top of the blue points. Or, in other words, the green, yellow, red points are a subset of the blue ones.
- The green points correspond to the subset of the blue ones for which the two CP-conserving minima conditions of Eqs. (7.19) and (7.20) are satisfied. Recall that those conditions are necessary ones, but not sufficient, and therefore not all green points will truly correspond to the existence of two minima. In fact, that happens typically for only half of these points. Notice the disproportion in size of the green region compared to the blue one: dual minima in the 2HDM potential are, in general, a rare occurrence.
- In yellow it is shown the subset of the green points for which the discriminant D from Eq. (7.22) is negative, i.e. the points for which, if two minima exist, “our” electroweak vacuum with $v = 246$ GeV will not be the deeper one.
- Finally in red, the subset of the yellow points for which: (a) two minima exist, (b) “our” electroweak vacuum is not the global minimum and (c) the tunneling time from “our” vacuum to the deeper true vacuum is less than the age of the universe.

The visible blue points in these figures are clearly safe combinations of parameters, for which the EW vacuum is not only safe but also unique. Several comments are in order to better interpret these plots. First, please take into account the fact that

these plots are dense in each of the colours. In other words, in the middle of the green, or yellow, or red points there are blue ones. Thus the red regions are not wholly excluded: though dangerous tunneling times seem to be found for specific areas in the $m_A - \lambda_5$ plane, those areas will in general also include perfectly acceptable blue (green, yellow) points for which there might not even be two minima. Second, there is no obvious pattern to the green, yellow or red regions: the existence of two minima, and dangerous tunneling times for the acceptable EW vacuum, depends on non-trivial relations between the potential's parameters, which are difficult to visualize in this 2-dimensional slice of what is in truth an 8-dimensional parameter space. Third, in general it seems easier to find two minima (and dangerous short-lived vacua) in model type II than in I. This is a consequence of the hard bound on the charged Higgs mass in model type II which arises from $b \rightarrow s\gamma$ constraints. This bound tends to privilege higher, positive, values of m_{12}^2 , for which the discriminant D is usually found to be positive (and thus “our” EW vacuum is the global minimum of the model).

To illustrate the frequency with which dangerous vacua are found in this blind scan, consider the results shown above for type I: the total number of generated (blue) points conforming to all theory and experimental constraints was above 120000; of these, roughly 21500 (green) points were found which might have two minima (satisfying Eqs. (7.19) and (7.20)): in fact, of those, two minima were found only for over 11000 points. The (yellow) points with $D < 0$, with possible local EW vacua with $v = 246$ GeV, totalled almost 9500, and out of these over 4200 were found for which the tunneling time to the global ($v \neq 246$ GeV) minimum is inferior to T_U . Thus the percentage of points of the initial parameter space excluded on tunneling time arguments is about 3.5%. For model type II, a similar accounting yields a percentage of excluded points of roughly 0.2%.

The distribution of dangerous (red) points in Fig. 7.5 is clearly not homogeneous, and the percentages of excluded points found in the previous paragraph are therefore not to be interpreted as, for instance, 3.5% of type I parameter space being ruled out on low tunneling times grounds. In fact, while certain regions of 2HDM parameter space are completely safe (the blue points visible in Fig. 7.5, for instance), others may yield a far larger percentage of dangerous minima than the numbers quoted above. To illustrate this let us now consider a few benchmark scenarios.

7.5.2 First benchmark scenarios: safe regions

As discussed above, the distribution of parameter space points for which dangerous short-lived false vacua occur in the 2HDM is not uniform. The regions of parameter space which conform to equations (7.19), (7.20) or have the discriminant (7.22) negative are usually not easily visualized in 2-dimensional slices, and as explained in Section 7.4, the tunneling time to lower vacua may depend crucially on the landscape

of saddle points in field space, and this will also depend in a non-trivial manner on the numerical values of the couplings, affecting the number of possible solutions of the minimisation conditions of Eq. (7.9). In the present subsection, we will give two examples of parameter choices for which, due to different reasons, the EW vacuum is perfectly safe. In all cases to follow we study model type I, and fix six of the parameters of the model, allowing two others to vary in such a manner as to comply with all theory and experimental constraints. Since we wish to have a physically interesting EW vacuum, we chose to specify the values of (in principle) observable 2HDM parameters, rather than the couplings of the potential in Eq. (7.2). To this end, we of course chose the value of $v = 246$ GeV and $m_h = 125$ GeV for the EW vacuum, and then proceed to select, for each benchmark scenario, the masses m_H and m_{H^\pm} , the value of $\tan \beta$ and of $\sin(\beta - \alpha)$ (thus, indirectly, the value of α). We chose $\sin(\beta - \alpha)$ because this quantity is already quite constrained to be close to unity by LHC data.

The 2HDM parameter scan we undertake therefore considers these six parameters fixed and then proceeds to choosing random values for two others, which we chose to be λ_5 and m_A ⁵. Each selection of parameters is then verified for theory and experimental constraints, and if all are obeyed a satisfactory EW vacuum is found. *A posteriori* the existence of a second minimum is checked, and if that second minimum is the global one, the tunneling time to the true vacuum is computed.

- Decoupling scenario

As a first example, we have chosen $m_H = 600$ GeV, $m_{H^\pm} = 700$ GeV, $\tan \beta = 1$ and $\sin(\beta - \alpha) = 0.99$. Though λ_5 was allowed to vary between -10 and 10 , only values in the window between ~ -6.3 and ~ -2.3 were found after all constraints applied. Likewise, the pseudoscalar mass is found to be constrained between roughly 620 and 705 GeV. It is well known that the electroweak precision constraints (namely the bounds on the Peskin-Takeuchi parameters S , T and U) force the extra scalar masses to be close in the high mass range, so these results are not surprising.

The high values for the extra scalar masses coupled with the fact that $\sin(\beta - \alpha)$ is extremely close to 1⁶, meaning that we are well within a decoupling regime for the model. Of course, one of the possible explanations for the current LHC results is the decoupling of all BSM particles, yielding a SM-like 125 GeV scalar. Thus the benchmark scenario chosen herein is of experimental interest.

For all 200000 points generated complying with the choices above for the parameters and all constraints, we observe that the conditions for the possible existence of two minima, Eqs. (7.19) and (7.20), are *never* satisfied. Thus, for this benchmark

⁵The reason for this is related to Eq. (7.11), which show it to be an efficient choice of parameters to fully specify the 2HDM potential.

⁶This implies that the coupling of h to Z or W bosons and to fermions is very much SM-like.

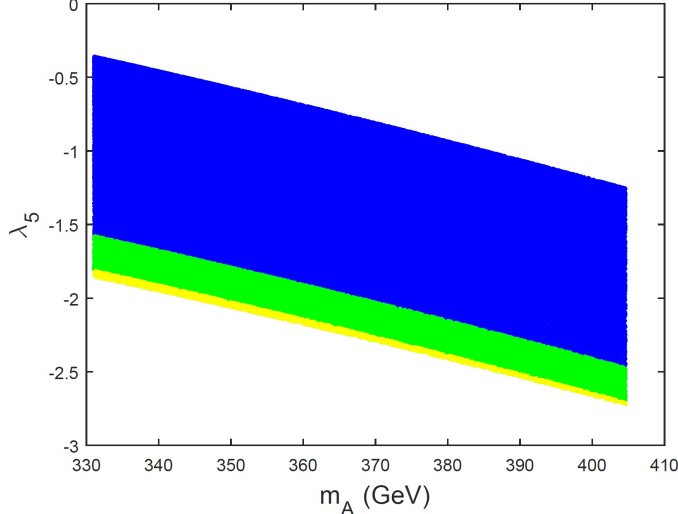


Figure 7.6: Scatter plots of λ_5 vs. m_A for the low mass stable benchmark scenario considered. The colour code is the same as in fig. 7.5.

scenario, the EW vacuum is unique, and thus (at tree-level at least) entirely stable. This does not mean that any choice of parameters in the decoupling regime will always fall into this category, although, as explained above for the type II model, large masses tend to yield stable EW vacua. Of course, there is no need to go into the decoupling regime to find parameters for which no non-degenerate vacua do not exist: the blue points in Fig. 7.5 show this to be true. Thus some regions of 2HDM parameter space have EW vacua which are unique at tree-level. Therefore, apart from the possibility of one-loop corrections to the potential originating deeper vacua as seems to be the case in the SM, the stability of the EW vacuum in such 2HDM parameter space regions is ensured and no tunneling calculations are needed.

- Low mass stable scenario

Consider now a different choice of parameters corresponding to much lower masses for the extra scalars: $m_H = 280$ GeV, $m_{H^\pm} = 400$ GeV, $\tan \beta = 2.3$ and again $\sin(\beta - \alpha) = 0.99$. This last choice all but ensures h has SM-like behaviour. The value of $\tan \beta$ is chosen such as to comply with the exclusion in the $\tan \beta$ - m_{H^\pm} plane stemming from B-physics constraints [143]. The low masses chosen for H and H^\pm are obviously interesting from the experimental point of view, as they raise the possibility of new particles discovered at LHC. As before, electroweak precision constraints force the pseudoscalar to be close in mass to the charged scalar, as can be appreciated from Fig. 7.6. In this plot it is shown a ‘‘phase diagram’’ of the 2HDM parameter space. Unlike the plots in Fig. 7.5 (the colour code is the same here than in those plots) the parameter space now being scanned is truly a two-dimensional one, and thus Fig. 7.6 gives us a clearer picture of regions having different vacuum structure.

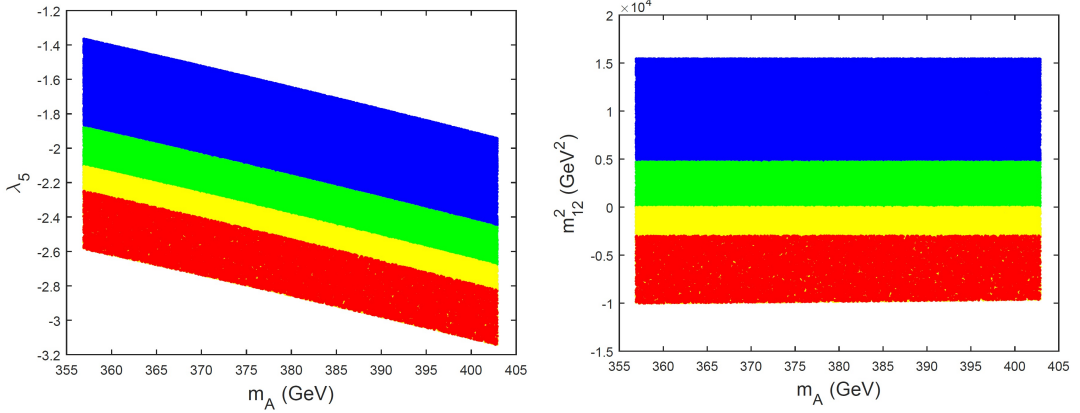


Figure 7.7: Scatter plots of λ_5 (left) and m_{12}^2 (right) *vs.* m_A for the benchmark scenario considered in Section 7.5.3. The colour code is the same as in fig. 7.5.

What we observe in Fig. 7.6 is the total absence of red points, and only a thin yellow strip where the EW vacuum could be the false vacuum. Indeed, for all points for which the EW vacuum is indeed a local minimum of the potential and not the global one, tunneling time calculations have revealed that the lifetime of the false vacuum is always far superior to the current age of the universe. Thus, even though for this benchmark scenario there may be dual minima, and “our” vacuum is not guaranteed to be the true vacuum of the model, it is nonetheless found to be either stable or incredibly long lived. Hence one must be careful to *not* exclude offhand regions of parameter space for which the discriminant D from Eq. (7.22) is negative: $D > 0$ is a necessary and sufficient condition for the EW vacuum with $v = 246$ GeV to be the global minimum of the theory, but as this example shows, points with $D < 0$ may be entirely acceptable, having lifetimes larger than T_U . One must therefore be cautious in excluding regions of parameter space using the sign of discriminant D , as was made in refs. [129, 166]: if $D < 0$, tunneling times involving two-field bounce equations need to be computed, lest one is needlessly refusing phenomenologically acceptable combinations of 2HDM parameters.

7.5.3 Second benchmark scenario: considerable exclusion

The vacuum stability of the 2HDM may however change dramatically even for seemingly small variations in its parameters. Consider yet another choice of parameters, still corresponding to low masses for the extra scalars: $m_H = 200$ GeV, $m_{H^\pm} = 400$ GeV, $\tan \beta = 2.5$ and again $\sin(\beta - \alpha) = 0.99$. Though this choice of parameters seems to be very similar to the previous benchmark considered, the allowed vacuum structure of the model is now quite different, as may be appreciated from Fig. 7.7. Notice how the region where two minima are in principle allowed (the yellow points) is now much larger, and how many red points now occur. In fact, for this region of parameter space, roughly 67% of all cases where “our” vacuum is the higher min-

imum yield a tunneling time inferior to the age of the universe. Globally, we find that for the points generated in this benchmark scenario which verify all theory and experimental constraints, roughly 11% have dangerous tunneling times. This is a much greater percentage than the one found for the blind parameter scan, showing that specific regions of the parameter space may be much more prone to dangerous false vacua than others. It is quite stunning how merely increasing by 0.2 the value of $\tan \beta$ and reducing by 80 GeV the value of the heavier CP-even scalar may have such a drastic effect in the vacuum structure of the 2HDM, but that simply reflects the complicated and non-obvious dependence on these parameters in Eqs. (7.9), (7.19), (7.20) and (7.22). This not to mention the susceptibility of the tunneling time calculations to the geometry of the potential (which may be heavily influenced by changes in the potential's couplings) as illustrated in Figs. 7.2 and 7.3. It is worth also to consider the importance of calculating the tunneling rates to the degenerate true vacua: as discussed in Section 7.4, despite that degeneracy originating physically equivalent vacua, the lifetime of the false vacuum can change immensely if one does not take into account the existence of two possible true vacua it can decay into. In this present case, doing the lifetime calculation correctly taking into account both lower vacua yielded roughly 50% more dangerous red points than if we considered tunneling to only one of the lower vacua.

In the right of Fig. 7.7 we plot m_{12}^2 against m_A , illustrating nicely how all EW false vacua can only occur for negative values of the soft breaking parameter. This is a known feature of the 2HDM: negative discriminant D seems to only occur for negative m_{12}^2 , though there is no demonstration of this property. It would imply a correlation in the signs of the two last terms in the definition of the discriminant in Eq. (7.22).

Chapter 8

Conclusions and outlook

In this thesis we studied several aspects on the topic of the stability analysis of the electroweak vacuum (where our entire Universe sits), using the formalism of the computation of a metastable vacuum decay rate through the bounce solutions of the euclidean equations of motion for scalar fields. In particular, we studied the impact of physics beyond the Standard Model on the stability condition of our Universe, considering both models in which we have new physics only around the Planck scale M_P , and models that provide new physics at lower scales. In this Chapter we summarize the main results presented in Chapters 4, 5, 6 and 7 of this thesis, i.e. the chapters based on the original works in Refs. [51, 83, 100, 114].

In Chapter 4 we studied the impact of very high energy NP (around the Planck scale M_P) on the stability condition of the EW vacuum by carrying the analysis in a curved spacetime background. In particular, we saw that taking into account the presence of gravity does not modify qualitatively the results of previous studies [54, 65, 71, 72], where the same analysis was carried in a flat spacetime background. In fact, as for this latter case, the main result is that we have new bounce solutions due to the New Physics modification to the RG improved Higgs effective potential, and these can have an enormous impact on the EW vacuum lifetime, by far dominating over the contribution that comes from the known solutions obtained with the unmodified Standard Model potential.

As in [54, 65, 71] we first performed the analysis by adding to the SM potential higher powers of the Higgs field, more precisely terms as ϕ^6/M_P^2 and ϕ^8/M_P^4 that are certainly generated in a quantum gravity context [167]. Then, following [73], we parametrized high energy new physics in a different manner, namely by adding to the SM potential a boson S and a fermion ψ , with very large masses M_S and M_f , coupled to the Higgs boson. As for the analysis carried in flat spacetime, in both models we actually find that the presence of new physics can have an enormous impact on the EW vacuum stability condition. In particular, these results definitely show that, irrespectively of the parametrization used to describe high energy new physics, it is not possible to ignore its presence when the stability analysis is performed. Then,

such analysis could be of the greatest importance for current studies and for model building of Beyond Standard Model physics, where we often have to take into account new physics at very high (Planckian and/or trans-Planckian) scales.

To be more specific, from the result obtained in the flat spacetime [54, 65, 71, 72], we know that New Physics introduced via this kind of models tends to destabilize the electroweak vacuum, even making the tunneling time less than the age of the Universe, and thus to move the instability line of the phase diagram in Fig. 4.1 towards the point corresponding to the central values of the masses of the Higgs boson and of the top quark, that is the point corresponding to our Universe. The results illustrated in this Chapter with the inclusion a minimal coupling of gravity with matter (i.e. considering a curved spacetime background with the only inclusion of the Einstein-Hilbert term) show that this destabilization effect of New Physics is still present and turns out to be dominant, although gravity tends to stabilize the electroweak vacuum, i.e. to suppress the nucleation of true vacuum bubbles [51].

In Chapter 5 we studied the impact of a direct coupling of the Higgs field ϕ with gravity on the stability of the electroweak vacuum when we include New Physics at high energy scales, describing this latter adding the higher order operator at the Planck scale ϕ^6/M_P^2 and ϕ^8/M_P^4 to the Higgs potential. In fact, in view of the destabilization effect induced by this kind of New Physics models, we want to search for a stabilization mechanism for the electroweak vacuum, and we showed that this direct coupling between gravity and matter could provide such a mechanism. This non minimal coupling is described adding to the lagrangian a term $\xi\phi^2R$, where R is the Ricci scalar and ξ is the coupling constant. The impact of this coupling considering only the Standard Model was studied in [77]: a part for a small region around the conformal value $\xi = 1/6$, this coupling tends to increase the electroweak vacuum lifetime τ value, respect to the minimal coupling case $\xi = 0$.

Once we include New Physics beyond Standard Model, the results presented in this Chapter show that the electroweak vacuum stability continue to strongly depend from the value of the coupling ξ : in fact, taking into account specific New Physics cases, i.e. fixing the values of the NP couplings, we find a behaviour of the tunneling time τ that presents a minimum as shown in Fig. 5.2, while moving away from this minimum, the $\tau(\xi)$ curve has a monotonous increasing behavior. Depending on the values of NP couplings, in a small interval around the minimum of $\tau(\xi)$ (which can include also the minimal coupling case $\xi = 0$), we can have values of the tunneling time less than the age of the Universe $\tau < T_U$, then a situation that can not describe our Universe.

However, for sufficiently large values of the coupling, but of the order of unity $|\xi| \sim 1$, the tunneling time becomes greater than the age of the Universe $\tau > T_U$ (a situation consistent with our Universe), i.e. the non minimal coupling solves the instability due to the presence of New Physics. If this were not enough, gravity with

non minimal coupling can have such a strong stabilizing effect that it completely *washes out* the effects of New Physics: this effect is shown in Fig. 5.2 where we see that the curve for $\tau(\xi)$ obtained with the inclusion of NP (with a specific values of the coupling) collapses on the corresponding SM curve for “large” values of $|\xi|$. This washing out effect of the non minimal coupling is present for a large region of the parameter space of the NP coupling, as can be seen in Figs. 5.3 and 5.4 [83].

In view of this enormous stabilizing effect induced by the term $\xi\phi^2R$ for values of ξ outside the small range around the minimum of $\tau(\xi)$, and under the assumption that the physical value (still unknown) of ξ lies outside this range, we are led to formulate the following conjecture, which we call “*Direct Coupling Stability Conjecture*”. An intrinsic stabilization mechanism that protects our Universe from any possible destabilization that could come from unknown New Physics beyond SM is provided by three simple and primordial ingredients: the quantum nature of the laws that govern the Universe, and the very existence of gravity and of the Higgs boson. This is all that is needed to require the presence of the direct coupling term between the Higgs field and the Ricci scalar.

It is worth to note that the results illustrated in this Chapter show how the washing out effect due to gravity is strictly related to the fact that for values of $|\xi|$ sufficiently large the center of the bounces, and therefore their maximum value, tends to be smaller and smaller, and this leads the bounce solutions obtained by including the New Physics to coincide with those obtained with the Standard Model only. Therefore, we can say that this electroweak vacuum stabilization mechanism could be due to a gravitational mechanism that tends to “flatten” the bounce solutions, i.e. to obtain solutions with an ever smaller center and an ever larger size.

In Chapter 6 we have studied the stability of the EW vacuum in the presence of Planck-scale suppressed operators of the form ϕ^{2n}/M^{2n-4} , where M is of order the Planck mass M_P , then a generalization of the higher order operators models considered in the previous chapters. As said above, such operators can no longer be excluded in the presence of gravity, as they could in principle be generated by quantum gravity effects. If these operators contribute with a negative sign to the SM effective potential, they will in general have a destabilizing effect on the EW vacuum, and therefore we have called them *harmful*. We have then evaluated the lifetime τ of the EW vacuum both in a flat and in a gravitational background for simple scenarios of Planckian NP with convex potentials in the presence of these harmful operators. Obviously, for $n = 3$ and $M = M_P$ we recover the results quoted in Chapter 4 [51]. For such scenarios, we have found that longevity of the EW vacuum requires $n \geq 4$, leading to a EW vacuum lifetime greater of the one obtained with the SM alone, $\tau \gtrsim \tau_{\text{SM}}$. Most remarkably, for theories with relatively lower scale M of quantum gravity, e.g. $M = M_P/10$, a safely stable EW vacuum implies that all harmful operators up to $n = 6$ need to be *either* accidentally suppressed *or* naturally

eliminated by the action of some symmetry.

Besides resorting to *ad hoc* accidental suppressions, in this Chapter we have explored the possibility whether the harmful Planck-scale operators of the form ϕ^{2n}/M^{2n-4} could be eliminated *naturally* to leading order because of the action of some symmetry. In this context, we have shown how minimal embeddings of the SM in SUGRA can stabilize the EW vacuum against these harmful operators up to very high values of the induced SUSY-violating A -couplings and the soft SUSY-breaking scale M_S . The scale M_S may even lie above the so-called SM instability scale of 10^{11} GeV. In particular, we have explicitly demonstrated how discrete R symmetries, such as Z_{2n-2}^R , could be invoked to suppress the harmful operators to arbitrary higher powers of n . In this minimal SUGRA framework, we have analyzed different scenarios of Planck-scale gravitational physics and derived lower limits on the power n that will be needed in order to render the EW vacuum sufficiently long-lived. We have presented numerical estimates for a few representative scenarios realising a low and high soft SUSY-breaking scale M_S , i.e. for $M_S = 10$ TeV and $M_S = 10^9$ TeV [100].

The results presented in this Chapter have revealed the severity of the stability problem for theories with low-scale quantum gravity. In particular, we have illustrated that such theories face serious difficulties in ensuring adequate longevity of our EW vacuum. These theories may have a string-theoretic origin [168] giving rise to realizations with a lower effective Planck mass, including models with large compact dimensions [169, 170]. It would be interesting to analyse the restrictions that can be derived from the evaluation of τ on the fundamental parameters of such theories.

In Chapter 7 we studied the EW vacuum stability condition in one of the most simple extension of the SM, the Two Higgs Doublet Model. This model presents a richer phenomenology than the SM, providing extra scalar particles. In particular it has a very rich vacuum structure, providing the possibility of the formation of a electroweak breaking, CP conserving true vacuum different from “our” vacuum also at the tree level, whereas in SM the EW vacuum metastability occurs due to radiative corrections to the potential. However, for the 2HDM we consider the stability analysis only for a flat spacetime background, postponing the study in a curved spacetime background in future works. We analysed in depth the possibility of using the lifetime of false vacua as an exclusion tool of regions of parameter space in 2HDM. The gauge freedom of the model allowed us to reduce the complexity of an *a priori* 8-field problem, and the physics of the models under discussion, coupled with the shape of the bounce equations describing the tunneling trajectories between vacua, permitted a further simplification. This is the first main result that we obtained in this Chapter: we have shown that, in the CP-conserving 2HDM potential the tunneling time calculation is reduced to a 2-field problem. The remaining fields do

not contribute, their bounce equations only allowing for trivial, vanishing solutions when the appropriate boundary conditions are taken into account.

However, the 2-field case produces a bizarre consequence, that is the second main result obtained in this Chapter. The 2HDM is invariant under a simultaneous sign redefinition for both scalar doublets, and no physical consequences should in principle arise from such a sign swap. Indeed, for any pair of solutions of the minimisation conditions of the potential, its symmetric is also a solution. This is a well-known, and trivial, property of 2HDM vacuum solutions. Any minimum found is in fact a “pair of minim”, degenerate, separate in field space, each producing exactly the same physics. We showed that this may have significant impact in the lifetime of false vacua: indeed, the false vacuum can decay to a pair of degenerate true vacua, separated in field space, and the trajectory to each of the true vacua will not be, in general, the same. Hence the partial decay rates to each of the deeper vacua will in general be different, and the landscape of maxima and saddle points found along the trajectories to each true vacuum can indeed yield vastly different tunneling rates. We find many instances where considering both tunneling possibilities yielded false vacua with lifetimes shorter than the age of the universe, whereas considering only one of the decaying possibilities seemed to indicate a stable false vacuum.

Applying the theoretical insights gained on generic scans of the 2HDM parameter space, we analysed which regions of that parameter space might be excluded on grounds of short EW vacuum lifetime. Generic scans over all allowed (under theory and experimental constraints) parameters show that the existence of non-degenerate minima is rare in the 2HDM, and that even when a false vacuum occurs, its lifetime is often found to be superior to the age of the universe. The percentage of 2HDM parameter space points excluded in generic scans is then found to be of the order of a few percent. However, care must be exercised in reading this result, since the regions of 2HDM parameter space where non-degenerate minima occur are not uniformly distributed, and neither is the subset of those for which short-lived false vacua occur.

We therefore proceeded to considering specific benchmark scenarios, illustrating how three very different regimes might occur. First we considered a choice for extra scalar masses and angles α and β (see Eqs. (7.7) and (7.8)) that pushed the theory well into the decoupling regime. Such a choice corresponds to a region of parameter space for which no non-degenerate minima exist in the potential, and as such the model is entirely stable at tree-level. The decoupling regime, of course, is not the only case where no non-degenerate vacua do not occur, the same does happen for smaller masses of the extra scalars. The second scenario considered studied a low-mass case for the extra scalars, and for which the possibility of a false EW vacuum now arises: certain regions of the considered parameter space had $D < 0$, the discriminant which characterizes false vacua (see Eq. (7.22)). However, for all such false vacua, the tunneling times towards the true vacuum were always found to be

larger than T_U , and therefore stability is ensured. Thus the mere existence of a false vacuum should not be used *per se* to exclude regions of parameter space for which $D < 0$: tunneling times should and must be computed, and parameter exclusion should only be decided after that calculation.

Finally, we considered a low-mass scenario for which a large swath of parameter space is excluded on grounds of the short lifetime of the false vacuum found. The importance of a proper lifetime calculation (taking into account the existence of a pair of lower true vacua, related by sign changes in the values of the vevs) was emphasised. In fact, the number of dangerous vacua found can increase by as much as 50% when the full vacuum structure is taken into account. Though dangerous vacua are hard to pinpoint in terms of relations between potential couplings or physical observables, we observed that a negative discriminant only seems to occur for a negative soft breaking term m_{12}^2 in the potential [114].

The overall conclusion of this work is that 2HDM vacuum instability at tree-level can have significant impact on parameter exclusion for certain regions of the parameter space, but that requires an appropriate calculation of the bounce solutions, taking into account the 2-field dynamics that CP-conservation allows us to study. Of crucial importance is also the seemingly trivial existence of pairs of degenerate, sign-swap-related, true vacua, since the lifetime of the false vacua may depend enormously on that fact. Generic blind scans of 2HDM parameters may suggest that the frequency of dangerous vacua is very small, but the results presented in this Chapter show that these vacua may be quite abundant for specific, experimentally-interesting, regions of parameter space. Though the current analysis was performed at tree-level, the significance of the results found is undeniable. Of course, from the existing SM studies, we can expect that radiative corrections will further complicate matters and bring more possibilities of vacuum instability. Thus a one-loop extension of the work presented in this Chapter should be undertaken.

Appendix A

Standard Model β and γ functions

Usually the β and γ function are computed diagrammatically and now we simply state it, as their computations are not a goal of this thesis. Here we want only to see how the Higgs scalar β and γ_m functions can be obtained from the effective potential (2.105) and from Eq. (2.107).

In fact we can write $V_{eff}(\phi) = V_0(\phi) + V_c(\phi)$, where $V_0(\phi)$ is the classical part of the Higgs effective potential, while

$$V_c(\phi) = V_s(\phi_c) + V_g(\phi_c) + V_f(\phi_c) \quad (\text{A.1})$$

is the radiative part. Then the Callan-Symanzik equation can be written as:

$$\begin{aligned} & \mu \frac{\partial}{\partial \mu} V_c(\phi) + \left(\beta \frac{\partial}{\partial \lambda} + m^2 \gamma_m \frac{\partial}{\partial m^2} + \phi \gamma \frac{\partial}{\partial \phi} \right) V_0(\phi) \\ &= \frac{1}{2} m^2 \left(\gamma_m + 2\gamma - \frac{24\lambda}{32\pi^2} \right) \phi^2 \\ &+ \frac{1}{4} \left(\beta + 4\lambda\gamma - \frac{1}{16\pi^2} \left[24\lambda^2 + \frac{3}{4} g^4 + \frac{4}{8} (g^2 + g'^2)^2 - 6y_t^4 \right] \right) \phi^4 = 0. \end{aligned} \quad (\text{A.2})$$

Hence we can read off

$$\beta + 4\lambda\gamma = \frac{1}{16\pi^2} \left(24\lambda^2 + \frac{3}{4} g^4 + \frac{4}{8} (g^2 + g'^2)^2 - 6y_t^4 \right) \quad (\text{A.3})$$

$$\gamma_m + 2\gamma = \frac{12\lambda}{16\pi^2}. \quad (\text{A.4})$$

The anomalous dimension have to be computed diagrammatically. In fact we know that the renormalized field ϕ and the bare field ϕ_0 (independent from the renormalization scale μ , but dependent on the cut-off scale Λ) are related

$$\phi = Z(g_i; \Lambda/\mu)^{-\frac{1}{2}} \phi_0, \quad (\text{A.5})$$

where the field strength renormalization Z is dimensionless, and then can depend on Λ and μ only through the ratio Λ/μ . Then substituting (A.5) in Eq. (2.109-a) we obtain:

$$\gamma = -\frac{1}{2} \mu \frac{d}{d\mu} \ln Z. \quad (\text{A.6})$$

The field strength renormalization Z can be computed diagrammatically from the external momentum p dependent part of the Higgs self-energy $\Sigma(p^2)$ as:

$$Z = 1 + \frac{\partial}{\partial p^2} \Sigma(p^2) \Big|_{p^2=m_H^2}, \quad (\text{A.7})$$

giving for the anomalous dimension:

$$\gamma = \frac{1}{16\pi^2} \left(\frac{3}{4} (3g^2 + g'^2) - 3y_t^2 \right). \quad (\text{A.8})$$

Substituting into Eqs. (A.3) and (A.4) then yields

$$\beta = \frac{1}{16\pi^2} \left(\lambda (24\lambda + 12y_t^2 - 9g^2 - 3g'^2) + \frac{3}{4}g^4 + \frac{3}{8}(g^2 + g'^2)^2 - 6y_t^4 \right) \quad (\text{A.9})$$

$$\gamma_m = \frac{1}{16\pi^2} \left(12\lambda - \frac{3}{2}(3g^2 + g'^2) + 6y_t^2 \right). \quad (\text{A.10})$$

It should be noted that the negative terms in Eq. (A.9), in particular the quartic Yukawa term y_t^4 , will have a reducing effect on the value of the coupling λ and could be responsible for causing any vacuum instability.

Finally, from the self-energy of the W and Z bosons, of the gluon boson and of the quark top, we can compute diagrammatically the respective field strength renormalizations Z_{g_i} and the coupling counterterms to relate the bare g_i to the renormalized ones, and then use Eq. (2.108) to compute the beta functions:

$$\beta_g = -\frac{19}{6} \frac{g^3}{16\pi^2} \quad \beta_{g'} = \frac{141}{6} \frac{g'^3}{16\pi^2} \quad \beta_{g_s} = -\frac{7g_s^3}{16\pi^2} \quad (\text{A.11})$$

$$\beta_{y_t} = \frac{1}{16\pi^2} \left(\frac{9}{2}y_t^3 - \left(8g_s^2 + \frac{9}{2}g^2 + \frac{17}{12}g'^2 \right) y_t \right). \quad (\text{A.12})$$

In conclusion, using Eqs. (A.9), (A.11) and (A.12), we can solve the differential equations in (2.117-a) with boundary conditions given by the value of the coupling g_i measured, for instance, at the EW scale v . The solution of this set of differential equations are the running coupling constant of the Standard Model. In particular, in Fig. 2.1 we have the Higgs scalar running coupling constant $\lambda(\mu)$.

Appendix B

Potential with a single minimum: computation of the functional determinant

We consider a potential with a single minimum as those shown in the left panel of Fig. B.1, in which the minimum is located in $q = q_0$ and for which we suppose $V(q_0) = 0$.

We want to compute the probability amplitude:

$$\langle q_0 | e^{-\frac{1}{\hbar} \hat{H}T} | q_0 \rangle = \mathcal{N} \int \mathcal{D}q(\tau) \exp \left\{ -\frac{1}{\hbar} S_E[q(\tau)] \right\}. \quad (\text{B.1})$$

The solution to the euclidean equation of motion that satisfies to the boundary conditions $q(-\frac{T}{2}) = q_0 = q(\frac{T}{2})$ is given by the constant solution $\bar{q}(\tau) = q_0$, shown in the right panel of Fig. B.1.

In this case, we have that $S_E[q_0] = 0$: in fact $V(q_0) = 0$ by hypothesis, while $\dot{q}_0 = 0$ as q_0 is a constant. Then, using Eq. (3.26), we obtain

$$\langle q_0 | e^{-\frac{1}{\hbar} \hat{H}T} | q_0 \rangle = \mathcal{N} [\det S''_E(q_0)]^{-\frac{1}{2}} = \mathcal{N} \prod_n \lambda_n^{-\frac{1}{2}}. \quad (\text{B.2})$$

As a consequence, we have to compute the eigenvalues λ_n of the operator $S''_E(q_0)$. Defining $\omega^2 = \frac{V''(q_0)}{m}$ and using Eqs. (3.17) and (3.20), to obtain λ_n we have to solve the eigenvalues equation:

$$\left[-m \frac{d^2}{d\tau^2} + m\omega^2 \right] \psi_n = \lambda_n \psi_n \quad (\text{B.3})$$

whose boundary conditions $\psi_n(\pm T/2) = 0$ are given by Eq. (3.22). The solution to this equation is:

$$\psi_n(\tau) = A_n \cos \left(\sqrt{\frac{\lambda_n}{m} - \omega^2} \tau \right).$$

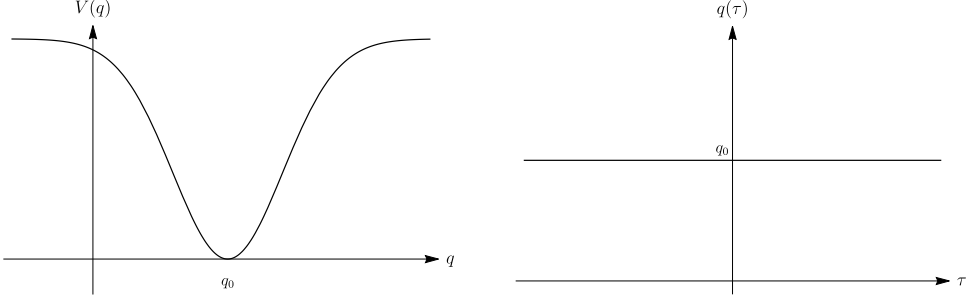


Figure B.1: *Left panel:* potential with a second minimum in q_0 . *Right panel:* trivial solution $q(\tau) = q_0$.

Imposing the boundary conditions, we obtain the eigenvalues λ_n :

$$\cos \left(\sqrt{\frac{\lambda_n}{m} - \omega^2} \frac{T}{2} \right) = 0 \quad \Rightarrow \quad \sqrt{\frac{\lambda_n}{m} - \omega^2} \frac{T}{2} = n \frac{\pi}{2} \quad \Rightarrow$$

$$\lambda_n = m \left[\omega^2 + \left(\frac{n\pi}{T} \right)^2 \right]. \quad (\text{B.4})$$

Consequently, Eq. (B.2) becomes:

$$\begin{aligned} \mathcal{N} \left[\det \left(-m \frac{d^2}{dt^2} + m\omega^2 \right) \right]^{-1/2} &= \mathcal{N} \prod_{n=1}^{\infty} \frac{1}{\sqrt{m \left[\omega^2 + \left(\frac{n\pi}{T} \right)^2 \right]}} \\ &= \mathcal{N} \prod_{n=1}^{\infty} \frac{1}{\sqrt{m \left(\frac{n\pi}{T} \right)^2}} \prod_{n=1}^{\infty} \frac{1}{\sqrt{1 + \left(\frac{\omega T}{n\pi} \right)^2}}. \end{aligned}$$

The first product is independent from ω , so that we denote with \mathcal{N}' the entire prefactor independent from ω

$$\mathcal{N} \prod_{n=1}^{\infty} \frac{1}{\sqrt{m \left(\frac{n\pi}{T} \right)^2}} \equiv \mathcal{N}'.$$

Instead, to compute the second product we use (see the demonstration behind):

$$\prod_{n=1}^{\infty} \left(1 + \frac{y^2}{n^2} \right) = \frac{\sinh \pi y}{\pi y}. \quad (\text{B.5})$$

Using Eq. (B.5), we have:

$$\prod_{n=1}^{\infty} \frac{1}{\sqrt{1 + \left(\frac{\omega T}{n\pi} \right)^2}} = \left\{ \prod_{n=1}^{\infty} \left[1 + \left(\frac{\omega T}{n\pi} \right)^2 \right] \right\}^{-1/2} = \left(\frac{\sinh \omega T}{\omega T} \right)^{-1/2}.$$

In conclusion, we find that the functional determinant is given by:

$$\mathcal{N} \left[\det \left(-m \frac{d^2}{dt^2} + m\omega^2 \right) \right]^{-1/2} = \mathcal{N}' \left(\frac{\sinh \omega T}{\omega T} \right)^{-1/2}.$$

In the limit $\omega \rightarrow 0$, this transition amplitude have to reduce to the corresponding amplitude for the euclidean free particle

$$K(q_0, q_0; -T/2, T/2) = \sqrt{\frac{m}{2\pi\hbar T}} e^{-\frac{1}{\hbar}S_{cl}}$$

where S_{cl} is the classical euclidean action of the free particle: however, once again, the action vanish, $S_{cl} = 0$, since the solution $q(\tau) = q_0$ is a constant. Then, since in the limit $\omega \rightarrow 0$, we have that $(\frac{\sinh \omega T}{\omega T})$ tends to 1:

$$\mathcal{N}' = \sqrt{\frac{m}{2\pi\hbar T}}.$$

In conclusion:

$$\mathcal{N} \left[\det \left(-m \frac{d^2}{dt^2} + m\omega^2 \right) \right]^{-1/2} = \left(\frac{m\omega}{2\pi\hbar} \right)^{1/2} \frac{1}{\sqrt{\sinh \omega T}}. \quad (\text{B.6})$$

Now, in the limit $\omega T \gg 1$ we have:

$$(\sinh \omega T)^{-1/2} = \left(\frac{e^{\omega T} - e^{-\omega T}}{2} \right)^{-1/2} \rightarrow \sqrt{2} e^{-\frac{1}{2}\omega T},$$

and then we obtain the result presented in Eq. (3.28)

$$\mathcal{N} \left[\det \left(-m \frac{d^2}{dt^2} + m\omega^2 \right) \right]^{-1/2} = \left(\frac{m\omega}{\pi\hbar} \right)^{1/2} e^{-\frac{1}{2}\omega T}.$$

Product

To demonstrate Eq. (B.5), we start from the Fourier expansion of the function $\cos(zx)$ in the variable $x \in (-\pi, \pi)$:

$$\cos(zx) = \frac{a_0}{2} + \sum_{k=1}^{\infty} a_k \cos(kx)$$

where the Fourier coefficient a_k are given by:

$$a_0 = \int_0^\pi \cos(zx) dx = \frac{2 \sin(\pi z)}{\pi z} \quad a_k = \frac{2}{\pi} \int_0^\pi \cos(zx) \cos(kx) dx.$$

Since $\cos(zx)$ is a function even in x , it is clear that in the Fourier expansion the terms with $\sin(kx)$ are not present, as the corresponding coefficient vanishes. At this point, using the sum formula of the cosine we have

$$\cos(zx) \cos(kx) = \frac{1}{2} [\cos((z+k)x) + \cos((z-k)x)].$$

Then we can compute explicitly the Fourier coefficients a_k :

$$a_k = \frac{2}{\pi} \int_0^\pi \cos(zx) \cos(kx) dx = \frac{1}{\pi} \left[\frac{\sin((z+k)x)}{z+k} + \frac{\sin((z-k)x)}{z-k} \right]_0^\pi =$$

$$= (-1)^k \frac{2z \sin(\pi z)}{\pi(z^2 - k^2)}.$$

As a consequence, for $-\pi < z < \pi$, we can expand $\cos(zx)$ as:

$$\cos(zx) = \frac{2z \sin(\pi z)}{\pi} \left[\frac{1}{2z^2} + \sum_{k=1}^{\infty} (-1)^k \frac{\cos(kx)}{z^2 - k^2} \right].$$

Setting $x = \pi$, we have $(-1)^k \cos(k\pi) = (-1)^k (-1)^k = (-1)^{2k} = 1$. Moreover, we have that:

$$\frac{2z}{z^2 - k^2} = \frac{1}{z - k} + \frac{1}{z + k}.$$

In conclusion, we can write the expansion for the function $\pi \cot(\pi z)$:

$$\pi \cot(\pi z) = \frac{1}{z} + \sum_{k=1}^{\infty} \left(\frac{1}{z - k} + \frac{1}{z + k} \right).$$

Such an expansion puts in evidence as the function $\pi \cot \pi z$ has simple poles of the first order for $z = 0, \pm 1, \pm 2, \dots$ with all the residues equal to 1. Now, we compute the following derivative:

$$\frac{d}{dz} \ln \left(\frac{\sin \pi z}{\pi z} \right) = \pi \cot \pi z - \frac{1}{z} = \sum_{n=1}^{\infty} \left(\frac{1}{z - n} + \frac{1}{z + n} \right),$$

where in the last step we used the expansion of $\pi \cot \pi z$ that we have just obtained. At this point, integrating terms by terms in the interval $0 \leq z \leq 1$ (chosen in such a way that the series is uniformly convergent), we obtain:

$$\begin{aligned} \ln \left(\frac{\sin \pi z}{\pi z} \right) &= \sum_{n=1}^{\infty} \left[\ln \left(\frac{z - n}{-n} \right) + \ln \left(\frac{z + n}{n} \right) \right] \\ &= \sum_{n=1}^{\infty} \ln \left(1 - \frac{z^2}{n^2} \right) \quad \Rightarrow \\ \frac{\sin \pi z}{\pi z} &= \prod_{n=1}^{\infty} \left(1 - \frac{z^2}{n^2} \right). \end{aligned}$$

Finally, setting $z = iy$ we obtain Eq. (B.5).

Appendix C

Mathematical appendix to the instanton computation

Computation of the instanton action S_I

Let us compute the action of the instanton in the double-well using Eq. (3.38):

$$S_I = \int_{-\frac{T}{2}}^{+\frac{T}{2}} m\dot{q}_I^2 d\tau = \int_{-\frac{T}{2}}^{+\frac{T}{2}} 2mV(q_I) d\tau .$$

To compute $V(q_I)$ we use Eqs. (3.30) and (3.34):

$$V(q_I) = \lambda(q_I^2 - a^2)^2 = \lambda a^4 \left\{ \tanh^2 \left[\frac{\omega}{2}(\tau - \tau_c) \right] - 1 \right\}^2 .$$

being $\omega^2 = 8\lambda a^2/m \Rightarrow a^4 = m^2\omega^4/64\lambda^2$. Moreover, denoting $u = \frac{\omega}{2}(\tau - \tau_c)$ we have $du = \frac{\omega}{2} d\tau$. Then, in the limit $T \rightarrow \pm\infty$

$$S_I = \frac{4m\lambda}{\omega} \frac{m^2\omega^4}{64\lambda^2} \int_{-\infty}^{+\infty} du (\tanh^2 u - 1)^2 .$$

We use the change of variables $t = \tanh u$, so that:

$$dt = \frac{d}{du} \frac{\sinh u}{\cosh u} du = \frac{\cosh^2 u - \sinh^2 u}{\cosh^2 u} du = (1 - \tanh^2 u) du .$$

Then, the integral in S_I becomes

$$S_I = \frac{m^3\omega^3}{16\lambda} \int_{-1}^1 dt (1 - t^2) = \frac{4}{3} \frac{m^3\omega^3}{16\lambda} \quad \Rightarrow \quad S_I = \frac{m^3\omega^3}{12\lambda} . \quad (\text{C.1})$$

This result put in evidence as the action computed in the instanton solution is translation invariant, since it does not depend of the centroid τ_c .

Computation of K

To compute K :

$$K = \left(\frac{S_I}{2\pi\hbar m} \right)^{1/2} \left[\frac{\det' S''(q_I)}{\det S''(a)} \right]^{-\frac{1}{2}} \quad (\text{C.2})$$

it is necessary to solve the eigenvalues equation for the operator $S''(q_I)$, where $\omega^2 = 8\lambda a^2/m$, while S_I is given by Eq. (C.1). The eigenvalue equation has the form:

$$-\frac{d^2 x_n(\tau)}{d\tau^n} + \frac{1}{m} V''(q_I(\tau)) x_n(\tau) = \epsilon_n x_n(\tau), \quad (\text{C.3})$$

where using Eqs. (3.30) and (3.34) it is easy to see

$$V''(q_I) = m\omega^2 \left(1 - \frac{3}{2 \cosh^2 \left[\frac{\omega}{2}(\tau - \tau_c) \right]} \right). \quad (\text{C.4})$$

It is clear that Eq. (C.3) is a Schroedinger equation with a potential $U(\tau) = \frac{1}{m} V''(q(\tau))$. From the form of this potential it is clear that there are discrete as well as continuous spectra.

The explicit form of the eigenvalues equation is:

$$\partial_\tau^2 x_n - (\omega^2 - \epsilon_n) x_n + \frac{3\omega^2}{2 \cosh^2 u} x_n = 0 \quad (\text{C.5})$$

where $u = \frac{\omega}{2}(\tau - \tau_c)$. To simplify this equation we make a change of variable:

$$\xi = \frac{q_I(\tau)}{a} = \tanh u.$$

Then:

$$\frac{1}{\cosh^2 u} = 1 - \xi^2.$$

$$\frac{d\xi}{d\tau} = \frac{\omega}{2}(1 - \xi^2) \quad \Rightarrow \quad \partial_\tau = \frac{\omega}{2}(1 - \xi^2)\partial_\xi,$$

In terms of ξ the equation becomes:

$$\frac{d}{d\xi}(1 - \xi^2) \frac{d}{d\xi} x_n + \left(a + \frac{b}{1 - \xi^2} \right) x_n = 0, \quad (\text{C.6})$$

where

$$a = 6 \quad b = \frac{4(\epsilon_n - \omega^2)}{\omega^2}.$$

Let be c a constant and set $x_n = (1 - \xi^2)^c \chi$ (c will be chosen appropriately later). Then, after a simple algebra, we get:

$$(1 - \xi^2) \frac{d^2 \chi}{d\xi^2} - (4c + 2)\xi \frac{d\chi}{d\xi} + \left(a - 2c - 4c^2 + \frac{b + 4c^2}{1 - \xi^2} \right) \chi = 0. \quad (\text{C.7})$$

We make a further change of variable:

$$z = \frac{1}{2}(1 - \xi) \quad (\text{C.8})$$

$$1 - z = \frac{1}{2}(1 + \xi) \quad 1 - \xi^2 = 4z(1 - z).$$

There is a correspondence in the asymptotic values of the variables:

$$\begin{aligned} \tau \rightarrow \infty &\Leftrightarrow \xi \rightarrow 1 \Leftrightarrow z \rightarrow 0 \\ \tau \rightarrow -\infty &\Leftrightarrow \xi \rightarrow -1 \Leftrightarrow z \rightarrow 1. \end{aligned}$$

Then the equation further simplifies to

$$z(1 - z) \frac{d^2\xi}{dz^2} + (2c + 1 - (4c + 2)z) \frac{d\xi}{dz} + \left(a - 2c - 4c^2 + \frac{b + 4c^2}{4z(1 - z)} \right) \xi = 0.$$

Now if we choose c such that $b + 4c^2 = 0$, we obtain the familiar hypergeometric equation

$$z(1 - z) \frac{d^2\chi}{dz^2} + (\gamma - (\alpha + \beta + 1)z) \frac{d\chi}{dz} - \alpha\beta\chi = 0 \quad (\text{C.9})$$

with

$$\gamma = 2c + 1 \quad \alpha + \beta = 4c + 1 \quad \alpha\beta = 4c^2 + 2c - a.$$

In our case with $a = 6$, these parameters simplify to:

$$\alpha = 2c - 2 \quad \beta = 2c + 3 \quad \gamma = 2c + 1. \quad (\text{C.10})$$

The solution to Eq. (C.9) is the hypergeometric function $F(\alpha, \beta, \gamma; z)$, which near $z = 0$ has the expansion:

$$F(\alpha, \beta, \gamma; z) = 1 + \frac{\alpha\beta}{\gamma} \frac{z}{1!} + \frac{\alpha(\alpha+1)\beta(\beta+1)}{\gamma(\gamma+1)} \frac{z^2}{2!} + \dots. \quad (\text{C.11})$$

- Continuous spectrum

For $\epsilon \geq \omega^2$, if we do not impose any asymptotic conditions, the spectrum is continuous, and it can be parametrized by the real positive momentum

$$p \equiv \sqrt{\epsilon - \omega^2} \quad \Leftrightarrow \quad k \equiv \frac{p}{\omega}. \quad (\text{C.12})$$

Since there is no barrier for $\epsilon > \omega^2$, we expect that the particle does not get reflected at all as it travels from $\tau = -\infty$ to $\tau = \infty$. This means that all the scattering dynamics is contained in the knowledge of the phase shift δ_p defined here as (setting $\tau_c = 0$):

$$\begin{aligned} x_p(\tau \rightarrow \infty) &= e^{ip\tau} \\ x_p(\tau \rightarrow -\infty) &= e^{ip\tau + i\delta_p}. \end{aligned}$$

As it will be shown, to compute the contribution to the determinant, the knowledge of δ_p will be enough.

Now for $\epsilon > \omega^2$, we have

$$\begin{aligned} b = \frac{4(\epsilon_n - \omega^2)}{\omega^2} \quad b + 4c^2 = 0 \quad \Rightarrow \\ b = -4c^2 = 4k^2 \quad \Rightarrow \quad c^2 = -k^2. \end{aligned}$$

The solution which has asymptotic behaviour $e^{ip\tau}$ as $\tau \rightarrow \infty$ (i.e. $z \rightarrow 0$) is, choosing $c = -ik$

$$x = (1 - \xi^2)^{-ik} F(\alpha, \beta, \gamma; z). \quad (\text{C.13})$$

In fact, using $u = \frac{1}{2}\omega\tau$ and hence $2uk = \omega\tau k = p\tau$, in the limit $\tau \rightarrow \infty$ we have:

$$(1 - \xi^2)^{-ik} = (\cosh^2 u)^{ik} \simeq (4e^{-2u})^{-ik} = 4^{-ik} e^{ip\tau}. \quad (\text{C.14})$$

To find the phase shift, we must analytically continue this solution to the one valid around $z = 1$, i.e. for $\tau \rightarrow -\infty$. In this limit, for the front factor we have:

$$(1 - \xi^2)^{-ik} \simeq (4e^{2u})^{-ik} = 4^{-ik} e^{-ip\tau}. \quad (\text{C.15})$$

Thus, this factor alone represents the reflected wave. On the other hand, the hypergeometric function must be rewritten as:

$$F(\alpha, \beta, \gamma; z) = F_1(1 - z) + F_2(1 - z) \quad (\text{C.16})$$

where

$$F_1(1 - z) \equiv \frac{\Gamma(\gamma)\Gamma(\gamma - \alpha - \beta)}{\Gamma(\gamma - \alpha)\Gamma(\gamma - \beta)} F(\alpha, \beta, \alpha + \beta - \gamma + 1; 1 - z) \quad (\text{C.17})$$

$$\begin{aligned} F_2(1 - z) \equiv & \frac{\Gamma(\gamma)\Gamma(\alpha + \beta - \gamma)}{\Gamma(\alpha)\Gamma(\beta)} (1 - z)^{\gamma - \alpha - \beta} \\ & \times F(\gamma - \alpha, \gamma - \beta, \gamma + 1 - \alpha - \beta; 1 - z) \end{aligned} \quad (\text{C.18})$$

with

$$\alpha = -2ik - 2 \quad \beta = -2ik + 3 \quad \gamma = -2ik + 1. \quad (\text{C.19})$$

It is easy to see that $F_1(1 - z)$ vanishes due to the denominator factor $\Gamma(\gamma - \beta) = \Gamma(-2)$ which diverges. This shows that indeed there is no reflected wave. The remaining part $(1 - \xi^2)^{-ik} F_2(1 - z)$ becomes

$$\begin{aligned} (1 - \xi^2)^{-ik} F_2(1 - z) &= \frac{\Gamma(-2ik + 1)\Gamma(-2ik)}{\Gamma(-2ik + 3)\Gamma(-2ik - 2)} (1 - z)^{2ik} \\ &\times (1 - \xi^2)^{-ik} (1 + \mathcal{O}(1 - z)) \\ &= \frac{(1 + 2ik)(1 + ik)}{(1 - 2ik)(1 - ik)} (1 - \xi^2)^{ik} 4^{-2ik} \\ &\times (1 + \mathcal{O}(1 - z)) \\ &\simeq \frac{(1 + 2ik)(1 + ik)}{(1 - 2ik)(1 - ik)} 4^{-ik} e^{ip\tau}. \end{aligned} \quad (\text{C.20})$$

Comparing with (C.14), we can read off the phase shift as

$$e^{i\delta_p} = \frac{(1 + 2ik)(1 + ik)}{(1 - 2ik)(1 - ik)}. \quad (\text{C.21})$$

- Discretization of the continuous spectrum

To compute the contribution to the determinant, we must regularize the continuous spectrum. The simplest way is to put the system in a box of interval $-T/2 < \tau < T/2$. As boundary conditions we take

$$x(-T/2) = x(T/2) = 0.$$

Because of this boundary conditions, there will be a reflected wave (which vanishes at $T \rightarrow \infty$) and we must consider the general solution. Since $x_p(-\tau)$ is obviously a solution independent of $x_p(\tau)$, such a solution is:

$$x = Ax_p(\tau) + Bx_p(-\tau). \quad (\text{C.22})$$

Applying the boundary conditions above, we get

$$\begin{aligned} Ax_p(T/2) + Bx_p(-T/2) &= 0 \\ Ax_p(-T/2) + Bx_p(T/2) &= 0. \end{aligned}$$

Non-trivial solution exists if and only if $A = \pm B$. this means

$$\frac{x_p(T/2)}{x_p(-T/2)} = \pm 1. \quad (\text{C.23})$$

Using the asymptotic form of the solution, the left hand side become $e^{ipT-i\delta_p} = \pm 1$. Hence the solutions are given by:

$$\tilde{p}_n = \frac{n\pi + \delta_p}{T}, \quad n = 0, 1, 2, \dots \quad (\text{C.24})$$

where we denote by \tilde{p}_n the (by definition positive) parameter p satisfying the above condition.

We now compute the contribution of these modes to the ratio of the determinant. We recall that for the harmonic oscillator case, the spectrum is

$$p_n = \frac{n\pi}{T}.$$

It is clear that in the limit $T \rightarrow \infty$, contribution from a finite number of eigenvalues with $n \sim \mathcal{O}(1)$ cancel against the contribution from the harmonic oscillator states as they both become ω^2 . Thus, the ratio to be computed can be taken as (by shifting a few levels and recalling $p = \sqrt{\epsilon - \omega^2} \Rightarrow \epsilon = \omega^2 + p^2$):

$$R \equiv \prod_{n=1}^{\infty} \frac{\omega^2 + \tilde{p}_n^2}{\omega^2 + p_n^2}. \quad (\text{C.25})$$

As $T \rightarrow \infty$, the difference $\bar{\Delta}p_n \equiv \tilde{p}_n - p_n = \delta_p/T \rightarrow 0$. Thus, we can expand in powers of $\bar{\Delta}p_n$ to the first order. Hence

$$R = \exp \left(\sum_{n=1}^{\infty} \ln \frac{\omega^2 + \tilde{p}_n^2}{\omega^2 + p_n^2} \right) \simeq \exp \left(\sum_{n=1}^{\infty} \frac{2p_n \bar{\Delta}p_n}{\omega^2 + p_n^2} \right). \quad (\text{C.26})$$

Moreover, the interval π/T goes to zero and we may convert Eq. (C.26) into the integral by noting

$$\bar{\Delta}p_n = \frac{\delta_p}{T} = \frac{\delta_p \pi}{\pi T} = \frac{\delta_p}{\pi} (p_{n+1} - p_n) = \frac{\delta_p}{\pi} \Delta p_n.$$

So we get

$$\begin{aligned} R &\simeq \exp \left(\frac{1}{\pi} \int_0^\infty \delta_p \frac{2p}{\omega^2 + p^2} dp \right) \\ &= \exp \left(\frac{1}{\pi} \int_0^\infty \delta_p \frac{d}{dp} \ln \left(1 + \frac{p^2}{\omega^2} \right) dp \right) \\ &= \exp \left(-\frac{1}{\pi} \int_0^\infty \delta_p \frac{d\delta_k}{dk} \ln (1 + k^2) dk \right) \end{aligned} \quad (\text{C.27})$$

where in the last step we used we integrate by parts. From Eq. (C.21) for the phase shift, we easily get

$$\frac{d\delta_k}{dk} = \frac{2}{1 + k^2} + \frac{4}{1 + 4k^2}. \quad (\text{C.28})$$

Now we use the formula

$$\int_0^\infty \frac{\ln(1 + k^2)}{1 + a^2 k^2} dk = \frac{\pi}{a} \ln \left(1 + \frac{1}{a} \right), \quad (\text{C.29})$$

to easily get:

$$R = e^{-\ln 9} = \frac{1}{9}. \quad (\text{C.30})$$

Remarkably, we have been able to compute the ratio of the determinant exactly.

- Discrete spectrum

Now we consider the discrete part of the spectrum in the case $\omega^2 - \epsilon_n > 0$. Thus, we should set

$$c = k \equiv \frac{\sqrt{\omega^2 - \epsilon_n}}{\omega} > 0. \quad (\text{C.31})$$

The solution to the Schroedinger equation which is finite near $z = 0$ (i.e. $\tau \rightarrow \infty$) is

$$x_n = (1 - \xi^2)^k F(\alpha, \beta, \gamma; z) \quad (\text{C.32})$$

where $F(\alpha, \beta, \gamma; z)$ is given by (C.11), with

$$\alpha = 2k - 2 \quad \beta = 2k + 3 \quad \gamma = 2k + 1. \quad (\text{C.33})$$

In order for this equation to be finite at $z = 1$ (i.e. as $\tau \rightarrow -\infty$), the series must terminate at finite terms. Since $\beta, \gamma, k > 0$ and $\alpha = 2k - 2 > -2$, it can occur only when

$$\begin{aligned} \alpha = 2k - 2 &= -n, \quad n = 0, 1 \quad \Rightarrow \\ k &= 2 \quad k = \frac{1}{2}. \end{aligned} \quad (\text{C.34})$$

Recalling the definition of k , this means that there are two discrete energy levels (bound states):

$$\epsilon_0 = 0 \quad \epsilon_1 = \frac{3}{4}\omega^2. \quad (\text{C.35})$$

The corresponding wave functions can be obtained using the form of the (truncated) hypergeometric function:

$$x_0(\tau) \sim \frac{1}{\cosh^2 \left[\frac{\omega}{2}(\tau - \tau_c) \right]} \xrightarrow{\tau \rightarrow \infty} e^{-\omega(\tau - \tau_c)} \quad (\text{C.36})$$

$$x_1(\tau) \sim \frac{\sinh \left[\frac{\omega}{2}(\tau - \tau_c) \right]}{\cosh^2 \left[\frac{\omega}{2}(\tau - \tau_c) \right]} \xrightarrow{\tau \rightarrow \infty} e^{-\frac{\omega}{2}(\tau - \tau_c)} \quad (\text{C.37})$$

It is easy to see that $x_0(\tau)$, i.e. the eigenfunction corresponding to the zero eigenvalue ϵ_0 , is proportional to $dq_I(\tau)/d\tau$. Then, we have found the zero mode that we have encountered and treated in Chapter 3.

Derrick theorem

In the computation of the exponent B of the vacuum decay amplitude we have used the *Derrick theorem* [34, 39]: we consider a vector of scalar fields in $D+1$ dimensions $\phi = (\phi_a)$, whose dynamics is described by the scalar lagrangian

$$\mathcal{L} = \frac{1}{2}\partial_\mu\phi\partial^\mu\phi - U(\phi) = \frac{1}{2}\partial_\mu\phi_a\partial^\mu\phi_a - U(\phi_a), \quad (\text{C.38})$$

where U is a non-negative function that vanishes in the ground states of the theory. The theorem establishes that for $D \geq 2$ the unique non-singular, static and finite energy solutions are the ground states.

To demonstrate the theorem, we define the two functionals

$$I_K = \frac{1}{2} \int d^D x (\nabla\phi_a)^2 \quad I_V = \int d^D x U(\phi_a). \quad (\text{C.39})$$

The two functionals I_K and I_V are non-negative and vanish simultaneously only on the ground states. We consider a solution of the equations of motion $\phi_S(\mathbf{x})$: since this function is a stationary point for the lagrangian in all the possible configurations space, then it will be *a fortiori* a stationary point for all the configuration subspaces to which it belongs. As a consequence, we define a set of functions through a parameter that defines a scaling of the lengths:

$$\phi_S(\mathbf{x}; \lambda) = \phi_S(\lambda\mathbf{x}) \quad \lambda > 0. \quad (\text{C.40})$$

The energy functional, in general, is given by the sum of the functionals in Eq. (C.39): computed in the solutions of Eq. (C.40), after the change of variables due to the scaling, we obtain

$$E_S(\lambda) = E_S[\phi_S(\lambda\mathbf{x})] = \lambda^{2-D} I_K + \lambda^{-D} I_V. \quad (\text{C.41})$$

Since $\phi_S(\mathbf{x})$ is a solution, the function $E_S(\lambda)$ has to be stationary for $\lambda = 1$: differentiating respect to the parameter λ we obtain

$$(D - 2)I_K + DI_V = 0. \quad (\text{C.42})$$

If $D > 2$, since $I_K \geq 0$ and $I_V \geq 0$, Eq. (C.42) can be satisfied only by $I_K = 0$ and $I_V = 0$. This implies that $\phi_S(\mathbf{x}) = \text{const}$, that is ϕ_S is a ground state. Instead, if $D = 2$ Eq. (C.42) implies that $I_V = 0$, so that the static solutions given by $\delta E_S[\phi]/\delta\phi = 0$ can be obtained also from $\delta I_K[\phi]/\delta\phi = 0$. The resulting equation is

$$\nabla^2\phi = 0. \quad (\text{C.43})$$

Then, an harmonic function in all the space \mathbb{R}^D is necessarily a constant function also in this case, $\phi_S(\mathbf{x}) = \text{const}$. This complete the demonstration of the theorem.

Appendix D

Numerical computation of the bounce solution

The search for the bounce solution is a boundary-value problem specified by the values of $\varphi'(0)$ and $\varphi(\infty)$. This can be turned into an initial-value problem using the shooting method, whereby $\varphi(\infty)$ is replaced by $\varphi(0)$, and the appropriate value for the latter quantity is found iteratively, solving Eq. (4.12) (or its curved-space generalization) for different initial values until the desired $\varphi(\infty)$ is obtained.

As will be clear below, knowledge of the asymptotic behavior of $\varphi(x)$ for $x \rightarrow 0$ and $x \rightarrow \infty$ is a crucial ingredient for the efficiency of the shooting algorithm. To find the expected behavior of $\varphi(x)$ in the relevant regimes, we begin by expanding $\varphi(x)$ around $x = 0$:

$$\varphi(x) = B_0 + B_2 x^2 + B_3 x^3 + \dots \quad (\text{D.1})$$

where the linear term is missing due to the condition $\varphi'(0) = 0$. Inserting this expansion in (4.12), with $U(\varphi)$ given by (4.14) we find that the coefficients of the odd-power terms vanish, $B_{2n+1} = 0$, while all the coefficients of the even-power terms B_{2n} are functions of the first coefficient B_0 (called B from now on). Truncating the expansion to the x^2 term:

$$\varphi(x) = B + \frac{B^3}{8} \left(\lambda_* + \frac{\alpha}{2} \ln B + \alpha \ln^2 B + \beta \ln^3 B + \beta \ln^4 B \right) x^2 + \dots \quad (\text{D.2})$$

The coefficient of x^2 turns out to be negative, so near the origin the bounce profile behaves as an upside-down parabola.

As for the behavior of $\varphi(x)$ for $x \rightarrow \infty$, we note that $U(\varphi) \rightarrow 0$ for $x \rightarrow \infty$, and $\varphi(x) \rightarrow 0$ for $x \rightarrow \infty$. Asymptotically Eq.(4.12) and the corresponding solution are then:

$$\varphi''(x) + \frac{3}{x} \varphi'(x) = 0 \quad \Rightarrow \quad \varphi(x) = \frac{A}{x^2}, \quad (\text{D.3})$$

where A is one of the integration constants, while the second additive integration constant vanishes due to the condition $\varphi(\infty) = 0$. In other words, for the bounce solution $x^2 \varphi(x)$ has to reach a *plateau* for $x \rightarrow \infty$.

Numerically, we have implemented a fully adaptive algorithm designed to: (i) pick an initial guess ($\varphi(0) = B$, $\varphi'(0) = 0$), (ii) integrate Eq. (4.12) numerically while monitoring the behavior of $\varphi(x)$, and (iii) iteratively restart the procedure with a suitably corrected B until the condition $\varphi(\infty) = 0$ is satisfied up to a prescribed tolerance. In practice, the numerical integration is carried out in the range $[x_{\min}, x_{\max}]$, where we have chosen $x_{\min} = 10^{-10}$ and $x_{\max} = 10^9$, so that the initial conditions for φ and φ' are given at $x = x_{\min}$ using Eq. (D.2). With this boundary conditions, we find a class of solutions $\varphi_B(x)$, parametrized by B . Following the *overshoot-undershoot argument* of Coleman [38], we want to tune the parameter B until we converge to the solution which reaches a plateau for $x \rightarrow \infty$.

We found that the characterization of the final state is of crucial importance to the effectiveness of the search. In particular, introducing the reference point $x_{\text{ref}} = x_{\max} - 10^3$ and a tolerance $\epsilon = 10^{-10}$, we found that the following three criteria are sufficient to lead the algorithm to the bounce solution in all cases (denoting $\tilde{\varphi}(x) = x^2 \varphi(x)$):

1. If $\tilde{\varphi}(x_{\max}) - \tilde{\varphi}(x_{\text{ref}}) > \epsilon$, the scalar field has reversed its direction before reaching $\varphi = 0$, and is returning towards its initial position. The initial guess for $\varphi(x_{\min})$ was therefore too low, and B is correspondingly increased by a quantity δ .
2. If $\tilde{\varphi}(x_{\max}) - \tilde{\varphi}(x_{\text{ref}}) < -\epsilon$, the scalar field is overshooting the top of the hill. The initial guess for $\varphi(x_{\min})$ was therefore too high, and B is correspondingly decreased by a quantity δ .
3. If $|\tilde{\varphi}(x_{\max}) - \tilde{\varphi}(x_{\text{ref}})| < \epsilon$, we consider that the plateau has been reached, i.e. that the bounce solution is found within the required precision.

Furthermore, the algorithm stores a state consisting of both B and its value for the two preceding iterations. It is therefore possible to detect oscillations in B and bisect (or otherwise decrease) δ . We found that decreasing δ to $\delta/10$ each time B changes trend leads to a particularly efficient search, that converges exponentially to the solution, as will be illustrated below.

The inclusion of gravity does not modify our algorithm, as we found that, for $x \rightarrow \infty$, the areal radius goes as $a \sim x + c$ (see Chapter 4), i.e. the curvature tends asymptotically to zero (the value of the constant c is given by $a(x) - x$ when the plateau is reached).

For this reason, the criteria for tuning the initial value of φ , introduced in the flat case, can also be used on a curved spacetime. Again, we implemented the boundary condition in x_{\min} :

$$\varphi(x_{\min}) = B \quad \varphi'(x_{\min}) = 0 \quad a(x_{\min}) = \epsilon' \quad a'(x_{\min}) = 1, \quad (\text{D.4})$$

with $\epsilon' \ll 1$ (clearly we cannot use $a(x_{\min}) = 0$ due to the factor a^{-1} in (4.17-a)).

After solving the equations, the size \mathcal{R} of the bounce solution is obtained and we can compute the integral in Eq. (4.19).

We go now back to the flat spacetime case and include the NP terms of (4.21), thus obtaining the (dimensionless) potential (4.22). The bonus for our analysis is that this potential does not modify the asymptotic behavior of the bounce solution $\varphi_b(x)$ for $x \rightarrow \infty$, as in this limit we still have $U(\varphi(x)) \rightarrow 0$. Therefore the inclusion of NP does not lead to any substantial change in our numerical method. The only modification with respect to the flat spacetime case concerns the expansion of the bounce solution around the origin $x = 0$. In the flat case, by considering the integration range $[x_{\min}, x_{\max}]$, we found that the initial values for solving Eq. (4.12) with the shooting method are obtained once we take the expansion (D.2) of $\varphi(x)$ and its first derivative at x_{\min} . Repeating the same analysis for the potential (4.22), we find that NP simply leads to additional terms in these expressions. Thus, the new expansion for $\varphi(x)$ is given by (again up to $O(x^2)$):

$$\varphi(x) = B + \frac{B^3}{8} \left(\lambda_* + \lambda_6 B^2 + \lambda_8 B^4 + \frac{\alpha}{2} \ln B + \alpha \ln^2 B + \beta \ln^3 B + \beta \ln^4 B \right) x^2 + \dots \quad (\text{D.5})$$

which we use to set initial conditions for $\varphi(x_{\min})$ and $\varphi'(x_{\min})$. An analogous approach is followed when we consider the alternative parametrization of NP given in Eq. (4.25). Just like in the case without new physics, when we include gravity we use the initial values (D.4), and the numerical integration of the equations of motion is reduced to the tuning of the parameter B .

Fig. D.1 illustrates the exponential convergence of our algorithm in the four cases presented in this appendix.

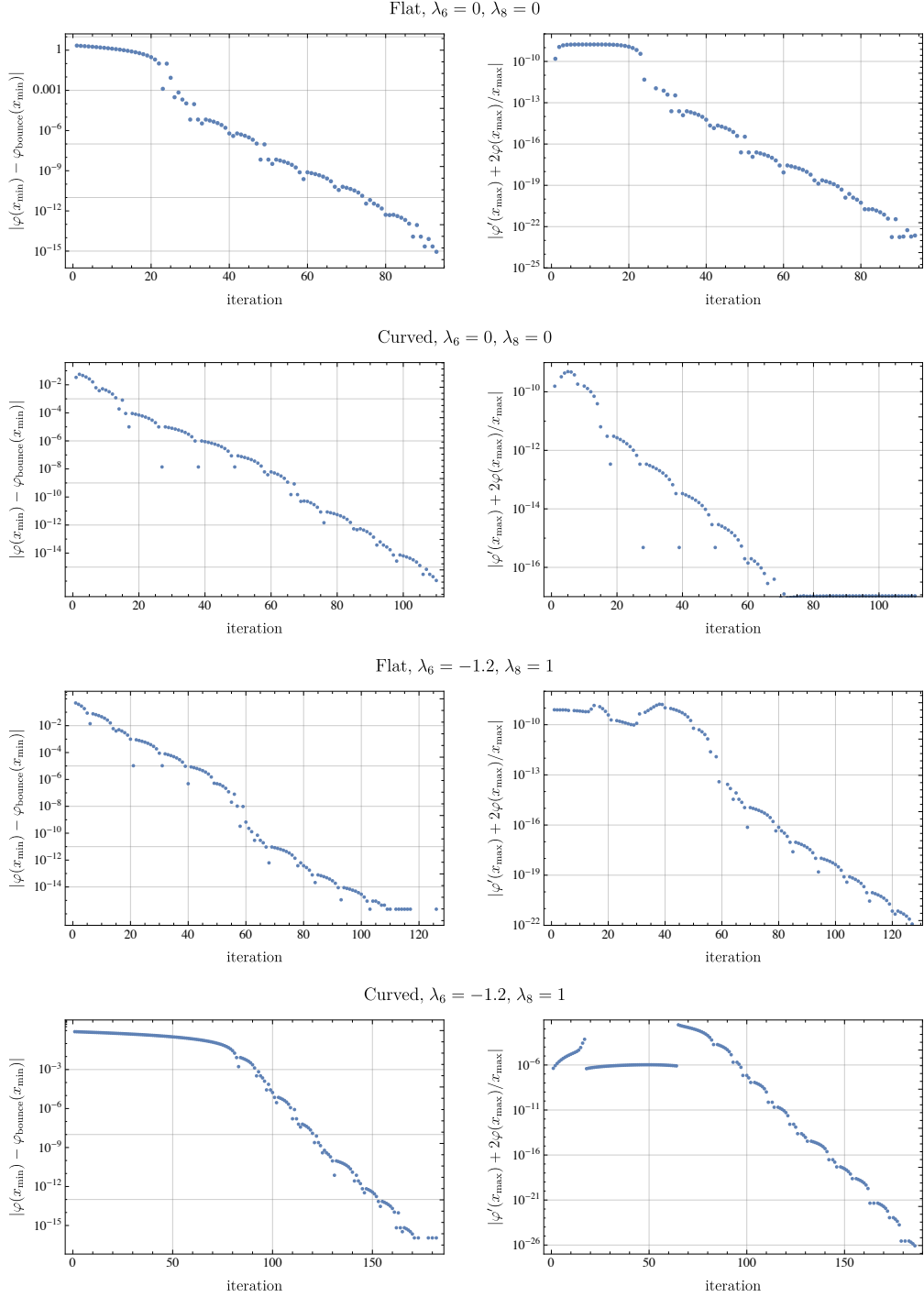


Figure D.1: Convergence of $\varphi(x_{\min})$ to its final value (left column), as well as of $\varphi'(x_{\max}) + 2\varphi(x_{\max})/x_{\max}$ to zero (right column), in the four cases (flat and curved, with and without new physics) discussed in the appendix.

Bibliography

- [1] O. Benhar L. Maiani and N. Cabibbo. Gauge Theories.
- [2] V. A. Rubakov. Classical Theory of Gauge Fields. *Princeton University Press*, 2007.
- [3] I. J. R. Aitchison and A. J. G. Hey. Gauge Theories in Particle Physics. *Adam Hilger, Bristol*, 1989.
- [4] T. Cheng and L. Li. Gauge Theory of Elementary Particle Physics. *Oxford University Press*, 1984.
- [5] C. Quigg. Gauge Theories of Strong, Weak and Electromagnetic Interactions. *Benjamin/ Cummings*, 1983.
- [6] F. Mandl and G. Shaw. Quantum Field Theory. *Wiley*, 2010.
- [7] M. E. Peskin and D. V. Schroeder. An Introduction to Quantum Field Theory. *Westview Press*, 1995.
- [8] L. H. Ryder. Quantum Field Theory. *Cambridge University Press*, 1996.
- [9] C. Itzikson and J. Zuber. Quantum Field Theory. *McGraw-Hill Book Company*, 1980.
- [10] S. Weinberg. The Quantum Theory of Fields-Modern Applications. *Cambridge University Press*, 1996.
- [11] S. Pokorski. Gauge Field Theories. *Cambridge University Press*, 2000.
- [12] J. C. Taylor. Gauge Theories of Weak Interactions. *Cambridge University Press*, 1976.
- [13] M. Maggiore. A Modern Introduction to Quantum Field Theory. *Oxford University Press*, 2010.
- [14] J. D. Jackson. Classical Electrodynamics. *Wiley*, 1975.
- [15] L. D. Landau and E. M. Lifshitz. Course of Theoretical Physics - The Classical Theory of Fields. *Pergamon Press*, 1979.

- [16] L. Maiani and O. Benhar. Meccanica Quantistica Relativistica - Introduzione alla Teoria Quantistica dei Campi. *Editori Riuniti University Press*, 2010.
- [17] L. B. Okun. Leptons and Quarks. *North-Holland*, 1982.
- [18] R. N. Cahn and G. Goldhaber. The Experimental Foundations of Particle Physics. *Cambridge University Press*, 1989.
- [19] D. Griffiths. Introduction to Elementary Physics. *Wiley*, 1987.
- [20] F. Halzen and A. D. Martin. Quarks and Leptons: An Introductory Course in Modern Particle Physics. *Wiley*, 1984.
- [21] D. H. Perkins. Introduction to High Energy Physics. *Addison-Wesley*, 1987.
- [22] G. Pagliaroli, A. Palladino, F.L. Villante, and F. Vissani. Testing nonradiative neutrino decay scenarios with IceCube data. *Phys. Rev. D*, 92(11):113008, 2015.
- [23] L. Maiani. Electroweak Interactions. *Editori Riuniti University Press*, 2013.
- [24] E. D. Commins and P. H. Bucksbaum. Weak Interactions of Leptons and Quarks. *Cambridge University Press*, 1983.
- [25] H. Georgi. Weak Interactions and Modern Particle Theory. *Benjamin/Cummings*, 1984.
- [26] Peter W. Higgs. Spontaneous Symmetry Breakdown without Massless Bosons. *Phys. Rev.*, 145:1156–1163, 1966.
- [27] Peter W. Higgs. Broken Symmetries and the Masses of Gauge Bosons. *Phys. Rev. Lett.*, 13:508–509, 1964.
- [28] Yoichiro Nambu. Quasiparticles and Gauge Invariance in the Theory of Superconductivity. *Phys. Rev.*, 117:648–663, 1960.
- [29] J. Goldstone. Field Theories with Superconductor Solutions. *Nuovo Cim.*, 19:154–164, 1961.
- [30] Jeffrey Goldstone, Abdus Salam, and Steven Weinberg. Broken Symmetries. *Phys. Rev.*, 127:965–970, 1962.
- [31] F. Englert and R. Brout. Broken Symmetry and the Mass of Gauge Vector Mesons. *Phys. Rev. Lett.*, 13:321–323, 1964.
- [32] G.S. Guralnik, C.R. Hagen, and T.W.B. Kibble. Global Conservation Laws and Massless Particles. *Phys. Rev. Lett.*, 13:585–587, 1964.

- [33] T.W.B. Kibble. Symmetry breaking in nonAbelian gauge theories. *Phys. Rev.*, 155:1554–1561, 1967.
- [34] C. Scrucca. Advanced Quantum Field Theory.
- [35] Marc Sher. Electroweak Higgs Potentials and Vacuum Stability. *Phys. Rept.*, 179:273–418, 1989.
- [36] S.Y. Lee and Alain M. Sciaccaluga. Evaluation of Higher Order Effective Potentials with Dimensional Regularization. *Nucl. Phys. B*, 96:435–444, 1975.
- [37] R. Rajaraman. Solitons and Instantons - An Introduction to Solitons and Instantons in Quantum Field Theory. *North-Holland*, 1989.
- [38] S. Coleman. Aspects of Symmetry: Selected Erice Lectures. *Cambridge University Press*, 1985.
- [39] E. J. Weinberg. Classical Solutions in Quantum Field Theory - Solitons and Instantons in High Energy Physics. *Cambridge University Press*, 2012.
- [40] Sidney R. Coleman. The Fate of the False Vacuum. 1. Semiclassical Theory. *Phys. Rev.*, D15:2929–2936, 1977. [Erratum: *Phys. Rev.* D16,1248(1977)].
- [41] Curtis G. Callan, Jr. and Sidney R. Coleman. The Fate of the False Vacuum. 2. First Quantum Corrections. *Phys. Rev.*, D16:1762–1768, 1977.
- [42] Anders Andreassen, David Farhi, William Frost, and Matthew D. Schwartz. Precision decay rate calculations in quantum field theory. *Phys. Rev. D*, 95(8):085011, 2017.
- [43] R. P. Feynman and A. R. Hibbs. Quantum Mechanics and Path Integrals. *McGraw-Hills*, 1965.
- [44] Sidney R. Coleman. Quantum Tunneling and Negative Eigenvalues. *Nucl. Phys. B*, 298:178–186, 1988.
- [45] Tom Banks, Carl M. Bender, and Tai Tsun Wu. Coupled anharmonic oscillators. 1. Equal mass case. *Phys. Rev. D*, 8:3346–3378, 1973.
- [46] Tom Banks and Carl M. Bender. Coupled anharmonic oscillators. ii. unequal-mass case. *Phys. Rev. D*, 8:3366–3378, 1973.
- [47] Gerald V. Dunne. Functional determinants in quantum field theory. *J. Phys. A*, 41:304006, 2008.
- [48] Erick J. Weinberg. Vacuum decay in theories with symmetry breaking by radiative corrections. *Phys. Rev. D*, 47:4614–4627, 1993.

- [49] G.H. Derrick. Comments on nonlinear wave equations as models for elementary particles. *J. Math. Phys.*, 5:1252–1254, 1964.
- [50] Sidney R. Coleman and Frank De Luccia. Gravitational Effects on and of Vacuum Decay. *Phys. Rev. D*, 21:3305, 1980.
- [51] E. Bentivegna, V. Branchina, F. Contino, and D. Zappalà. Impact of New Physics on the EW vacuum stability in a curved spacetime background. *JHEP*, 12:100, 2017.
- [52] Georges Aad et al. Combined search for the Standard Model Higgs boson using up to 4.9 fb^{-1} of pp collision data at $\sqrt{s} = 7 \text{ TeV}$ with the ATLAS detector at the LHC. *Phys. Lett. B*, 710:49–66, 2012.
- [53] Serguei Chatrchyan et al. Combined results of searches for the standard model Higgs boson in pp collisions at $\sqrt{s} = 7 \text{ TeV}$. *Phys. Lett. B*, 710:26–48, 2012.
- [54] Vincenzo Branchina and Emanuele Messina. Stability, Higgs Boson Mass and New Physics. *Phys. Rev. Lett.*, 111:241801, 2013.
- [55] First combination of Tevatron and LHC measurements of the top-quark mass. 2014.
- [56] Pier Paolo Giardino, Kristjan Kannike, Isabella Masina, Martti Raidal, and Alessandro Strumia. The universal Higgs fit. *JHEP*, 05:046, 2014.
- [57] Georges Aad et al. Measurements of Higgs boson production and couplings in diboson final states with the ATLAS detector at the LHC. *Phys. Lett. B*, 726:88–119, 2013. [Erratum: *Phys.Lett.B* 734, 406–406 (2014)].
- [58] Serguei Chatrchyan et al. Measurement of the Properties of a Higgs Boson in the Four-Lepton Final State. *Phys. Rev. D*, 89(9):092007, 2014.
- [59] Measurements of the properties of the Higgs-like boson in the two photon decay channel with the ATLAS detector using 25 fb^{-1} of proton-proton collision data. 3 2013.
- [60] Updated measurements of the Higgs boson at 125 GeV in the two photon decay channel. 3 2013.
- [61] J. Ellis, J.R. Espinosa, G.F. Giudice, A. Hoecker, and A. Riotto. The Probable Fate of the Standard Model. *Phys. Lett. B*, 679:369–375, 2009.
- [62] Joan Elias-Miro, Jose R. Espinosa, Gian F. Giudice, Gino Isidori, Antonio Riotto, and Alessandro Strumia. Higgs mass implications on the stability of the electroweak vacuum. *Phys. Lett. B*, 709:222–228, 2012.

- [63] Giuseppe Degrassi, Stefano Di Vita, Joan Elias-Miro, Jose R. Espinosa, Gian F. Giudice, Gino Isidori, and Alessandro Strumia. Higgs mass and vacuum stability in the Standard Model at NNLO. *JHEP*, 08:098, 2012.
- [64] Dario Buttazzo, Giuseppe Degrassi, Pier Paolo Giardino, Gian F. Giudice, Filippo Sala, Alberto Salvio, and Alessandro Strumia. Investigating the near-criticality of the Higgs boson. *JHEP*, 12:089, 2013.
- [65] Vincenzo Branchina, Emanuele Messina, and Alessia Platania. Top mass determination, Higgs inflation, and vacuum stability. *JHEP*, 09:182, 2014.
- [66] Gino Isidori, Giovanni Ridolfi, and Alessandro Strumia. On the metastability of the standard model vacuum. *Nucl. Phys. B*, 609:387–409, 2001.
- [67] J. R. Espinosa, G. F. Giudice, and A. Riotto. Cosmological implications of the Higgs mass measurement. *JCAP*, 0805:002, 2008.
- [68] Fedor Bezrukov, Mikhail Yu. Kalmykov, Bernd A. Kniehl, and Mikhail Shaposhnikov. Higgs Boson Mass and New Physics. *JHEP*, 10:140, 2012. [,275(2012)].
- [69] K.G. Chetyrkin and M.F. Zoller. Three-loop β – functions for top – Yukawa and the Higgs self – interaction in the Standard Model. *JHEP*, 06 : 033, 2012.
- [70] Luminita N. Mihaila, Jens Salomon, and Matthias Steinhauser. Gauge Coupling Beta Functions in the Standard Model to Three Loops. *Phys. Rev. Lett.*, 108:151602, 2012.
- [71] Vincenzo Branchina, Emanuele Messina, and Marc Sher. Lifetime of the electroweak vacuum and sensitivity to Planck scale physics. *Phys. Rev.*, D91:013003, 2015.
- [72] Vincenzo Branchina and Emanuele Messina. Stability and UV completion of the Standard Model. *EPL*, 117(6):61002, 2017.
- [73] Vincenzo Branchina, Emanuele Messina, and Dario Zappala. Impact of Gravity on Vacuum Stability. *EPL*, 116(2):21001, 2016.
- [74] A. Aguirre, T. Banks, and M. Johnson. Regulating eternal inflation. II. The Great divide. *JHEP*, 08:065, 2006.
- [75] Raphael Bousso, Ben Freivogel, and Matthew Lippert. Probabilities in the landscape: The Decay of nearly flat space. *Phys. Rev. D*, 74:046008, 2006.

- [76] Ali Masoumi, Sonia Paban, and Erick J. Weinberg. Tunneling from a Minkowski vacuum to an AdS vacuum: A new thin-wall regime. *Phys. Rev. D*, 94(2):025023, 2016.
- [77] Artu Rajantie and Stephen Stopyra. Standard Model vacuum decay with gravity. *Phys. Rev. D*, 95(2):025008, 2017.
- [78] Sidney R. Coleman and Erick J. Weinberg. Radiative Corrections as the Origin of Spontaneous Symmetry Breaking. *Phys. Rev. D*, 7:1888–1910, 1973.
- [79] Philipp Burda, Ruth Gregory, and Ian Moss. The fate of the Higgs vacuum. *JHEP*, 06:025, 2016.
- [80] Jose R. Espinosa, Gian F. Giudice, Enrico Morgante, Antonio Riotto, Leonardo Senatore, Alessandro Strumia, and Nikolaos Tetradis. The cosmological Higgstory of the vacuum instability. *JHEP*, 09:174, 2015.
- [81] P.Q. Hung and Marc Sher. Implications of a Higgs discovery at LEP. *Phys. Lett. B*, 374:138–144, 1996.
- [82] J.A. Casas, V. Di Clemente, and M. Quiros. The Standard model instability and the scale of new physics. *Nucl. Phys. B*, 581:61–72, 2000.
- [83] Vincenzo Branchina, Eloisa Bentivegna, Filippo Contino, and Dario Zappalà. Direct Higgs-gravity interaction and stability of our Universe. *Phys. Rev. D*, 99(9):096029, 2019.
- [84] Jr. Callan, Curtis G., Sidney R. Coleman, and Roman Jackiw. A New improved energy - momentum tensor. *Annals Phys.*, 59:42–73, 1970.
- [85] N.D. Birrell and P.C.W. Davies. *Quantum Fields in Curved Space*. Cambridge Monographs on Mathematical Physics. Cambridge Univ. Press, Cambridge, UK, 2 1984.
- [86] Peter Brockway Arnold and Stamatis Vokos. Instability of hot electroweak theory: bounds on $m(H)$ and $M(t)$. *Phys. Rev. D*, 44:3620–3627, 1991.
- [87] Marc Sher. Precise vacuum stability bound in the standard model. *Phys. Lett.*, B317:159–163, 1993. [Addendum: *Phys. Lett.*B331,448(1994)].
- [88] Guido Altarelli and G. Isidori. Lower limit on the Higgs mass in the standard model: An Update. *Phys. Lett.*, B337:141–144, 1994.
- [89] Ricardo A. Flores and Marc Sher. Upper Limits to Fermion Masses in the Glashow-Weinberg-Salam Model. *Phys. Rev.*, D27:1679, 1983.

- [90] N. Cabibbo, L. Maiani, G. Parisi, and R. Petronzio. Bounds on the Fermions and Higgs Boson Masses in Grand Unified Theories. *Nucl. Phys.*, B158:295–305, 1979.
- [91] M. Lindner. Implications of triviality for the standard model. *Zeitschrift für Physik C Particles and Fields*, 31(2):295–300, 1986.
- [92] Manfred Lindner, Marc Sher, and Helmut W. Zaglauer. Probing Vacuum Stability Bounds at the Fermilab Collider. *Phys. Lett.*, B228:139–143, 1989.
- [93] C. Ford, D. R. T. Jones, P. W. Stephenson, and M. B. Einhorn. The Effective potential and the renormalization group. *Nucl. Phys.*, B395:17–34, 1993.
- [94] J. A. Casas, J. R. Espinosa, and M. Quiros. Standard model stability bounds for new physics within LHC reach. *Phys. Lett.*, B382:374–382, 1996.
- [95] J. A. Casas, J. R. Espinosa, and M. Quiros. Improved Higgs mass stability bound in the standard model and implications for supersymmetry. *Phys. Lett.*, B342:171–179, 1995.
- [96] Bum-Hoon Lee and Wonwoo Lee. Vacuum bubbles in a de Sitter background and black hole pair creation. *Class. Quant. Grav.*, 26:225002, 2009.
- [97] Bum-Hoon Lee, Wonwoo Lee, Changheon Oh, Daeho Ro, and Dong-han Yeom. Fubini instantons in curved space. *JHEP*, 06:003, 2013.
- [98] Bum-Hoon Lee, Wonwoo Lee, Daeho Ro, and Dong-han Yeom. Oscillating Fubini instantons in curved space. *Phys. Rev.*, D91(12):124044, 2015.
- [99] Hans Peter Nilles. Supersymmetry, Supergravity and Particle Physics. *Phys. Rept.*, 110:1–162, 1984.
- [100] Vincenzo Branchina, Filippo Contino, and Apostolos Pilaftsis. Protecting the stability of the electroweak vacuum from Planck-scale gravitational effects. *Phys. Rev. D*, 98(7):075001, 2018.
- [101] Marcela Carena, John R. Ellis, A. Pilaftsis, and C. E. M. Wagner. Renormalization group improved effective potential for the MSSM Higgs sector with explicit CP violation. *Nucl. Phys.*, B586:92–140, 2000.
- [102] Abdelhak Djouadi. The Anatomy of electro-weak symmetry breaking. II. The Higgs bosons in the minimal supersymmetric model. *Phys. Rept.*, 459:1–241, 2008.
- [103] Nima Arkani-Hamed and Savas Dimopoulos. Supersymmetric unification without low energy supersymmetry and signatures for fine-tuning at the LHC. *JHEP*, 06:073, 2005.

- [104] G. F. Giudice and A. Romanino. Split supersymmetry. *Nucl. Phys.*, B699:65–89, 2004. [Erratum: Nucl. Phys.B706,487(2005)].
- [105] T. D. Lee. A Theory of Spontaneous T Violation. *Phys. Rev.*, D8:1226–1239, 1973.
- [106] G. C. Branco, P. M. Ferreira, L. Lavoura, M. N. Rebelo, Marc Sher, and Joao P. Silva. Theory and phenomenology of two-Higgs-doublet models. *Phys. Rept.*, 516:1–102, 2012.
- [107] P. M. Ferreira, R. Santos, and A. Barroso. Stability of the tree-level vacuum in two Higgs doublet models against charge or CP spontaneous violation. *Phys. Lett.*, B603:219–229, 2004. [Erratum: Phys. Lett. **B629**, 114 (2005)].
- [108] A. Barroso, P. M. Ferreira, and R. Santos. Charge and CP symmetry breaking in two Higgs doublet models. *Phys. Lett.*, B632:684–687, 2006.
- [109] I. P. Ivanov. Minkowski space structure of the Higgs potential in 2HDM. *Phys. Rev.*, D75:035001, 2007. [Erratum: Phys. Rev. **D76**, 039902 (2007)].
- [110] Igor P. Ivanov. Minkowski space structure of the Higgs potential in 2HDM. II. Minima, symmetries, and topology. *Phys. Rev.*, D77:015017, 2008.
- [111] A. Barroso, P. M. Ferreira, and R. Santos. Neutral minima in two-Higgs doublet models. *Phys. Lett.*, B652:181–193, 2007.
- [112] A. Barroso, P. M. Ferreira, I. P. Ivanov, Rui Santos, and Joao P. Silva. Evading death by vacuum. *Eur. Phys. J.*, C73:2537, 2013.
- [113] A. Barroso, P. M. Ferreira, I. P. Ivanov, and Rui Santos. Metastability bounds on the two Higgs doublet model. *JHEP*, 06:045, 2013.
- [114] V. Branchina, F. Contino, and P.M. Ferreira. Electroweak vacuum lifetime in two Higgs doublet models. *JHEP*, 11:107, 2018.
- [115] John F. Gunion and Howard E. Haber. The CP conserving two Higgs doublet model: The Approach to the decoupling limit. *Phys. Rev.*, D67:075019, 2003.
- [116] Sheldon L. Glashow and Steven Weinberg. Natural Conservation Laws for Neutral Currents. *Phys. Rev.*, D15:1958, 1977.
- [117] E. A. Paschos. Diagonal Neutral Currents. *Phys. Rev.*, D15:1966, 1977.
- [118] Nilendra G. Deshpande and Ernest Ma. Pattern of Symmetry Breaking with Two Higgs Doublets. *Phys. Rev.*, D18:2574, 1978.

- [119] Shinya Kanemura, Takahiro Kubota, and Eiichi Takasugi. Lee-Quigg-Thacker bounds for Higgs boson masses in a two doublet model. *Phys. Lett.*, B313:155–160, 1993.
- [120] Andrew G. Akeroyd, Abdesslam Arhrib, and El-Mokhtar Naimi. Note on tree level unitarity in the general two Higgs doublet model. *Phys. Lett.*, B490:119–124, 2000.
- [121] J. Horejsi and M. Kladiva. Tree-unitarity bounds for THDM Higgs masses revisited. *Eur. Phys. J.*, C46:81–91, 2006.
- [122] Nabarun Chakrabarty, Ujjal Kumar Dey, and Biswarup Mukhopadhyaya. High-scale validity of a two-Higgs doublet scenario: a study including LHC data. *JHEP*, 12:166, 2014.
- [123] Dipankar Das and Ipsita Saha. Search for a stable alignment limit in two-Higgs-doublet models. *Phys. Rev.*, D91(9):095024, 2015.
- [124] Debdosh Chowdhury and Otto Eberhardt. Global fits of the two-loop renormalized Two-Higgs-Doublet model with soft Z_2 breaking. *JHEP*, 11:052, 2015.
- [125] Pedro Ferreira, Howard E. Haber, and Edward Santos. Preserving the validity of the Two-Higgs Doublet Model up to the Planck scale. *Phys. Rev.*, D92:033003, 2015. [Erratum: *Phys. Rev.* **D94**, no.5, 059903 (2016)].
- [126] Nabarun Chakrabarty and Biswarup Mukhopadhyaya. High-scale validity of a two Higgs doublet scenario: metastability included. *Eur. Phys. J.*, C77(3):153, 2017.
- [127] Nabarun Chakrabarty and Biswarup Mukhopadhyaya. High-scale validity of a two Higgs doublet scenario: predicting collider signals. 2017.
- [128] Stefania Gori, Howard E. Haber, and Edward Santos. High scale flavor alignment in two-Higgs doublet models and its phenomenology. *JHEP*, 06:110, 2017.
- [129] Philipp Basler, Pedro M. Ferreira, Margarete Mühlleitner, and Rui Santos. High scale impact in alignment and decoupling in two-Higgs doublet models. *Phys. Rev.*, D97:095024, 2018.
- [130] Benjamín Grinstein, Christopher W. Murphy, and Patipan Uttayarat. One-loop corrections to the perturbative unitarity bounds in the CP-conserving two-Higgs doublet model with a softly broken Z_2 symmetry. *JHEP*, 06:070, 2016.

- [131] Vincenzo Cacchio, Debashish Chowdhury, Otto Eberhardt, and Christopher W. Murphy. Next-to-leading order unitarity fits in Two-Higgs-Doublet models with soft \mathbb{Z}_2 breaking. *JHEP*, 11:026, 2016.
- [132] Michael E. Peskin and Tatsu Takeuchi. A New constraint on a strongly interacting Higgs sector. *Phys. Rev. Lett.*, 65:964–967, 1990.
- [133] Michael E. Peskin and Tatsu Takeuchi. Estimation of oblique electroweak corrections. *Phys. Rev.*, D46:381–409, 1992.
- [134] I. Maksymyk, C. P. Burgess, and David London. Beyond S, T and U. *Phys. Rev.*, D50:529–535, 1994.
- [135] M. Baak, J. Cúth, J. Haller, A. Hoecker, R. Kogler, K. Mönig, M. Schott, and J. Stelzer. The global electroweak fit at NNLO and prospects for the LHC and ILC. *Eur. Phys. J.*, C74:3046, 2014.
- [136] G. Abbiendi et al. Search for Charged Higgs bosons: Combined Results Using LEP Data. *Eur. Phys. J.*, C73:2463, 2013.
- [137] O. Deschamps, S. Descotes-Genon, S. Monteil, V. Niess, S. T'Jampens, and V. Tisserand. The Two Higgs Doublet of Type II facing flavour physics data. *Phys. Rev.*, D82:073012, 2010.
- [138] Farvah Mahmoudi and Oscar Stal. Flavor constraints on the two-Higgs-doublet model with general Yukawa couplings. *Phys. Rev.*, D81:035016, 2010.
- [139] Thomas Hermann, Mikolaj Misiak, and Matthias Steinhauser. $\bar{B} \rightarrow X_s \gamma$ in the Two Higgs Doublet Model up to Next-to-Next-to-Leading Order in QCD. *JHEP*, 11:036, 2012.
- [140] M. Misiak et al. Updated NNLO QCD predictions for the weak radiative B-meson decays. *Phys. Rev. Lett.*, 114(22):221801, 2015.
- [141] Mikolaj Misiak and Matthias Steinhauser. Weak Radiative Decays of the B Meson and Bounds on M_{H^\pm} in the Two-Higgs-Doublet Model. *Eur. Phys. J.*, C77(3):201, 2017.
- [142] Howard E. Haber and Heather E. Logan. Radiative corrections to the Z b anti-b vertex and constraints on extended Higgs sectors. *Phys. Rev.*, D62:015011, 2000.
- [143] A. Arbey, F. Mahmoudi, O. Stal, and T. Stefaniak. Status of the Charged Higgs Boson in Two Higgs Doublet Models. *Eur. Phys. J.*, C78(3):182, 2018.

- [144] Georges Aad et al. Measurements of the Higgs boson production and decay rates and constraints on its couplings from a combined ATLAS and CMS analysis of the LHC pp collision data at $\sqrt{s} = 7$ and 8 TeV. *JHEP*, 08:045, 2016.
- [145] Robert V. Harlander, Stefan Liebler, and Hendrik Mantler. SusHi: A program for the calculation of Higgs production in gluon fusion and bottom-quark annihilation in the Standard Model and the MSSM. *Comput. Phys. Commun.*, 184:1605–1617, 2013.
- [146] Robert V. Harlander, Stefan Liebler, and Hendrik Mantler. SusHi Bento: Beyond NNLO and the heavy-top limit. *Comput. Phys. Commun.*, 212:239–257, 2017.
- [147] Lei Wang, Feng Zhang, and Xiao-Fang Han. Two-Higgs-doublet model of type-II confronted with the LHC run-I and run-II data. *Phys. Rev.*, D95(11):115014, 2017.
- [148] Pedro M. Ferreira, Stefan Liebler, and Jonas Wittbrodt. $pp \rightarrow A \rightarrow Zh$ and the wrong-sign limit of the two-Higgs-doublet model. *Phys. Rev.*, D97(5):055008, 2018.
- [149] P. M. Ferreira, John F. Gunion, Howard E. Haber, and Rui Santos. Probing wrong-sign Yukawa couplings at the LHC and a future linear collider. *Phys. Rev.*, D89(11):115003, 2014.
- [150] P. M. Ferreira, Renato Guedes, Marco O. P. Sampaio, and Rui Santos. Wrong sign and symmetric limits and non-decoupling in 2HDMs. *JHEP*, 12:067, 2014.
- [151] Beranger Dumont, John F. Gunion, Yun Jiang, and Sabine Kraml. Constraints on and future prospects for Two-Higgs-Doublet Models in light of the LHC Higgs signal. *Phys. Rev.*, D90:035021, 2014.
- [152] Duarte Fontes, J. C. Romão, and João P. Silva. A reappraisal of the wrong-sign $hb\bar{b}$ coupling and the study of $h \rightarrow Z\gamma$. *Phys. Rev.*, D90(1):015021, 2014.
- [153] Jeremy Bernon, John F. Gunion, Yun Jiang, and Sabine Kraml. Light Higgs bosons in Two-Higgs-Doublet Models. *Phys. Rev.*, D91(7):075019, 2015.
- [154] Ambalika Biswas and Amitabha Lahiri. Alignment, reverse alignment, and wrong sign Yukawa couplings in two Higgs doublet models. *Phys. Rev.*, D93(11):115017, 2016.
- [155] Tanmoy Modak, Jorge C. Romão, Soumya Sadhukhan, João P. Silva, and Rahul Srivastava. Constraining wrong-sign $hb\bar{b}$ couplings with $h \rightarrow \Upsilon\gamma$. *Phys. Rev.*, D94(7):075017, 2016.

- [156] Ali Masoumi, Ken D. Olum, and Benjamin Shlaer. Efficient numerical solution to vacuum decay with many fields. *JCAP*, 1701(01):051, 2017.
- [157] Ilya F. Ginzburg, Maria Krawczyk, and Per Osland. Two Higgs doublet models with CP violation. In *Linear colliders. Proceedings, International Workshop on physics and experiments with future electron-positron linear colliders, LCWS 2002, Seogwipo, Jeju Island, Korea, August 26-30, 2002*, pages 703–706, 2002. [,703(2002)].
- [158] Wafaa Khater and Per Osland. CP violation in top quark production at the LHC and two Higgs doublet models. *Nucl. Phys.*, B661:209–234, 2003.
- [159] Abdul Wahab El Kaffas, Per Osland, and Odd Magne Ogreid. CP violation, stability and unitarity of the two Higgs doublet model. *Nonlin. Phenom. Complex Syst.*, 10:347–357, 2007.
- [160] Abdul Wahab El Kaffas, Wafaa Khater, Odd Magne Ogreid, and Per Osland. Consistency of the two Higgs doublet model and CP violation in top production at the LHC. *Nucl. Phys.*, B775:45–77, 2007.
- [161] Abdul Wahab El Kaffas, Per Osland, and Odd Magne Ogreid. Constraining the Two-Higgs-Doublet-Model parameter space. *Phys. Rev.*, D76:095001, 2007.
- [162] Per Osland, P. N. Pandita, and Levent Selbuz. Trilinear Higgs couplings in the two Higgs doublet model with CP violation. *Phys. Rev.*, D78:015003, 2008.
- [163] B. Grzadkowski and P. Osland. Tempered Two-Higgs-Doublet Model. *Phys. Rev.*, D82:125026, 2010.
- [164] A. Arhrib, E. Christova, H. Eberl, and E. Ginina. CP violation in charged Higgs production and decays in the Complex Two Higgs Doublet Model. *JHEP*, 04:089, 2011.
- [165] A. Barroso, P. M. Ferreira, Rui Santos, and Joao P. Silva. Probing the scalar-pseudoscalar mixing in the 125 GeV Higgs particle with current data. *Phys. Rev.*, D86:015022, 2012.
- [166] Florian Staub. Reopen parameter regions in Two-Higgs Doublet Models. *Phys. Lett.*, B776:407–411, 2018.
- [167] Florian Loebbert and Jan Plefka. Quantum Gravitational Contributions to the Standard Model Effective Potential and Vacuum Stability. *Mod. Phys. Lett. A*, 30(34):1550189, 2015.
- [168] Petr Horava and Edward Witten. Heterotic and type I string dynamics from eleven-dimensions. *Nucl. Phys.*, B460:506–524, 1996. [,397(1995)].

- [169] Ignatios Antoniadis, Nima Arkani-Hamed, Savas Dimopoulos, and G. R. Dvali.
New dimensions at a millimeter to a Fermi and superstrings at a TeV. *Phys. Lett.*, B436:257–263, 1998.
- [170] Lisa Randall and Raman Sundrum. A Large mass hierarchy from a small extra dimension. *Phys. Rev. Lett.*, 83:3370–3373, 1999.